ATMOSPHERIC   STRUCTURE :

EXPLORATION OVER   ANTARCTICA

AND INTERHEMISPHERIC   COMPARISON
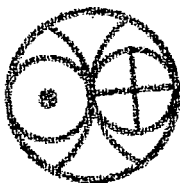

THESIS

Submitted   to   the

GUJARAT   UNIVERSITY

for   the   degree   of

DOCTOR   OF   PHILOSOPHY

(Science)

by

PARMJIT   SINGH   SEHRA

October 1976

Physical Research Laboratory

Ahmedabad 380009

India

D E D I C A T E D   T O

MY   PARENTS

Shri Mohinder Singh Sehra

and

Shrimati Satwinder Kaur

who induced into me a great inspiration and

cultivated a keen interest for

scientific adventures and

exploratory work

C E R T I F I C A T E

I hereby declare that the work presented in this thesis 'Atmospheric Structure : Exploration over Antarctica and Interhemispheric Comparison' is original and has not formed the basis for the award of any degree or diploma by any University or Institution.

PARMJIT SINGH SEHRA
(Author)

Certified by

P. R. Pisharoty
(Guide & Professor-in-charge)

C O N T E N T S

CHAPTER - II

THE M-100 METEOROLOGICAL ROCKET SOUNDING SYSTEM   35-62

CHAPTER - III

CHAPTER - V

ATMOSPHERIC TEMPERATURE, PRESSURE AND DENSITY VARIATIONS IN ANTARCTICA

S T A T E M E N T

In 1970, the Department of Atomic Energy, Government of India and the Hydrometeorological Service of the USSR signed a joint agreement for collaborative meteorological rocket soundings of the upper atmosphere from the Thumba Equatorial Rocket Launching Station ($8^{\circ}32'N$, $76^{\circ}52'E$) using Soviet 'M-100' meteorological rockets. The author was the Project Scientist for the rocket soundings from Molodezhnaya ($67^{\circ}40'S$, $45^{\circ}51'E$) in Antarctica during the Soviet Antarctic Expedition, 1971-73. The author directly participated in the M-100 rocketsonde data acquisition and processing both at Molodezhnaya in Antarctica and Thumba equatorial station in South India. This forms the major source of data for the thesis. A brief review of the atmospheric structure is given in Chapter I.

In 1972 about 60 rockets were launched from the Antarctic station Molodezhnaya out of which 52 flights were successful and 16 of them carried an additional wind sensor 'chaff' for measuring upper mesospheric winds. The M-100 rockets probe the atmosphere up to an altitude of about 90 km carrying a payload of 66.65 kg. Atmospheric winds are derived from the drift of the trajectory of the

descending parachute and chaff while the temperatures are measured by 4 variable resistance thermometers with 40 micron tungsten-rhenium wire. The M-100 rocket sounding system and the M-100 rocketsonde data reduction and processing are discussed in Chapters II and III. Accuracy of wind measurement is about 5 to 10 ms^{-1} while the mean square error in temperature measurement is 3 to $10^{o}C$.

The analysis of the Antarctic M-100 rocketsonde data was carried out for the southern summer (December to February), autumn (March to May), winter (June to August) and spring (September to November). The Antarctic summer was characterised by light easterly winds increasing in strength with altitude. The winter exhibited strong westerly winds of speed about 50 to 100 ms^{-1} increasing in magnitude as the season progressed. However, autumn and spring were the wind reversal periods marked by the change of summer easterly winds to the winter westerlies and vice versa.

Complete reversal of winds from easterlies to westerlies occurred in the stratosphere in the first week of February and in the troposphere in the last week of February. On the other hand the change from westerlies to easterlies took place in the third week of November in the

stratosphere and during the first week of December in the troposphere, suggesting that the reversal first occurred in the upper layers and was propagated downwards. Exploration of atmospheric structure over Antarctica with an emphasis on seasonal wind variations is discussed in Chapter IV.

The investigation of the Antarctic atmosphere shows that the most unsettled period in the South Polar regions was the winter and the early spring which was marked by **large perturbations** in the wind and thermal structure. The rapid shifts in both **zo**nal and meridional components of the upper atmospheric winds, particularly during the period from May to July, were accompanied by sudden changes in the temperature distribution as revealed by the stratospheric and mesospheric warming and cooling. During September when the winter westerlies changed to the summer easterlies the upper atmosphere experienced a warming of about $40^{o}C$ at 40 km. Apart from the general warmings and coolings of the Antarctic stratosphere and mesosphere, there were a few occasions in May and July when sudden warmings were also observed.

The average summer tropopause over Antarctica was located at 9 km with a temperature of $-53^{o}C$ while during the southern winter it was ill-defined due to its multiple

occurrences. The Antarctic stratopause in the southern summer was located at 47 km with a temperature of $7^{\circ}C$ while in the winter it was at 46 km with a temperature of $-12^{\circ}C$. The Antarctic upper mesosphere in an altitude region from about 60 to 80 km in winter was found warmer than its summer counterpart. Atmospheric temperature, pressure and density variations in Antarctic are discussed in Chapter V.

A study of the equatorial atmospheric structure is also made and the results of this investigation are discussed in Chapter VI. A comparison of the South Polar and equatorial atmospheric structure is made in Chapter VII. It is found that the summer tropopause and stratopause in the Southern Hemisphere over Antarctica were about $27^{\circ}C$ and $13^{\circ}C$ warmer than the corresponding equatorial tropopause and stratopause. Also, the South Polar tropopause and stratopause were located at altitudes about 8 km and 2 km lower than their corresponding equatorial counterparts. The Antarctic tropopause and stratopause in the southern winter were apparently about $5^{\circ}C$ and $8^{\circ}C$ colder and located at altitudes about 3 km and 2 km higher than the corresponding equatorial tropopause and stratopause contrary to the summer-time atmospheric structure.

The actual results obtained from the rocket soundings in 1972 are also compared with the Groves (1971) atmospheric model and the corresponding deviations of the actuals from the Groves model are worked out. The departures of the actual zonal winds and of the temperatures over Molodezhnaya, Antarctica and over Thumba equatorial station from the corresponding Groves atmospheric model profiles were found to be quite significant. The Groves model is based on data from the Northern Hemisphere. The departures are because the Southern Hemisphere is more oceanic and more symmetric and has a vigorous general circulation as compared to the Northern Hemisphere. Also, the Antarctic continent is located at a higher elevation and has a higher albedo than the Arctic.

Likewise for the Thumba latitude in the Eastern Hemisphere, the Groves atmospheric model is based on data from all longitudes mostly from the Western Hemisphere. Departures of the equatorial actuals from the Groves profiles may, therefore, be the evidence of longitudinal asymmetries between the Eastern and the Western Hemisphere.

In addition to the Antarctic exploration, and equatorial study an interhemispheric comparison of the atmospheric structure is also carried out in Chapter VIII

employing meridional cross section analysis. Data were taken
from the meteorological rocket soundings along two meridional
zones : 40°E to 90°E in the Eastern Hemisphere and 35°W to
95°W in the Western Hemisphere. The results obtained from
the Eastern Meridional Network of stations from the 'M-100'
rocket soundings in 1972 at Heiss Island (80°37'N), Volgograd
(48°41'N), Thumba (8°32'N), Mobile ships in the Indian
Ocean and Molodezhnaya (67°40'S) are presented as mean
profiles, time-height cross sections and lateral cross
sections. Rocketsonde data for the Western Meridional Network
are taken from the stations Thule (76°33'N), Fort Churchill
(58°44'N), Wallops Island (37°50'N), Cape Kennedy (28°27'N),
Antigua (17°09'N), Fort Sherman (9°20'N), Natal (5°55'S),
and Mar Chiquita (37°45'S).

Finally, a summary of the work done and the principal
conclusions drawn from the investigation "Atmospheric
Structure: Exploration over Antarctica and Interhemispheric
Comparison" are presented in Chapter IX.

PARMJIT   SINGH   SEHRA
(Author)

Approved by

P. R. Pisharoty
(Guide & Professor-in-charge)

INTRODUCTION

1.1   General

In Greek atmosphere means atmos,"vapour" ;sphaira ,
"sphere" i.e. gaseous envelope covering a planet. It is the
ocean of air in which we move and have our being, which
flows around us and sustains life on Earth. The ever changing
sky has always inspired and intrigued mankind. Depending
on the good graces of the weather for so many of his
pursuits, man recognised early the necessity of studying
the weather. The farmer watched the sunset and the motions
of the clouds to determine if the next day would bring rain.
The mariner watched the same signs and as ships ranged
around the world mariners prepared weather charts. A
disastrous flood, a drought or a long severe winter arouses
even today the desire to trace back the event to some
specific cause. For practical and observational reasons,
attention has been largely concentrated in the past on the
study of the processes in the lowest layer (up to about
10-15 km) of the atmosphere which give rise to weather.

Investigation of the upper air began in 1749 when Alexander Wilson attached a thermometer to a kite. With the development of the balloon in the late 18th century, scientific ballooning began with manned flights. Extensive application to research started in 1892 when Gustave Hermite and George Besancon began to use small unmanned balloons (balloon sondes) carrying instruments. In 1894, Albert Rotch used large kites tethered by steel wire, but meteorological kite flying was gradually abandoned.

Between 1899 and 1902 balloon experiments led Richard Assmann and L.P.Teisserence de Bort to the discovery of the stratosphere, and the first two decades of the 20th century saw an immense development of the balloon sounding technique, yielding considerable information about the lowest layer of the atmosphere. In the period 1927-36 advances in radio techniques made possible the development of the radiosonde. This instrument, attached to a free balloon, sends radio signals that can be translated into numerical values of temperature, humidity, and pressure. During World War II and later, radiosonde techniques were further developed, radar was applied to wind measurements, meteorological instrumentation for aircraft was greatly advanced, and the sounding rocket came into use. Regular

meteorological rocket soundings commenced in 1962. Satellites are now being employed for determining the temperature profiles of the atmosphere up to about 30-40 km by infrared radiation measurements.

1.2   Various techniques of sounding the atmosphere

Detailed exploration of the atmospheric structure awaited the development of suitable vehicles for the transport of instrumentation into the relatively inaccessible region, stratosphere and mesosphere. Radiosonde method has been widely employed all over the globe. The rubber balloons used for routine meteorological soundings burst near the tropopause. The American 'Darex' and the Japanese 'Totex', each 1200 gm, have been found to reach altitudes of about 30-35 km. On account of its strong neck and sturdy structure, a 'Totex' balloon is preferred when higher rate of ascent, 24 km hr^{-1} is desired and the launching is to be carried out in rough weather and gusty wind conditions although its cost is higher and it attains a relatively lower altitude. The trajectory of the hydrogen gas filled balloon released with radiosonde and reflector is tracked by radar and telemetery system and the meteorological parameters recorded. Small corner

aluminium reflectors of 250 gm are used for rawin ascents. At the Thumba Equatorial Rocket Launching Station (TERLS) there are two radiosonde systems working on 401 MHz and 1680 MHz. The Soviet 'RKZ-2' radiosonde system working on 1780 MHz was also employed.

The development of rockets capable of carrying instruments much higher above the earth's surface has now made it possible to make direct measurements of atmospheric winds, temperature, pressure and density above the balloon altitudes. The investigation of the upper atmosphere necessiated the development of small and less expensive meteorological rockets which could be fired on a routine basis for synoptic studies. The British 'Skua' , the Polish 'Meteor-1' , the United States 'Lokidart' , 'Judidart' and 'Arcas' , the Japanese 'MT-135' and 'MT-160' and the Australian 'Kookaburra' meteorological rocket systems are now being regularly used for sounding the upper atmosphere (Webb, 1969). For the present investigation of the upper atmospheric structure, the Soviet 'M-100' meteorological rocket sounding system was employed which is discussed separately in Chapter - II.

The M-100 rocket sounding system incorporates parachute and chaff as wind sensors and four tungsten-rhenium (40 microns) wire thermometers as temperature sensors. The two-stage M-100 rocket measures 8.906 m, has a diameter of 25 cm and weighs about 480 kg when fully charged. It can reach a maximum altitude of 100 km when launched vertically with a solid propellant made of nitrocellulose base. For meteorological investigations it is usually fired at 83° effective elevation with a payload of about 66 kg. The steeple portion containing the temperature sensors opens around 60 sec after the lift off. The whole payload is separated at 70 sec around 70 km and it attains an apogee of about 90 km around 140 sec from the take-off. About 400 gm of chaff, in a special container divided into two parts, is ejected at rocket apogee. The chaff consists of aluminium-coated glass fibres with a diameter of about 0.025 mm. After ejection from the M-100 rocket, it is tracked by a high sensitivity Meteor-2 radar. Conventionally, three or four fibre glass chaff bundles are ejected at intervals of ten km in downward direction starting from 90 km and the different chaff clouds are tracked by a single radar system. Also, at apogee the parachute consisting of a non-reflecting hemispherical mylar with a surface area of 35 m^2 exerts a stabilising influence on the payload and

fully opens during descent at an altitude of 60-65 km around
200 sec after the take-off. The parachute is tracked by the
Meteor-1 radar operating at 1780 MHz in the transponder mode.
Atmospheric winds are derived from the drift of the trajectory
of the descending parachute and chaff. An unbalanced wheat-
stone bridge arrangement is used for telemetering the
atmospheric temperature data from the 40 μm tungsten-rhenium
wire thermometers to the ground. Two telemetry receivers with
panoramic and photographic attachments record the temperature
data along with the timing pulses from the take-off. The
reduction and processing of the meteorological data obtained
from the M-100 rocket sounding system and the various
corrections applied are discussed in Chapter - III.

Various types of rocket-borne wind and temperature
sounding instruments are now used throughout the world to
study the atmospheric structure in the region from about
20 to 100 km. Wind profiles are determined on a routine
basis as high as 65 to 85 km with passive radar targets
'chaff' , inflatable sphere 'Robin' and parachutes. The two
main temperature sensors used in the rocket payloads for
temperature measurements are thermistor and wire resistance
types. Other techniques for measuring the atmospheric winds
and temperatures are falling sphere, grenade, vapour cloud

(Sodium, Trimethyl Aluminium and Barium) and pitot tubes which are limited due to their complexity, cost and accuracy. The wide range of environmental conditions which characterise the stratosphere and mesosphere preclude the application of any one measuring system over the entire range of interest. Consequently, various techniques have to be used for sounding the terrestrial atmosphere. Bollermann (1970) has given a survey of the various techniques used for atmospheric sounding.

1.3   Present state of knowledge

Since the establishment of the Meteorological Rocket Network (MRN) there has been a substantial increase in the number of measurements of atmospheric structure by sounding rockets. An attempt is made to summarise some of the important results obtained so far.

1.3.1   Earlier studies of the atmospheric structure

Our initial knowledge of the atmospheric structure came from a variety of instrumentation systems. A good deal of information on atmospheric winds and temperatures was deduced indirectly from other experiments based on phenomena such as observations of solar spectrum. In addition certain naturally occurring phenomena such as meteors, aurora and

noctilucent clouds have provided valuable information so
that with the help of theoretical considerations a general
picture of winds and temperatures over the globe could be
built up to considerably higher levels, for example as given
by Kellog and Schilling (1951), Pant (1956) and Deb (1953).
Investigations such as those of Murgatroyed (1957), Batten
(1961) and Finger, Teweles and Mason (1963) have established
that in summer an anticyclonic vortex develops around the
poles but in winter the circulation changes to a cyclonic
circumpolar vortex. These vortices develop earlier and more
rapidly at higher levels and penetrate downward and equator-
ward with advance of season.

The 50 mb (about 20 km) constant pressure chart shows
in summer a warm high situated near the pole, the temperature
and contour height decreasing steadily towards the equator.
The thermal winds are therefore easterly. Although at 50 mb
itself the actual winds are light, at higher levels (around
25 km) a marked easterly circulation prevails at all
latitudes. In winter, a cold low is located near the pole.
Temperature and contour height rise rapidly from the pole
up to about $50^{\circ}N$ where a ridge is noticeable. Winds are
already westerly at 50 mb and continue to increase in speed
upwards. Equatorward of $50^{\circ}N$ the westerlies weaken and even
change at low latitudes to easterlies.

The easterly zonal flow of summer, although weak, is steady, being affected only by occasional mild perturbations. On the other hand the stronger winter circulation is dynamically unstable. Not only are both zonal wind and wind shear larger than in summer, but also the vertical temperature gradient continues to be negative even above the tropopause, at high latitudes. Consequently, the Richardson number becomes small. As a result of baroclinic instability it is found that disturbances of wave number usually 2 or 3 (which set in through essentially barotropic development) get accentuated. Sometimes the polar cyclonic vortex shrinks (the low latitude anticyclonic belt advances poleward) and local anticyclones develop which shift towards the winter pole at some latitudes. On other occasions, there is a complete reversal of the circulation and of the normal winter-time meridional temperature gradient. In the latter kind of circulation disturbance, which may be termed 'major' the stratosphere seems capable of generating its own kinetic energy, and operating as a heat engine ; in the former or 'minor' kind, the stratosphere is probably a sink of kinetic energy consuming energy perhaps supplied by the troposphere below (Julian, 1967). These break-downs rarely occur when the winter circulation is at its early stage but are common during winter and the final spring reversal periods. They closely precede sudden stratospheric warmings.

1.3.2   Synoptic studies in the Northern Hemisphere

In the Northern Hemisphere, a regular feature of the summer months is a polar anticyclone which reaches peak intensity in July. Summer conditions are generally steady and symmetrical in longitude. Thereafter the system decays slowly and by the end of August high latitude cyclonic activity may be expected to appear at 36 km. As the cyclone cools the anticyclonic circulation retreats southward reaching low latitudes by late October so that most of the hemisphere is involved in an apparently steady nearly circumpolar westerly circulation. This situation is usually soon terminated by a warming with anticyclonic activity appearing over the Aleutian area possibly before the end of October. A typical winter situation is difficult to define on account of the non-steady conditions. The Aleutian anticyclone generally intensifies and displaces the polar low towards northern Europe or Eurasia. It may later fill in and subsequently intensify.

When the temperature gradient between the high and low pressure systems increases, strong northerly winds develop over North Canada. The main changes that occur in the winter and early spring are associated with pulsations and displacements of the Aleutian high and with the occurrence

of stratospheric warmings. The final phase occurs in late
March or early April when a cyclone usually dominates the
polar area again for a brief period before a warm polar
anticyclone develops in response to spring time radiational
heating. Up to 30 km complete coverage in longitude has been
provided for the Northern Hemisphere since the IGY by high-
level balloons. Infra-Red (IR) sensing by satellites of CO_2
emissions in the 15 μ m spectral region has more recently
provided a new tool for synoptic studies in both the Northern
and Southern Hemispheres. A single-channel radiometer in
TIROS VII provided observational results over one seasonal
cycle of the temperature field smoothed in altitude with
maximum weighting at 20 km. Over 70 percent of the total
received radiation originated at altitudes between 10 and
30 km (Kennedy and Nordberg, 1967). The differences between
the summer and winter synoptic situations were in general
agreement with the rocketsonde results. Synoptic charts have
been prepared by Johnson and McInturff (1970) from the
NIMBUS 3 results.

1.3.3   Synoptic studies in the Southern Hemisphere

In the Southern Hemisphere the number of available
observations on the atmospheric structure have always been
sparse. For CIRA 1965 the number of launchings carried out

were 30 for Ascension Island at 8°S, 22 for Woomera at 31°S
and just 14 for McMurdo Sound at 78°S. At Woomera, the
seasonal wind pattern appeared similar to that at 30°N sites
judged by these few observations which did not cover all
months of the year. From the few available observations at
McMurdo Sound it appeared that midwinter warmings of the
Antarctic were similar in many respects to Arctic warmings,
the circumpolar vortex tending to elongate and split
(Quiroz, 1966). The observations were, however, not sufficient
to show whether the winter flow was disrupted in the Southern
Hemisphere to the same extent as in the Northern Hemisphere.

Different Southern Hemisphere winters, particularly
atballoon altitudes, have behaved in quite different ways in
terms of the detailed temperature structure but they have not
shown the large amplitude variability found in the Arctic.
In late winter, August and September, warm cells, principally
in the Australian Sector, produce perceptible perturbations
in the otherwise zonal flow, which develop into the final
warming. Asymmetries in atmospheric heating and circulation
between the two hemispheres may be expected to arise from the
very different distributions of land and sea, although the
effects in the stratosphere and mesosphere may not be large.
Total ozone amounts which were measured at 17 stations during
the IGY showed quite a distinct asymmetry. The maximum

concentration in the Southern Hemisphere occurred at 50 to 55° latitude throughout the year with decreasing concentration towards the pole, whereas in the Northern Hemisphere the maximum occurred at 60° to 70° moving to above 80° during spring (MacDowell, 1960). The upwards extension of such asymmetries has been uncertain due to the small number of observations.

Since 1966, additional data in the southern Hemisphere have been obtained from the Experimental Inter-American Meteorological Rocket Network (EXAMETNET). In view of the large ocean areas in the Southern Hemisphere, shipboard launchings have provided a means of extending coverage in latitude (Finger and Woolf, 1967 a),(Theon and Horvarth, 1968). Vertical distribution of the main meteorological parameters and large-scale processes in the stratosphere and mesosphere has been discussed by Gaigerov et al in a paper presented at 13th COSPAR Meeting, Leningrad, 1970. It was found that the summer anticyclonic circulation is symmetric about the pole and is practically the same in both hemispheres, the winter circulation in the Southern Hemisphere is less perturbed than in the Northern Hemisphere and that during the transitional season, April and October the two zonal flows are from the west.

Zonal flows at times of the year other than April
and October are in opposite directions in the two hemispheres
except at low latitudes where they merge along a sub-tropical
ridge line in the winter hemispheres. When the sub-tropical
ridge is displaced southward due to deepening of the middle
latitude trough, westerlies replace easterlies in the
sub-tropics. At mid or high latitudes during wintertime the
meridional wind speeds at times may be comparable with the
zonal wind speeds. At other times, meridional wind velocities
are generally small compared with zonal velocities and
consequently their seasonal pattern is not so readily apparent
as that for the zonal winds.

1.3.4   Transient and standing eddies

A distinction can be made between transient eddies
which give rise to time variations in the meridional wind
at a particular site and standing eddies which are related
to the longitudinal variations in the time-averaged value.
When evalued for the troposphere in terms of appropriate
standard deviations, both transient and standing eddies were
found to be largest in the vicinity of the mid-latitude jet
stream at 10 km altitude (Newell, Wallace and Mahoney, 1966).
The standing eddies are smaller in summer than winter, and
even in winter their standard deviations are small in

comparison with those of the transient eddies, which show little seasonal change and have a maximum standard deviation of 15 ms^{-1}. Transient eddies in the lower stratosphere tend to increase with latitude and values of the order of 10 ms^{-1} were found in the above study at high latitudes. Polewards of 30° latitude, a seasonal variation in the transient eddy velocity was present. With regard to height dependence, transient eddies were least in the region of 24 km. Above 24 km the longitudinal coverage by balloon observations has been inadequate for zonal averaging and analysis of standing eddies and the meridional circulation. Above the transient eddy minimum at 24 km, values were found to increase to a maximum at 50 km or more and to reach 25 ms^{-1} at high latitude in winter. Seasonal dependence is prominent in stratospheric transient eddies in comparison with the tropospheric ones possibly due to the seasonal reversal of the stratospheric vortex. Standing eddies are expected to be an important feature of the circulation at rocket heights as well as at balloon heights. A more detailed analysis of these parameters of meridional flow awaits a better global distribution of data.

1.3.5 Diurnal variations

The increased amount of data from meteorological rocket soundings has revealed the existence of diurnal tidal motions with amplitudes of several ms^{-1}. Diurnal components

are more readily resolved in meridional winds than zonal winds, which are subject to large seasonal variations. At 50 km a diurnal amplitude of 8 ms^{-1} has been found using summer data over a number of years, the maximum south-to-north flow occurring close to noon (Groves, 1967). Diurnal variations in meridional flow have also been resolved at Ascension Island and high latitude sites (Reed, McKenzie and Vyverberg, 1966). The main thermal drives for the diurnal tide, insolation absorption by O_3 and H_2O, have been described by Lindzen (1967). It is apparent that a complicated wind field is set up by relatively simple thermal drives. The results are a first approximation which may possibly be improved when the thermal drives are better known. At midlatitudes, the phase of the 24-hour tide changes rapidly with latitude and is therefore sensitive to the relative thermal input between low and high latitudes that is assumed. Seasonal changes in the thermal input will also have an effect.

The amplitude and phase of the diurnal variation in the zonal wind components at $30^{\circ}N$ has also been obtained (Reed, Oard and Sieminski, 1969). Except near 40 km, the phase difference between the two components is about 90° corresponding to a clockwise rotation of the wind vector with time. Seasonal variations in tidal components for $31.5^{\circ}N$ have been investigated by Groves and Makarious (1968).

Quite significant variations of phase with season occur particularly in the diurnal component where phases may change rapidly with height. Attempts have been made to observe diurnal variations in stratosphere temperatures but the amplitudes obtained have been consistently greater than those predicted by tidal theory. A limited sample of rocketsonde temperature and wind data gathered during a series of launchings at Wallops Island suggests that the diurnal range of observed temperature consists of components that can be ascribed to the real diurnal variation and radiation error of the rocketsonde instrument (Finger and Woolf, 1967 b). Corresponding diurnal dependences will also be present in pressures and densities. Diurnal variations derived from temperatures measured at White Sands, $32^{\circ}N$, have given an amplitude of 4 to 7 percent in pressure and 3 to 5 percent in density for the 52-58 km layer (Thiele, 1966). Although these variations are small, they are comparable with the seasonal variation at latitudes of less than 30°.

Diurnal variations in wind components above 60 km have been most extensively observed by the radar-meteor method. The 24 hour, 12 hour and 8 hour solar components are usually extracted by harmonic analysis. Amplitudes and phases can be expected from theoretical considerations to be both latitudinally and seasonally dependent. At latitudes

50 to 55°N, the 12 hour component is found to be the main periodic variation exceeding the 24 hour component by a factor of 3 to 4. In contrast to the 24 hour component, seasonal changes in the 12 hour component follow a regular pattern. For most of the year, the phase of the zonal component leads that of the meridional component by about 3 hours corresponding to a clockwise rotation of the wind vector. Muller (1966) and Sprenger, Greisiger and Schminder (1969) have discussed the diurnal variations above 60 km. For altitudes above 90 km, tidal period winds have been sought by analysis of data from chemical releases (Hines,1966) and (Woodrum, Justus and Roper 1969). In spite of the attenuation of the upward tidal energy flux, the decrease of ambient density with height tends to maintain velocity amplitudes so that tidal components still contribute significantly to the total wind vector.

1.3.6   Seasonal variations

One of the main variation of the stratospheric and mesospheric structure is the seasonal variation (Belmont and Dartt, 1970). At mid and high latitudes, there is a well established pattern of easterlies in summer and stronger westerlies in winter. The easterlies recur very regularly each year but the westerlies show year-to-year variations

in the winter and early spring. At low latitudes, the summer-
time easterlies at 40 km extend across the equator into the
winter hemisphere, giving rise to a semiannual variation. Due
to the presence of the quasi-biennial oscillation the annual
cycles are significantly modified. The semi-annual variation
was quite well represented by the CIRA 1965 zonal wind model,
considering the small amount of low-latitude data then
available. Using the data from Ascension Island and other sites
up to September 1964, the semi-annual variation was estimated
to have a maximum amplitude of 30 ms^{-1} near 50 km with the
core of the summer easterlies located at 15° latitude (Reed,
1966). The levels of maximum easterlies at several low-latitude
sites have been studied by Rao and Joseph (1969) and the
structure of the semi-annual variation at different longitudes
has been investigated by Quiroz and Miller (1967).

There is a seasonal asymmetry between the Northern
and the Southern Hemispheres. The easterlies from the Southern
Hemisphere penetrate further into the Northern Hemisphere
than do the Northern Hemisphere easterlies into the Southern
Hemisphere. The Southern Hemisphere westerlies extend further
towards the equator than the Northern Hemisphere westerlies
as part of the same asymmetry. Although data are lacking
at mid and high latitude in the Southern Hemisphere, both

winter and summer regimes in the Southern Hemisphere appear
to be more intense or more extensive in latitude than their
Northern Hemisphere counterparts. A hemispheric asymmetry
also appears in temperature data at maximum balloon altitudes.
Differences of up to $15^{O}K$ have been reported for the same
season in opposite hemispheres but annual means differ by only
2 to $3^{O}K$ between the two hemispheres for the same latitude
(Smith, McMurray and Crutcher, 1961). Southern Hemisphere
data are still two few for separate consideration of the two
hemispheres over a wide range of latitude.

Chemical trail releases and ground-based techniques
have now provided new data for higher altitudes. In 1964,
zonal wind patterns for January and July were extended to
120 km for latitudes up to $75^{O}N$ using Adelaide radio-meteor
results and chemical release data from Wallops Island, Eglin
AFB and Woomera, Australia (Kantor and Cole, 1964). In 1969
the model was updated at low latitudes on the basis of the
wind results from the Barbados gun-launched probes (Murphy,1969).
Although equatorial winds appear to be from the east at
heights of 95 $\pm$ 15 km throughout the year, a slight shifting
of the wind belt north and south of the equator results in a
seasonal reversal being observed at the Barbados latitude
(Groves, 1969).

Murgatroyd (1965) has developed mean latitudinal cross sections of zonal winds for both the equinoxes and solstices using data obtained by the radio-meteor and E-layer drift techniques. In summer the easterlies changed to westerlies in the E-layer, and above 120 km a return to easterlies was thought to be indicated by sodium trail data. This description agrees with the July profile, but in winter the westerlies were taken to extend to only 100-110 km before reversing to easterlies, whereas the January profile shows them extending to 120 km.

The analysis of the meridional circulation in the stratosphere and the mesosphere is rather more difficult than zonal circulation on account of the smaller flow velocities involved. In the upper mesosphere, however, meridional components are often observed which equal or exceed zonal components. Tidal components contribute significantly at these heights to both zonal and meridional components but even when these have been extracted as with the radar-meteor technique, prevailing meridional velocities of the order of tens of ms^{-1} remain. A prominent feature of the meridional components is the flow from the summer hemisphere to the winter hemisphere at 85 to 105 km, the heights accessible for observation by the radar-meteor technique. Observations are, however, needed at other longitudes to obtain the zonally

averaged meridional flow.

1.3.7   Quasi-biennial oscillation

Superimposed on the annual cycle of winds described above, there is in the equatorial stratosphere, a quasi-biennial oscillation (QBO) of period nearly 26 months. This is associated with oscillations of a similar period in temperature and ozone (Ebdon, 1960), (Ramanathan, 1963) and (Staley, 1963). The quasi-biennial wind oscillation has its maximum amplitude near the equator where it is far more prominent than the annual oscillation. With increasing latitude, the amplitude decreases, becoming small near the 30° latitude circle. In the vertical, there is a rapid increase in amplitude from near zero values close to the tropopause, to a maximum at about 25 km. Further upwards, the amplitude decreases slowly with height to about half the maximum value at 50 km. The QBO is characterised by a downward propagation of phase at the rate of approximately 1 km per month. The variation of amplitude or phase with longitude is not significant.

Long period variations in the zonal wind have recently been studied on global basis using 1950-64 balloon data from 200 stations (Dartt and Belmont, 1970). The primary variation is the QBO of the equatorial stratosphere and its extension to higher latitudes. The first observations of the QBO above

30 km were obtained from rocket soundings at Ascension Island,
8°S between October 1962 and October 1964 as discussed by
Reed (1965).The zonal wind oscillation was found to decrease
in amplitude with increasing altitude above the 25 km level
and to propagate downwards in phase at a rate of 2 km per
month. Angell and Korshover (1965) showed that at temperate
latitudes the amplitudes increased with height so that above
55 km the QBO zonal wind oscillation was larger than at tropical
latitudes and the downwards propagation of phase was faster
than at low latitudes, being 5 or more km per month. A review
of the QBO has been given by Rahmatullah (1968).

The QBO in wind is accompanied by a corresponding
temperature oscillation, the latter being relatively more
difficult to trace. At 80 mb level the temperature amplitu'e
is 3 to 4°C and this decreases upwards to about 2°C at 30 mb.
The temperature oscillation goes through a minimum at about
17°N. At 30°N, the phase change from equator is π radians,
the amplitude attaining a secondary maximum of only about
1°C. Further north the amplitude decreases becoming insignificant
near 40-50°N. Geostrophic equilibrium is obtained within
this oscillation in the low latitude stratosphere and the
temperature and wind oscillations are found to obey well the
thermal wind relationship.

Ramanathan (1963) has observed a two year ozone periodicity : a year of high ozone in high latitudes occurring when there is low ozone in **low** latitudes. Rising and sinking motions of a cellular type in the meridional plane are suggested to explain the ozone variation. This agrees with a similar suggestion by Reed (1964) to explain the temperature QBO. Sparrow and Unthank (1964) found that the periods of westerly winds at Christchurch, New Zealand coincide with minimum ozone amounts at Aspendale and Brisbane in Australia. The downward progress of the temperature wave with time has led Angell and Korshover (1962) to infer that the likely cause is small scale eddy heat flux. Tucker (1965) has found a sinusoidal oscillation in the eddy flux gradient which is consistent with the QBO in wind. Difference between the tropical and temperate parts of the oscillation have also been reported for the Southern Hemisphere from an analysis of 1958-66 balloon data over Australia (Tucker and Hopwood, 1968). The maximum amplitude which occurs at about 25 km in the tropics was not found in the southern latitudes below 30.5 km, the effective altitude limit of observations. The presence of a QBO in other atmospheric parameters at low latitudes is not so apparent as in the zonal wind.

1.3.8 Stratospheric warmings

As was first observed by Scherhag (1960) and later by others (Sheppard, 1963), the temperature in the stratosphere rises suddenly in mid-winter, especially in the region 30-40 km where temperature may rise in a typical case from -50°C to -5°C in less than 48 hours. The warmings occur first in the vicinity of the stratopause around 48 km and appear to travel gradually down to the tropopause. The energy transformations associated with the stratospheric warmings have been discussed by Teweles (1965). The zonally available potential energy which originates primarily from latitudinal variation in solar heating and which may be expressed in terms of the mean meridional temperature gradient is converted into eddy potential energy by perturbations of wave number 2 appearing through essentially baratropic development in the strong westerlies. Eddy available potential energy may also be generated in situ by latitudinal differences in albedo and heat capacity of adjacent land and sea areas. Under conditions favourable for the formation of vortices, eddy potential energy is converted into eddy kinetic energy. While some of the eddy kinetic energy passes through a cascade process into shorter and shorter wavelengths until finally dissipated as frictional heat, a considerable fraction is converted into zonal kinetic energy. With the intense closed low centres

below the Arctic circle, the zonally averaged flow at high latitudes is easterly. The thermal winds associated with the layers where this flow increases with height require higher temperature on the side of polar darkness. Thus a portion of the zonal kinetic energy has been converted into zonal potential energy through the mechanism of eddies and an indirect meridional circulation. This potential energy is rapidly destroyed by radiative heat loss from the warm air in the polar region, with the ultimate result that the hemispheric circulation is left operating with a much lower energy than before.

A survey of Northern Hemisphere stratospheric warmings has been given by Kreister (1968). There are two general categories of warmings, 1 : mid-winter warmings, which may be divided into minor and major warmings and 2 : final warmings which may be divided into early or late final warmings. A major stratospheric warming occurred in December 1967 which was unusual in that it began one month earlier than previous early warmings (Johnson, 1969). Midwinter warmings in the Northern Hemisphere in the first quarter of 1966 have been analysed by Labitzke (1969) at the 30 km and 35 km levels where balloon observations are available at many longitudes. The mean temperature differences between these two levels for January were in very good

agreement with the CIRA 1965 differences. For February, however, when a major warming occurred, temperature differences as well as temperatures were longitudinally dependent, indicating a rapid change with height in the form of the longitudinal dependence. Such vertical structure is clearly apparent in the NIMBUS 4 observations with westward tilts of a few degrees longitude per kilometer height (Barnett et al 1971). Midwinter stratospheric warmings in the Northern Hemisphere occur locally 3 to 4 times during November to February or March. The final warming occurs in spring between mid-February to mid-April when there is rapid and large general rise in temperature throughout the depth of the stratosphere and the cold low near the poles is replaced by a warm high. It is also observed that during final warming stratospheric temperature overshoots a little before settling down to the early summer temperature value.

Longitudinal variations in density are associated with those in temperature and may significantly affect the re-entry heating and dynamics of space vehicles. For the December 1967 warming, horizontal density gradients in the Arctic regions as large as 0.04 g m^{-3} deg^{-1} latitude occurred at 40 km (typical density 3 g m^{-3}), corresponding to an increase in the normal latitude gradient by about a

factor of three. Strong winds are associated with stratospheric warmings as horizontal temperature gradients increase. The highest wind speed recorded in the stratosphere so far appears to be 198 ms^{-1} over Heiss Island on Ist February 1966 which occurred at the relatively low height of 39 km (Quiroz, 1969).

It may be mentioned that in the Southern Hemisphere only occasional midwinter warmings of the 'minor' type (tropospheric-stratospheric compensation mechanism) have been reported to take place and no major warming energetically and dynamically similar to those in the Southern Hemisphere has been satisfactorily observed (Julian, 1967). The final warming in the Antarctic stratosphere, however, is well marked. Antarctic stratospheric warmings have now also been observed by satellites IR radiometry. TIROS VII was operational for the winter 1963 and detected one midwinter minor warming and two later winter warmings at latitudes of less than 60° which moved eastwards from Australia and the South Indian Ocean (Shen, Nicholas and Belmont , 1968). The Southern Hemisphere winter of 1969 was observed by the polar-orbiting NIMBUS 3 up to the 30 mb (23km) level as discussed by Miller, Finger and Gelman (1970). A warm area developed in the Indian Ocean and moved to the South Pacific Ocean during August passing south of Australia where the decrease in westerly flow was

observed at balloon levels. This eastwards drift appears to have been shared by the temperature field over the whole South Polar region.

Some interesting explanations have been advanced to account for the stratospheric warmings. It is curious that the source level of sudden warmings (close to the stratopause) coincides with the portion of the ozone layer heated most strongly by solar radiation. Yet, the explanation perhaps favoured most is that local subsidence associated with the break-down of the winter circulation is responsible for the warmings. Willet (1968), however, basing his arguments on the outstanding differences between observed phenomena in the Arctic and Antarctic stratosphere considers the explanation in terms of latitudinal transport, vertical mixing and dynamic heating rather unsatisfactory. According to him, the marked correlation of auroral activity with Arctic and Antarctic regimes and sudden changes of stratospheric temperature and total ozone indicate a dependence on the variability of the solar wind (solar corpuscular) invasions causing and controlling. auroral, magnetic, ozonal as well as thermal phenomena.

1.3.9   Dependence on solar activity

Sprenger and Schminder (1969) have shown that the prevailing zonal wind component increased with increasing solar activity from about 15 ms^{-1} towards the east at solar

minimum to nearly 40 ms^{-1} towards the east at solar maximum indicating a possible solar-cycle dependence. Other components also appear to have been affected. Evidence of a possible solar-cycle dependence in other atmospheric parameters has also been cited. Winter temperatures at 80 km at Fort Churchill, 59°N show an average decrease of about 30°K between solar maximum and solar minimum, and summer temperatures also show a small decrease (Groves, 1968). Meteor counting rates (Lindblad, 1967) and falling-sphere densities (Lindblad, 1968) have also been analysed showing a solar-cycle effect at mesospheric heights.

An intriguing feature of the global temperature field in the meso-stratospheric region is that while at the stratopause level the atmospheric temperature falls as should be expected but at the mesopause level it is reversed with the dark winter pole being warmer than the summer pole. To explain this reversal several causes have been considered, for example : recombination of atomic oxygen brought down from higher levels (Kellog,1961), up-gradient transfer of energy by eddies (Sheppard, 1963), degradation of energy of internal gravity waves (Hines, 1963) and release of energy from auroral particles (Maeda, 1963). However, a completely satisfactory solution for this problem is yet to come.

1.4   Indo-Soviet collaboration and author's contribution

The Indian Space Research Organisation, Government of India entered into a joint agreement with the Hydrometeorological Service of the USSR for collaborative meteorological rocket soundings of the upper atmosphere from Thumba Equatorial Rocket Launching Station ($8^{\circ}32'$N, $76^{\circ}52'$E) using Soviet M-100 rockets. The Indo-Soviet collaborative meteorological programme commenced from Thumba on December 9, 1970 and is being continued with the M-100 rocket soundings weekly once on Wednesdays. The author worked at Thumba, assisted in the execution of the collaborative programme and directly participated in the collection of the M-100 rocketsonde data.

Under the joint Indo-Soviet agreement, the author participated in the Soviet Antarctic Expedition during 1971-73, circumnavigated the Antarctic continent, wintered at the South Polar Ice-cap and also took part in a 1500-km tractor-driven sledge odyssey from the coastal observatory Mirny ($66^{\circ}33'$S, $93^{\circ}01'$E) to the geomagnetic South Pole Vostok ($78^{\circ}27'$S, $106^{\circ}48'$E at 3488 m above M.S.L.) which is the world's coldest place (Caffin, 1975)[1].

In particular, the author worked at the Soviet Antarctic station Molodezhnaya ($67^\circ 40' S$, $45^\circ 51' E$) and carried out meteorological rocket soundings of the upper atmosphere over Antarctica during 1971-73. In this programme M-100 rockets were launched weekly once (**twice in the southern winter regime May to August**) from Molodezhnaya as part of the synoptic study to understand the Arctic-Antarctic circulation and the atmospheric structure in the Eastern Hemisphere. Results of the exploration of atmospheric structure over Antarctica are discussed in Chapters IV & V. A study of the equatorial atmospheric structure is made in Chapter VI and a comparison of the South Polar atmospheric structure results with those obtained at Thumba Equatorial Rocket Launching Station for the corresponding periods is given in Chapter VII. The results obtained from the Eastern Meridional Network (along $70^\circ E$) are compared with the corresponding results from the Western Meridional Network (along $70^\circ W$) in Chapter VIII. A summary of the work done and principal conclusions drawn from this investigation are given in Chapter IX.

Some of these studies have been published in the following papers :

Papers published

1. Upper mesospheric wind structure in Antartica, Nature, Vol. 252, No. 5485, pp. 683-686, December 20/27, 1974.

2. Upper atmospheric thermal structure in Antarctica, Nature, Vol. 254, No. 5499, pp. 401-404, April 3, 1975.

3. Antarctic Atmosphere : Temperature Exploration and Seasonal Variations, Journal of Geophysical Research, Vol. 81, No. 21, pp. 3715-3718, July 20, 1976.

4. Atmospheric Circulation : Exploration over Antarctica and Seasonal Variations, Geophysical Research Letters, (in press), 1976.

5. Exploration of atmospheric wind structure in Antarctica, To appear in Tellus, 1976/1977.

6. Structure of the Atmosphere over South Polar and Equatorial Regions, Journal of the Meteorological Society of Japan, Vol. 54, No. 2, pp. 105-117, April 28, 1976.

7. Atmospheric structure : Exploration over Antarctica and Equatorial Comparison , _Indian Journal of Radio and Space Physics_, Vol. 5, No. 1, pp. 66-74, March 1976.

8. Atmospheric Structure over Antarctica and equatorial India in southern summer , _Indian Journal of Meteorology, Hydrology and Geophysics_, Vol. 27, No. 3, July 1976.

9. Indian Scientist worked at Soviet Antarctic Station, _Antarctic_ , Published quarterly by the New Zealand Antarctic Society, Vol. 7, No. 7, pp. 224-225, September 1975, (Editor, J.M.Caffin).

THE M-100 METEOROLOGICAL ROCKET SOUNDING SYSTEM

The Soviet method of sounding the upper atmosphere for acquiring high altitude meteorological data incorporates M-100 rocketsonde and a suitable radiosonde which have been regularly launched since the Meteorological Rocket Network started and are being continued. The present investigation of the upper atmosphere has been made with the M-100 meteorological rocket sounding system both over Molodezhnaya ($67^{\circ}40'S$, $45^{\circ}52'E$) in Antarctica and Thumba ($8^{\circ}32'N$, $76^{\circ}52'E$) in equatorial India. The author worked at both these stations and directly participated in the collection of data. The soundings over Heiss Island ($80^{\circ}37'N$, $58^{\circ}03'E$), Volgograd ($48^{\circ}41'N$, $44^{\circ}21'E$) and mobile ships in the Indian Ocean were also carried out with the M-100 rocket system.

2.1   The 'RKZ-2' radiosonde

Each M-100 rocket flight is preceded by a radiosonde. The most commonly used radiosonde is RKZ-2 which operates at a frequency of 1780 MHz. The carrier frequency is interrupted according to the ambient temperature. The RKZ-2 radiosonde is made of two sections, the meteorological unit and the radio unit. The meteorological unit consists of a rod thermistor as temperature sensor , a

gold-beater skin as the humidity sensor, a fixed high stability resistor and a baroswitch. The radio unit consists of a measuring oscillator, modulator, transponder, radio frequency oscillator and power supply. Each of the units is discussed below :

2.1.1   Temperature sensor

The temperature sensor is a rod thermistor of negative temperature coefficient of resistance with a reflective coating to reduce undesirable effect of radiation. It is designed to measure temperature between + $50^{O}C$ and $-80^{O}C$ within a root mean square error of $0.7^{O}C$. A feature of this type of thermistor is that its mass and surface area are less compared to that in the 1680 MHz radiosondes. This configuration helps to reduce lag coefficient and increases sensitivity percentage. The thermistor is mounted on a special frame with connecting leads. One end of the frame is exposed to air, while the other end is clamped to the top of the radiosonde case. All thermistors of RKZ-2 system are calibrated individually by the manufacturer. Ground base check is carried out prior to each flight for checking the calibration of each instrument and to detect zero shift, if any, in the calibration curves.

2.1.2   Humidity sensor

A diaphragm made of organic film is employed as a humidity sensor in the RKZ-2 radiosonde. Sagging on the centre of the diaphragm depends on the relative humidity. This sagging is communicated to a sliding arm of a rheostat. The position of the pointer on the rheostat can respond to humidity variation between 15 % and 100 % with root mean square error of 7 % at positive temperatures. The humidity pick-up is connected to the radio unit by a two pin plug. This unit is securely fixed in the hole provided on the top of the radiosonde case which is protected by a visor to avoid direct exposure to any prevailing weather.

2.1.3   Baroswitch

It switches the various sensor resistors in or out of the circuit to obtain the three types of signals in a sequence. It is actuated by double aneroid cells which operate in tandem. One end is fixed and the other end is connected to the switching arm through a lever system. The contact arm slides over the commutator plate according to the changes of the atmospheric pressure. The commutator is made out of perspex and consists of alternate conducting and insulating strips. The insulating portion is of larger width than the conducting ones. This facilitates temperature sampling for a larger duration compared to the other parameters. The baroswitch

is designed to operate over a pressure range from 1060 mb to 5 mb . The pressure is computed from the height, temperature and humidity measurements.

When the contact of the baroswitch is on the reference conductor, a high stability fixed resistor is connected into the grid circuit of the measuring oscillator which generates a reference frequency lying in the range from 2070 to 2110 Hz depending upon the power supply of the radiosonde. Normally a deviation of 115 Hz from the chart value is permissible.

2.1.4   Radio unit

It contains a measuring oscillator, a modulator and 1780 MHz carrier oscillator. The measuring oscillator generates negative voltage pulses. The frequency of these pulses depends upon the value of resistance incorporated in its grid circuit. As the radiosonde sensors are connected to the same grid circuit by the baroswitch the frequency of the negative voltage pulses is naturally a function of the temperature and humidity. The modulator section of the radio unit acts as transponder necessary for the automatic tracking of the balloon or rocket by the Meteor radar. Both the modulator and oscillator are coupled to the carrier oscillator in such a manner that the oscillation of the latter are interrupted at the respective frequencies of the former. Thus the transmitted frequency has two components, radio frequency 1780 MHz and the audio frequency 0-3 KHz.

The power supply comprises of three voltages with high tension plate supply voltage as 178 to 212 V, first filament supply voltage 5.45 to 6.68 V and the second filament supply voltage equal to 2.15 to 2.65 V . This power pack is activated 30 minutes before the time of balloon release. It can give sufficient power for more than two hours. Ground checks of power supply and calibration curves are taken in each flight. A uniform shift of $\pm$ 1°C throughout the range is not taken into account for redrawing calibration curves. Humidity calibration is checked for ambient condition and the accuracy assumed is within 20 %.

An added advantage of this radiosonde is that no separate reflector target is required for range tracking as in the other radiosonde systems. Moreover, it ensures an efficient performance check for the Meteor radar prior to each M-100 rocket flight.

2.1.5   Sources of error

The major source of error in the radiosonde measurements is due to the error in elevation and azimuth when the elevation angle of the balloon is below 15°. Short term fluctuations in the rate of ascent caused by turbulence are difficult to deal with. Under such circumstances radar has the advantage that it does not depend on any assumption but measures directly the slant range of the balloon. A handicap

in the detailed measurement of the vertical wind and temperature
profiles lies in the averaging process over discrete time
intervals. When there is no reversal of wind direction at
great heights, large errors in stratospheric wind measurement
may be expected. A semi-objective method for smoothing
employed in the data processing further reduces the error.

The source of error in the small elevation angles
may be eleminated by using relay stations under the strong
jet stream conditions as done in Japan. More accuracy in the
wind measurement in the stratosphere is ensured by the use
of standard corner reflectors. Swaying motion of the
reflector may be disturbing especially when the reflected
signal is already weak due to a large range and consequently
reception may finally become impossible. In order to remedy
this limitation with a large range, the passive reflector
on the balloon may be replaced by an active transponder
which provides an accuracy in measurement of $\pm\ 0.1^{\circ}$ in angle
and $\pm\ 50$ m in range. With such a system the upper limit of
the range is about 200 km.

Another correction for the radiosonde measurements
becomes necessary when the distance between the balloon and
the station exceeds a certain threshhold value brought about
by the earth's curvature. This correction for height is

$$L^2 / 2R$$

where L is the distance and R the radius of the earth, both
in km. Corresponding to a distance of 80 km this correction
factor is about 500 m. As the balloon drift is mostly within
80 km, this correction is less than averaging height interval
of 600 m (2 minutes interval) and hence neglegible.

Finally a fairly good accuracy within a root mean
square error of about 2 ms^{-1} could be obtained in the
radiosonde wind measurements from the Meteor radar tracking.

2.2   The M-100 rocket sounding system

The M-100 rocket is a two-stage meteorological rocket
lifted by a solid propellant made of nitrocellulose base. It
can reach a maximum altitude of 100 km when launched vertically.
For meteorological experiments it is usually fired at 83°
effective elevation with a payload weighing 67 kg. The standard
M-100 rocket payload consists of four tungsten-rhenium
(40 microns) wire thermometers for measuring atmospheric
temperature in two different ranges and other supplementary
thermometers for monitoring payload housing temperature.
The payload incorporates necessary electronic devices, a
mechanical 60 channel commutator, a 22 MHz telemetery trans-
mitter, a 1780 MHz radar transponder, antenna system and
power supply sources.

An unbalanced wheat-stone bridge arrangement is used for telemetering the thermometer data to the ground. Two telemetry receivers with panoramic and photographic attachments record them along with the timing pulses (10 pps) from lift-off. The steeple portion containing the sensors opens around 60 seconds after take-off while the whole payload is separated around 70 km after 70 seconds and it attains an apogee of about 90 km at 140 seconds. At apogee, a hemispherical mylar non-reflecting parachute with 35 m^2 area exerts a stabilising influence on the payload and fully opens during descent at an altitude of 60-65 km around 200 seconds after the take-off. The Meteor radar working on 1780 MHz tracks the payload in the transponder mode and the trajectory data azimuth, elevation and slant range are photographed every second for the first 10 minutes and recorded on a paper tape for the rest of the trajectory. The rocket splash-down occurs after about 45 minutes. After the rocket launching, the data reduction, processing and analysis are carried out. The experimental detail of the M-100 rocketsonde system are described below :

2.2.1   Launching of M-100 rocket

Launching of the M-100 rocket is carried out through launcher system U-100 P . Technical characteristics of the rocket are given in Table 2.1.

At the time of launch, an electric impulse is sent through firing panel from ground power-source to the squib of the first stage pyrounit, and then the igniter fires. Powder gases and burning powder grains of igniter ignite the outer and the inner surfaces of the propellant. Rocket takes off along the launcher rails, and starts moving along the trajectory due to thrusting. After powder charge burns out, first-stage engine stops operating and for some time rocket keeps moving reducing flight speed. After 8 seconds of launching, timer mechanisms come into action and the second-stage engine gets fired. After separation the second stage moves along the trajectory due to thrusting. After powder charge burns out the second-stage engine stops operating and consequently the second stage separates. At the ascending branch of the trajectory (at an altitude of about 70 km), the head part with the instruments separates from the rocket and flies to an altitude of about 95 km. At the upper section of the trajectory a parachute exerts a stabilizing influence upon the flight of the head part. The parachute fully develops during descent at altitudes of about 60-65 km.

2.2.2   Rocket Payload

It consists of two major parts, the steeple and the instrument bay. The steeple incorporates a cone bay, a unit of transmitters and measuring equipment and protective

Table - 2.1

Technical characteristics of the 'M-100' Meteorological rocket

Rocket weight at the launch	.....	480 kg
Diameter	.....	0.250 m
Rocket total length	.....	8.240 m
First-stage engine weight	.....	290 kg
Second-stage engine weight	.....	122 kg
Head part weight	.....	66.7 kg
Weight of the first-stage propellant	.....	132.4 kg
Weight of the second-stage propellant	.....	64.7 kg
First and second stages fin span	.....	0.680 m
Temperature range of rocket firing	.....	+ 40 to -40°C
Time of stage separation	.....	8 sec
Time of jettison of steeple	.....	60 sec
Time of head part separation	.....	70 sec
Altitude of head part separation	.....	68-74 km
Maximum probing altitude with 85° effective elevation	.....	95 km

casing flaps. The steeple contains the temperature transmitters (resistance thermometers) which are set in the working position perpendicular to the steeple by springs and held in this position by the appropriate latches l. The steeple is supported in the protective casing by two pertinax forks and by two supporting rubber half-washers.

The instrument bay houses the radiotelemetering system for the temperature transmitters and also incorporates radar responder, heater supply unit, power supply unit, batteries, command unit and other accessories. Heater supply unit is used to apply voltage to the valves of radiotelemetering transmitter, radar responder, and to switching device motor of telemetering system. The power supply unit serves to apply anode voltage to the radiotelemetering transmitter. The batteries are connected in series with the anode voltage supply unit to increase the voltage applied to the anode of the radar responder. One power supply unit is used to apply voltage through the distant tubes to the separation motor squib and to the nose section (with parachute bay) and rocket propelling plant separation device. The instrument bay is closed with protective covers used for transportation purposes.

The physical values characterising the processes taking place in the upper layers of the atmosphere are

converted with the aid of the instruments (transmitters), into electrical voltage variable in amplitude. With the aid of the switching device of the telemetering system, the voltages of the instruments are applied in turn to the input of radio transmitter where these voltages are converted into radio signals modulated in frequency. The frequency-modulated radio signals are transmitted through an antenna which are then received and photographed by the ground receiving and recording equipment.

Radar measurements during movement of the nose section on the whole flight path of the meteorological rocket are carried out with the aid of the radar system incorporating the rocket-borne radar responder and a ground radar station. During the flight of the nose section, this system is used to determine the trajectory data (slant range, azimuth and elevation) which are recorded by the typing device of the Meteor radar on a paper tape.

The power supply unit provides the whole rocket-borne equipment and instruments with necessary voltages through the special power supply and control plug connector of the article. The command unit with self-contained power supply is designed for applying the signals at the given time to the protective casing squib to open and throw the steeple

protective flaps, and to the squibs of the separation unit and separation motor to separate the nose section from the rocket second stage.

2.2.3   Wind measuring sensors

Atmospheric wind measurements in the M-100 rocket system are made from the drift of the descending parachute and chaff tracked by Meteor-1 and Meteor-2 radars. The Meteor-1 radar operates in a frequency range of 1770 to 1795 MHz in the rocket-borne transponder mode. It tracks the 35 m^2 mylar parachute which fully opens around 60 km during the descent. The trajectory data elevation, azimuth and slant range from the radar yield the wind speed and direction.

Since the parachute gives the winds only from 60 km to down below, another wind sensor 'chaff' has to be used for the measurement of upper mesospheric winds. The chaff used in the M-100 rocket at Molodezhnaya, Antarctica consisted of cylindrical aluminium -coated glass fibres having a diameter of about 0.025 mm. About 400 gm of chaff, in a special container divided into two parts, was ejected at rocket apogee. The descending chaff was then tracked by high sensitivity Meteor-2 radar. At the time of ejection at rocket apogee, above 80 km, the chaff fell at a high speed about 160 ms^{-1} but as it descended further it slowed

down to about 4 ms^{-1} at around 56 km because of the greater
density and viscosity of the air at lower altitudes. The
Meteor-2 radar data on the drift of the trajectory of the
chaff were used to measure the wind speed and direction in
the mesospheric region from about 80 to 60 km. Corrections
for changes in the wind with altitude were also applied.
The accuracy in measuring the wind speed was about 6 to
10 ms^{-1}. Thus the chaff yielded the winds from about 80 to
60 km and the parachute for the lower altitudes from 60 km
to down below. Lally and Leviton (1958) have discussed errors
in wind determination due to falling objects, e.g. in the
cases when parachute and chaff are employed.

2.2.4   Temperature transmitters

The temperature transmitters are basically resistance
thermometers also known as cross thermometers, which are
designed for measuring the temperature of free atmosphere up
to about 80 km. The operating principle of the rocket-borne
thermometers is based on the relation of thin electrical wire
resistance versus the temperature, given by

$$R_t = R_0 \ (1 + \alpha t + \beta t^2 + \qquad)$$

where R_t is the electrical resistance of thermometer at
temperature $t^\circ C$ and R_0 at $0^\circ C$ while α and β are the thermal

factors of wire resistance.

The rocket-borne thermometers are made of tungsten alloy 'BP-20' wire, diameter about 40 microns ; or of the same alloy wire, diameter 35 microns ; or coated with alloy Au + 10% Pd (gold and palladium). Wound on the middle part of the temperature transmitter tube is another resistance thermometer of enamelled copper wire Taw which serves to control the temperature of the thermometer tube. The temperature sensor commonly used in the M-100 rocket is a 40 micron tungsten-rhenium wire. The measuring instruments are connected to the arms of a wheatstone bridge. The bridges of all the measuring instruments have a common DC power supply source of V_o = 3.11 volts. The temperature transmitters have two sub-ranges a and b in order to increase the accuracy of measurements. The temperature transmitters T_1, T_2, T_3 and T_4 and the reference thermometers Tab, Tag and Taw have the following sub-ranges: T_{1a} from -20 to 200°C, T_{1b} from 90 to 350°C, T_{2a} from -100 to 120°C, T_{2b} from 0 to 250°C, T_{3a} from -30 to 200°C, T_{3b} from 80 to 350°C, T_{4a} from -100 to + 100°C, T_{4b} from 0 to 250°C, Tab from 0 to 150°C, Tag from -50 to 300°C, and Taw from -50 to 100°C. The resistance of measuring thermometers T_1, T_2, T_3 and T_4 is about 225 ohms at 20°C, while that of the reference thermometers Tab, Tag, and Taw is about 152 ohms.

2.2.5   Temperature sensors calibration

The thermometer calibration consists in setting up accurate measurement of the required temperature in a special thermostat chamber with the rocket steeple placed inside. It includes accurate measurement of steeple thermometer resistance at two different temperatures, calibration of thermometer resistance bridge, and measurement of data processing to receive thermometers calibration characteristics in the whole range of the temperature measurement.

Such a calibration carried out about 5 days before the take-off considerably increases accuracy of the rocket sounding measurements. Necessary instruments and equipment for the thermometer calibration are thermostat chamber, thermostat TC-16 A, potentiometer P-30 f, standard resistance coil (100 ohms), switch distributor, platinum thermometer TC-MHI, galvanometer M-95, resistance box, power supply unit, contact thermometer TK-6 and mercury thermometer ($0-100^{o}C$) of $0.1^{o}C$ accuracy.

The rocket steeple is inserted in the thermo-isolated chamber consisting of two bays with double walls between which water is circulating. Water is pumped through the thermostat TC-16 A. A small ventilator is installed

inside the chamber to reduce temperature stabilization time.
Water temperature in the thermostat is held constant by
contact thermometer TK-6. Temperature in the thermostat TC-16 A
is measured by mercury thermometer with an accuracy of $0.1^{\circ}C$.
First calibration is carried out at room temperature about
$30^{\circ}C$. Second calibration is carried out at a temperature of
$75-80^{\circ}C$. Temperature in the chamber is recorded by a platinum
thermometer TCMH-1 with an accuracy of $0.01^{\circ}C$.

Stabilization time to reach constant water temperature
is about 5-6 hours both at room temperature and at $75-80^{\circ}C$.
Readings of the platinum thermometer are taken through
potentiometer P-37 when they are stable i.e. when the pointer
of null-galvanometer would not deflect. Difference in the
readings of the thermostat mercury thermometer and the
chamber platinumthermometer at room temperature (about $30^{\circ}C$)
in stable state is of the order of 0.1 to $0.2^{\circ}C$ and at higher
temperature ($75-80^{\circ}C$) is 0.5 to $0.7^{\circ}C$. D.C.Potentiometer P-37
with micro-ammeter M-95 as a null-galvanometer is used for
thermometers resistance measurements. The voltage drop across
the standard resistance coil (100 ohms) and across the
steeple thermometer is taken in turn by the potentiometer.
To reduce thermometer filaments foul heating effect,ballast
resistance of 1500 ohms (resistance box MCP-63) is placed
in series with the measuring circuits. At each of the two

temperature calibrations a series of 3 measurements is taken, and average temperature value obtained by platinum thermometer and by each payload thermometer is calculated.

Thermometer resistance is calculated from the formula

$$R_t = \frac{U_t}{U_{st}} R_{st}$$

where R_t is the thermometer resistance, U_t the voltage drop across the thermometer filament, Ust the voltage drop against the standard resistance coil and Rst is the resistance of the standard coil (100 ohms). Resistance of the leads from the platinum thermometer to potentiometer and from payload thermometers to potentiometer is measured beforehand by the measuring bridge and is taken into account in the processing of the data. The calibration of the temperature measuring sensors consists in determining the parameters α and R_o from the equation:

$$R_t = R_o (1 + \alpha t + \beta t^2)$$

where R_t is the thermometer resistance at a temperature of $t^o C$, R_o the thermometer resistance at $0^o C$, α the first temperature coefficient and β is the second temperature coefficient. While β is taken as the value supplied by the maker, the value of α is calculated for each payload. This is done by measuring the R_t values at two known calibration temperatures t_1 ($30^o C$) and t_2 ($80^o C$) with R_1 and R_2 as the

corresponding resistances using the formula –

$$\alpha = \frac{(R_2-R_1) + \beta(R_2 t_1^2 - R_1 t_2^2)}{(R_1 t_2 - R_2 t_1)}$$

After having calculated the values of α and R_o as described above, the temperature t for certain values of thermometer resistance over the range 180 to 340 ohms is determined at intervals of 20 ohms. It is done by using the standard resistance thermometer equation. The exact value of the two calibration temperatures t_1 and t_2 are determined from the standard tables of calibration temperatures versus thermometer resistance.

After the calibration of the temperature sensors the rocket-borne bridge circuits are calibrated. For the same values of thermometer resistance from 180 to 340 ohms as described earlier, the rocket-borne bridge circuit output voltages for all the four thermometers are measured. For this purpose a special test bench K11M with potentiometer P-37 is used. A standard resistance box is connected in the bridge circuit instead of steeple thermometers. Measurements of the output voltage as a function of box resistance are then taken in succession for each subrange of each thermo-meter. Using the values of these output voltages and the thermometer filament temperatures already calculated, the manufacturer's calibration curves for the resistance thermo-meters are redrawn and thus corrected.

2.2.6 The M-100 radiotelemetry system

The multi-channel radiotelemetering system is designed
to transmit information about variations of transmitters
voltages from the meteorological rocket to the ground and
to receive and record this information. The radiotelemetering
system is based on the principle of alternate transmission of
data with mechanical switching of the channels. The carrier
frequency of the transmitter is frequency-modulated. The
system equipment is divided into the ground and the rocket-
borne equipment. The system ground equipment is designed to
convert the output voltages of transmitter carrier frequency
and to transmit this frequency to the ground receiving station.
The system has got 60 channels, 5 of which are allotted for
transmitting five reference levels. The rocket-borne equipment
incorporates the switching device, transmitter, antenna and
electric power supply sources. The radio transmitter consists
of a reactance valve, self-oscillator, frequency doubler and
power amplifier. Technical characteristics of the Radio
Telemetery in the M-100 rocket system are given in Table 2.2.

The ground equipment of the radiotelemetering system
is designed to receive and record the signals of the rocket-
borne transmitter. The ground equipment incorporates an
antenna, a radio transmitter, a panoramic attachment and a
photorecorder with timing system unit and the measurements

Table - 2.2

Technical characteristics of Radio Telemetry in the 'M-100' rocket system

(A) Radio Receiver

Type	: FM/AM super heterodyne
Frequency range	: 1 to 25 MHz in 6 bands
First oscillator	: Continuously tunable
I.F.Band width	: 300 Hz to 5 KHz (adjustable)
Sensitivity	: 1.5 to 2.0 micro volts
Operating range	: 100 km

(B) Radio Transmitter

Transmitter frequency	: 22150 KHz $\pm$ 100 KHz
Type of modulation	: Frequency modulation
Input resistance	: 20 ohms
Power output	: 1.8 W
Continuous operation	: 2 hours for normal power supply
No.of transmitting channels:	: 60 including 5 reference channels
Switching time for channels(one cycle)	: 5 sec

(C) Panoramic Adapter

Type	: P 317
Observational Band	: 100 KHz,10 KHz and 2.5 KHz in all the receiver bands.
Sensitivity	: 2 micro volts with signal to noise ratio 3:1
Frequency scale RMS error	: 3.5 KHz in 100 KHz band,0.7 KHz in 10 KHz and 150 Hz in 2.5 KHz band

(D) Antenna

Type	: Full wave,non-symmetral length
Position	: Fixed
Beam width	: 50°
Polarisation	: Linear

(E) Recorder

Type	: KH3
Speed	: Low
Type of film	: 35 mm
Sensitivity	: 20 DIN/180 ASA
Film conumption	: 1 cm sec^{-1}

are recorded by photographing the image on the screen of
a cathode ray tube **in the telemetry**. The radio communication
line of the system is designed for operation within the range
of 22150 ± 100 K Hz. Deviation of the radio transmitter
carrier frequency does not exceed ± 50 KHz, provided ± 100 mV
are applied to the transmitter input. The input resistance of
radio transmitter equals 20 K ohms. Power of the radio
transmitter is not less than 18 W. Operating range of the
radiotelemetering system is not less than 100 km.

The rocket-borne equipment of radiotelemetering
system incorporates a switching device (PTS switch board) and
a radio transmitting device. The switching device is used to
periodically connect the transmitters to supply their voltages
under measurements to the rocket-borne radiotelemetering
transmitter. The switching device provides alternative
connection of sixty channels to which the voltage under
measurements are applied. It also provides switching of slowly
variable potentials applied from the transmitters and changed
within the limits of -100 mV to + 100 mV. Provision is made
in the device to connect five voltage-calibrating levels - 100 mV,
-50 mV, 0, + 50 mV and + 100 mV to the five channels. The
time required for interrogating the sixty channels of the
switching device equals 5 seconds. The switching device
motor is supplied with electrical power from 23 ± 1 V DC

source. The current consumed by the motor equals 5 ma. The
bridges of transmitters and the calibrating level dividers
are fed from 3.11 - 3.12 V DC source.

The radio-transmitting device consists of a control
stage with reactance valve, sine-voltage oscillator and
frequency doubler and a power amplifier. The master oscillator
(sine-voltage oscillator) produces the high frequency
oscillations. The frequency doubler is used to obtain the
radiated frequency. The sine voltage from the doubler is
applied to the input of the power amplifier. The antenna is
essentially a half-wave vibrator with the input resistance
of 75 ohms. The receiving antenna of the ground radio-
telemetering system provides reception of the signals of the
rocket-borne radio-transmitter within the range of 3-25 MHz.
In order to facilitate processing the film, increase the
processing accuracy and to decrease the amount of the film
consumed for recording, provision is made for the brightness
indication of the signals.

2.2.7   The M-100 radar system

The radar system is used to take distant measurements
during the flight of the meteorological rocket i.e. to
determine the slant range, azimuth and angle of elevation
of the rocket nose section. The radar data is then used to

determine the wind velocity and direction. The system consists
of the ground Meteor radar and rocket-borne radar responder.

The Meteor radar . used in the M-100 rocket
has the   technical characteristics as given in Table 2.3.
The radar operates within the frequency range from 1770 to
1795 MHz and it incorporates the transmitter, receiver, antenna,
feeder system, indicator and the units providing the automatic
range and elevation tracking and the co-ordinates recording.
The transmitting device generates the electro-magnetic power
of high frequency and radiates it by a narrow beam
(interrogation pulse) through the antenna. The interrogation
pulse actuates the responder installed in the rocket nose
section. The responder transmits a response signal which is
received by the radar antenna and applied to the range
indicator through the receiver. The slant range is determined
by the delay time of the rocket-transmitted response signal
relative to the radar interrogation pulse. The angular
co-ordinates are determined by the method of the equisignal
zone (equisignal direction).

It incorporates a super high frequency (SHF)
oscillator and a modulator which are housed in the
M-100 rocket pay-load . The SHF oscillator radiates radio
signals at the frequency of the ground radar station
(1770-1795 MHz), receives the interrogation pulses of the

ground radar station, changes the nature of radiated
oscillations and produces response radio signals which make
it possible to determine the slant range. The modulator
produces the auxiliary sine oscillations of about 800 KHz
to ensure operation of the SHF oscillator in super-
regenerative mode. As a result of this, the SHF oscillator
becomes sensitive to the interrogation pulses radiated by the
ground radar station. During modulation, the SHF oscillator
radiates intermittent oscillations with a frequency of
800 KHz. The responder antenna radiates electro-magnetic
energy of the SHF oscillator in the space. At the same time
the responder antenna serves as a receiving antenna which
receives the interrogation pulse radio signals of the ground
radar station.

2.2.8   The M-100 power supply unit

The power supply of the M-100 rocket sounding
system units are designed to apply the required voltages
to the nose section equipment. The power supply units provide
the following voltages :

3.11   V for the electrical measuring circuit ,

23   V for the PTS switching device motor ,

6.1-6.0V for heating the PTS transmitter and radar responder,

132-120V to feed anodes of the PTS transmitter valves, and

Table - 2.3

Technical characteristics of the Meteor radar in the M-100 rocket system

Wave band of the station	:	1770-1795 MHz
Main pulse repetition frequency	:	833 pulses sec^{-1}
Transmitter peak output	:	200 KW
Pulse duration of the transmitter	:	0.8 micro second
Sensitivity of the receiving system	:	6.5×10^{-13} W
Parabolioid diameter	:	1.83 m
Width of half-amplitude beam	:	6.5 ± 1°
Range of automatic tracking with recording	:	150 km
Operating range in azimuth	:	Unlimited
Operating range in elevation	:	0.50-15.0 mils (1 mil $= 0.06^{o}$)
Mean error in determining range	:	25 m
Mean error in determining azimuth and elevation		0.02 mils
Supply voltage	:	220 V at 400 Hz
Power consumption	:	13.5 KW
Time of deployment	:	20 minutes
Rate of recording of meteorological data	:	5 sec
Rate of recording of spherical co-ordinates and time	:	30 sec
Accuracy in angular co-ordinates measurement		1 mil
Accuracy in range measurement	:	10 m
Accuracy in frequency measurement	:	1 Hz

270-250 V to feed anodes of the radar responder valves. The power supply units provide proper operation of the equipment for 1.5 hours. The system incorporates one storage battery unit, two anode batteries and four additional batteries. The power supply unit is housed in the rocket payload.

The anodes of the radio-telemetering transmitter valves are supplied with current from the dry anode batteries. The anodes of the radar responder valves are supplied from the anode battery of the PTS transmitter to which two twined dry batteries are connected in series with the anode in the form of a self contained box to ensure convenient arrangements. The storage battery unit apply supply-voltages to the electrical measuring circuit, switching device motor, and to the heater valves of the PTS transmitter and radar responder. To obtain the other voltages, use is made of the silver zinc storage battery assembled in the respective supply groups.

2.2.9   General remarks

The M-100 rocket sounding system was designed and developed by the USSR before the commencement of the International Geophysical Year and has been extensively used for meteorological exploration of the upper atmosphere from various stations e.g. Heiss Island ($80^{o}37'N$, $58^{o}03'E$)

and Volgograd (48°41'N, 44°21'E). The M-100 soundings from
Thumba started on December 9, 1970 and are being continued
weekly once on Wednesdays. In the middle of 1969, regular
stratospheric and mesospheric sounding by the M-100 rockets
was started at the Antarctic Station Molodezhnaya (67°41'S,
45°51'E) and the results of these soundings were presented
by Koshelkov (1972).Under a joint Indo-Soviet agreement the
author participated in the Soviet Antarctic Expedition
during 1971-73 and carried out the upper atmospheric soundings.
The experience has shown that the M-100 rocket sounding system
is quite efficient and satisfactory for probing the upper
atmosphere below 100 km.

C H A P T E R - III

M-100 ROCKETSONDE DATA REDUCTION AND PROCESSING

During the M-100 meteorological rocket flight time
the atmospheric parameters are registered by the instruments
carried by the rocket. The air temperature and pressure are
calculated with the help of equations interconnecting the
parameters of the thermometers and the characteristics of
the free atmosphere. In computation, an allowance is made
for such factors as the low-density flow, the inertial
characteristics of the instruments, the interaction with the
solar radiation and others that exert influence upon the
measuring instruments. The preliminary processing of the
data collected from the meteorological radiosonde and M-100
rocketsonde are first done manually, while the final data
reduction and processing are carried out with the Minsk-2
or IBM-360 computers using standard programmes.

3.1   Radiosonde data reduction

The radiosonde data is important because it is used
in the processing of the M-100 rocketsonde data. The monthly
average radiosonde apogees at Molodezhnaya from January to
December in 1972 were 32.4, 30.4, 28.5, 37.2, 33.5, 32.0,
34.7, 37.1, 38.7, 39.7, 35.6 and 29.2 km, respectively.

Meteorological data was obtained from the radiosonde flight records and the Meteor radar. Temperature and relative humidity values at 2 minutes interval and at any other significant levels, for example isotherm or inversion not covered by the values at 2 minutes interval, were determined by standard temperature and humidity evaluators applying the necessary zero correction from the ground base checks. Pressure computation was carried out by a standard computer programme incorporating height, temperature, humidity and surface pressure values. The accuracy in wind measurement was about 3 ms^{-1} while the root mean square error in temperature measurement ranged from 2 to 4°C.

3.2   Meteor radar data reduction

The Meteor radar used for automatic tracking of the balloon with radiosonde and the M-100 rocket in transponder mode is L-band radar (1770-1795 MHz) with a peak power of 200 W . The Meteor-1 radar tracks the descending parachute while the Meteor-2 radar which has a higher sensitivity tracks the descending chaff made of aluminium-coated glass fibres. For the first 10 minutes of rocket flight the parachute trajectory data are recorded on a photographic film with a camera fitted in the Meteor-1 radar system. Splash-down of the payload occurs after 45-50 minutes from the take-off. The parachute and the chaff trajectory data
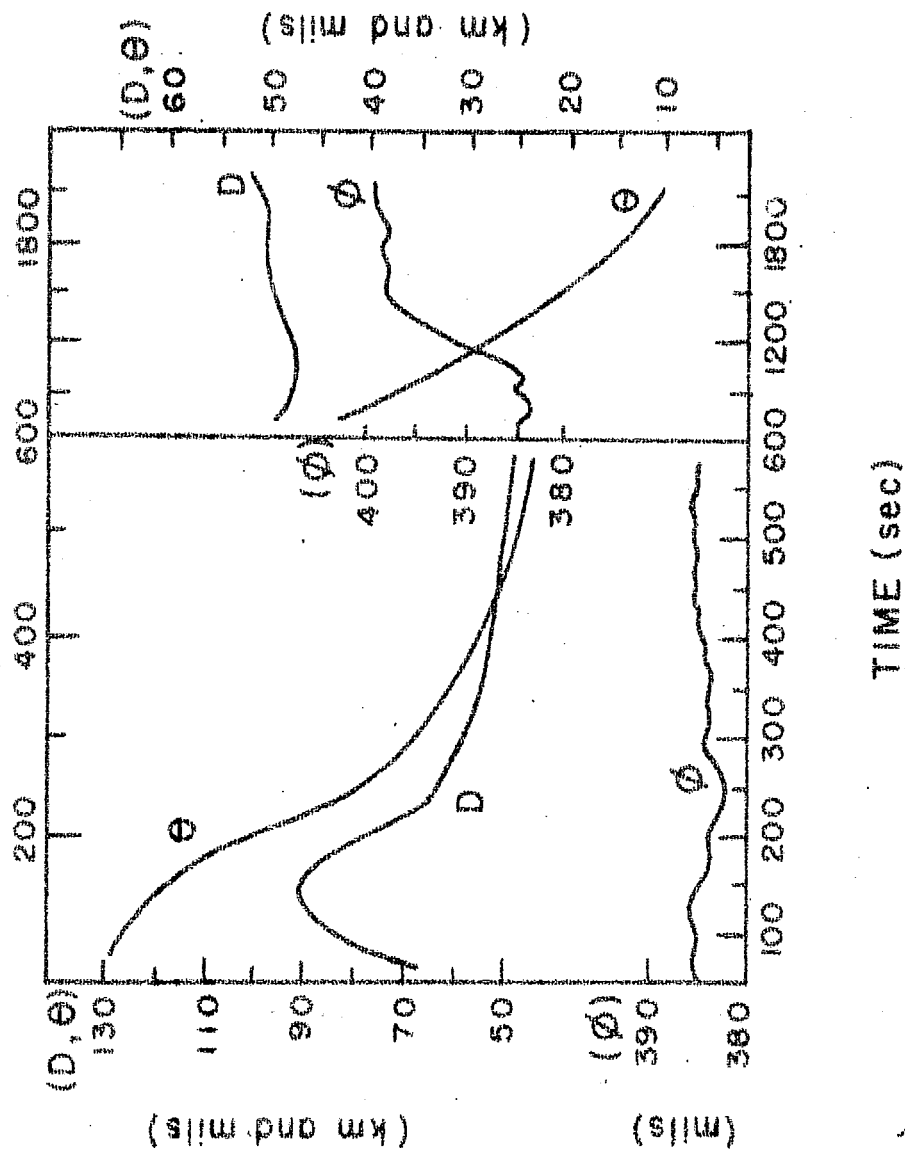
Smoothed Meteor radar data: elevation (θ) and azimuth (ø) in mils, and slant range (D) in km from a typical M-100 rocket sounding.

(Fig. 3.1)

(elevation, azimuth and slant range) are recorded by the Meteor-1 and Meteor-2 radars on a paper tape at an interval of 5 seconds.

The Meteor-1 radar data on the drift of the parachute trajectory recorded on the photographic film is projected on an illuminated microscope and the corresponding elevation (mils), azimuth (mils) and slant range (tens of metres) readings are tabulated at every 5 seconds interval starting from 70 seconds to 600 seconds. From the paper tape print output, readings are taken at 30 seconds interval till elevation falls below 100 mils (6 degrees). These readings are plotted against time and smoothed as shown in Fig. 3.1. Whenever radar tracking is not good, smoothed readings are taken from the graph accurate to 0.01 km for slant range and one mil each for elevation and azimuth. The Meteor-2 radar records the chaff trajectory data (elevation and azimuth in degrees and slant range in tens of metres) on a paper tape with two values for each 5-second interval corresponding to two most active centres of the descending chaff cloud. This data is likewise plotted against time and smoothed. The smoothed values of the tracked data (elevation, azimuth and slant range) taken from the graphs are then used for computing the rocket trajectory, co-ordinates and the wind speed and direction. The computer print out results are
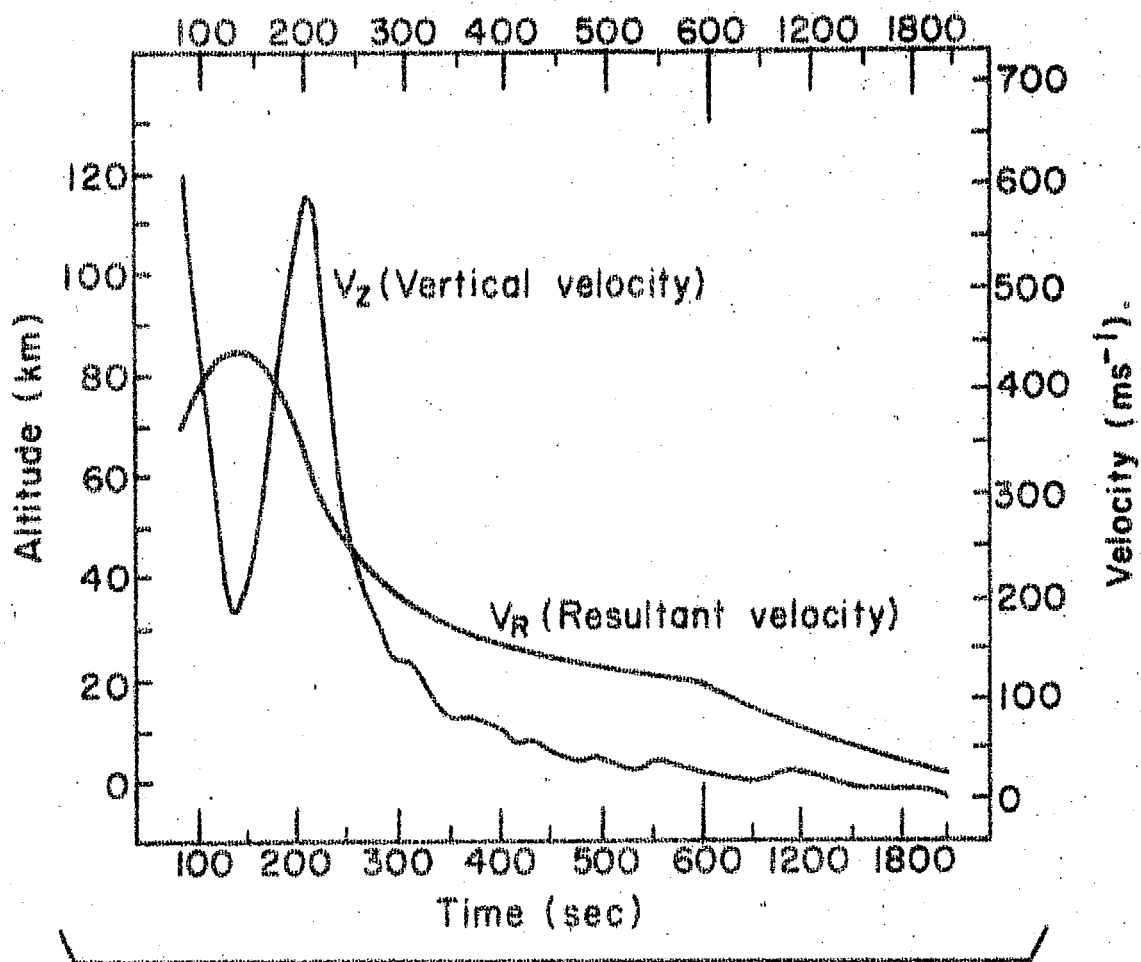
Time-height & velocity-height curve for a typical M-100 rocket sounding.

(Fig. 3·2)

plotted for further analysis and checking in respect of velocity and altitude. Typical M-100 rocket flight results presenting time-height and velocity-height curves are shown in Fig. 3.2. Various formulae used in these computations are discussed separately.

3.3   Telemetry data reduction

All signals of the telemetering system that characterise the readings of the rocket transmitters are recorded on a photographic film. Each signal is registered on the film as three points that are plotted close to one another. These points are usually well distinguished from uninterrupted or chaotically scattered signals caused by continuously acting or short time interference. The vertical displacement of a signal from the zero line on the photographic film varies proportionally to the voltage supplied from the transmitter to the sender output and depends upon the value of a parameter to be measured. The initial processing of the telemetered data includes a deciphering of the signals on the film in certain time intervals and their conversion into the values of temperature and pressure with the help of graduated graphs.

3.3.1   Timing the film

The telemetry film is developed after the rocket launching is successfully carried out and then dried. It is timed automatically with a timer from the take-off to splashdown at one second interval. However, it is important to check it and make an appropriate correction if found necessary. The film is timed from the moment of the rocket launching determined on it by the point where a continuous straight line on the perforation ends. This line on the film is exposed by a lamp of the timing system during the pre-launching drawing of the film. The signals are usually disturbed at the moment of launching. Each one second interval is a shorter exposed line on the perforation plus a gap between this line and the adjacent one. When determining the moment of launching, it may be borne in mind that the first gap between the continuous exposed line and the shorter exposed line that follows can be very small or even almost unnoticeable. It is convenient from the practical point of view to fix the time of the first longer exposed line and to compose a time table of similar exposed lines that follows after each complete cycle of 60 seconds.

3.3.2   Deciphering the signals

The signals are deciphered by means of a decoder as in Table 3.1, which makes possible projecting the

enlarged signals from the telemetering film to a special
screen of the decoder. The voltage obtained during operation
of the transmitters can be taken from the film with the use
of numbered scales of movable board secured on the screen of
the decoder. The timed film is inserted into the decoder so
that the emulsion faces the mirror. The positive signals in
this case are projected on the upper portion of the screen.
The acting code table of the signal transmission within every
cycle is given in Table 3.1. In the Table, B1 and B2 are
the readings of the pirani-hot wire manometers which are
now obsolete, while T1, T2, T3, & T4 are the tungsten-rhenium
wire thermometer readings in the two subranges a and b. Tab,
Taw and Tag are the temperature values of reference
thermometers in the piranic manometer, resistance thermometers
and the membrane pressure transmitters respectively, while
Al and A2 are the ranges of the pressure transmitters.

For deciphering, the zero pilot signals on the
telemetry film are brought to the vertical reference line on
the screen of the decoder . By moving the decoder board or
mirror the signals are set at the board scale readings
obtained for them during the reference deciphering before
the rocket launching. It is an important precaution to see
that the zero pilot signals are not displaced from the
scale reference values. The first pilot signal

Table - 3.1

Telemetry signal deciphering code

No.	Signal	No.	Signal	No.	Signal	No.	Signal
1	K_1	16	B_{1a}	31	T_{1a}	46	B_{2a}
2	K_2	17	T_{3b}	32	T_{2a}	47	B_{2b}
3	O	18	T_{3a}	33	T_{3a}	48	A_1
4	K_3	19	B_{1b}	34	T_{4a}	49	A_2
5	K_4	20	O	35	O	50	O
6	B_{1a}	21	T_{1b}	36	B_{1a}	51	T_{1b}
7	B_{1b}	22	T_{2b}	37	B_{1b}	52	T_{2b}
8	B_{2a}	23	T_{3b}	38	B_{1a}	53	T_{3b}
9	B_{2b}	24	T_{4b}	39	B_{1b}	54	T_{4a}
10	O	25	O	40	O	55	O
11	T_{1a}	26	T_{1a}	41	A_1	56	T_{1a}
12	T_{2a}	27	T_{1b}	42	T_{ab}	57	T_{2a}
13	T_{3a}	28	T_{2a}	43	T_{aw}	58	B_{1a}
14	T_{4a}	29	T_{2b}	44	T_{ag}	59	B_{1b}
15	O	30	O	45	O	60	O

(of an order of -100 ± 2 mV) is then brought to the vertical reference line and the lower half of the board is shifted horizontally so that it is against the board scale reading corresponding to the value of this pilot signal (e.g.-98 mV). Repeat this procedure for the second pilot signal (e.g.-48 mV). The upper half of the board scale is also similarly set with reference to the third and fourth pilot signals. The upper and the lower halves of the board scale are checked for correct position before the deciphering of every cycle of signals and adjusted, if necessary. All signals of the cycle are successively brought to the vertical reference line and their values determined in milli-volts with the help of a scale formed on the board by inclined lines.

The standard code in the Table 3.1 makes it possible to distribute all signals among the transmitters. In case zero pilot signals in a cycle follow irregularly (travel), the board zero is set in relation to the travelling zeroes. The values of all signals (in milli volts) are recorded in the log containing the code Table. The time values (in seconds) are also recorded adjacent to the respective nearest signals as soon as the time marks approach the vertical reference line. Deciphering of the telemetry film is carried out for all the cycles one by one beginning from the 70th second up to the 300th second,

every second cycle beginning from the 300th second to the 600th second, every third cycle starting from the 600th second to the 1000th second and every tenth cycle (i.e.a cycle every 50 seconds because one cycle completes in 5 seconds) beginning from the 1000th second up to the end of the film. In case the film has many marks caused by interference which makes the decoding difficult and doubtful, all the decodeable signals for the first ten minutes are deciphered.

3.3.3   Converting the telemetered signals into atmospheric parameters

The voltages (mV) taken from the film are converted in to the values of temperature (for the thermometers) and the values of pressure in mm Hg (for the membrane pressure transmitters) with the help of graduated curves. For this purpose either the graduated curves obtained a few days before the rocket launching are used or the Manufacturer's curves corrected according to the data of the reference deciphering with the aid of D.C.potentiometers are taken.

3.3.3.1   Correcting the graduated curves

The graduated curves are corrected by plotting a point for every thermometer on the respective graph and drawing a new curve parallel to the Manufacturer's curves through this point. The position of this point is

determined by the average voltage (mV) for a given thermo-
meter obtained during the reference deciphering and by the
air temperature for this particular case. The Manufacturer's
curves are thus corrected with the calibration data. Correction
is not necessary if the graduated curve in the case of plotted
point is at a distance of less than 1 mV from the
Manufacturer's graduated curve.

3.3.3.2 Plotting graduated bar graph

For plotting graduated bar graph elevan lines are
drawn one under another at every 5 mm on a piece of graph
paper (70 x 10 cm). Eight lines are intended for four
thermometers (atmospheric temperature transmitters) within
the ranges a and b, two lines are used for pressure
transmitters A_1 and A_2 and one line is meant for the thermo-
meter T_{aw}. A temperature scale is plotted along the paper
to the scale of the graduated graphs (1 cm = $10^{o}C$) and the
values of the lower temperature are marked from the left.
The bar graph and the graduated curve for the given thermo-
meter are placed together such that the temperature scales
of both are matched. The voltages at every 5 mV are
converted into the temperature values with the help of the
corrected graduated curves and the values marked on the
temperature scale of the graduated bar graph.

The same procedure is repeated for the other thermometers also and the ranges a & b are marked with the pencils of different colours. Similarly the voltages (every 5 mV) from the pressure transmitters A_1 and A_2 are converted into the corresponding pressure values (mm Hg) and noted on the bar graph to a scale of 1 cm = 10 mm Hg. It is important that the zero points of the pressure scale and the temperature scale coincide.

3.3.3.3   Voltages conversion and plotting with typewriter

The conversion of the voltages (mV) into the values of temperature (degrees) or pressure (mm Hg) and the plotting of graphs showing the dependence of these parameters upon the time from the moment of the rocket launching is done simultaneously with the aid of a special typewriter provided with a plate to secure the graduated bar graph and a transparent rule with a central vertical line on its movable carriage used for plotting |.   The keys of the typewriter are designated with the thermometers (T_1, T_2, T_3, T_4, T_{aw}), ranges (A_1, A_2) and the pirani hot-wire manometers (B_1, B_2). The graph taken for plotting is about 45 cm wide and 3 m long. Time scale is taken from top to bottom along the Y-axis of the graph paper to a scale of 1 cm = 2 sec beginning from 50th second to 300th second, 1 cm = 10 sec from 300th second to 1000th second and 1 cm = 20 sec from

1000th second onwards. The temperature scale (1 cm = 10^0), pressure scale for the membrane transmitters within the range of A_1 and A_2 (1 cm = 10 mm Hg) and the scale of pressure logarithms for the pirani manometers (1 cm = 0.1) are taken across the graph paper along the X-axis. The zeros of the three scales should coincide and be about 15-20 cm from the right-hand edge of the graph. The temperature scale is graduated both in ^0C and ^0K.

The graduated bar graph is fixed on the typewriter plate used in plotting so that during printing the marks are precisely at the zero of the temperature scale when the central vertical line of the rule on the movable carriage is brought to the zero of the temperature scale on the bar graph. A group of three persons is usually engaged in decoding the data on the telemetering film and plotting them on the graph paper. One person in this case decodes the film and dictates the obtained values to the second person who records them in the log, while the third person plots the data on the graph with the aid of the typewriter. This procedure is considered quite favourable and efficient. All the plotted data of the thermometers T_1, T_2, T_3 and T_4 is then used to draw an average curve of the thermometer wire temperature (T_w) and the steeple temperature (T_{aw}) as a function of time. It is a good practice to use a

Temperature (°K)

273   373   473   573

STEEPLE
TEMPERATURE

WIRE
TEPERATURE

Time (sec)

140
150
160
170
180
190
200
210
220
230
240
250

Time (sec)

140
150
160
170
180
190
200
210
220
230
240
250

0   100   200   300
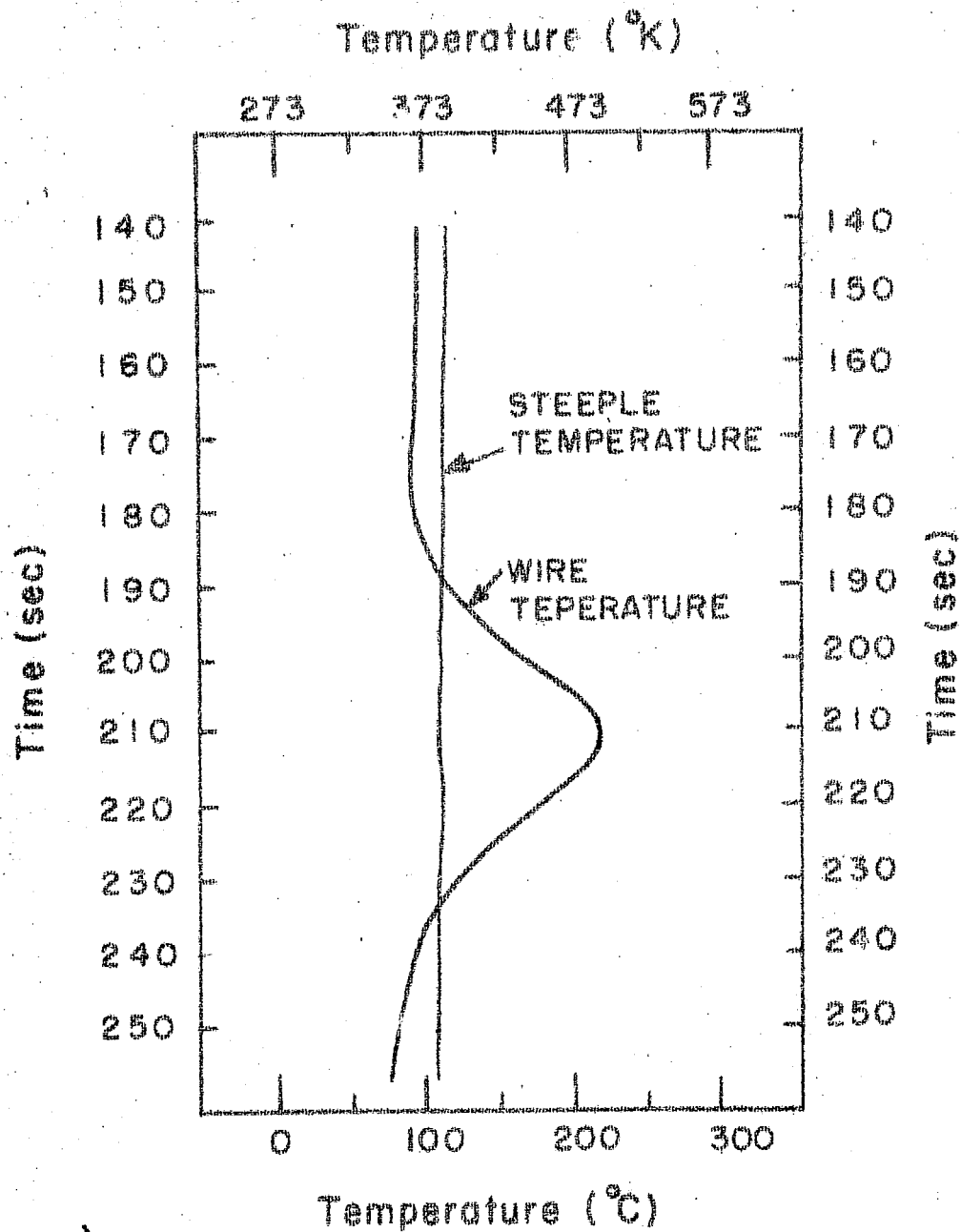
Temperature (°C)

Average temperature curve of the decoded
telemetry data from a typical M-100 rocket
sounding.   (Fig 3·3)

transparent rule or a templet for plotting these curves.
An average and smoothed temperature curve plotted with the
typewriter is shown in Fig.3.**3.**

3.4   Computer processing of the data

        Manually reduced and smoothed data from the radar
tracking and telemetry are taken at 5 seconds interval,
tabulated, punched on a tape and fed to Minsk-2/IBM-360
computer along with the standard M-100 computer programme for
final data processing. The computer programme permits the
preparation of original data for processing, processing of
radar data, correction of original data to standard altitude
and restoration of the results of tracking, processing of
telemetery data and storage and formulation of the results.
Verification of the input data, identification of correction
in case of detection of errors, searching for anomalous points
and their elemination and smoothing of the original data are
carried out first. This is followed by the calculations of
the co-ordinates of the rocket trajectory, component and total
velocity of the descending parachute or chaff and calculation
of the wind speed and direction. Correlation of the results
of radar tracking and telemetry measurements and restoration
of the vertical and total velocity of the descending parachute
or chaff is done by the equations of motion. Calculation of

the atmospheric temperature, pressure and density at standard altitudes is carried out using the results of the thermometer measurements. Storage and formulation of the results incorporate recording the results on magnetic tape for prolonged storage and printing the data bulletins. The computer print out results are plotted for further analysis and checking in respect of velocity, altitude, temperature, density and wind.

3.5   Computing wind velocity and direction

The M-100 rocket is located in space by slant range (D), elevation ($\odot$) and azimuth ($\emptyset$) measured by the Meteor radar . The vertical angle $\odot$ varies from 0 to 1500 mils (1 mil = 0.06°) and the horizontal angle $\emptyset$ from 0 to 6000 mils, while the slant range is measured in tens of metres (0.1 = 1 m). For observations taken from a ship, the marine variant of the meteorological radar is equipped with a device that allows an automatic introduction of the ship's course. The radar data is then smoothed by plotting it against time on a graph paper. The averaged values of the angles and slant range are used for computing the rocket co-ordinates and speed, as well as for computing the wind velocity.

The horizontal co-ordinates are given by -

$$X = D \cos \odot \cos \emptyset$$
$$Y = D \cos \odot \sin \emptyset \qquad\qquad - (1)$$

and the vertical co-ordinates by -

$$Z = D \sin \theta \qquad\qquad - (2)$$

where X is the meridian axis (the sign " + " being northward) and
Y the regional axis (the sign " + " being eastward).
The altitude H is found from the formula

$$H = Z + \Delta H$$

where, ΔH is the correction for the curvature of the Earth,
which is neglegible if the horizontal distance of the rocket
from the radar ($D_H = D \cos \theta$) is less than 50 km. The values
of the correction ΔH at $D_H = 50, 60, 70, 80, 90, 100, 110,$
120, and 130 km are 0.20, 0.28, 0.38, 0.50, 0.64, 0.79, 0.94,
1.13 and 1.32 km respectively.

The components of the parachute (or chaff) speed are
determined with an accuracy of 1 ms^{-1} by the method of finite
differences from the following relations -

$$V_x = \frac{X_2 - X_1}{t_2 - t_1}$$

$$V_y = \frac{Y_2 - Y_1}{t_2 - t_1} \qquad\qquad - (3)$$

$$V_z = \frac{Z_2 - Z_1}{t_2 - t_1}$$

where X_1, Y_1, Z_1 and X_2, Y_2, Z_2 are the co-ordinates of the
rocket at times t_1 and t_2.

A speed found for a definite interval of time is actually at the middle moment of that interval. V_x, V_y, V_z are then plotted against time and the resulting curves are smoothed. The smoothed values V_x', V_y', and V_z' are taken from these curves for calculating the parachute (or chaff) speed and the wind velocity.

3.6 Error in wind determination

We will here examine the error in the ability of the falling object itself (parachute or chaff) to follow the vertical wind pattern. Let M be the mass (kg) of the falling object, A the drag cross-section (m^2), g the accelration due to gravity (m/s^2), P the density (kg/m^3), a_D the accelration due to drag (m/s^2), Z the height of the object (m), $\dot{Z}$ the vertical velocity of the object (m/s), $\ddot{Z}$ the vertical accelration of the object (m/s^2), $\dot{X}$ the horizontal velocity of the object (m/s), $\ddot{X}$ the horizontal accelration of the object (m/s^2), C_D the drag coefficient, W_s the wind shear (units/s) and W the horizontal wind speed. Then the horizontal wind relative to the falling object or wind error $\dot{X} - W$ is determined as follows:

Since $\ddot{Z}$ $= -g + a_D$
the drag force can be written as

$$Ma_D = \frac{C_D AP (\dot{Z})^2}{2}$$

The equation of motion of the falling object will be

$$\ddot{Z} = -g + \frac{C_D A P}{2 M} (\dot{Z})^2$$

if both the vertical winds and the coriolis accelration are neglected.

If $K = \dfrac{C_D A}{2 Mg}$ — (4)

the expression for vertical accelration becomes

$$\ddot{Z} = -g + K Pg (\dot{Z})^2$$ — (5)

Solving for $\dot{Z}$ we get

$$\dot{Z} = \left(\frac{1}{K P} (1 + \frac{\ddot{Z}}{g}) \right)^{\frac{1}{2}}$$

If we further assume that $\ddot{Z} \ll g$, then

$$\dot{Z} = (\frac{1}{KP})^{\frac{1}{2}}$$ — (6)

We will now derive an expression for the error in wind determination as a function of fall velocity. The complete expression for the horizontal accelration of a falling object in a wind field assuming a planar flow is

$$\ddot{X} = \frac{C_D A P}{2 M} (\dot{X} - W) \left((\dot{X} - W)^2 + (\dot{Z})^2 \right)^{\frac{1}{2}}$$ — (7)

If the difference between the horizontal velocity of the object and the horizontal wind velocity is very much less than the fall velocity, i.e., $\dot{X} - W \ll \dot{Z}$, then the above equation simplifies to :

$$\ddot{X} = K \, P \, g \, (\dot{X} - W) \, \dot{Z}$$

Substituting $KP = \dfrac{1}{(\dot{Z})^2}$

$$\ddot{X} = \dfrac{g \, (\dot{X} - W)}{\dot{Z}} \qquad\qquad - (8)$$

This equation indicates that the horizontal accelration on the object, tending to pull it into the wind field, is proportional to the relative wind and inversely proportional to the fall velocity. Equation (8) may be written as –

$$\dot{X} - W = \dot{Z} \, \dfrac{\ddot{X}}{g} \qquad\qquad - (9)$$

More strictly, vertical accelration $\ddot{Z}$ should be incorporated in g. Then

$$\dot{X} - W = \dot{Z} \, \dfrac{\ddot{X}}{\ddot{Z} + g} \qquad\qquad -(10)$$

If we assume that the horizontal wind, or wind error, relative to the falling object remains constant as it passes through a zone of constant wind shear, then

$$\dot{X} - W = \text{Constant}$$

and $\quad \ddot{X} = \dfrac{dW}{dt}$

The vertical wind shear W_s is defined as

$$W_s = \dfrac{dW}{dZ}$$

$$= \dfrac{dW}{dt} \, \dfrac{dt}{dZ}$$

$$W_s = \dfrac{\ddot{X}}{\dot{Z}} \qquad\qquad -(11)$$
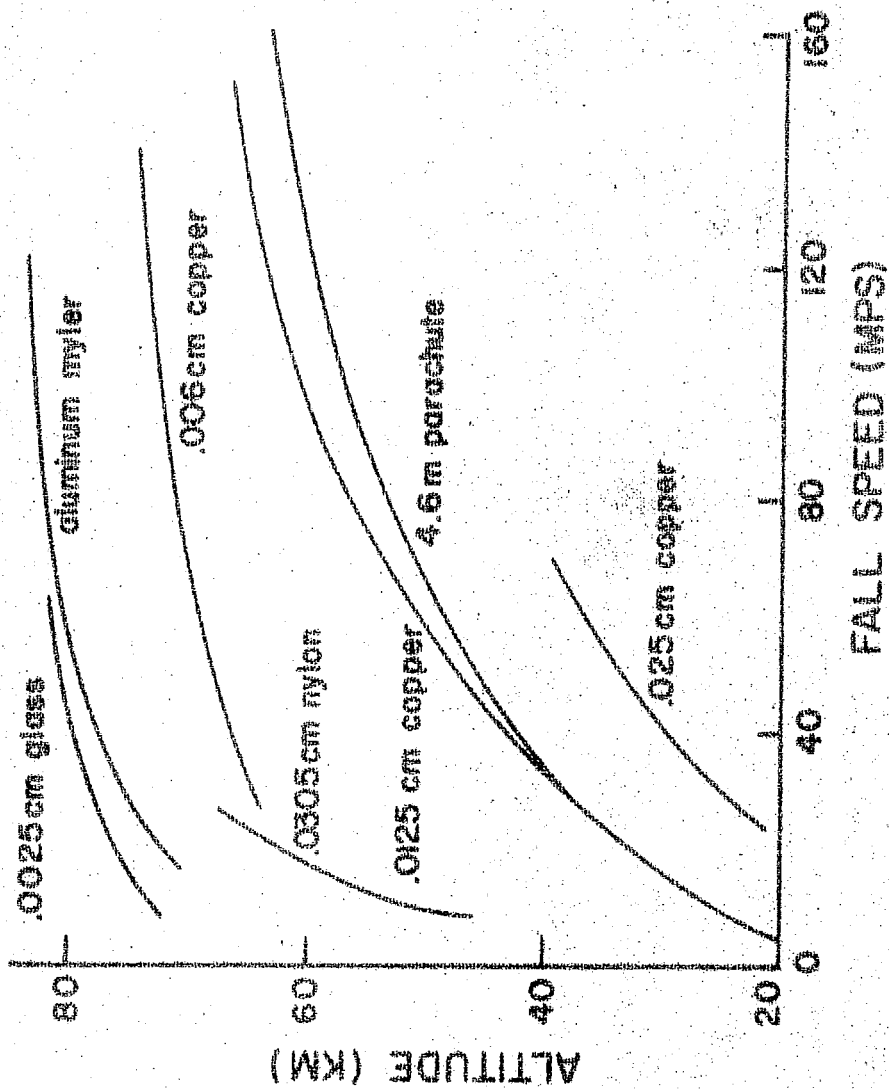
(Fig. 3.4) Radar chaff fall velocities. Data in this figure compiled from studies of Beyers et al (1962), Morris (1957) and Smith (1960).

Combining equations (8) and (11)

$$\ddot{X} = W_s \, \dot{Z} = \frac{g(\dot{X}-W)}{\dot{Z}} \qquad -(12)$$

$$W_s = \frac{g(\dot{X}-W)}{(\dot{Z})^2}$$

$$\dot{X}-W = \frac{W_s \, (\dot{Z})^2}{g} \qquad -(13)$$

This expression shows that for a given constant wind shear W_s, the error in the horizontal wind determined by tracking a falling object (parachute or chaff) is a function of the square of the fall velocity provided the fall velocity is much larger than the relative horizontal wind. Lally (1958) has worked out the values of the wind error for various fall velocities and wind shears. Fall velocities of various chaffs and of 4.6 m parachute are presented in Fig.3.4. The wind error analysis gives an immediate answer on how accurately an object falling at a known velocity will represent the wind field. If we wish to be able to measure the wind field to an accuracy of 10 m/s within a zone where the wind shear is 0.02 units/sec, then the fall velocity of our tracked object must be less than 70 m/s. An object falling at twice this speed will be in error by four times as much. A typical chaff fall speed (m/s) obtained from one of the M-100 rocket soundings versus altitude is shown in Fig.3.5. The chaff used consisted of cylindrical aluminium-coated glass fibres having a

(Fig.3.8)
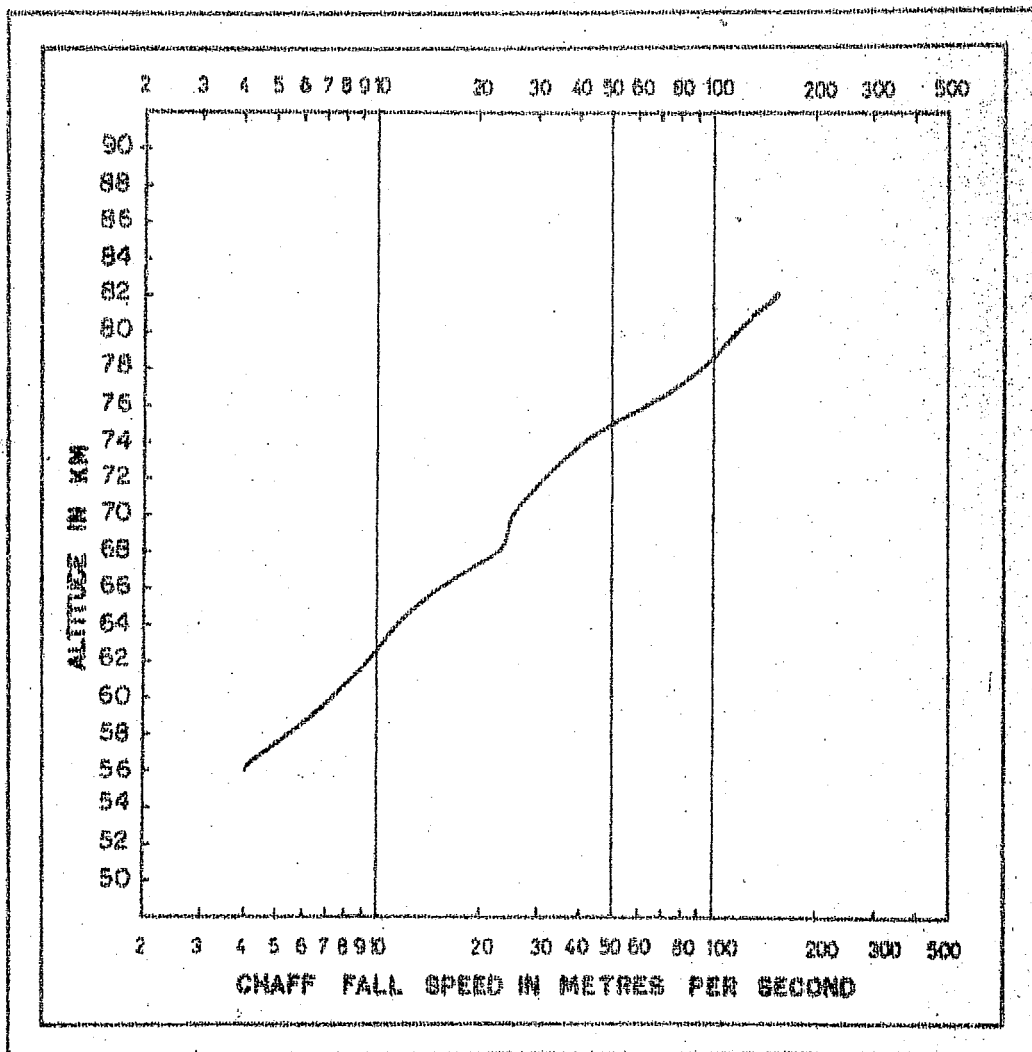
Meteor radar chaff fall velocity (m/s) from a typical M-100 rocket sounding.

diameter of about 0.0025 cm. It gave an accuracy of about 5-10 m/s in upper mesospheric wind determination.

3.7   Correction of wind errors

The total speed of the descending parachute (or chaff) is computed from the relation -

$$V_R = ((V_x')^2 + (V_y')^2 + (V_z')^2)^{\frac{1}{2}} \qquad -(14)$$

within the range of altitudes 30-58 km. When there are large wind shears in the vertical, the descending parachute/chaff may not respond instantaneously to the wind of each level. The differences between the components of the wind velocity and those of the descending parachute or chaff speed (ms^{-1}) are calculated from equation (10) by replacing $\dot{X}$-W by ΔX, $\dot{Z}$ by V_z', $\ddot{X}$ by a_x, $\ddot{Z}$ by a_z and g by 9.7 (m/s^2) .The expression (10) thus becomes $\Delta X = V_z' \dfrac{a_x}{a_z + 9.7}$

Similarly

$$\Delta Y = V_z' \frac{a_y}{a_z + 9.7} \qquad -(15)$$

where a_x, a_y and a_z are the components of the descending parachute/chaff acceleration given by

$$a_x = \frac{(V'_x)_2 - (V'_x)_1}{t_2 - t_1}$$

$$a_y = \frac{(V'_y)_2 - (V'_y)_1}{t_2 - t_1} \qquad -(16)$$

$$a_z = \frac{(V'_z)_2 - (V'_z)_1}{t_2 - t_1}$$

Within the range of 30-50 km (as a rule within the 240-420th seconds during descent), the wind velocity components V_{1x} and V_{1y} are calculated by the following equations

$$V_{1x} = V'_x + \Delta X$$

$$V_{1y} = V'_y + \Delta Y \qquad -(17)$$

However, at altitudes below 30 km these components are simply the smoothed values of V'_x and V'_y i.e.

$$V_{1x} = V'_x$$

$$V_{1y} = V'_y \qquad -(18)$$

Having obtained the wind components V_{1x} and V_{1y} for all standard altitudes up to about 50 km, total wind velocity and its direction are determined by using the aerological disk or from the following formulae

$$V = ((V_{1x})^2 + (V_{1y})^2)^{\frac{1}{2}}$$

$$d = \tan^{-1}\left(\frac{V_{1y}}{V_{1x}}\right) \qquad -(19)$$

The upper atmospheric wind speed and direction are thus calculated from the drift of the trajectory of the descending chaff and parachute using the above formulae. Chaff is used for wind measurements in the mesosphere while parachute in the stratosphere and the troposphere with a view to minimising the wind errors as discussed in section 3.6. An example of computing the wind speed and direction from the Meteor radar data and applying the wind error corrections is given in Table 3.2 (a, b). The accuracy in measuring the wind speed is about 5-10 ms^{-1} after applying the above corrections. It is very important that for wind computations the radar data must be smoothed before feeding it to the computer. The computer further smoothes the data according to a standard programme and yields reasonably accurate results.

3.8   Computing the atmospheric temperature

A brief account of determining the atmospheric temperature, pressure, and density from the data of resistance thermometers is given below :

At altitudes below 15-18 km, atmospheric temperature T_A is equal to the thermometer wire temperature T_w, and is taken from the average smoothed curve of the telemetry decoded data e.g. Fig. 3.4. At altitudes in excess of 15-18 km the thermometer wire temperature is corrected by the

Table - 3.2(a)

Computation of the upper atmospheric wind speed and direction from one of the chaff-borne M-100 rocket flights over Molodezhnaya, Antarctica

(Dated January 5, 1972)

Time t (sec)	Elevation (θ) (deg)	Azimuth φ (deg)	Slant range D (km)	Chaff co-ordinates			Altitude H (km)	Chaff velocity components		
				X (km)	Y (km)	Z (km)		V_x (m/s)	V_y (m/s)	V_z (m/s)
1	2	3	4	5	6	7	8	9	10	11
140	68.6	298.9	88.50	15.61	-28.30	82.40	82.42	-	-	-
170	68.0	298.6	86.90	15.58	-28.58	80.57	80.59	-3	-11	-51
200	67.5	298.0	85.85	15.42	-29.00	79.31	79.34	-6	-21	-38
230	66.8	297.0	85.15	15.23	-29.88	78.26	78.29	-8	-30	-27
260	66.2	295.8	84.89	14.91	-30.84	77.67	77.70	-12	-30	-24
290	65.2	294.6	84.65	14.50	-31.68	76.84	76.89	-2	-50	-18
300	64.8	294.3	84.63	14.83	-32.84	76.57	76.63	9	-60	-21
350	63.2	293.1	84.70	15.03	-35.25	75.60	75.68	6	-46	-20
400	61.5	292.5	84.90	15.50	-37.43	74.61	74.71	10	-40	-20
450	60.0	292.3	84.95	16.12	-39.29	73.57	73.69	8	-41	-20
500	58.4	291.5	85.15	16.35	-41.51	72.52	72.67	2	-47	-19
550	56.8	290.3	85.65	16.27	-43.98	71.67	71.74	-2	-54	-15
600	55.1	289.0	86.65	16.14	-46.87	71.07	71.27	6	-48	-11

more

Table - 3.2(a) contd. 2

1	2	3	4	5	6	7	8	9	10	11
700	52.0	288.3	88.80	17.17	-51.90	69.97	70.17	2	-50	-9
800	49.4	286.3	91.10	16.64	-56.91	69.17	69.37	-3	-48	-8
900	47.0	285.5	93.60	17.06	-61.52	68.46	68.77	6	-32	-7
1000	45.2	285.4	95.40	17.85	-63.46	67.70	68.05	4	-30	-10
1200	41.9	284.7	97.80	18.49	-70.49	65.31	65.71	5	-31	-10
1400	39.2	284.6	101.00	19.73	-75.73	63.83	64.31	1	-27	-6
1600	36.9	283.1	104.50	18.94	-81.40	62.74	63.28	-3	-35	-6
1800	34.1	281.8	109.70	18.58	-88.92	61.50	62.14	1	-42	-4
2000	31.4	281.1	117.30	19.27	-98.25	61.11	61.90	-	-	-

Table - 3.2(b)

Computation of the upper atmospheric wind speed and direction from one of the M-100 rocket flights over Molodezhnaya, Antarctica (dated January 5, 1972). Values to integer altitudes are obtained by plotting the corresponding graphs

Time t (sec)	Smoothed chaff velocity components			Wind error components		Altitude H (km)	Corrected wind velocity components		Resultant wind direction and speed	
	V'_x (m/s)	V'_y (m/s)	V'_z (m/s)	ΔX (m/s)	ΔY (m/s)		V_{1x} (m/s)	V_{1y} (m/s)	d (deg)	V (m/s)
1	2	3	4	5	6	7	8	9	10	11
140	-	-	-	-	-	82.42	-	-	-	-
170	-4	-11	-51	-4	-11	80.59	-8	-22	70	23
200	-7	-21	-37	-2	-9	79.34	-9	-30	72	32
230	-8	-30	-29	0	-8	78.29	-8	-38	78	39
260	-7	-40	-24	2	-7	77.60	-5	-47	85	47
290	-2	-49	-22	2	-6	76.89	0	-55	90	55
300	0	-51	-22	1	1	76.63	1	-50	91	50
350	10	-46	-21	1	2	75.68	11	-44	105	45
400	10	-39	-20	1	1	74.71	11	-38	107	40
450	8	-41	-20	0	1	73.69	8	-40	102	42
500	8	-47	-20	-1	0	72.67	7	-47	98	48
550	6	-45	-19	1	1	71.74	7	-45	99	45

more

Table - 3.2(b) contd..2

	2	3	4	5	6	7	8	9	10	11
0	6	-46	-19	1	-1	71.27	7	-47	98	47
0	3	-49	-9	-1	-1	70.17	2	-50	92	50
0	-4	-48	-8	1	1	69.37	-3	-47	85	48
0	5	-31	-7	1	-1	68.77	6	-32	101	33
00	3	-30	-10	1	0	68.05	4	-30	98	30
00	6	-32	-10	-1	1	65.71	5	-31	100	31
00	1	-28	-6	0	1	64.31	1	-27	92	27
00	-4	-34	-6	1	-1	63.28	-3	-35	86	35
00	1	-43	-4	0	1	62.14	1	-42	91	42
00	-	-	-	-	-	61.90	-	-	-	-

	7	8	9	10	11
	80	-8.8	-25.5	71	27
	78	-6.7	-42.5	81	43
	76	-6.7	-47.5	98	48
	74	10.6	-39.6	105	41
	72	7.2	-45.4	99	46
	70	0.9	-50.0	92	50
	68	4.8	-30.6	99	31
	66	4.7	-29.6	99	30
	64	2.0	-27.1	94	28
	62	-0.7	-38.0	89	38

following formula

$$T_W' = T_W + \Delta T_{aw}$$

$$= T_W + 0.06 \ (T_W - T_{aw}) \qquad -(20)$$

where T_{aw} is the temperature measured by the steeple thermo-
meter and ΔT_{aw} is an allowance for a thermal contact between
the thermometer wire and the insulating blocks. Within the
range of altitudes from about 15 to 30 km, the temperature
T_A is considered equal to the value T_W' , because all other
factors influencing the wire temperature are neglegible.

Within the range of altitudes from about 30 to 50 km
the wire temperature is allowed for speed correction ΔT_V.
The atmospheric temperature in this case is determined as
follows

$$T_A = T_W - \Delta T_V$$

$$= T_W - \ (4.98 \times 10^{-4} \times r \times (\bar{V}_z)^2 \qquad -(21)$$

where, r is the temperature recovery co-efficient and
$\bar{V}_z$ the average air flow velocity (ms^{-1}) relative to the
thermometers (in case of employment of a parachute) determined
from the formula

$$\bar{V}_z = (\ (V_z')^2 + (\Delta X)^2 + (\Delta Y)^2 \ )^{\frac{1}{2}} \qquad -(22)$$

where V_z' is the smoothed value calculated from the relation
given in (3) and ΔX, ΔY are calculated from (15) as

discussed in section 3.7. At altitudes below 40 km values V'_z do not differ much from the values $\bar{V}_z$. At altitudes exceeding 45 km the atmospheric temperature T_A is calculated by the following formula

$$T_A = T'_w - 4.98 \times 10^{-4} \times r \times V^2 + \tau \frac{dT'_w}{dt} + \frac{\xi_\sigma (T'_w)^4}{h}$$

$$- \frac{Q}{S.h} - \frac{\Sigma q}{h} \qquad\qquad -(23)$$

At altitudes below 55 km the value V_z determined by formula (22) is considered to be the air flow velocity V relative to the transmitters. At altitudes exceeding 60 km the value V is considered equal to the full speed of the rocket. The values of the recovery coefficient (r) are taken from the standard tables. Correction for the thermometer thermal inertia depends upon the rate of change of the thermometer wire temperature $(\frac{d\;T'_w}{dt})$ during the rocket flight and upon the time constant (τ) of the thermometer thermal equilibrium. Time constant τ depends upon the diameter (d) of the thermometer, its thermal characteristics and on a heat exchange coefficient (h). It is given by $\tau = \frac{C.\rho.d}{4h}$ $\qquad -(24)$

where C is the thermal capacity of the thermometer, ρ the density and d the diameter of the thermometer wire. The time constant of the standard thermometers employed at the present time equals

$$\tau = \frac{6.5 \times 10^{-4}}{h} \qquad\qquad -(25)$$

Heat exchange co-efficient (h) of the thermometer is calculated from

$$h = \frac{0.1241 \times 10^{-4} \times T_A \ (T_A)^{\frac{1}{2}} \times N_u}{T_A + 110.5} \qquad -(26)$$

The Nusselt number (N_u) used in formula (26) depends upon Knudsen number (Kn) and Mach number (Mn) given by the following formulae

$$Kn = \frac{3.10 \times 10^{-5} \times T_A}{d \times P_A(1 + \frac{110.5}{T_A})} \qquad -(27)$$

where d is the thermometer wire diameter (0.004 cm) and P_A the atmospheric pressure in mb. The Knudsen number Kn is a function of the values P_A and T_A at the given diameter d. The values of Kn are given in standard tables. The Mach number Mn is defined as the ratio of the total chaff speed (V_R) to a sonic speed (V_s) and is given by

$$Mn = \frac{V_R}{V_s} \qquad -(28)$$

where

$$V_s = 20.05 \ (T_A)^{\frac{1}{2}} \qquad -(29)$$

The values of V_s as a function of the atmospheric temperature are taken from standard tables. The temperature recovery co-efficient (r) is taken from the graph:

$$r = f \ (Mn, \log Kn) \qquad -(30)$$

which is plotted by using the data from the standard tables.
The Knudsen number (Kn) is related to the Nusselt number (Nu)
and Mach number (Mn). The values of the temperature recovery
co-efficient (r) in terms of (Mn) and (log Kn) are given in
Table 3.3. The Table 3.4 presents the values of the Nusselt
number as a function of the Mach number and the logarithm of
Knudsen number.

It is quite evident that the temperature recovery
co-efficient (r) depends only upon the Mach number (Mn) when
the Knudsen number Kn $>$ 11 and can be interpolated from
Tables 3.3 and 3.4.

The value of the heat exchange co-efficient (h) is
found from the values of the Nusselt number (Nu) using the
relation

$$h = A. \; Nu \hspace{5cm} -(31)$$

where A depends upon the atmospheric temperature T_A and is
taken from the standard tables. As is obvious from the
relation (26)

$$A = \frac{0.1241 \times 10^{-4} \times T_A \; (T_A)^{\frac{1}{2}}}{T_A + 110.5} \hspace{3cm} -(32)$$

The correction for the thermometer wire heat radiation equals

$$\frac{\sigma \; \xi (T_W')^4}{h}$$

Table - 3.3

The temperature recovery co-efficient (r) as a function of the Mach number (Mn) and logarithm of the Knudsen number (log Kn)

Log Kn \ Mn	0.5	1.0	1.5	2.0	2.5	3.0
-2.0	0.579	0.790	0.857	0.890	0.910	0.926
-1.5	0.590	0.802	0.871	0.899	0.915	0.929
-1.0	0.699	0.884	0.940	0.955	0.967	0.976
-0.5	1.080	1.079	1.062	1.061	1.060	1.069
0.0	1.459	1.299	1.214	1.186	1.155	1.145
0.5	1.633	1.471	1.333	1.289	1.226	1.208
1.0	1.680	1.540	1.412	1.331	1.261	1.237
1.5	1.680	1.540	1.420	1.340	1.261	1.240
2.0	1.680	1.540	1.420	1.340	1.261	1.240
2.5	1.680	1.540	1.420	1.340	1.261	1.240

Table - 3.4

The values of the Nusselt number (Nu) as a function of the Mach number (Mn) and the logarithm of the Knudsen number (log Kn)

Mn / Log Kn	0.3	0.5	1.0	1.5	2.0	2.5	3.0
-2.0	2.951	3.802	5.754	7.413	10.00	12.88	15.85
-1.5	1.664	2.089	3.020	3.715	5.012	6.310	8.128
-1.0	0.933	1.096	1.514	1.862	2.399	2.951	3.981
-0.5	0.4677	0.5248	0.6918	0.9511	1.096	1.380	1.862
0.0	0.2089	0.2291	0.2951	0.3613	0.4677	0.5888	0.7762
0.5	0.08128	0.09120	0.1122	0.1349	0.1862	0.2239	0.3020
1.0	0.02884	0.03236	0.03802	0.04571	0.06457	0.07762	0.1047
1.5	0.008913	0.01000	0.01200	0.01479	0.02042	0.02455	0.03236
2.0	0.002818	0.003236	0.003715	0.004786	0.006457	0.007762	0.01026
2.5	0.0008891	0.001000	0.001175	0.001479	0.002089	0.002399	0.003162

where ξ is the radiation co-efficient dependent upon the thermometer wire temperature and σ, the Stefan-Boltzman constant (1.375×10^{-12} cal cm^{-2} deg^{-1}). Radiation co-efficient ξ for a tungsten-rhenium wire used at the present time in rocket thermometers linearly rises with an increase of the thermometer wire temperature. Value $\xi = 0.129$ at T_w' $= 300^\circ$ and the value $\xi = 0.204$ at $T_w' = 500^\circ$ are used for the calculation of $\xi \sigma (T_w')^4 = f (T_w')$.

The term $\frac{Q}{S.h}$ gives the correction for the ohmic heating of the thermometer by electric current, where (Q) is the heat effect of the resistance thermometer and (S) the thermo-meter surface area. The heat effect Q of the thermometer is given by the equation

$$Q = \frac{0.239 \times V_1^2 \times R_o (1 + \alpha t_w')}{(R + R_o (1 + \alpha t_w'))^2} \qquad -(33)$$

where $t_w' = T_w' - 273^\circ$, R_o the thermometer resistance at 0°C, V_1 the voltage of the thermometer bridge supply (3.11 to 3.12 volts) and R the resistance of the thermometer bridge arm.

The length of the thermometer wire consists of eight sections, 13.3 cm each. Thus the total length of the wire equals 106 cm, wire diameter $d = 0.004$ cm and its surface area $S = 1.34$ cm^2. If, for example, $R_o = 221$ ohms,

$\alpha = 147 \times 10^{-3}$ and $R = 250$ ohms, the value Q will be 0.230 $\times 10^{-2}$, 0.232 $\times 10^{-2}$ and 0.231 $\times 10^{-2}$ at $t_w' = 0°$, $100°$ and $200°C$ respectively. It follows that under the specified parameters the temperature variation of the thermometer wire for first minutes of the rocket flight does not practically influence the value Q. It is, therefore, quite possible to dispense with the calculation of the value $\frac{Q}{S}$ for every altitude of measuring atmospheric temperature T_A and take it as a constant value for all altitudes of a given rocket launching. For the present case the value $-\frac{Q}{S}$ is 17.2 $\times$ 10^{-4}. In case of simultaneous operation of the four thermometers mean arithmatic value of $-\frac{Q}{S}$ is used for the atmospheric temperature calculations. In practice the value $-\frac{Q}{S}$ may be used for processing the data obtained by a number of launchings because the parameters R_o, α, R and V_i influencing its value turn to be the same.

The correction $\frac{\Sigma q}{h}$ allowing for a heat of a long-wave radiation and especially of a short-wave radiation inflowing to the resistance thermometers may be found from the relations

$$\Sigma q = \xi \sigma (T_w')^4 - \frac{Q}{S} + h(T_w' - T_e) + 6.5 \times 10^{-4}$$
$$\times \frac{d\, T_w'}{dt} \qquad\qquad -(34)$$

$$T_e = T_A(1 + 0.2r \times M_n^2) \qquad\qquad -(35)$$

where T_e is the equilibrium temperature i.e. the temperature
at which the convective heat exchange of the resistance
thermometers in the atmosphere equals zero, all other values
of the formula being calculated for the peak of the trajectory.

By summing up the numerators of the terms involving
(h) in the equation (23) one gets a simplified formula for
temperature calculations.

$$T_A = T_W' - \Delta T_v + \frac{S'}{h} \qquad -(36)$$

where

$$S' = 6.5 \times 10^{-4} \times \frac{d\,T_W'}{dt} + \xi\sigma(T_W')^4 - \Sigma q - \frac{Q}{S} \quad -(37)$$

It is expedient to calculate the atmospheric temperature by
formula (36) , values S' in this case are to be computed for
every altitude.

Since the value Q does not depend upon the thermometer
wire temperature, substituting (34) into (37)

$$S' = 6.5 \times 10^{-4} \times \frac{d\,T'_w}{dt} + \xi\sigma(T_W')^4 - (\xi\sigma(T_W')^4$$
$$+ h\,(T_W' - T_e) + 6.5 \times 10^{-4} \times \frac{d\,T_W'}{dt}) \qquad -(38)$$

The last 3rd term (in the brackets) may be denoted by $\Sigma q'$.
The calculations by the relation (23) produce an atmospheric
temperature in the first approximation which is corrected
to good accuracy by the method of iterations. The measurements

show that an accidental root mean square error in determining
the atmospheric temperature by the resistance thermometers
equals $3^{\circ}C$ at an altitude of 40 km, $5^{\circ}C$ at an altitude of
50 km, and $7-10^{\circ}C$ at altitudes 60-80 km.

3.9   Computing the atmospheric pressure and density

Having found the pressure at a certain lower level by
radiosonde data, the atmospheric pressure at the higher levels
is determined from the formula

$$K = \log P_1 - \log P_2 = \frac{g\,(H_2 - H_1)}{2.302 \times R_v \times T_A} \qquad -(39)$$

where P_1 and P_2 are the pressure values at lower level H_1
and upper level H_2 (in km), R_v the gas constant of the air
($R_v = 28.7$) and g the free-fall acceleration (m sec^{-2})
respectively.

The values of K are found out from the standard tables.
Thus the atmospheric pressure at a higher altitude is
given by $\log P_2 = \log P_1 - K$ $\qquad -(40)$

The same procedure is used for calculating $\log P_2$
and the pressure values for all the upper layers are thus
determined.

The temperature and pressure values of the last
approximation are then used to calculate the atmospheric
density given by the relation

$$\rho_A = 348.4 \, \frac{P_A}{T_A} \qquad -(41)$$

where ρ_A is in gm^{-3}, P_A in mb and T_A in $^{\circ}K$.

In modern practice an ever greater part of the meteorological rocket data is processed by the computing machines. The advantages of the data processing by computing machines over that by hand consist in a time saving in obtaining the final results and in a higher reliability of the processed data. The data processing of the M-100 rocket system is not very simple as it is very time consuming and complex.However, it has more redundancy in the observations and correcting and checking methods. The preflight calibration of the sensors and the determination of (α) value are important facotors in the M-100 rocket data processing and it is checked with the factory value.

C H A P T E R - IV

EXPLORATION OF ATMOSPHERIC STRUCTURE OVER ANTARCTICA

For centuries, the poles have driven hardy men to exploration motivated by curiosity, adventure, promise of rewarding harvests of seals and whales or by the search for shorter trade routes. The annals of early polar exploration tell of daring exploits and killing hardships. Ironically, some of more tragic early expeditions contributed a lot to our knowledge of the polar regions as for example, Shakelton's remarkable Antarctic odyssey after his ship 'Endurance' had been crushed by pack ice in the Weddel Sea, and the ill-fated Franklin expedition into the Arctic. Because survival in the harsh environment demanded so much of the early explorers, their contributions to our knowledge of the polar regions were largely limited to the discovery and mapping of land features.

The polar regions of the Earth are still comparatively less explored . This especially applies to the Antarctic which was discogered just two centuries ago. Scientific investigations of Antarctica started in 1901 when expeditions were sent to the Antarctic continent under various national flags. Polar investigation entered a new

era during the International Geophysical Year, IGY in 1957-58
which marked the end of random exploration and the beginning
of systematic scientific research. Broad features of the
polar environment are now known to a reasonable extent.
However, some specific significant problems, largely inter-
disciplinary in nature, that will lead to a better under-
standing of the total global environment remain yet unsolved.
The polar regions are integral parts of the total global
environment and understanding of polar processes and
phenomena is essential to the solution of earth-wide problems.
For example, polar atmospheric circulations strongly
influence weather and climate at the lower latitudes, and
the polar oceans can be considered the high-latitude portions
of the world oceans. Removal of the sea-ice cover of polar
seas, either accidently or deliberately, would certainly
have a profound effect on the global heat balance and hence
on the world's weather and climate and consequently on the
atmospheric structure and circulation. We have yet to
uncover and explain many of the basic secrets of the polar
environment, to relate them to their global counterparts
and to weigh the interlocking consequences of environmental
modifications. The study of the polar atmospheric structure
particularly over Antarctica which is the last terra incognita
on the Earth and the least investigated so far is, therefore,
very essential.

4.1   Soviet Antarctic Expedition

Under a joint Indo-Soviet agreement ratified in 1970, the author participated in the 17th Soviet Antarctic Expedition during the period 1971 to 1973, wintered at the South Polar Ice-Cap and circumnavigated the Antarctic Continent (Caffin,1975). Some of the stations visited by the author during his Antarctic Odyssey, 1971-73 are shown in Fig.4.1. Visit to the station Vostok (78°28'S, 106°48'E), the pole of cold located at the geomagnetic South Pole at a height of 3488 m above M.S.L. was of special interest because it involved a trekking of about 1500 km with tractor sledge and footsore.

The author wintered at the station Molodezhnaya located at 67°40'S, 45°51'E at a height of 42 m above M.S.L. and carried out meteorological rocket soundings of the upper atmosphere in addition to other observations. The station Molodezhnaya was formally opened on January 14, 1963 and the atmospheric soundings with meteorological rockets were started from mid 1969 (Koshelkov, 1972). At the station there is a series of east-west ridges made of some exposed bedrocks. The ridges are separated by ice-filled valleys with elevations ranging from about 20 to 200 m along the coast. Some of the ridges terminate in cliffs at the adjacent bay, Alasheyev Bight. The major bedrocks are magmatized, granitized and pegmatized

WEST 0° EAST 30° AFRICA
SOUTH ATLANTIC OCEAN
45°W 50° SOUTH INDIAN OCEAN 45°E
SOUTH AMERICA
BELLINGS- HAUSEN NOVOLAZAR- EVSKAYA
MOLODEZHNAYA
KERGU- ELEN
90°W POLE 80° MIRNY 90°E
ANTARCTIC CIRCLE VOSTOK McMURDO
LENINGRAD- SKAYA
ANTARCTIC CONVERGENCE
SOUTH PACIFIC OCEAN
TASMANIA AUSTRALIA
135°W 135°E
NEW ZEALAND
WEST 180° EAST
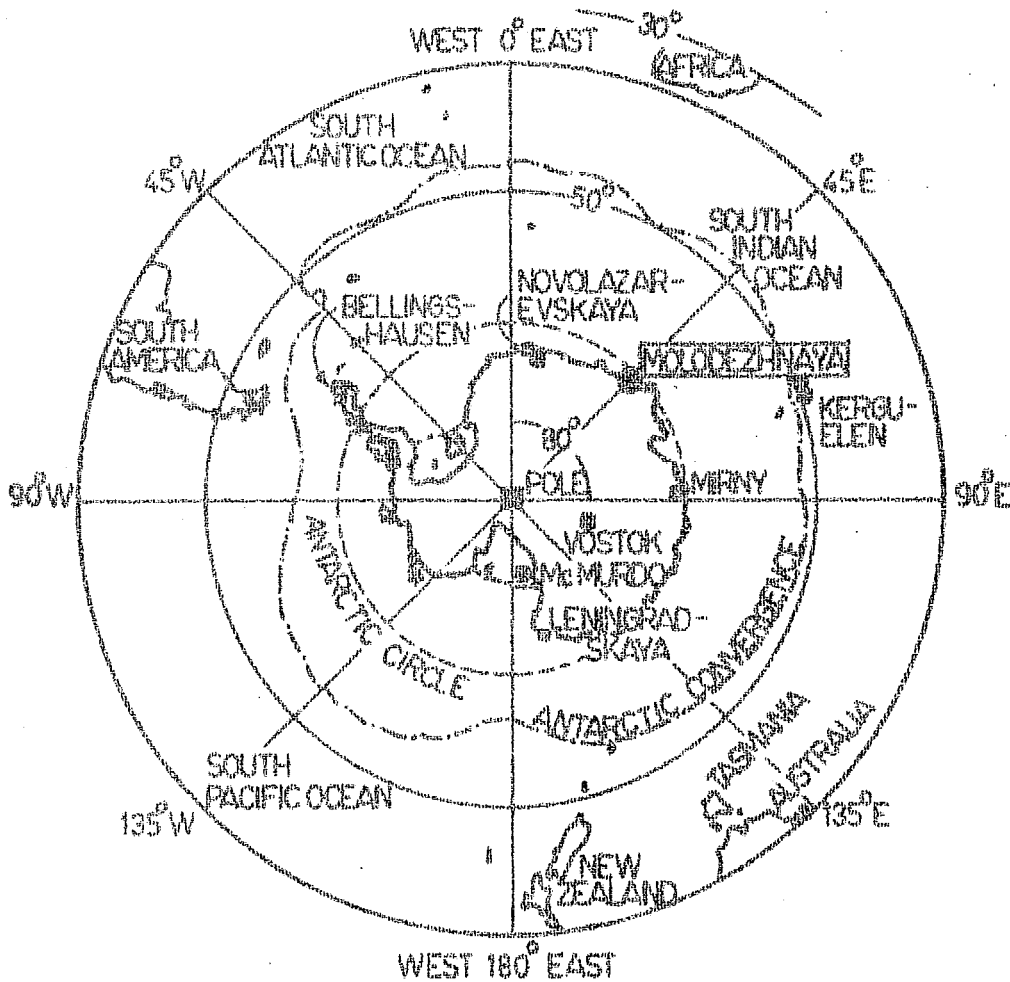
(Fig. 4.1)
Map of Antarctica and surrounding area showing the
location of the station Molodezhnaya. Some other
stations visited by the author are also shown.

Precambrian gneisses of the crystalline basement of the
Antarctic platform. In a narrow zone about 10 km wide
parallel to the coast, exposed rock and soil are found in
abundance which are, however, very rare inland. Although the
station bed itself is confined to erratic and frost-churned
mixed materials, yet nearby there are two outlet glaciers,
Campbell and Hays, which form active moraines.

4.2   Some physical characteristics of Antarctic Meteorology

The weather and climate of Antarctica are the result
of several factors, for example its location near the South
Pole of the Earth with the implied astronomical influences,
its great elevation which intensifies the polar climate, its
perpetual snow cover with strong reflective and radiative
characteristics and its complete isolation from all other
continents by a completely surrounding ocean of relatively
warmer water. The Antarctic atmosphere has the same composition
as that of the rest of the world, except that the principal
variable gaseous component, water vapour, has only about one-
tenth of the average concentration, of what it has in middle
latitudes.

Table 4.1 presents the surface meteorological results
at the Antarctic station Molodezhnaya ($67^{\circ}40'S$, $45^{\circ}51'E$, 42 m
above M.S.L.) in 1972. It is obvious from the Table 4.1 that in

1972 the mean annual temperature observed at the station was $-10.5^{o}C$ varying from a lowest minimum of $-35.8^{o}C$ to a highest maximum of $7.0^{o}C$. South-east winds prevailed at the surface with frequent gusts of 21-41 m/s. Annual mean relative humidity was 65 % and the annual mean precipation observed was 0.14 cm. Table 4.2 gives the atmospheric winds and temperatures at the station level from 1963 to 1971, while Table 4.3 gives the extreme results since when the station was established i.e. from 1963 . The surface meteorological results collected from the various stations in 1972 during the author's participation in the Soviet Antarctic Expedition, 1971-73 are compared in Table 4.4 showing the latitudinal differences in atmospheric pressure, air temperature, wind speed, wind gust, relative humidity and average cloudiness from the Antarctic Peninsula $(62^{o}S)$ to the geomagnetic South Pole $(78^{o}S)$.

Excluding the Antarctic Peninsula, the monthly mean temperature during the warmest month is around $0^{o}C$ in the coastal region and from -34 to $-20^{o}C$ in the interior. The water vapour concentration can be higher than about 4.8 and 0.2 g m^{-3} respectively. In winter the coldest monthly mean temperature is from about -30 to $-20^{o}C$ in the coastal region and from -70 to $-40^{o}C$ in the interior, while the water vapour concentration is less than 0.3 and 0.003 g m^{-3} respectively. The carbon dioxide content is between

Table - 4.1

Surface meteorological results at Molodezhnaya, Antarctica in 1972

Meteorological parameter	Jan	Feb	Mar	Apr	May	June	July	Aug	Sept	Oct	Nov	Dec
	2	3	4	5	6	7	8	9	10	11	12	13
temperature	0.2	-3.4	-9.3	-10.5	-15.3	-17.4	-18.3	-14.9	-15.2	-13.6	-7.6	-0.3
maximum temperature	7.0	4.7	-0.7	0.0	-4.0	-4.4	-7.1	-3.2	-3.4	-1.5	1.6	7.2
date of maximum temperature	1	3	6	20	3,4	23	7	19	3	31	30	22
minimum temperature	-7.1	-11.6	-19.5	-21.6	-28.7	-29.9	-31.6	-35.8	-30.6	-26.5	-16.5	-8.9
date of minimum temperature	6	13,27,29	15	12	31	1	13,31	1	14	12	18	5
atmospheric pressure	988.3	985.2	986.4	989.2	987.0	990.5	984.3	988.2	982.3	978.3	976.7	987.6
maximum atmospheric pressure	1004.3	1005.6	1000.3	1003.7	1002.3	1007.0	996.8	1006.7	1015.2	1002.8	985.6	1001.3
date of maximum pressure	28	19	30	27	16	17	30	15	2	24	30	27

more

Table – 4.1 contd /2/.

	2	3	4	5	6	7	8	9	10	11	12	13
num atmospheric pressure	980.7	974.9	967.6	959.7	966.2	965.9	970.2	956.5	957.1	947.7	956.0	975.6
of minimum ...sure	4	20	25	19	21	16	21	3	23	17	13	7
absolute ...ity	3.8	2.9	2.1	1.9	1.4	1.0	1.1	1.5	1.6	1.6	2.2	3.1
relative ...ity	63	60	60	64	69	59	67	71	72	69	62	64
overall ...liness (per ten)	7.4	8.0	7.6	7.4	7.5	7.2	8.1	7.2	8.3	8.4	7.5	5.1
...iling wind ...tion	ESE	E	SE	SE	SE	SE	SE	E	E	SE	SE	SE
wind speed	4.5	7.9	12.1	13.3	12.7	15.2	8.9	10.4	10.8	9.7	8.3	4.8
um wind speed	17	29	22	34	32	35	24	30	35	26	21	20
of maximum speed	21	20	16	27	18	4	11	18	12	3	13	21
um wind gust	21	34	28	41	41	41	28	34	39	31	37	23
of maximum thrust	21	20	25, 26	29	19	5	3	12	12	22	18	21
precipitation (mm)	0.0	42.5	53.0	34.3	37.7	13.9	16.7	90.9	129.5	65.1	8.1	7.0
days with ...a australis	-	-	10	13	15	13	9	8	11	3	-	-

Table - 4.2

Surface meteorological results, wind speeds (m/s) and temperature (°C) at the Antarctic station Molodezhnaya from 1963 to 1971

Year	Jan	Feb	Mar	Apr	May	June	July	Aug	Sept	Oct	Nov	Dec	Annual Mean
	2	3	4	5	6	7	8	9	10	11	12	13	14
1963													
nd:Average	-	-	14.0	14.6	15.0	16.0	11.1	14.8	8.8	8.8	7.4	8.2	10.8
Maximum		27	46	44	36	46	38	48	39	47	31	30	48
p:Average		-4.0	-10.6	-11.4	-14.3	-16.2	-18.7	-16.5	-14.0	-15.3	-7.6	-1.7	-12.1
p:Maximum		-2.0	2.0	-1.6	-3.5	-4.0	-5.3	-6.4	-2.6	-5.4	0.5	8.5	8.5
Minimum	-14.0	-14.0	-22.4	-	-25.4	-27.8	-36.8	-28.1	-25.7	-28.2	-22.8	-13.7	-36.8
1964													
nd:Average	6.0	7.2	11.4	14.8	13.1	14.6	10.5	12.5	8.9	11.0	7.4	5.4	10.2
Maximum	27	25	41	41	30	25	37	38	32	38	23	28	41
Average	-0.7	-5.4	-8.2	-11.3	-15.5	-17.2	-14.7	-14.9	-18.8	-14.6	-5.5	-0.9	-10.6
p:Maximum	3.8	3.2	0.2	-1.5	-3.6	-2.3	-4.2	-3.5	-6.9	-4.5	3.1	6.3	6.3
Minimum	-8.6	-13.6	-19.5	-22.0	-29.5	-28.8	-26.8	-31.1	-33.2	-23.1	-20.2	-7.2	-33.2
1965													
nd:Average	6.1	8.2	12.2	12.7	12.6	12.4	10.1	9.8	9.8	9.8	8.3	5.2	9.8
Maximum	22	36	30	35	28	38	32	35	30	31	30	19	38
Average	-0.7	-3.5	-8.7	-9.8	-11.2	-15.4	-22.8	-19.0	-20.8	-14.4	-9.6	-1.1	-11.4
p:Maximum	5.2	3.9	2.4	2.9	-2.6	-6.3	-9.5	-5.3	-8.8	-6.6	-0.4	7.1	7.1
Minimum	-8.1	-16.8	-	-26.1	-26.7	-26.5	-35.8	-37.1	-37.5	-28.6	-23.2	-11.4	-37.5

more

Table - 4.2 contd..2..

1	2	3	4	5	6	7	8	9	10	11	12	13	14
1966													
ind:Average	5.0	8.2	11.5	17.0	15.6	11.4	12.6	8.2	11.7	10.1	8.9	7.3	10.6
Maximum	21	32	27	36	45	41	38	34	40	33	24	27	45
emp:Average	-1.7	-4.8	-7.2	-14.2	-13.2	-17.8	-19.4	-20.9	-15.1	-15.9	-6.5	0.8	-11.5
Maximum	3.9	1.6	0.3	-1.9	-4.3	-4.9	-6.5	-9.5	-4.1	-7.5	0.6	5.0	5.0
Minimum	-8.5	-13.7	-18.7	-26.7	-25.9	-29.9	-33.5	-34.3	-33.3	-26.5	-16.3	-8.7	-34.3
1967													
ind:Average	4.5	5.6	11.1	13.9	12.4	13.2	10.9	10.5	10.1	8.1	8.2	6.7	9.6
Maximum	20	23	30	34	35	33	38	38	30	30	39	30	38
emp:Average	0.8	-4.9	-7.6	-10.5	-12.0	-14.6	-17.4	-18.2	-18.2	-12.2	-5.4	-1.0	-10.1
Maximum	8.3	2.7	2.3	-2.7	-3.1	-5.4	-6.7	-8.1	-4.5	-0.4	2.6	8.2	8.3
Minimum	-8.9	-14.2	-22.1	-22.0	-22.5	-26.5	-31.5	-35.1	-30.5	-21.6	-17.8	-11.3	-35.1
1968													
ind:Average	6.2	9.2	13.3	13.3	15.1	13.3	10.6	11.3	9.8	9.9	8.5	5.6	10.5
Maximum	30	34	35	37	42	43	35	42	38	36	40	40	43
emp:Average	-0.7	-4.2	-7.3	-10.3	-13.0	-16.0	-18.8	-16.9	-19.2	-13.5	-6.5	-2.5	-10.7
Maximum	7.1	5.2	0.1	1.6	-1.5	-2.0	-5.9	-8.0	-7.8	-3.5	3.5	3.5	7.1
Minimum	-8.2	-14.3	-16.2	-18.7	-23.2	-24.0	-29.2	-32.7	-30.5	-29.2	-16.8	-10.1	-32.7
1969													
ind:Average	6.7	8.2	13.0	12.8	14.0	14.7	9.6	9.7	9.4	10.1	8.6	5.4	10.0
Maximum	30	36	36	36	48	46	39	43	41	38	33	25	48
emp:Average	0.0	-2.4	-7.4	-11.2	-14.2	-14.5	-18.3	-21.9	-18.6	-13.2	-6.6	-1.0	-10.7
Maximum	8.4	3.9	0.9	-1.0	-4.3	-5.8	-9.4	-10.4	-6.2	-3.4	2.9	7.4	8.4
Minimum	-9.8	-12.5	-18.4	-23.3	-25.1	-24.0	-36.4	-36.7	-30.2	-25.3	-19.3	-13.8	-9.8

Table - 4.2 contd...3

	2	3	4	5	6	7	8	9	10	11	12	13	14
1970													
d: Average	5.8	8.2	10.9	14.7	12.0	13.8	11.8	9.4	10.4	12.6	9.8	7.0	10.5
Maximum	28	33	27	34	34	44	51	44	48	52	37	32	52
p: Average	-0.7	-4.4	-5.8	-10.7	-14.3	-17.0	-17.3	-20.6	-20.0	-12.0	-6.4	11.1	-10.9
Maximum	6.7	1.6	2.8	-2.5	-4.9	-7.1	-5.3	-7.7	-8.6	-1.3	1.6	7.3	7.3
Minimum	-9.8	-14.1	-17.8	-20.0	-27.4	-28.7	-36.2	-34.0	-33.4	-28.3	-19.1	-12.7	-36.2
1971													
d: Average	5.3	10.3	12.6	11.6	13.9	12.6	13.6	11.9	11.3	10.0	8.2	4.8	10.5
Maximum	30	35	33	29	42	33	44	35	39	35	31	33	44
p: Average	-0.4	-2.8	-8.9	-12.6	-17.2	-17.9	-19.6	-19.1	-16.3	-12.6	-7.5	0.1	-11.3
Maximum	7.0	3.6	-0.5	-1.6	-5.8	-5.1	-6.1	-6.7	-5.6	-3.4	3.1	7.2	7.2
Minimum	-9.5	-12.7	-18.2	-22.6	-29.7	-35.2	-31.6	-32.8	-29.3	-23.8	-18.4	-8.9	-35.2

Table - 4.3

Extreme surface meteorological results at Molodezhnaya, Antarctica

No.	Meteorological Parameter	Value	Date
1	2	3	4
	Maximum of the mean temperature recorded during a month	0.8°C	January 1967
	Minimum of the mean temperature recorded during a month	-22.8°C	July 1965
	Maximum temperature recorded	8.5°C	December 30, 1963
	Minimum temperature recorded	-37.5°C	September 8, 1965
	Maximum of the mean atmospheric pressure recorded during a month	997.8 mb	July 1964
	Minimum of the mean atmospheric pressure recorded during a month	966.0 mb	October 1965
	Maximum atmospheric pressure recorded	1017.2 mb	June 7, 1964
	Minimum atmospheric pressure recorded	936.3 mb	September 8, 1969
	Maximum atmospheric pressure increase during three hours	23.8 mb	September 8, 1969
	Maximum atmospheric pressure decrease during three hours	22.3 mb	June 27, 1966

more

Table – 4.3 contd..2..

2	3	4
Maximum of the mean wind speed recorded during a month	17.0 m/s	April 1966
Minimum of the mean wind speed recorded during a month	4.5 m/s	January 1967
Maximum of wind speed recorded	39 m/s	April 12, 1963
Maximum wind thrust (gust) recorded	48 m/s	August 24, 1963 & May 1, 1969
Maximum number of days with wind speed 15 m/s recorded month-wise.	30	May 1968
Maximum number of days with wind speed 30 m/s recorded month-wise	6	May 1968
Maximum number of clear days	13	December 1964 & July 1966
Maximum number of overcast days recorded during a month	23	August 1968

310 and 315 parts per million, about the same as other parts of the world. Total atmospheric ozone is at a maximum in spring, usually November, while the limited dark-season data indicate minimum during the winter. Dust and other pollutants are practically unknown.

The total of the incoming direct and diffuse solar radiation reaches values of 75-85 % of the solar constant depending on the altitude of the station. The high values are partly due to the Earth's being at perihelion (point of its orbit nearest the sun) during the Southern Hemisphere summer, but the clear and dry atmosphere and high elevation of Antarctica are important factors. However, as much as 80-90 % of the incoming short wave radiation is reflected by the snow surface. Only the upper 1-1.5 metres of the snow-cover absorb appreciable amounts of the solar energy and it is quickly lost again in the dark season because the dry atmosphere has little blanketing effect. Small amounts of cloud do not appreciably reduce the total amount of solar radiation reaching the surface, since there is a high multiple reflection caused by the snow surface and the underside of the clouds. In some cases this can even raise the total of the direct and diffuse radiation reaching the surface to a value higher than that of the solar constant, i.e. the amount of radiation from the sun reaching the top of the atmosphere. The albedo, or

reflectivity of the snow surface varies from about 75 to 90 %
and the values tend to be lowest after periods of ablation
(e.g. sublimation, melting, evaporation) and wind erosion ,
and highest after fresh snow-fall. The albedo has a seasonal
as well as shorter period variation.

The mean annual temperature isotherms over Antarctica
generally approximate the terrain contours with warmer temp-
eratures near the low-lying coast and the coldest temperatures
on the high plateau in the interior of East Antarctica, which
averages between 790-1100 metres higher than the South Pole
elevation of 2800 metres. The annual mean on the plateau is
about $-56^{o}C$ and temperatures below $-80^{o}C$ are very common as
is obvious from Table 4.4. The lowest temperature ever
observed in the world is $-88.3^{o}C$ which was recorded at
Vostok ($78^{o}28'S$, $106^{o}48'E$, 3488 m above M.S.L.), the
geomagnetic South Pole. Although it is the world's coldest
continent, Antarctica is not uniformly cold. Variations in
the atmospheric circulation bring about considerable
differences in temperature, both in time and in space. The
minimum temperatures at one place do not always occur during
the same month from one year to another, and places several
hundred miles apart may be under completely different
temperature regimes at the same time. A rise and fall of
as much as $8^{o}C$ in the monthly mean temperature can take place

in successive months during the winter. Under conditions of large-scale flow of air from the oceans to the continent, a rise of as much as 14°C in one day can occur. Increased cloudiness inhibits the loss of heat by radiation from the snow surface as well as increase the amount of heat radiated downward to the snow surface.

The main supply of heat to Antarctica in winter is the warm air carried by the atmospheric currents. The first strong radiational cooling in winter causes an early winter temperature minimum, but the atmosphere reacts to it by changing its circulation to bring in the warmer air. Finally, at the end of the winter radiational cooling again becomes dominant and late winter minimum temperatures are noted usually just before the return of the sun. The cyclonic storms that move around Antarctica often pass through the West Antarctica highland and even across the South Pole, but only rarely over the higher plateau of East Antarctica. The exchange of air horizontally in the levels from about 2440-4570 m is such that a temperature fall of only about 8°C is noted in the monthly mean values from summer to winter. The very lowest layers of the atmosphere lose heat by radiation and by contact with the snow surface. The result in these cases is inversion i.e. the temperature increases with height and a gradient of 28°C in 305 m is not uncommon as is obvious from Table 4.4.

Table - 4.4

Surface meteorological results in 1972 at the Antarctic stations :

I – Bellingshausen (62°12'S, 58°56'W)

II – Mirny (66°33'S, 93°01'E)

III – Molodezhnaya (67°40'S, 45°51'E)

IV – Leningradskaya (69°30'S, 154°23'E)

V – Novolazarevskaya (70°46'S, 11°50'E)

VI – Vostok (78°28'S, 106°48'E at 3488 m above M.S.L.)

Station	Atmospheric pressure (mb)			Air temperature (°C)			Wind speed (m/s)		Max gust (m/s)	Relative humidity (%)	Average cloudiness (units/ten)
	Mean	Max	Min	Mean	Max	Min	Mean	Max			
2	3	4	5	6	7	8	9	10	11	12	13
I	995.2	1009.7	975.4	1.1	5.8	– 2.3	7.5	34	40	84	9.2
II	993.9	1002.6	977.5	– 0.3	5.9	– 7.3	9.5	23	32	73	7.5
III	988.3	1004.3	980.7	0.2	7.0	– 7.1	4.5	17	21	63	7.4
IV	956.5	970.7	940.2	– 2.7	2.8	– 7.4	12.4	29	41	92	9.3
V	981.9	992.2	974.3	– 0.8	5.1	– 7.6	4.1	14	22	63	7.2
VI	638.2	648.4	627.2	–31.1	–21.5	–41.2	3.7	8	14	74	4.0
I	993.3	1006.0	974.3	0.6	5.8	– 4.6	7.1	22	30	88	9.8
II	988.5	1010.5	972.2	– 4.8	2.7	–17.9	8.6	18	25	74	5.9
III	985.2	1005.6	974.9	– 3.4	4.7	–11.6	7.9	29	34	60	8.0
IV	952.1	969.6	936.9	– 6.1	1.2	–14.7	9.1	29	38	78	7.7
V	977.2	995.5	956.8	– 3.0	4.3	–12.8	8.1	22	35	46	5.1
VI	630.9	949.5	616.3	–44.9	–26.6	–61.0	4.8	8	12	72	3.7

Table - 4.4 contd..2..

2	3	4	5	6	7	8	9	10	11	12	13
I	991.9	1009.2	977.1	0.0	6.2	-6.6	7.5	17	23	89	9.7
II	984.2	1000.6	977.9	-9.4	0.4	-19.1	10.8	20	32	82	6.5
III	986.4	1000.3	967.6	-9.3	0.7	-19.5	12.1	22	28	60	7.6
IV	953.0	964.8	939.4	-11.3	-3.4	-21.8	9.8	35	44	67	7.7
V	979.4	989.5	959.6	-8.7	0.9	-19.0	9.8	21	29	46	9.4
VI	927.9	646.5	615.7	-57.7	-47.8	-66.0	5.7	10	14	70	3.8
I	989.5	1011.9	954.9	-2.7	4.3	-11.9	7.5	18	30	86	9.1
II	992.2	1011.5	970.4	-12.5	2.6	-23.9	13.1	28	40	78	7.1
III	989.2	1003.7	959.7	-10.5	0.0	-21.6	13.3	34	41	64	7.4
IV	954.0	969.8	936.3	-13.2	-3.7	-24.4	10.9	38	47	76	9.2
V	979.2	990.4	963.4	-9.8	-4.3	-22.2	12.0	28	40	50	5.9
VI	627.7	641.3	618.5	-65.0	-53.5	-73.5	5.7	10	14	69	3.8
I	994.8	1016.4	962.7	3.7	3.7	-14.6	7.2	20	26	87	9.2
II	990.3	1012.4	971.3	-19.8	8.7	-29.4	11.1	19	27	74	4.0
III	987.0	1002.3	966.2	-15.3	-4.0	-28.7	12.7	32	41	69	7.5
IV	951.0	968.0	932.3	-19.1	-8.8	-29.6	8.1	30	38	63	5.4
V	977.4	995.2	960.2	-14.2	-3.1	-27.4	10.6	30	43	50	6.5
VI	622.3	633.7	615.0	-65.8	-49.5	-75.7	5.5	10	15	68	5.0
I	995.2	1018.5	968.0	-7.2	0.7	-22.2	7.4	16	24	86	8.7
II	989.6	1006.9	972.5	-12.2	2.8	-26.2	13.2	31	47	88	8.1
III	990.5	1007.0	965.9	-17.4	-4.4	-29.9	15.2	35	41	59	7.2
IV	957.1	978.9	936.8	-18.2	-6.4	-32.4	7.7	31	32	64	5.7
V	980.4	996.7	957.5	-13.2	-4.9	-24.5	14.1	37	59	48	6.4
VI	630.8	642.0	614.6	-66.4	-37.8	-78.0	5.5	17	22	68	3.0
I	991.6	1008.6	969.0	5.8	1.3	-19.7	8.6	20	28	88	9.1
II	989.3	1008.8	969.5	-16.7	3.4	-33.8	13.0	27	38	79	5.4
III	984.3	996.8	970.2	-18.3	-7.1	-31.6	8.9	24	28	67	8.1
IV	951.6	967.2	930.1	-18.7	1.2	-33.7	9.4	35	52	69	6.3
V	981.0	997.8	969.7	-22.0	-11.0	-35.4	6.5	15	25	38	3.8
VI	622.2	644.4	606.9	-68.8	-52.7	-80.7	5.5	11	14	68	2.7

Table – 4.4 contd...3...

2	3	4	5	6	7	8	9	10	11	12	13
I	1002.5	1029.1	980.1	-10.0	0.4	-24.8	6.3	17	31	89	8.6
II	985.6	1016.3	957.1	-12.3	-3.2	-26.4	14.8	30	38	81	5.2
III	988.2	1006.7	965.5	-14.9	-3.2	-35.8	10.4	30	34	71	7.2
IV	957.1	971.1	938.3	-21.6	-7.5	-35.6	7.2	24	40	64	5.7
V	967.3	998.6	954.7	-14.1	-5.6	-31.6	15.0	40	60	50	8.1
VI	630.6	653.5	614.2	-61.6	-34.9	-78.6	5.6	11	16	70	5.2
I	989.9	1015.9	958.3	-4.5	0.9	-17.8	7.8	19	29	91	9.3
II	983.6	1010.8	962.6	-18.1	-3.7	-31.2	11.2	31	37	73	5.0
III	982.3	1015.2	957.1	-15.2	-3.4	-30.6	10.8	35	39	72	8.3
IV	946.4	970.9	928.4	-19.8	-6.5	-29.3	9.3	25	39	75	6.5
V	969.3	991.9	964.7	-14.8	-5.6	-24.0	12.9	32	47	50	6.5
VI	621.2	639.7	604.7	-62.4	-39.5	-76.6	5.1	11	16	70	4.5
I	996.2	1017.9	962.6	2.4	2.7	-10.4	6.4	17	24	88	9.3
II	977.4	1003.4	954.7	-17.2	-3.4	-29.4	8.8	20	26	69	4.7
III	978.3	1002.8	947.7	-13.6	-1.5	-26.5	9.7	26	31	69	8.4
IV	938.6	954.1	923.1	-19.6	-8.5	-32.6	6.4	28	38	67	6.8
V	982.3	1001.4	963.0	-14.6	-4.1	-27.5	10.4	30	54	50	6.4
VI	615.8	637.1	604.5	-56.6	-38.4	-77.1	6.3	11	20	70	4.2
I	993.6	1013.5	972.6	-1.3	2.5	-7.2	7.0	20	27	84	9.2
II	985.3	1004.2	964.7	-8.4	-1.2	-18.6	9.0	23	31	70	5.6
III	976.7	985.6	956.0	-7.5	-1.6	-16.5	8.3	21	37	62	7.5
IV	948.4	960.2	930.7	-11.2	-5.3	-21.2	7.2	30	40	73	7.2
V	991.3	1001.7	970.7	-8.7	-1.6	-17.8	8.5	32	39	55	6.2
VI	623.4	632.2	616.8	-46.4	-29.8	-60.3	5.8	17	29	68	5.3
I	994.8	1010.3	983.5	-0.7	3.4	5.4	7.7	22	30	80	9.1
II	993.5	1005.2	984.2	-1.8	5.6	9.3	9.1	25	33	71	6.0
III	987.6	1001.3	975.6	-0.3	7.2	8.9	4.8	20	23	64	5.1
IV	957.9	969.2	941.4	-5.5	-0.5	-10.0	9.6	26	32	80	8.0
V	003.1	1003.5	980.7	-0.8	4.7	7.7	6.6	24	34	58	6.5
VI	636.2	644.1	630.2	-30.7	-21.3	-42.4	6.2	14	14	72	5.0

t

The air trajectory and the contrast between ocean and continental underlying surface are the principal factors in the development of weather at a given spot as a result of which cyclones on the polar front attain great intensity and size. The great storms and blizzards of long duration are related to deep disturbances extending in many cases from sea level to the tropopause (located at about 10 km) . Storms of blowing snow accompany the disturbances and even persist for some hours after the passage of initial storms. The shallow storms tend to move quickly around the periphery of the continent and are not related to the large-scale planetary waves in the atmosphere. The large storms move in arc-like, clockwise trajectories, generally from the north-west to the southeast and remain north of the coastline in most cases. The high level of the continent, the strong gravitational outflow of the cold air in contact with the surface and the procession of storms act against the formation of large polar anticyclones, although the sea level pressure at some coastal stations has gone above 1035 milibars. Some of the cold anticyclones have provided sufficient cold air both from West Antarctica and from East Antarctica to reach other Southern Hemisphere continents, although much modified by over water trajectories of several thousand kilometeres.

The jet stream, the core of winds of maximum velocity, found usually just below the tropopause and in regions of maximum horizontal temperature gradient, tends to broaden its latitudinal extent and strengthen in winter and tends to narrow and weaken in summer. Surface winds frequently attain speeds of 160 km per hour or more during the passage of storms along the coast of East Antarctica as is obvious from the Tables 4.1 to 4.4. The temperature field along the steep slopes of the continent affects the horizontal temperature gradient and thus modifies the **winds** in these cases. Along low-lying coastlines, the maximum force of wind is usually less. The extension of the 'effective' continent as much as 6° of latitude farther north of its summer coastline comes about through the freezing of the surface layers of the ocean in winter. This inhibits the vertical exchange of heat between ocean and atmosphere and also provides a longer continental trajectory for the air of oceanic origin that reaches the continent. This is one reason for lower average cloudiness in winter than in summer.

The condensation of water vapour carried in the air not only adds to the snow cover but also contributes about 14 % of the net heat energy transported by the atmosphere. It is estimated that on an average about 12-20 cm of water equivalent are deposited in the form of snow over Antarctica

in one year. The coastal regions have up to ten or more times the 2-inch snow fall (water equivalent) deposited on the interior of Antarctica, the polar ice-cap. During the winter lot of snow is accumulated over the South Polar Ice-Cap and the camps of the wintering teams are often burried under the snow. It is due to the frequent blizzards and snow drift.

4.3   Tropospheric and Stratospheric winds over Antarctica

While the author was the Project Scientist in Antarctica, sixty M-100 meteorological rockets were launched from Molodez- hnaya in 1972 out of which 52 flights were successful and 16 of them carried chaff also. A summary of all the 52 successful M-100 rocket soundings carried out from Molodezhnaya, Antarctica in 1972 is given in Table 4.5. Time-height cross sections of the zonal and the meridional components of winds data are drawn in Figs. 4.2 and 4.3 using the conventional linear interpolation method. For showing the seasonal reversal of stratospheric winds, Webb (1964) calculated an average flow over a layer 10 km thick centred at 50 km between 45 and 55 km and called it Stratospheric Circulation Index (SCI). Using the same method average values of the zonal and meridional components of winds are computed for the

Table – 4.5

Summary of the successful M-100 meteorological rocket launchings from Molodezhnaya, Antarctica in 1972 showing the Meridional (NS) and Zonal (EW) components of Tropospheric and Stratospheric Circulation Indices (TCI & SCI) respectively

Date	Time (GMT)	Rocket apogee (km)	Wind track (km)	Components (m/s)	5-15km TCI$_{10}$	15-25km TCI$_{20}$	25-35km SCI$_{30}$	35-45km SCI$_{40}$	45-55km SCI$_{50}$
1	2	3	4	5	6	7	8	9	10
Jan 5	1450	82.80	80-10	NS	-0.8	-1.6	1.5	-0.2	-1.1
				EW	1.7	4.6	-13.3	-15.8	-33.6
Jan 12	1425	86.00	48-10	NS	-7.5	-1.5	-2.4	-11.8	N/A
				EW	3.7	4.2	9.2	-7.5	N/A
Jan 19	1440	84.65	84-10	NS	-4.5	-2.3	0.6	0.9	N/A
				EW	9.1	5.2	8.5	8.8	N/A
Jan 26	1435	88.03	86-10	NS	-5.3	-3.6	1.0	5.4	4.3
				EW	3.1	2.1	5.4	-12.8	-27.3
Average	-----	85.37	-----	NS	-4.5	-2.3	0.2	-1.4	1.6
				EW	4.4	4.0	9.1	-11.2	-30.5
Feb 2	1448	90.94	48-10	NS	8.8	-0.5	-10.6	4.8	N/A
				EW	6.0	0.2	-13.4	-21.1	N/A
Feb 16	1535	83.70	82-10	NS	-5.5	-0.9	0.5	-4.5	-19.3
				EW	5.1	1.5	-2.9	6.8	27.8

more

Table – 4.5 contd..2..

1	2	3	4	5	6	7	8	9	10
Feb 23	1530	84.14	55–10	NS	– 4.4	0.3	4.6	– 4.4	–23.7
				EW	–10.8	– 0.2	– 3.8	15.1	35.2
Average)	----	86–26	----	NS	– 0.4	– 0.4	– 1.8	– 1.4	–21.5
				EW	– 3.9	0.5	6.7	0.3	31.5
Mar 8	1506	88.80	60–10	NS	0.7	– 4.1	3.8	7.1	– 1.5
				EW	4.3	3.0	9.1	22.5	50.9
Mar 22	1500	90.84	49–10	NS	8.9	8.3	6.2	–10.5	N/A
				EW	1.5	9.1	13.3	31.9	N/A
Mar 29	1500	84.00	60–10	NS	6.3	5.4	1.5	– 6.2	–21.3
				EW	14.1	8.2	13.4	26.7	45.3
Average)	----	87.79	----	NS	– 0.6	– 2.3	– 2.8	– 3.2	–11.4
				EW	6.6	6.8	11.9	27.0	48.1
Apr 5	1400	87.85	57–10	NS	– 7.5	– 0.6	– 0.4	– 0.1	–46.3
				EW	6.4	9.0	13.0	25.0	48.2
Apr 12	1400	77.40	57–10	NS	8.1	–0.1	– 6.9	–36.0	–11.8
				EW	25.1	20.7	25.6	55.9	64.9
Apr 19	1405	94.90	40–10	NS	2.5	– 2.8	1.6	N/A	N/A
				EW	0.3	9.2	29.1	N/A	N/A
Average)	----	86.72	----	NS	1.0	– 1.2	– 1.9	–18.1	–29.1
				EW	10.6	13.0	22.6	40.5	56.6

Table - 4.5 contd...3

1	2	3	4	5	6	7	8	9	10
y 3	1400	88.00	84–10	NS	11.8	1.9	-0.1	9.9	7.9
				EW	4.9	21.3	27.9	47.3	42.4
y 10	1405	87.67	55–10	NS	-1.5	1.1	6.4	-10.3	6.2
				EW	18.3	30.7	44.0	64.7	62.1
y 17	1750	87.94	84–10	NS	11.7	8.7	-1.4	-3.5	-8.1
				EW	17.3	28.1	43.0	49.8	32.8
y 20	1855	92.50	60–10	NS	-0.6	-0.3	0.5	-4.5	4.2
				EW	10.7	32.0	43.4	37.5	40.5
y 24	1400	91.20	57–10	NS	2.0	2.2	0.1	-3.8	-12.5
				EW	10.9	25.1	38.7	54.1	56.9
y 31	1435	90.90	50–10	NS	24.1	23.5	13.8	3.1	N/A
				EW	15.9	35.5	52.4	65.3	N/A
(Average)	----	89.96	----	NS	4.0	6.2	3.2	-1.5	-0.5
				EW	13.0	28.8	41.6	53.1	46.9
ne	1407	90.40	56–10	NS	9.0	2.4	5.6	3.6	-8.1
				EW	26.6	39.8	59.0	63.2	49.7
ne 28	1405	88.40	84–10	NS	-4.9	1.1	1.5	-1.5	7.4
				EW	9.2	39.9	53.0	45.9	55.5
(erage)	----	90.55	----	NS	2.1	1.8	3.6	1.1	-0.4
				EW	17.9	39.9	56.0	54.6	52.6
ly 1	1400	94.00	57–10	NS	-2.5	-11.5	-21.1	-16.3	-44.7
				EW	18.5	44.7	63.1	56.6	77.6
ly 5	1400	86.70	84–100	NS	-3.2	-11.6	-22.2	-13.8	-1.9
				EW	5.2	28.5	52.8	66.6	57.0

more

Table - 4.5 contd...4

1	2	3	4	5	6	7	8	9	10
July 12	1400	88.30	40-10	NS EW	-0.7 6.7	2.2 13.9	-18.9 34.8	N/A N/A	N/A N/A
July 19	1400	85.30	84-10	NS EW	-6.5 7.8	-1.3 31.7	-7.4 50.4	-13.3 38.7	-5.5 52.5
July 22	1400	91.02	60-10	NS EW	-2.7 3.0	0.3 17.0	-7.3 34.6	-5.2 38.5	25.3 40.3
July 26	1400	86.25	60-10	NS EW	-3.1 11.1	1.7 22.3	10.6 35.7	6.5 55.4	-14.4 52.7
Average)	---	88.60	---	NS EW	-3.1 8.7	-3.4 26.4	-11.1 45.2	-8.4 51.2	-8.2 56.0
ug 2	1400	93.65	55-10	NS EW	-11.1 8.7	-6.7 50.4	8.4 89.5	10.6 95.0	-6.8 69.6
ug 6	1400	88.47	55-10	NS EW	-9.4 8.7	-6.0 45.9	8.8 88.9	-6.6 119.5	6.2 80.2
ug 9	1400	89.88	55-10	NS EW	-1.8 14.1	4.5 53.6	3.4 87.3	3.7 97.5	5.1 86.4
ug 16	1400	89.90	57-10	NS EW	-19.9 6.8	-9.1 24.0	-7.2 38.0	-22.7 67.0	-10.4 55.4
ug 20	1350	92.18	55-10	NS EW	-13.3 3.9	-4.1 48.7	6.1 74.0	11.1 57.5	-28.6 32.2
ug 23	1405	87.57	56-10	NS EW	-22.4 6.5	-6.7 40.3	7.5 70.0	12.7 78.2	-3.3 82.2
ug 30	1410	90.03	62.10	NS EW	-0.3 8.1	-7.1 46.8	-25.4 81.8	-23.0 93.0	-18.1 63.8

more

Table - 4.5 contd..5

1	2	3	4	5	6	7	8	9	10
(Average)	---	90.24	---	NS	-11.2	-5.0	0.2	-3.5	-8.0
				EW	8.1	44.2	75.6	86.8	67.1
Sept 6	1400	88.44	82-10	NS	-2.5	-6.3	-9.4	-19.6	-33.5
				EW	12.9	48.2	67.1	67.1	64.4
Sept 13	1400	88.58	45-10	NS	-14.3	-19.1	-1.4	-0.5	N/A
				EW	6.8	24.5	-3.8	-1.7	N/A
Sept 20	1405	86.55	66-10	NS	-8.4	-2.0	-10.3	-30.7	-63.2
				EW	15.8	35.7	47.0	39.5	-6.5
Sept 27	1400	93.50	60-10	NS	-7.7	-11.1	-12.6	-25.0	-13.8
				EW	17.5	29.5	48.5	69.9	71.7
(Average)	---	89.27	---	NS	-8.2	-9.6	-8.4	-19.0	-36.8
				EW	13.3	34.5	39.7	43.7	43.2
Oct 4	1353	86.50	80-10	NS	-13.3	-5.5	4.0	-0.4	7.8
				EW	3.7	11.9	87.5	75.6	83.8
Oct 11	1430	92.64	55-10	NS	2.5	-5.1	-39.1	-49.6	-35.1
				EW	12.4	19.9	28.9	19.5	-21.1
Oct 18	1425	88.28	63-10	NS	-5.7	-2.3	8.2	-2.1	-13.0
				EW	-4.1	47.3	92.2	67.5	-15.1
Oct 25	1443	88.62	60-10	NS	-7.0	-15.5	5.5	20.0	25.8
				EW	29.3	49.5	41.2	-9.8	-27.6
(Average)	---	89.01	---	NS	-5.9	-7.1	-5.4	-8.0	-3.6
				EW	10.3	32.2	62.5	38.2	12.6

more

Table - 4.5 contd...6

1	2	3	4	5	6	7	8	9	10
Nov 15	1426	89.10	60–10	NS	1.9	-2.5	-11.1	-1.5	-9.4
				EW	2.9	11.9	-1.9	8.2	33.0
Nov 22	1430	90.84	60–10	NS	10.0	9.4	-3.0	-0.3	36.8
				EW	10.0	10.2	-6.2	-9.0	-15.1
Nov 29	1430	91.80	60–10	NS	2.4	-2.0	-1.6	1.0	14.1
				EW	1.3	10.8	-3.0	-13.0	-17.1
Average	---	90.58	---	NS	4.8	1.6	0.1	-0.3	13.8
				EW	4.7	11.0	-3.7	-4.6	0.3
Dec 6	1430	87.91	56–10	NS	-10.8	-2.3	-2.5	-2.9	-7.4
				EW	-1.1	-6.1	-8.6	-11.6	-10.7
Dec 13	1430	87.60	60–10	NS	-4.3	1.0	5.6	-7.5	-18.3
				EW	5.5	3.2	-4.1	-27.5	-22.7
Dec 20	1430	81.98	80–10	NS	-7.9	-1.6	-0.3	0.5	-1.5
				EW	-2.0	-4.4	-10.5	-14.7	-21.5
Dec 27	1400	86.80	55–10	NS	-12.1	-3.3	-2.6	6.9	20.8
				EW	-7.3	-0.4	-9.1	-16.6	-16.6
Average	---	86.07	---	NS	-8.8	-1.6	0.1	-0.8	-1.6
				EW	-1.2	-1.9	-8.1	-17.6	-17.9

layers centred at 10, 15, 20, 30, 40, 45 and 50 km between 5-15, 10-20, 15-25, 25-35, 35-45, 40-50, and 45-55 km, respectively and termed as Tropospheric Circulation Index (TCI) up to 25 km and Stratospheric Circulation Index (SCI) aloft, up to 55 km. The circulation indices TCI_{10}, TCI_{20}, SCI_{30}, SCI_{40}, and SCI_{50} in which suffix indicates the centre of the layer are given in Table 4.5. The Tropospheric Circulation Index for the layer between 10-20 km centred at 15 km (TCI_{15}) and the Stratospheric Circulation Index for the layer between 40-50 km centred at 45 km (SCI_{45}) are plotted in Fig.4.4 which give the seasonal reversal of the tropospheric and the stratospheric winds. Data for the altitude region from surface to 10 km was taken from the balloon soundings which preceded each rocket flight.

4.3.1   Zonal Winds

Fig. 4.2 shows that the zonal winds over Molodezhnaya, Antarctica in 1972 were predominantly easterly in the southern summer (December to February) and westerly in the winter (June to August) with reversal of winds from easterly to westerly during autumn (March to May) and from westerly to easterly during spring (September to November). The winds in the lower troposphere up to an altitude of about 5 to 10 km were predominantly easterly throughout the year with speed less than 24 ms^{-1}. In December and February during summer,
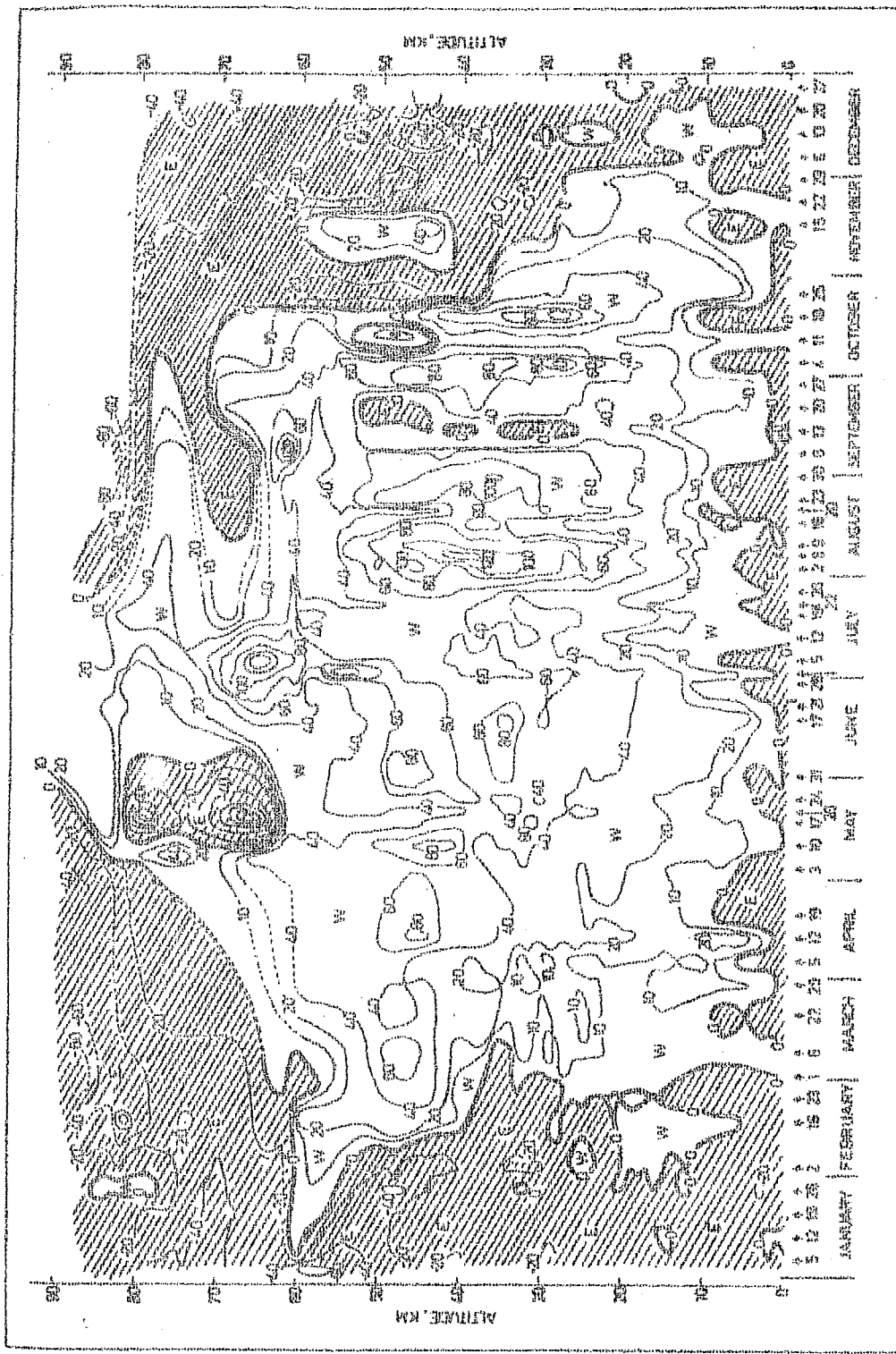
(Fig. 4.2)

The height cross section of the zonal wind component (m/s) at Molodezhnaya, Antarctic in 1972. Positive components are the westerly winds, while negative components shown by shaded areas are the easterly winds. Dashed lines present extrapolated data. Arrows above the abscissa show the days on which the data were obtained.
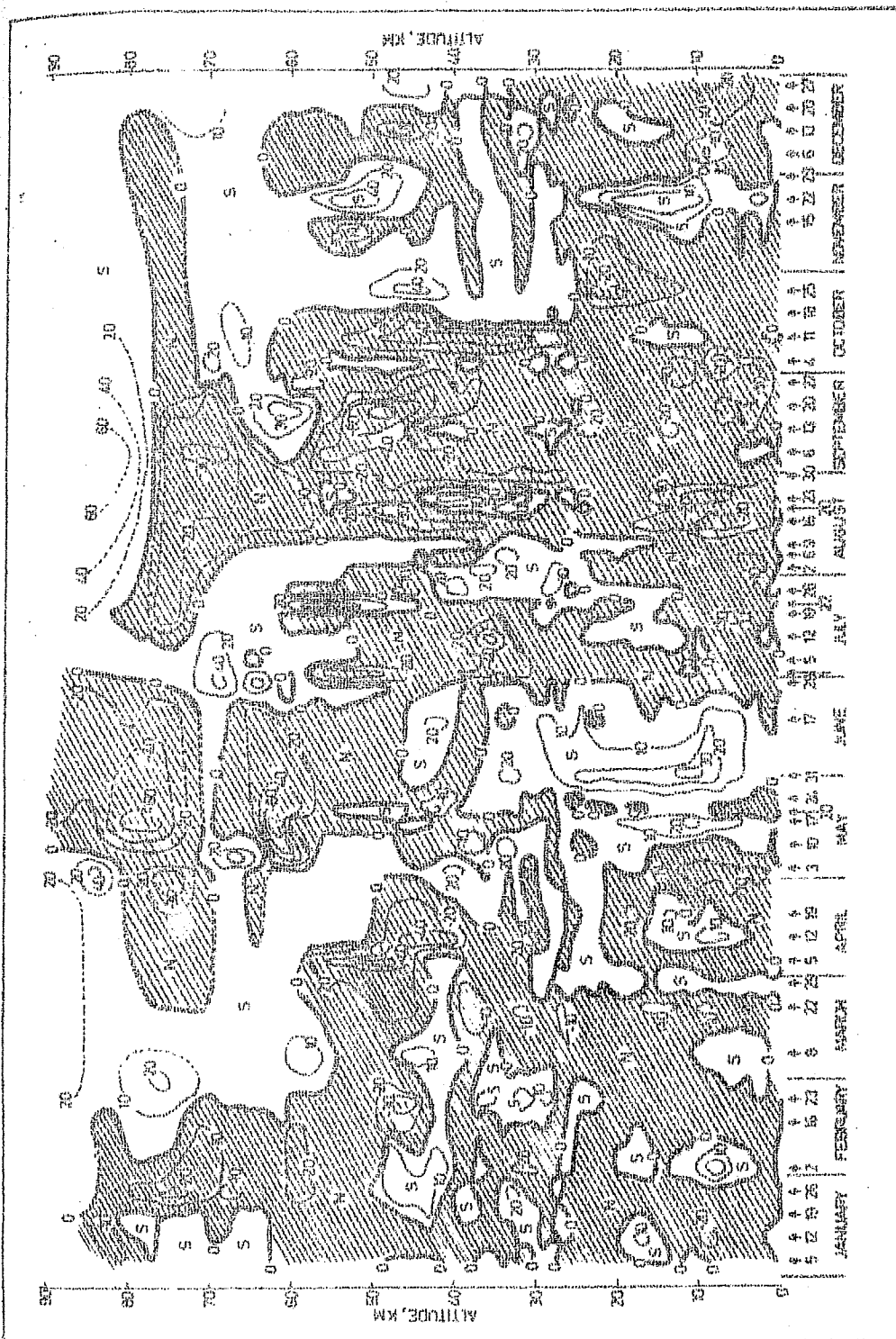
a core of weak westerly winds with speed less than 9 ms^{-1} was detected in an altitude region from 4 to 20 km which extended up to 30 km in mid-December. In February there was a strong westerly flow with wind speed less than 49 ms^{-1} in an altitude region from 40 to 60 km which became weaker as it ascended. During the summer the stratospheric easterlies had a maximum speed of 53 ms^{-1} at 45 km in mid-December. The summer easterly flow in the upper atmosphere up to 60 km was completely replaced by westerly winds during the autumn period (March to May) with a maximum speed of 97 ms^{-1} at 49 km in May end.

In the southern winter (June to August) the zonal winds were westerly throughout the atmosphere with jet speeds in the stratosphere. The stratospheric westerly jet attained a maximum speed of 139 ms^{-1} at 40 km in early August with a secondary maximum of 101 ms^{-1} at 36 km in August end. During the spring period (September to November) the zonal winds were predominantly westerly with erratic easterlies of speed less than 40 ms^{-1} in an altitude region from 26 to 52 km in mid-September. A similar core of strong easterly winds was also detected in mid-October in the layer from 44 to 54 km which had a maximum speed of 47 ms^{-1} at 47 km. Fig. 4.2 shows that the reversal of westerlies to easterlies occurred in the upper mesosphere in early September and subsequently in the lower mesosphere and the upper stratosphere in late

October with complete reversal in the stratosphere by
November end. In Mid-November there was a core of strong
westerly winds with speeds ranging from 10 to 52 ms^{-1} in an
altitude region from 40 to 60 km. In early October during
the spring, the westerly winds attained jet speed in the
lower stratosphere with a maximum of 110 ms^{-1} at 28 km. It
is obvious from the Figure 4.2 that a normal reversal of winds
occurred in the Antarctic atmosphere with the transition from
winter to summer.

4.3.2   Meridional winds

Fig. 4.3 shows that the meridional components of winds
over Molodezhnaya, Antarctica in 1972 were of variable nature
with the northerly winds somewhat more predominant than the
southerlies which were erratically distributed. In the
southern summer (December to February) although the meridional
flow was predominantly northerly, it had some significant
cores of southerly winds throughout the atmosphere. The
southerly winds attained a maximum speed of 51 ms^{-1} at 48 km
in early February, while the northerlies had a maximum speed
of 52 ms^{-1} at 46 km in February end. Fig. 4.3 also shows that
in the summer the meridional winds in the stratospheric layer
from 40-50 km were predominantly southerly and in the mesosphere
northerly, particularly during February which attained speeds
raning from 5 to 25 ms^{-1} and changed to weak southerly in

Fig. 4.5

Fig.—The cross section of the meridional (N/S) and longitudinal (W/E) wind components above Antarctica. The zonal components are the southerly winds shown by shaded areas, while the negative components are the northerly winds. Dashed lines present extrapolated data. Arrows above the abscissa show the dates on which the data were obtained.

December. The autumn period (March to May) was again marked by erratic northerly and southerly winds which were weaker in the troposphere, relatively stronger in the stratosphere and strongest, in the mesosphere. The northerly components had a maximum speed of 56 ms^{-1} at 42 km in the stratosphere in mid-April, while in the troposphere the southerly compo- nents had a maximum speed of 34 ms^{-1} at 11 km in May end.

The meridional winds during the southern winter in June were predominantly southerly in the troposphere and stratosphere with speed less than 26 ms^{-1} and strong northerly in the mesosphere having speeds up to 60 ms^{-1}. In June end the tropospheric and stratospheric southerlies changed to northerly winds and attained a maximum speed of 54 ms^{-1} at 35 km in mid-July. The northerlies in the layer from 10 to 45 km again changed to southerly winds and attained a maximum speed of 30 ms^{-1} at 40 km in July end with a reversal to the northerlies around mid-August which had speeds ranging from 10 to 35 ms^{-1}. However, towards the end of August there was a core of southerly winds with speeds less than 35 ms^{-1} in an altitude region from 30 to 45 km.

From September to about mid-October during the spring the meridional flow was mainly characterised by northerly winds from surface up to 60 km with weaker winds in the troposphere and stronger in the stratosphere. Maximum wind

speed of the northerlies in the troposphere was found to be 22 ms^{-1} at 8 km in early October, while in the stratosphere it was 80 ms^{-1} at 48 km around mid-September. However, in the lower mesospheric region from 57 to 66 km there were southerly winds of speeds ranging from 3 to 32 ms^{-1} with a similar core of strength less than 10 ms^{-1} in the region from 9 to 18 km around mid-October. From about mid-October to mid-November during the spring, the meridional winds in the troposphere and the lower stratosphere up to 25 km were predominantly northerly with speeds less than 30 ms^{-1}, while aloft they were predominantly southerly having a maximum speed of 46 ms^{-1} at 45 km in October end. In November end also, similar southerly cores were detected, one having a maximum strength of 58 ms^{-1} at 52 km and another 17 ms^{-1} at 13 km. It is thus evident from the Figure 4.3 that in the southern spring (September to November) the meridional flow was primarily composed of northerly winds which changed to erratic southerlies in November as the summer approached.
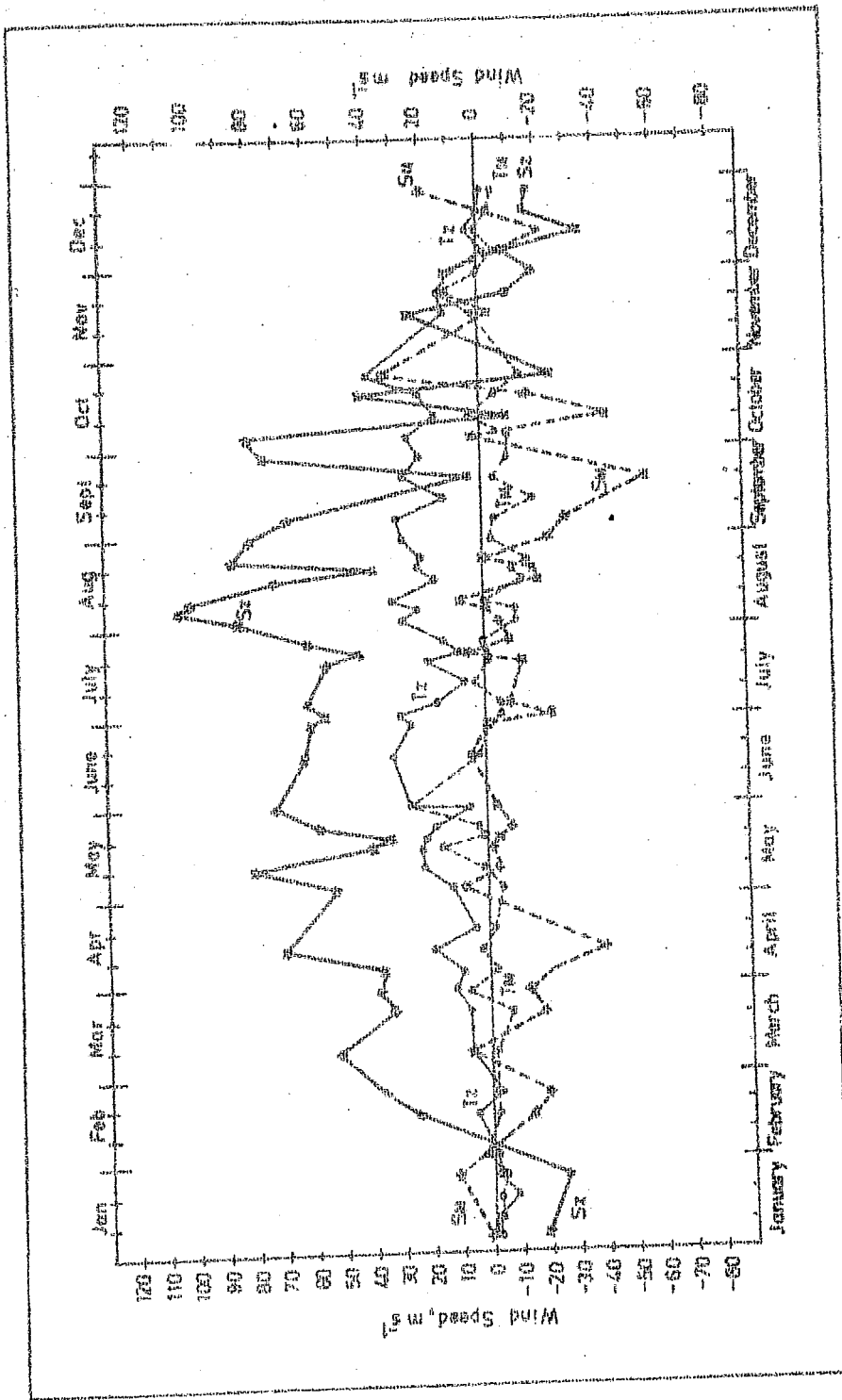
4.3.3   Tropospheric and Stratospheric Circulation Indices (TCI, SCI)

In order to study the seasonal reversal of winds over Molodezhnaya, Antarctic at different times, Tropospheric and Stratospheric Circulation Indices (TCI & SCI) were

computed using the method devised by Webb (1964)', The indices

for the layers 10 km thick centred at 10, 20, 30, 40 and

50 km are given in Table 4.5, while those for the layers

between 10-20 km and 40-50 km centred at 15 and 45 km,

respectively are illustrated in Fig. 4.4.

The solid curve (T_Z) passing through the solid circled

data points in Fig. 4.4 shows that the tropospheric zonal

circulation over Antarctica in 1972 was predominantly easterly

during the southern summer (December to February) having a

maximum speed of 8.1 ms^{-1} on January 19 and pronounced westerly

during the rest of the period having a maximum speed of

39.7 ms^{-1} on October 25. The reversal of the winds from the

summer easterlies to westerlies occurred in February end and

from the winter westerlies to easterlies around December 4.

The meridional circulation in the troposphere over Antarctica

given by the dashed curve (T_M) passing through the open

circled data points in Fig. 4.4 shows that the meridional flow

was of variable nature having an erratic distribution of

noertherly and southerly winds. The northerly components had

a maximum speed of 18.2 ms^{-1} on September 13, while the

southerlies had the maximum 25.9 ms^{-1} on May 31.

The solid curve (S_Z) passing through the cross marked

data points in Fig. 4.4 gives the zonal stratospheric

circulation index over Molodezhnaya, Antarctica in 1972.

(Fig 4.7)

Tropospheric and Stratospheric Circulation Indices at Molodezhnaya, Antarctica in 1972

T_z, T_m = Zonal and Meridional Components of the Tropospheric Circulation Index

S_z, S_m = Zonal and Meridional Components of the Stratospheric Circulation Index

It shows that the zonal winds in the stratosphere over Antarctica were completely easterly in December and January during the southern summer having a maximum speed of 35.7 ms^{-1} on December 13 and were pronounced westerly during the period from February to September with a maximum speed of 105.1 ms^{-1} on August 6 in the winter. From October to about mid-November during the spring, there were sudden reversals in the zonal winds indicating some significant changes in the stratospheric temperature distribution. The wind reversal from the summer easterlies to westerlies occurred around February 6 and from the winter westerlies to easterlies around November 20. The meridional circulation in the stratosphere over Antarctica is given by the dashed curve (S_M) passing through the crossed data points in Fig.4.4. It shows that the stratospheric meridional flow was also of variable nature with the northerly and southerly winds erratically distributed throughout the year. However, the northerlies were relatively more predominant which attained a maximum speed of 57.9 ms^{-1} on September 20, while the southerlies had a maximum speed of 33.8 ms^{-1} on October 25. During the spring period (September to November) there were sudden reversals of winds from northerlies to southerlies and vice versa which may be due to some perturbations in the stratospheric temperature distribution.

4.4   Upper mesospheric wind structure in Antarctica

Out of the sixty M-100 meteorological rockets launched from Molodezhnaya in 1972, sixteen of the 52 successful soundings carried an additional wind sensor chaff for determining the mesospheric winds. Most of the flights were successful and the average rocket apogee reached was 86.93 km. A summary of the chaff-borne flights, evenly distributed throughout 1972, is given in Table 4.6. The results derived for the region 50-90 km (mostly for the 60-80 km layer in the upper mesosphere) are presented here. This is the first meteorological study of the upper mesospheric winds carried out in Antarctica.

The chaff used consisted of cylindrical aluminium-coated glass fibres having a diameter of about 0.025 mm. About 400 g of chaff, in a special container divided into two parts, was ejected at rocket apogee. The descending chaff cloud was then tracked by a high sensitivity Meteor-2 radar. Table 4.6 gives the corresponding wind tracks of all such flights. At the time of ejection at rocket apogee, above 80 km, the chaff fell at a high speed, about 160 ms^{-1}, but as it descended further it slowed down to about 4 ms^{-1} at around 56 km because of the greater density and viscosity of the air at lower altitudes.

Table - 4.6

Summary of the 16 launchings of rockets containing a chaff sensor launched from Molodezhnaya, Antarctica, in 1972 showing the Meridional (NS) and Zonal (EW) Components of Mesospheric Circulation Index (MsCI)

Date	Time (GMT)	Rocket apogee (km)	Wind track (km)	Compo-nents.	60-70 km MsCi65 (9m/s)	65-75 km MsCI70 (m/s)	70-80 km MsCI75 (m/s)	75-85 km MsCI80 (m/s)
1	2	3	4	5	6	7	8	9
Jan 5	1450	82.80	80-62	NS EW	N/A N/A	6.1 -40.1	2.4 -41.5	N/A N/A
Jan 19	14.0	84.65	84-64	NS EW	N/A N/A	3.3 -38.2	5.5 -29.3	-2.5 -16.4
Jan 26	1435	88.03	86-62	NS EW	N/A N/A	-14.9 -33.3	-16.4 -13.1	-6.7 6.2
Feb 16	1535	83.70	82-60	NS EW	-3.4 -21.2	-2.6 -26.7	5.1 -30.5	N/A N/A
Mar 1	0330	87.50	86-56	NS EW	9.3 -12.4	9.3 -26.3	14.5 -33.9	12.8 -46.0
May 3	1400	88.00	84-56	NS EW	1.9 29.0	-12.7 11.3	-24.2 2.3	6.4 -21.1

more

Table – 4.6 :contd..2..

1	2	3	4	5	6	7	8	9
May 6	1410	91.50	90–58	NS	3.4	20.9	-3.9	-6.2
				EW	45.0	27.7	33.0	19.6
May 17	1750	87.94	84–56	NS	-31.1	-17.8	-50.1	-44.0
				EW	-61.5	-57.0	-37.5	9.5
June 21	1400	92.85	88–56	NS	-5.8	-8.1	-18.2	-25.6
				EW	54.2	34.2	13.6	14.0
June 28	1405	88.40	84–54	NS	29.7	23.0	5.4	-6.4
				EW	89.2	60.6	16.8	17.2
July 5	1400	86.70	84–54	NS	12.1	17.9	14.7	16.2
				EW	116.6	74.0	32.5	16.3
July 19	1400	85.30	84–56	NS	10.1	0.4	-12.7	-0.9
				EW	32.4	21.7	38.9	41.3
Sept 6	1400	88.44	82–62	NS	-15.6	-28.0	0.2	N/A
				EW	36.2	0.9	10.4	N/A
Sept 20	1405	86.55	66–52	NS	4.3	N/A	N/A	N/A
				EW	50.9	N/A	N/A	N/A
Oct 4	1353	86.50	80–58	NS	6.7	4.3	3.1	N/A
				EW	12.8	4.7	1.6	N/A
Dec 20	1430	81.98	80–64	NS	N/A	10.6	7.5	N/A
				EW	N/A	-36.3	-38.7	N/A

The radar data on the drift of the trajectory of the chaff were used to measure the wind speed and direction in the mesospheric region under study. Corrections for changes in the wind with altitude were also applied. The accuracy in measuring the wind speed at higher altitudes was about 6-10 ms^{-1}. Time-height cross sections for zonal and meridional winds are plotted using the conventional interpolation method in Figs. 4.5 and 4.6.

4.4.1 Upper mesospheric zonal winds

The zonal components over Molodezhnaya, Antarctica, show that in the upper mesosphere the winds were predominantly easterly in the summer half and westerly in the winter half, Fig. 4.5. In January and February (southern summer) the speeds of the easterly winds ranged from 10 to 50 ms^{-1} in the 60-80 km region for which the chaff data were available. On January 26, 1972 however, the zonal wind structure was found to have a small core of weak westerlies with wind speed about 10-15 ms^{-1} in a narrow altitude region from 77 to 85 km. In February the easterly winds were stronger and attained a maximum speed of 96 ms^{-1} at 82 km. During March there was only one rocket flight and during April there were none. During the first week of May, westerly winds of about 20 to 60 ms^{-1} were detected. During the second week of May, however, the winds again became strong easterlies with a maximum speed of 113 ms^{-1} at 66 km and a secondary maximum of 79ms^{-1} at 80 km.

Fig. 4.10
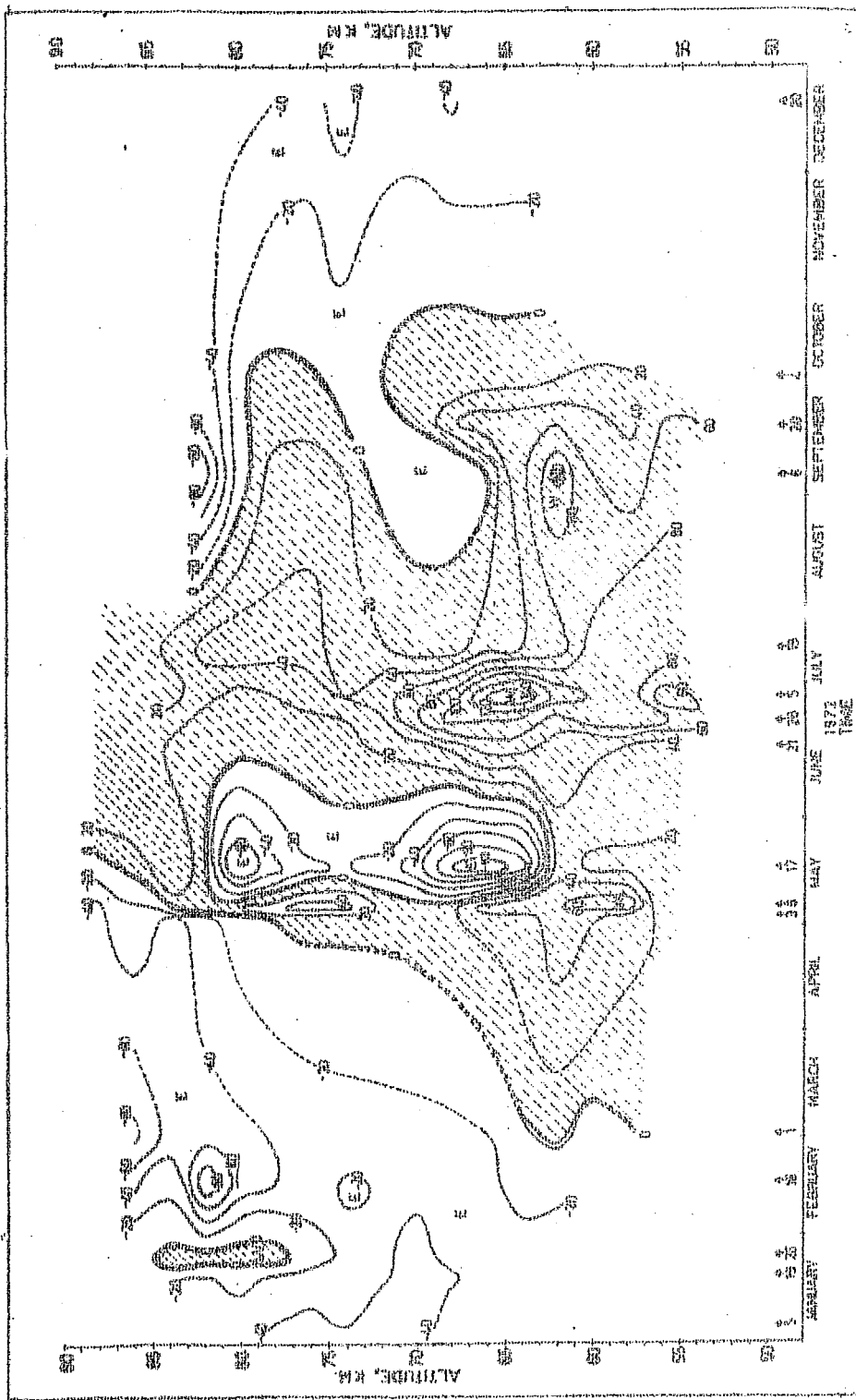
X-height cross-section for Malone's 1972 with east (+) and west (-) zonal components m/s. Dashed lines present extra-tropical data of altitudes 20km and above. Arrows show is dates on which data were obtained.

In June and July (southern winter) a westerly jet was formed which attained a maximum speed of 157 ms^{-1} at 64 km and became weak at higher altitudes. The strong westerly winds started to weaken in September-October (southern spring) in the 60-70 km region and weak easterlies started developing above 70 km. There were no ascents with chaff payloads during August and November. In December the zonal flow was characterised by easterlies of about 20-40 ms^{-1}.

4.4.2 Upper mesospheric meridional winds

The meridional cross section of the winds show that they were of variable nature, Fig. 4.6. In January, weak southerly winds of about 5-15 ms^{-1} predominated in the upper mesosphere. In February the winds were mainly northerlies, ranging from 5-25 ms^{-1}. In May the northerly winds became stronger and formed a jet which had a maximum speed of 88 ms^{-1} at around 60 km, with a secondary maximum of 79 ms^{-1} at 78 km. In the narrow region 65-70 km there was a small core of southerlies having a maximum speed of 57 ms^{-1} at 68 km. In June and July the northerly winds changed to southerly ones with a maximum speed of 48 ms^{-1} at 64 km. In September and October the winds were mainly southerlies of about 10-60 ms^{-1} with lower values at around 60 km and higher values at around 82 km. There was a core of weak northerlies at around 75 km.
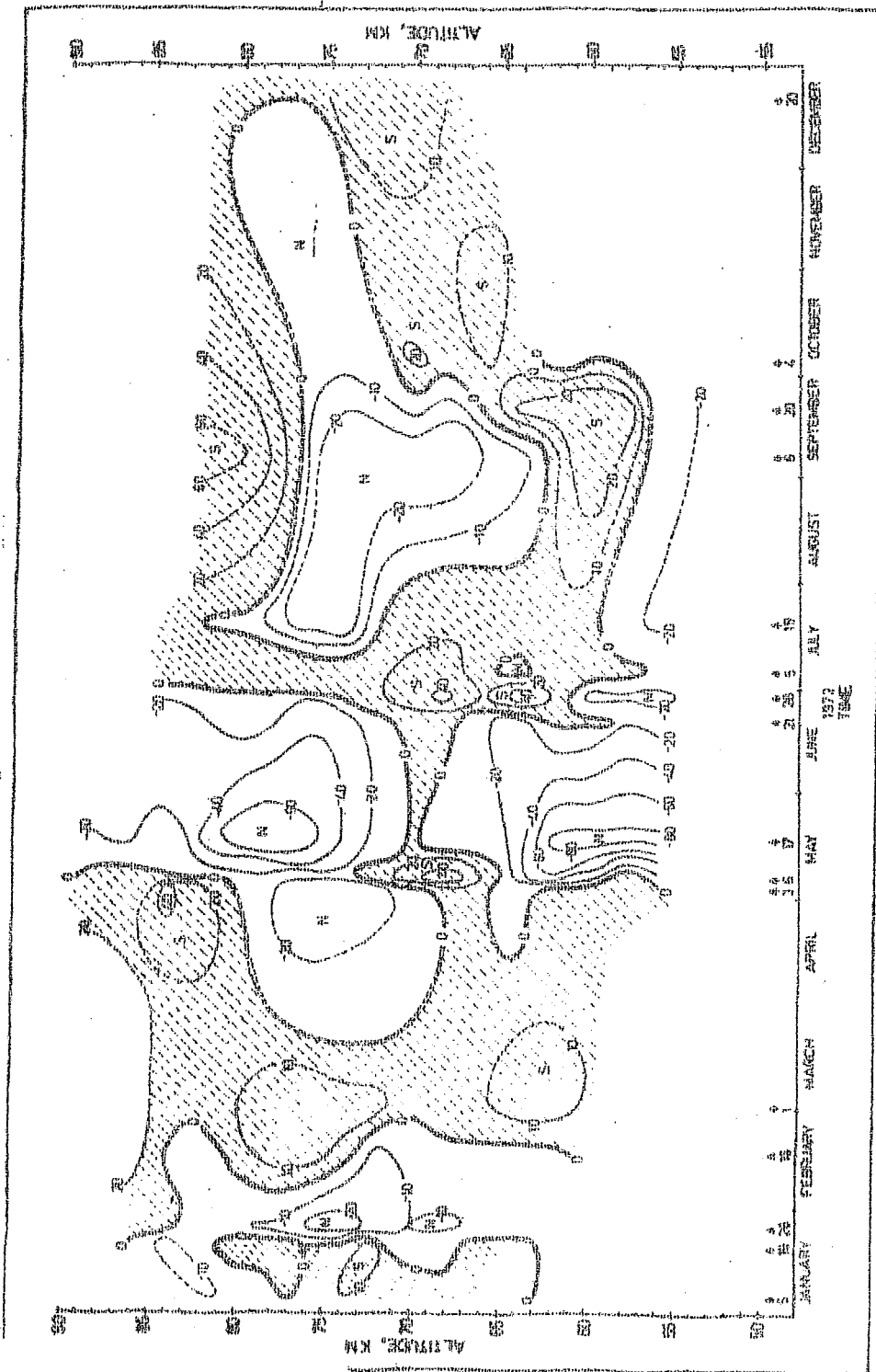
Time-height cross section for motionizate meridional winds (1972) with north (+) and south (-) ending ageostaphic components in m/s. Dashed lines present stratospheric data. Arrows above the dates show the dates on which data were obtained.

Fig. 4.5

In December the meridional flow was characterised by weak southerlies of about 5-15 ms^{-1}.

4.4.3 Mesospheric Circulation Index (MsCI)

The seasonal reversal of winds at different times of the year can be shown clearly by a method devised by Webb (1964). Adopting the same method mean values of the wind speeds were computed from the individual soundings by averaging over a 10 km layer centred at each of the altitudes 65, 70, 75 and 80 km as given in Table 4.6. Since this presents an average flow of the mesosphere under study, it is termed the Mesospheric Circulation Index (MsCI). Its values for the 70-80 km layer centred at 75 km, MsCI$_{75}$, are plotted in Fig. 4.7.

It was found that zonal winds were predominantly easterly in the summer half and westerly in the winter half whereas the meridional winds were variable. From the analysis of the MsCI in Fig. 4.7 , it is obvious that the summer easterly flow changed to a westerly flow in the first week of May, followed by a rapid reversal to an easterly flow in the second week. The easterly flow again changed to westerly flow in mid June. The meridional flow also showed a rapid shift from northerlies to southerlies in the last week of June.
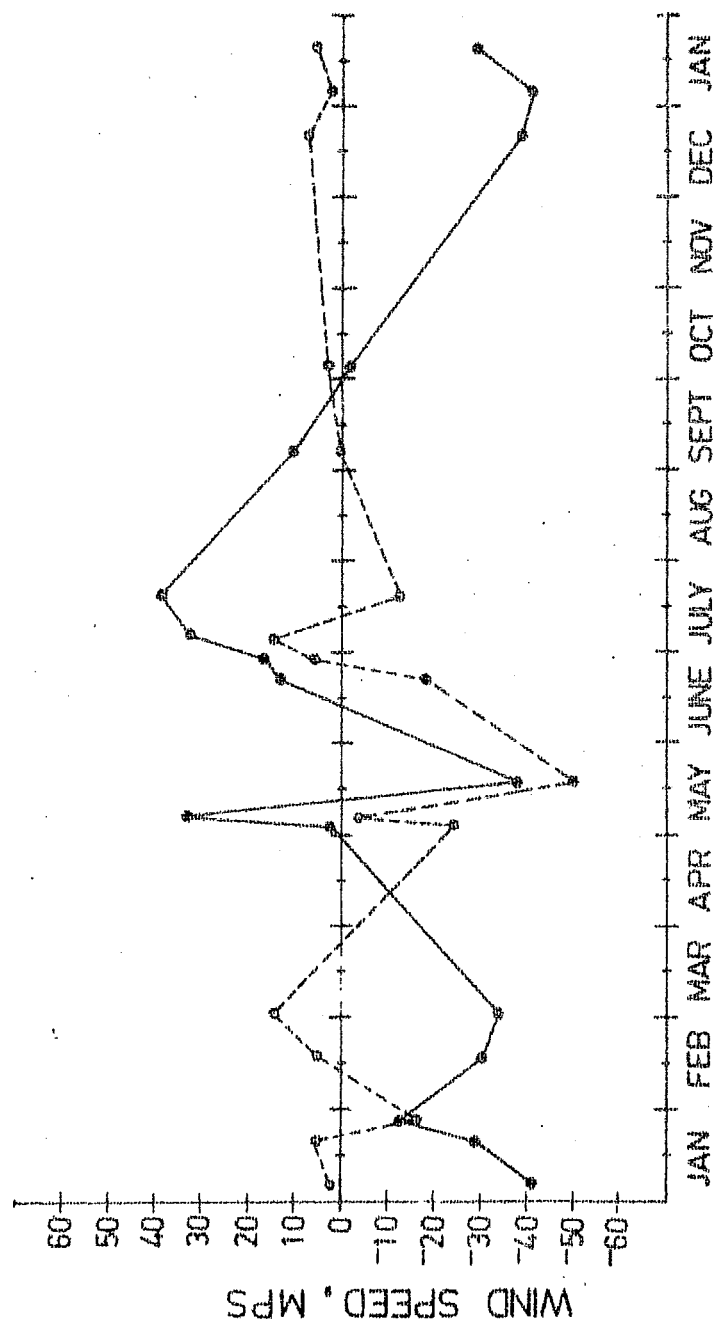
(Fig.4.7)

...onal flow (solid curve) obtained by averaging winds from the individual soundings over a 10-km layer centred at 75 km (Mesospheric Circulation Index, MsCI). Dashed curve presents the meridional flow component of the MsCI. Positive values refer to west and south components, while the negative to east and north. Wind speed in m/s.

The southerly flow again rapidly changed to northerly flow in mid July. These rapid shifts in both zonal and meridional components indicated sudden 'explosive' change in temperature distribution which might have occurred in the upper mesosphere. It is discussed separately. The winter westerly flow changed to the summer easterly flow at about the end of September. It seems that both for the zonal and the meridional flows the summer to winter shift was a rapid and dramatic change, whereas the winter to summer shift was slow and unspectacular.

4.5   Seasonal wind variations over Antarctica

Seasonal variations of the tropospheric, stratospheric and mesospheric winds over Antarctica in an altitude region from surface up to about 80 km are studied in this section. The data are used from all the 52 successful M-100 meteorological rocket soundings carried out at Molodezhnaya in 1972. The data are enalysed for the following seasons : southern summer from December to February, autumn from March to May, winter from June to August and spring from September to November. Seasonal averages of the zonal and meridional components of winds were computed for each km level and plotted in Fig. 4. 8 (I & II), while their corresponding standard deviations at 5 km interval are given in Table 4.7. In order to measure the wind persistance, steadiness factor(S_f)

Table - 4.7

Standard deviations of the zonal (Sz) and meridional (Sm) components of winds over Molodezhnaya, Antarctica in 1972 for the southern summer (December to February), autumn (March to May), winter (June to August) and spring (September to November). N is number of observations.

Altitude (km)	Summer			Autumn			Winter			Spring		
	Sz	Sm	N	Sz	Sm	N	Sz	Sm	N	Sz	Sm	N
1	2	3	4	5	6	7	8	9	10	11	12	13
0	4.3	5.1	11	4.5	6.3	12	4.8	5.1	15	7.2	2.4	13
5	4.4	5.6	11	9.5	7.8	12	8.9	8.1	15	10.2	4.5	11
10	7.0	7.7	11	8.8	12.5	12	7.5	10.2	15	10.0	8.6	11
15	3.2	2.5	11	6.3	9.0	12	7.4	5.9	15	8.0	8.8	11
20	3.9	2.0	11	10.7	8.4	12	12.9	6.2	15	15.4	8.4	11
25	5.6	2.6	11	13.4	7.1	12	18.2	7.8	15	25.6	8.1	11
30	10.1	12.5	11	16.6	8.6	12	20.0	10.6	15	37.8	14.0	11
35	4.3	4.8	11	18.6	6.2	12	26.1	19.3	15	38.3	17.0	11
40	9.8	3.7	11	19.0	16.4	12	24.9	16.3	15	41.8	17.8	11
45	28.8	24.1	11	21.8	19.3	11	23.2	11.2	14	41.0	30.2	11
50	24.3	9.7	8	22.8	18.3	10	16.5	18.6	14	42.0	34.8	10

more

Table - 4.7 contd....2..

1	2	3	4	5	6	7	8	9	10	11	12	13
55	26.1	4.6	8	12.7	18.4	9	22.5	21.9	14	31.8	21.1	10
60	39.4	10.6	5	25.9	22.7	7	25.5	19.2	7	29.4	16.0	8
65	6.4	5.2	5	62.6	10.3	4	40.2	19.7	4	18.4	13.3	3
70	7.5	8.0	5	24.6	15.9	4	27.1	12.8	4	19.6	25.2	3
75	10.0	12.6	5	31.7	26.7	4	11.6	17.9	4	14.0	9.0	2
80	23.1	6.5	5	37.0	32.1	4	21.2	9.7	4	2.0	17.0	2

was introduced which is the ratio of the speeds of the resultant wind to the mean scaler wind expressed in per cent and given by -

$$S_f = \frac{\left(\left(\frac{\Sigma U}{N}\right)^2 + \left(\frac{\Sigma V}{N}\right)^2 \right)^{\frac{1}{2}}}{\left(\left(\frac{\Sigma IUI}{N}\right)^2 + \left(\frac{\Sigma IVI}{N}\right)^2 \right)^{\frac{1}{2}}} \times 100$$

where U, V are the zonal and meridional components of winds with west and south positive, respectively, while IUI and IVI are their corresponding absolute values and N the number of observations. If the wind persistence i.e. the steadiness factor (S_f) is 100 %, it means that the wind always blows from the same direction and if it is 0, it connotes that either the wind is equally likely from all the directions or blows half the time from one direction and half the time from the opposite. S_f was computed for each season at 5 km interval and its values are plotted in Fig. 4.6 (III).

4.5.1   Seasonal zonal wind variations

The solid curve (S) in Fig. 4.8 (I) shows that in the southern summer (December to February), average zonal flows was easterly throughout the atmospyere from surface up to 80 km. The flow had a speed less than 13 ms^{-1} in the

troposphere and the stratosphere. It became stronger in the mesosphere and attained a speed of 41 ms^{-1} at 70 km with a standard deviation of about 7 ms^{-1}. In an altitude region from about 10 to 20 km the zonal winds were very weak and calm with speeds less than 3 ms^{-1} indicating that there was no turbulence at the boundary of the troposphere and the stratosphere in the summer. The dashed curve (A) in Fig.4.8(I), which gives average autumn wind profile shows that the summer easterly flow changed to westerly flow during the autumn period (March to May) with weaker winds in the troposphere and stronger in the stratosphere. The stratospheric westerly flow attained a maximum speed of 56 ms^{-1} at 47 km, However, in the upper mesosphere above 65 km the zonal flow remained predominantly easterly with speed less than 30 ms^{-1}.

Average wind profile for the southern winter (June to August) given by the solid curve (W) passing through cross marks in Fig. 4.8 (I) shows that in the winter the zonal winds were strong westerly throughout the atmosphere from about 5 to 80 km with weak easterly winds of speed less than 8 ms^{-1} in the lower troposphere below 5 km. The winter westerly flow attained jet speed in the stratosphere and the mesosphere which had a maximum of 90 ms^{-1} at 64 km with a secondary maximum of 71 ms^{-1} at 44 km. Also, a large wind

(Fig. 4-9)
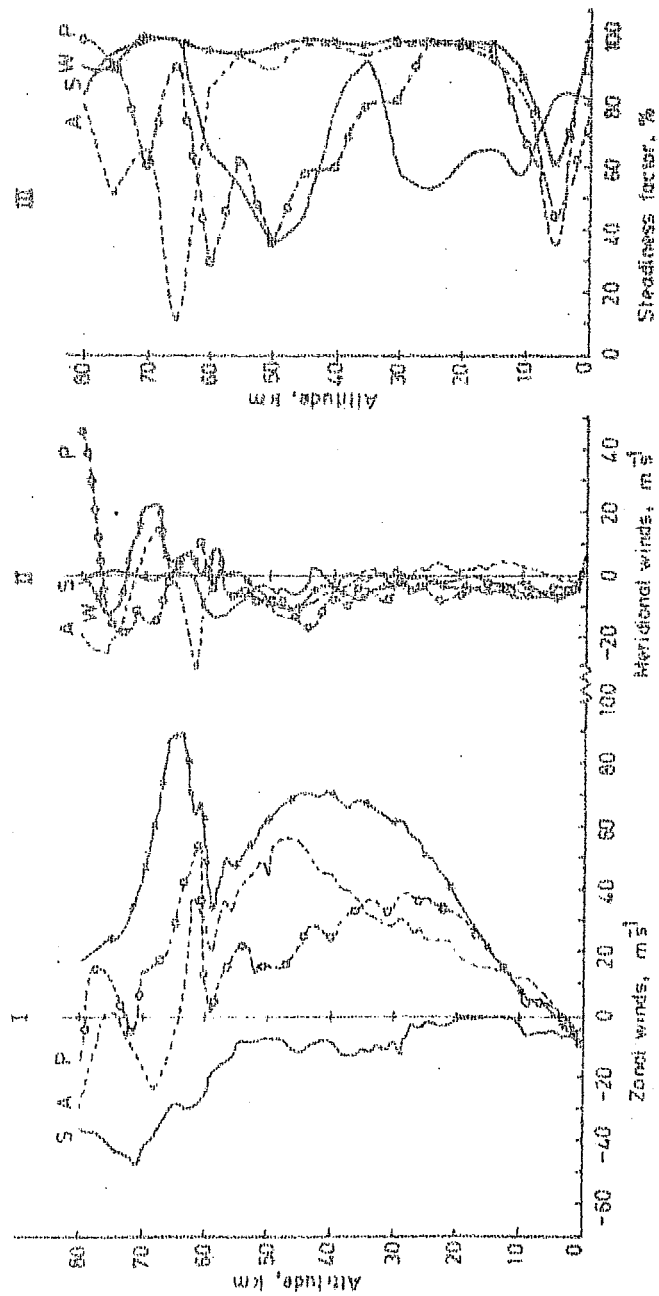
SEASONAL WIND VARIATIONS OF THE ATMOSPHERE IN ANTARCTICA (MOLODEZHNAYA, 1972)

S=SUMMER (DEC.,JAN.,FEB); A = AUTUMN (MAR.,APR.,MAY);
W=WINTER (JUNE,JULY,AUG); P=SPRING (SEPT.,OCT.,NOV)

shear of about 0.0113 s^{-1} was detected in an altitude region from 59 to 64 km. The dashed curve (P) passing through open circles in Fig. 4.8 (I) which gives an average profile of the zonal winds during the spring (September to November) shows that the winter westerly flow persisted in the spring with the stratospheric maximum of 39 ms^{-1} at 28 km and mesospheric maximum of 56 ms^{-1} at 61 km having a large wind shear of 0.0472 s^{-1} around 60 km.

4.5.2   Seasonal meridional wind variations

Fig. 4.8 (II) which gives the seasonal average profiles of meridional winds over Molodezhnaya, Antarctica in 1972 shows that the meridional wind components were variable throughout the atmosphere with weaker winds from surface up to the lower mesosphere and relatively stronger aloft. In the southern summer the meridional winds were predominantly northerly having a maximum speed of 13 ms^{-1} with a standard deviation of 9 ms^{-1} at 59 km as is obvious from the solid curve (S) in Fig. 4.8 (II), while in the autumn the meridional flow was mostly weak southerly with speed less than 5 ms^{-1} up to an altitude of about 35 km and predominantly northerly aloft having a maximum speed of about 30 ms^{-1} at 62 km. There was also a small core of southerlies of speed less than 16 ms^{-1} in a narrow altitude region from 66 to 71 km as shown by the dashed curve (A) in the Figure

The solid curve (W) passing through cross marks in Fig. 4.8 (II) shows that in the southern winter, average meridional flow was predominantly weak northerly up to an altitude of 54 km having a maximum speed of 11 ms^{-1} with a standard deviation of 14 ms^{-1} at 47 km. However, in the mesosphere from 55 to 72 km the flow was in toto southerly having a maximum speed of 23 ms^{-1} with a standard deviation of 14 ms^{-1} at 68 km which again became northerly aloft. In the spring the meridional winds were predominantly weak northerly throughout the atmosphere with a maximum speed of 19 ms^{-1} at 74 km in the upper mesosphere as shown by the dashed curve (P) passing through open circles. However, from 60 to 65 km there was a core of weak southerly winds with speed less than 11 ms^{-1}. A stronger southerly core was also detected in an altitude region from 77 to 80 km with speed less than 46 ms^{-1}.

4.5.3 Seasonal wind persistence

Fig. 4.8 (III) gives the steadiness factor S_f in per cent over Molodezhnaya, Antarctica in 1972 computed from the seasonal average of the zonal and the meridional components of winds as mentioned earlier. It is a measure of wind persistence. The solid curve (S) in Fig. 4.8 (III) shows that in the southern summer the wind in the upper

mesospheric layer from about 65 km to 80 km was steady since the steadiness factor, S_f in that region was large lying between 80 and 100 %, while in the lower region the horizontal flow was not as much steady. In the autumn the mesosphere was subjected to large wind perturbations as revealed by the smaller S_f values with a minimum of 11 % at 65 km, while the stratospheric flow was quite steady with the S_f lying between 90 and 100 % as shown by the dahsed curve (A) in the Figure.

The solid curve (W) passing through cross marks in Fig. 4.8 (III) shows that during the southern winter the horizontal flow over Antarctica was quite steady throughout the atmosphere from about 10 to 80 km with the S_f lying between 38 and 100 %. In the altitude region from 15 to 70 km the S_f was more than 95 % which connotes that the wind flow (predominantly westerly) was always from the same direction in that region during the winter. However, in the lower troposphere around 5 km the winds were not as much steady because there the S_f was smaller. During the autumn and the spring large wind perturbations were noticed with the S_f ranging from 11 to 100 % indicating that the horizontal flow was in turbulence as shown by the dashed curves (A) and (P) in the Figure 4.8 (III). However, in the altitude region from 15 to 25 km the flow was quite steady since the S_f was more than 95 % there.

4.6   Comparison with the Groves Atmospheric Model

Table 4.8 presents a comparison of the seasonal average zonal wind components over Molodezhnaya, Antarctica at 68°S with the corresponding Groves atmospheric model average values in the Arctic at 70°N shifted six months in time. The Groves seasonal averages were computed from the atmospheric model (Groves, 1971). The Table shows good agreement between the actual average zonal winds and the Groves model average winds in the summer with departures lying in a range of -4 to +8 ms^{-1} in the stratosphere and -19 to +2 ms^{-1} in the mesosphere. There is also an indication that in the Antarctic atmosphere the summer period with easterly winds grew in duration with height more rapidly than in the Arctic resulting relatively larger departures in the upper mesosphere. Around the stratopause from 50 to 55 km the average summer easterly wind speed was lower than in the Arctic. The zonal wind departures in the autumn ranged from -24 to + 42 ms^{-1} having larger values in the stratosphere with the maximum at 45 km.

In the winter, average speeds of the westerly winds over Antarctica were considerably higher than those over the derived from the Groves Model with a maximum departure of 84 ms^{-1} at 65 km in the mesosphere. In the stratosphere during winter, average wind speeds of the westerlies over

Table - 4.8

Comparison of the 1972 seasonal average zonal wind components (m/s) over Molodezhnaya Antarctica at 68°S with the corresponding Groves Atmospheric Model average values at 70°N shifted six months in time

	Summer			Autumn			Winter			Spring		
	Actual	Groves	Depar-ture	Actual	Groves	Depar-ture	Actual	Groves	Depar-ture	Actual	Groves	Depar-ture
	2	3	4	5	6	7	8	9	10	11	12	13
	- 2.8	- 6.5	3.7	23.9	6.8	17.0	50.1	15.0	35.1	37.8	- 4.8	42.6
	- 8.3	- 6.5	- 1.8	28.7	10.3	18.4	61.4	29.3	32.1	34.6	- 1.3	35.9
	-10.5	- 7.0	- 3.5	33.8	12.3	21.5	68.2	36.0	32.2	33.7	0.0	33.7
	- 8.9	- 7.8	- 1.1	44.7	13.8	30.9	70.5	34.5	36.0	24.4	- 1.3	25.7
	-12.0	- 9.8	- 2.2	55.1	13.5	41.6	70.8	25.5	45.3	22.3	- 5.0	27.3
	- 7.6	-13.3	5.7	43.9	12.5	31.4	62.1	12.8	49.3	15.2	-11.0	26.2
	- 8.7	-17.0	8.3	40.0	10.5	29.5	47.8	3.3	44.5	21.8	-16.0	37.8
	-24.2	-23.5	- 0.7	29.0	4.0	25.0	53.3	0.8	52.5	8.3	-15.5	23.8
	-28.4	-30.5	2.1	- 5.0	0.5	- 4.5	89.3	5.5	83.8	30.7	-10.0	40.7
	-41.0	-28.0	-13.0	-15.3	-2.0	-13.3	45.8	10.0	35.8	14.0	- 4.3	18.3
	-31.0	-19.5	-11.5	1.0	-6.0	5.0	25.0	10.3	14.7	11.0	- 0.8	11.8
	-25.6	- 6.5	-19.1	-29.5	-5.5	-24.0	17.5	8.0	9.5	-14.0	- 1.0	-13.0

Antarctica in the Southern Hemisphere were found to be in excess by about 30 to 50 ms^{-1} of those over the Arctic in the Northern Hemisphere as revealed by the Groves atmospheric model average values at 70°N given in Table 4.8. There is an indication of the reversal of meridional temperature gradient in the upper-most layers over Antarctica while the central polar region was warmer than the periphery of the continent. In the spring the average zonal winds over Antarctica were still predominantly westerly while over the Arctic they were replaced by light easterlies as is obvious from the Table 4.8. It suggests that the spring reversal from winter westerlies to summer easterlies occurred over the Arctic earlier than over the Antarctic. The vernal change of zonal wind direction in the upper atmosphere over Antarctica in the Southern Hemisphere generally occurred in November, while the date of change might vary from year to year. The spring average zonal wind departures from the Groves atmospheric model ranged from about -18 to + 43 ms^{-1} with smaller values in the upper mesosphere with the actual winds in excess of those of the Model.

4.7   Discussion of results

The above ivestigation shows that the zonal flow over Antarctica in the summer was characterised by light easterly winds and in the winter by strong westerly winds which

increased in strength as the season advanced and attained jet speeds, while the meridional flow was of variable nature. The autumn and spring were the wind reversal periods marked by change of summer easterly winds to winter westerly flow and vice versa. The spring period was quite turbulent marked by strong reversal of winds which was followed by return to normal summer circulation. Complete reversal of winds from easterlies to westerlies occurred in the stratosphere in the first week of February, while in the troposphere it occurred in February end. The reversal from westerlies to easterlies occurred in the third week of November in the stratosphere and in the first week of December in the troposphere suggesting that the reversal first took place in the stratosphere and subsequently in the troposphere. It shows a downward propagation of the disturbance which is in agreement with the results given by Miers(1963). The analysis also reveals that the summer to winter shift was a rapid change while the winter to summer shift was slow. It is found that in the upper mesosphere over Antarctica the summer to winter shift occurred somewhat late while in the stratosphere it occurred earlier. The analysis also shows that the spring reversal from winter westerlies to summer easterlies occurred over the Arctic earlier than over the Antarctic.

The Antarctic winter regime comprising late autumn and early spring (May to September) was found to be the most

unsettled period characterised by a strong westerly jet of speed up to about 100 ms^{-1} in the stratosphere and the mesosphere. In the southern winter (June to August) ,the atmospheric steadiness factor was found to be as high as 95 to 100 % showing that the winter jet stream was always blowing from the same direction, mostly from the west. The autumn transfer from easterly to westerly winds over Antarctica depicted a rapid retreat of high pressure belt from polar to middle latitudes. The spring reversal of the Antarctic circulation was first noted in the upper layers suggesting that the stratospheric warm region advancing southwards during the spring was located farther to the south than the high pressure belt.

Comparison of the Antarctic average zonal winds with the corresponding Groves atmospheric model values showed a good agreement in the summer easterly circulation. However, in the winter the departures of the actuals from the Groves Model were found to be quite significant and the Antartic wind values were considerably in excess of those of the Arctic. This is apparently because the Groves atmospheric model is based on the data from the Northern Hemisphere which differs from the Southern Hemisphere in many respects, e.g., the Southern Hemisphere is more oceanic, more symmetric and has a vigorous general circulation. Also, Antarctica has a higher albedo and is located at a higher elevation as compared with the Arctic.

C H A P T E R – V

ATMOSPHERIC TEMPERATURE, PRESSURE AND DENSITY VARIATIONS IN ANTARCTICA

In this chapter, seasonal variations and other changes in the atmospheric temperature over Antarctica are studied. Variations in the Antarctic atmospheric pressure and density are also investigated and the results are presented here.

5.1   Seasonal variations of atmospheric temperature over Antarctica

Time–height cross section of the atmospheric temperature from the 52 successful M-100 meteorological rocket soundings carried out at Molodezhnaya, Antarctica in 1972 is drawn in Fig. 5.1. Seasonal and annual mean temperatures and their corresponding standard deviations are computed. The departures of the southern summer (December to February) and the winter (June to August) average temperatures from the annual mean temperature are worked out in Table 5.1. Also, the departures of the monthly average temperatures from the annual mean from 10 to 70 km at 10 km interval are shown in Fig. 5.2.

5.1.1   Tropospheric temperatures

In Fig. 5.1 the dashed curves (T) and (S) present the annual variation of the Antarctic atmospheric temperature minimum (tropopause which changed to a complex quasi-tropopause during the winter regime) and the temperature maximum (stratopause) respectively. The shaded areas in the Figure are the regions of warmer temperatures with positive values. It is found that the lower atmospheric temperature over Antarctica in an altitude region from surface to 10 km varied from about + 5 to -75°C throughout the year, while the tropopause during the southern summer (December to February) was located in an altitude region from about 8 to 11 km with the temperature ranging from -50 to -60°C as shown by the dashed curve (T) in the Figure. The well-defined summer tropopause showed a sudden disruption during the southern autumn (March to May) with the lower atmospheric temperature minimum varying from -54 to -74°C in an altitude region from about 8 to 29 km indicating a differential cooling set in the atmosphere which weakened the tropopause and persisted throughout the winter regime.

As the sunlight almost totally disappeared during the southern winter (June to August) the Antarctic troposphere cooled further and the winter temperature minimum was
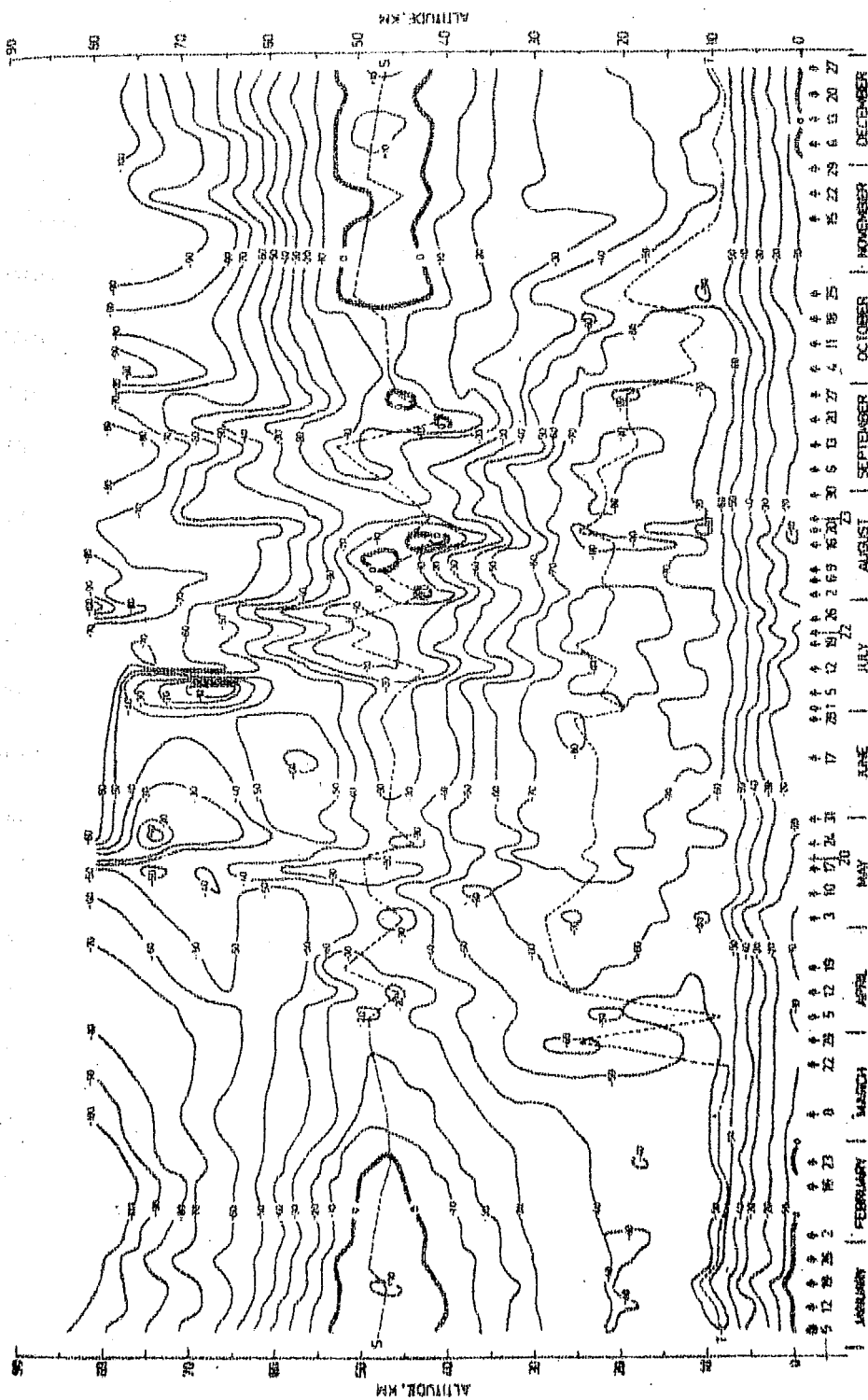
(Fig.5.1)

...me-height cross section of the atmospheric temperature (°C) at Molodezhnaya,Antarctica in 1972. ...e dashed lines (T) and (S) present the annual variation of the atmospheric temperature minimum ...ropopause) and the temperature maximum (stratopause) respectively. The arrows above the abscissa ...ow the dates on which the data were obtained.

located in an altitude region from 20 to 25 km varying from
-79 to -87°C . The winter polar tropopause was found to be
complex and locally ill-defined because several tropopause
occurrences were noted on a single sounding in an altitude
range from 10 to 25 km. However, it appears that the winter
tropopause was located at a relatively higher altitude than
the summer tropopause. As the sunlight returned and the spring
season (September to November) progressed the polar troposphere
in the southern hemisphere warmed with a maximum warming of
22°C at 11 km on October 25 and the normal summer regime set
in by mid-November. It was also found that during the summer
regime the temperature lapse rate in the Antarctic atmosphere
in an altitude region from about 10 to 30 km did not exceed
+ 1.0°C km^{-1} showing that the temperature structure was quasi-
isothermal in that region. During the winter regime also the
steep lapse rate of the Antarctic troposphere stopped around
10 km where the first tropopause occurrence was noted with
subsequent ones aloft.

5.1.2   Stratospheric temperatures

The dashed curve (S) in Fig. 5.1 shows the annual
variation of the polar atmospheric temperature maximum
(stratopause) in the southern hemisphere. It is obvious from
the Figure that during the southern summer (December to February)

the stratopause was located in a warm region between 47 and 49 km with the temperature maximum found on December 13 having a peak value of + 13°C, at 48 km and a secondary maximum of + 10°C at 47 km on January 19. The Antarctic stratopause cooled during the autumn period (March to May) and varied from about 44 to 52 km with the temperature ranging from -13 to -35°C having the maximum at 50 km on May 17, while there was a warming of 23°C **from May 10 to 17 followed by** an equal cooling from May 17 to 20.

The winter polar stratopause in the southern hemisphere showed a wide variation with the altitude ranging from 41 to 52 km and the temperature carrying from -28 to + 6°C. The winter stratopause temperature minimum of -28°C was found on July 3 at an altitude of 46 km, while the maximum of + 6°C at 47 km on August 9. Also, in August contours of warmer temperatures with positive values were detected around the stratopause showing stratospheric warming during the winter. It is obvious from the Figure 5.1 that the polar stratosphere in the southern hemisphere was subjected to significant warming and cooling with the pronounced ones around May 17, July 12, August 16 and September 20. The Antarctic stratopause during the southern spring (September to November) was located in an altitude region from about 41 to 53 km having a minimum temperature of -10°C at 47 km on October 4 and a

maximum of + 8°C at 49 km on November 29. Commencing October 25, the spring stratopause temperature minimum was found in a warm region with the return of the sunlight permitting the atmospheric ozone to absorb solar ultra-violet radiation and thus warm the stratosphere which returned to normal summer regime by the end of November.

5.1.3   Mesospheric temperatures

The polar mesopause in the southern hemisphere was not found to be well defined. It may be due to the fact that the atmospheric temperature data over Milodezhnaya, Antarctica could be obtained most satisfactorily only up to about 75 km and apparently the mesopause was lying above that level. Fig. 5.1 shows that the Antarctic mesospheric temperature varied from about -5 to -110°C and that the normal summer temperature distribution was disrupted in May (late autumn) which presented throughout the winter and early spring. Consequently, the Antarctic mesosphere was subjected to large thermal perturbations during the winter regime marked by sudden warming and cooling with the most prominent ones having occurred around May 17, July 5, July 19 to 26, August 20 and September 20. A quantitative investigation of the stratospheric and mesospheric warmings and coolings is discussed separately.

5.1.4   Antarctic tropopause, stratopause and mesopause

Table 5.1 shows that on an average the Antarctic tropopause in the southern summer (December to February) was located at 9 km with a temperature of $-53^\circ C$ and corresponding standard deviation of $4^\circ C$, while in the winter (June to August) it was ill-defined due to its multiple occurrences in an altitude region from about 10 to 25 km with a temperature of $-67^\circ C$ at 10 km and the lowest minimum of $-81^\circ C$ at 21 km. During the south polar winter night the Antarctic tropospheric temperature decreased due to differential cooling of the atmosphere which weakened the tropopause and at times wiped it out thus forming a quasi-tropopause with a complex structure located in an altitude range from about 10 to 25 km during the winter regime. The differential cooling might be due to the ventilation of the Antarctic atmosphere by warm marine air with intense horizontal advection in the troposphere and a weak advection through the strong stratospheric jetstream encircling Antarctica. The Antarctic tropopause was found to be ill-defined during the autumn, while in the spring it was located around 11 km with a temperature of $-64^\circ C$.

The average polar stratopause over Antarctica in the southern summer was located at 47 km with a temperature of $7^\circ C$ and corresponding standard deviation of $4^\circ C$, while in the

winter it was found at 46 km with a temperature of $-12^{\circ}C$ and corresponding standard deviation of $10^{\circ}C$ showing that the winter polar stratopause was about $19^{\circ}C$ colder than the summer stratopause. During the equinoxes the Antarctic stratopause was located at 47 km with an average temperature of $-26^{\circ}C$ in the southern autumn (March to May) and about $-4^{\circ}C$ in the spring (September to November). The Antarctic mesopause was not found to be well-defined since no satisfactory temperature data was available above 75 km, the possible location of the mesopause.

5.1.5   Temperature departures from the annual mean

As obvious from the Table 5.1 the departures of the Antarctic summer and winter average atmospheric temperatures from the annual mean ranged from about -22 to $+24^{\circ}C$ with larger amplitudes in the stratosphere which were caused by warmer summers and colder winters. The south polar stratosphere was warmer in the summer because Antarctica has a large albedo of about 80 to 90 per cent due to which a high intensity of the solar radiation (which is almost continuous during summer) was reflected back, thereby permitting the ozone in the Antarctic stratosphere to reabsorb the reflected solar radiation and thus achieve a higher temperature. The Antarctic stratosphere was colder in the southern winter because there was very little warm air advection through

Table - 5.1

Seasonal variation of the atmospheric temperature (°C) from the successful M-100 meteorological rocket launchings at Molodezhnaya, Antarctica in 1972. T gives the average temperature, St the corresponding standard deviation, N the number of observations and D the respective departures from the annual mean temperature

Altitude (km)	Southern Summer (December to February)				Southern winter (June to August)				Annual Temperature (January to December)		
1	T	St	N	D	T	St	N	D	T	St	N
	2	3	4	5	6	7	8	9	10	11	12
0	1.3	2.4	11	10.9	-14.5	5.9	15	-4.9	-9.6	8.4	49
2	-12.5	2.0	11	6.0	-21.3	4.8	15	-2.8	-18.5	5.6	49
4	-22.7	4.0	11	6.1	-32.1	4.3	15	-3.3	-28.8	8.8	49
6	-35.2	3.8	11	7.3	-44.9	4.6	15	-2.4	-42.5	2.8	49
8	-48.9	3.1	11	5.8	-57.5	4.2	15	-2.8	-54.7	3.7	49
9	-53.0	4.0	11	6.3	-63.8	3.2	15	-2.8	-59.3	5.4	49
10	-50.8	4.5	11	8.8	-67.0	3.2	15	-4.5	-59.6	9.5	49
12	-45.1	3.8	11	15.0	-69.9	4.9	15	-7.4	-60.1	11.9	49
14	-43.6	2.4	11	14.9	-72.8	4.9	15	-9.8	-58.5	13.4	49
16	-42.3	1.2	11	18.5	-76.0	4.8	15	-14.3	-60.8	15.1	49
18	-40.2	1.1	11	19.8	-78.5	4.5	15	-15.2	-60.0	21.3	49
20	-39.6	1.7	11	22.0	-80.1	3.9	15	-18.5	-61.6	19.7	49

more

Table - 5.1 contd..2..

1	2	3	4	5	6	7	8	9	10	11	12
22	-39.1	1.7	11	23.2	-80.3	3.9	15	-18.0	-62.3	17.6	49
24	-37.5	1.6	11	23.6	-79.9	3.3	15	-18.8	-61.1	19.3	49
26	-36.1	1.9	11	22.2	-77.1	3.8	15	-18.8	-58.3	18.9	49
28	-34.1	2.0	11	20.9	-70.9	4.1	14	-15.9	-55.0	17.2	46
30	-30.3	3.0	11	20.8	-63.9	6.5	14	-12.8	-51.1	13.2	46
32	-25.7	3.4	11	19.4	-57.1	7.6	14	-12.0	-45.1	16.7	46
34	-21.3	3.4	11	18.4	-50.2	8.0	14	-10.5	-39.7	14.0	46
36	-15.6	4.0	11	18.1	-41.8	11.0	14	-8.1	-33.7	10.0	46
38	-10.2	5.0	11	17.7	-33.5	11.1	14	-5.6	-27.9	16.6	46
40	-5.1	4.2	11	16.0	-23.3	12.2	14	-2.2	-21.1	15.8	46
42	-0.7	3.8	11	15.0	-16.7	12.3	14	-1.0	-15.7	15.0	46
44	3.3	3.6	11	15.1	-13.4	10.4	14	-1.6	-11.8	14.7	46
46	6.0	3.6	11	16.0	-12.0	10.0	14	-2.0	-10.0	13.8	46
47	7.0	4.0	11	16.3	-12.9	10.1	14	-3.6	-9.3	14.2	46
48	6.9	4.2	11	16.6	-14.3	10.7	14	-4.6	-9.7	14.7	46
50	5.1	4.2	11	17.3	-17.5	11.6	13	-5.3	-12.2	15.6	45
52	-0.4	4.1	11	16.6	-23.8	13.2	13	-6.8	-17.0	16.3	45
54	-8.5	4.6	11	14.6	-31.5	13.8	13	-8.4	-23.1	15.5	44
56	-18.3	4.9	11	12.4	-38.8	14.0	13	-8.1	-30.7	14.1	43

more

162

Table - 5.1 contd..3..

2	3	4	5	6	7	8	9	10	11	12
-27.9	5.4	11	9.4	-42.8	12.4	12	-5.5	-37.3	11.5	42
-27.5	6.5	11	7.2	-47.1	12.1	12	-2.4	-44.7	7.0	42
-47.6	5.6	11	2.1	-50.3	12.2	12	-0.6	-49.7	10.0	40
-56.2	5.3	11	-2.1	-52.1	15.9	12	2.0	-54.1	12.8	40
-63.3	4.9	11	-5.5	-53.6	17.2	12	4.2	-57.8	14.5	40
-69.2	5.0	11	-8.5	-53.4	16.3	12	7.3	-60.7	16.4	39
-74.3	5.2	11	-9.8	-57.9	16.0	12	6.6	-64.5	19.3	39
-7?.8	5.4	11	-10.6	-65.0	16.4	10	4.2	-69.2	17.9	35
-87.4	7.0	9	-15.0	-70.0	7.2	8	2.4	-72.4	20.4	25
-93.5	7.0	8	-19.2	-68.3	7.2	6	6.0	-74.3	21.1	20
-95.8	6.3	5	-18.4	-76.8	10.5	5	0.6	-77.4	21.5	14
-102.3	7.5	3	-21.7	---	---	-	---	-80.6	25.2	11

the strong stratospheric jet-stream encircling Antarctica thus permitting the average stratospheric temperature to fall steadily at the rate of about $0.25^{o}C$ per day. Thus the high latitude stratopause region appears to gain energy through radiative processes in the summer and to lose energy through radiative process in the winter which was found to hold good for the entire upper stratosphere and the lower mesosphere.

However, the Antarctic upper mesosphere in an altitude region from about 64 to 80 km in the summer was found colder than its winter counterpart with the average summer and winter temperature departures from the annual mean lying in a range of about -22 to + $7^{o}C$ as shown by the Table 5.1. The polar winter upper mesosphere in the southern hemisphere may be warmer due to a large-scale meridional transport of heat in one form or another by the atmosphere resulting from a mean meridional circulation or from large-scale eddy processes.

5.1.6   Temperature lapse rates

Average temperature lapse rates in the troposphere, stratosphere and mesosphere over Antarctica in the summer were about -6.0 + 1.5 and $-3.4^{o}C$ km^{-1}, respectively with a quasi-isothermal structure in the layer from 10 to 30 km which had a lapse rate of less than + $1.0^{o}C$ km^{-1}. The average temperature lapse rates in the Antarctic winter were as follows:

in the altitude region from surface to 10 km it was $-1.3^{\circ}C$ km^{-1}, in the stratosphere above 20 km its value was $+ 2.7^{\circ}C$ km^{-1} and in the mesosphere the lapse rate was about $-2.0^{\circ}C$ km^{-1}.

Annual mean and corresponding standard deviation of the atmospheric temperature over Molodezhnaya, Antarctica in 1972 are also given in Table 5.1. It is found that the annual tropospheric temperature ranged from about -10 to $-60^{\circ}C$ and that the lower atmospheric temperature minimum occurred at 22 km with a temperature of $-62.3^{\circ}C$ and corresponding standard deviation of $17.6^{\circ}C$, while the temperature at 9 km (possible tropopause) was $-59.3^{\circ}C$ with a standard deviation of 5. Annual mean lapse rate in the layer from 10 to 30 km was found to be $+ 0.4^{\circ}C$ km^{-1} showing a quasi-isothermal temperature structure in that region. The annual mean Antarctic stratospheric temperature also varied from about -10 to $-62^{\circ}C$ with the maximum at the stratopause which was located at 47 km with a temperature of $-9.3^{\circ}C$ and corresponding standard deviation of $14.2^{\circ}C$. The annual mean temperature lapse rate in the Antarctic upper stratosphere was about $+ 2.5^{\circ}C$ km^{-1}, while it was about $-2.3^{\circ}C$ km^{-1} in the mesosphere. The mesospheric temperature at 75 km was $-72.3^{\circ}C$ with a standard deviation of $20.4^{\circ}C$.

5.2   Warmings and Coolings of the Antarctic stratosphere and mesosphere

The mesospheric wind results derived for atmospheric altitudes between 50 and 90 km from meteorological rocket flights carried out at Molodezhnaya station ($67^{\circ}40'S$, $45^{\circ}51'E$) in Antarctica have been discussed in Section 4.4. The rapid shifts in both zonal and meridional components of the winds during May to July indicated a sudden 'explosive' change in temperature distribution in the upper mesosphere over Antarctica in the winter regime. This phenomenon is investigated and the study extended down to the stratosphere. The results of this investigation here are discussed. The meridional and the zonal temperature gradients at altitudes of 65, 70 and 75 km, derived from the thermal wind equations using the corresponding upper wind and temperature results are also studied as in Table 5.2.

5.2.1   Atmospheric temperature disruption

Departures of the monthly average temperatures from the annual mean over Molodezhnaya, Antarctica in an altitude region from 10 to 70 km are also worked out. These departures at 10 km altitude interval are plotted in Fig.5.2. Time-height cross sections of the mesospheric temperatures in the region 50 to 80 km are plotted using linear interpolation in Fig. 5.3.
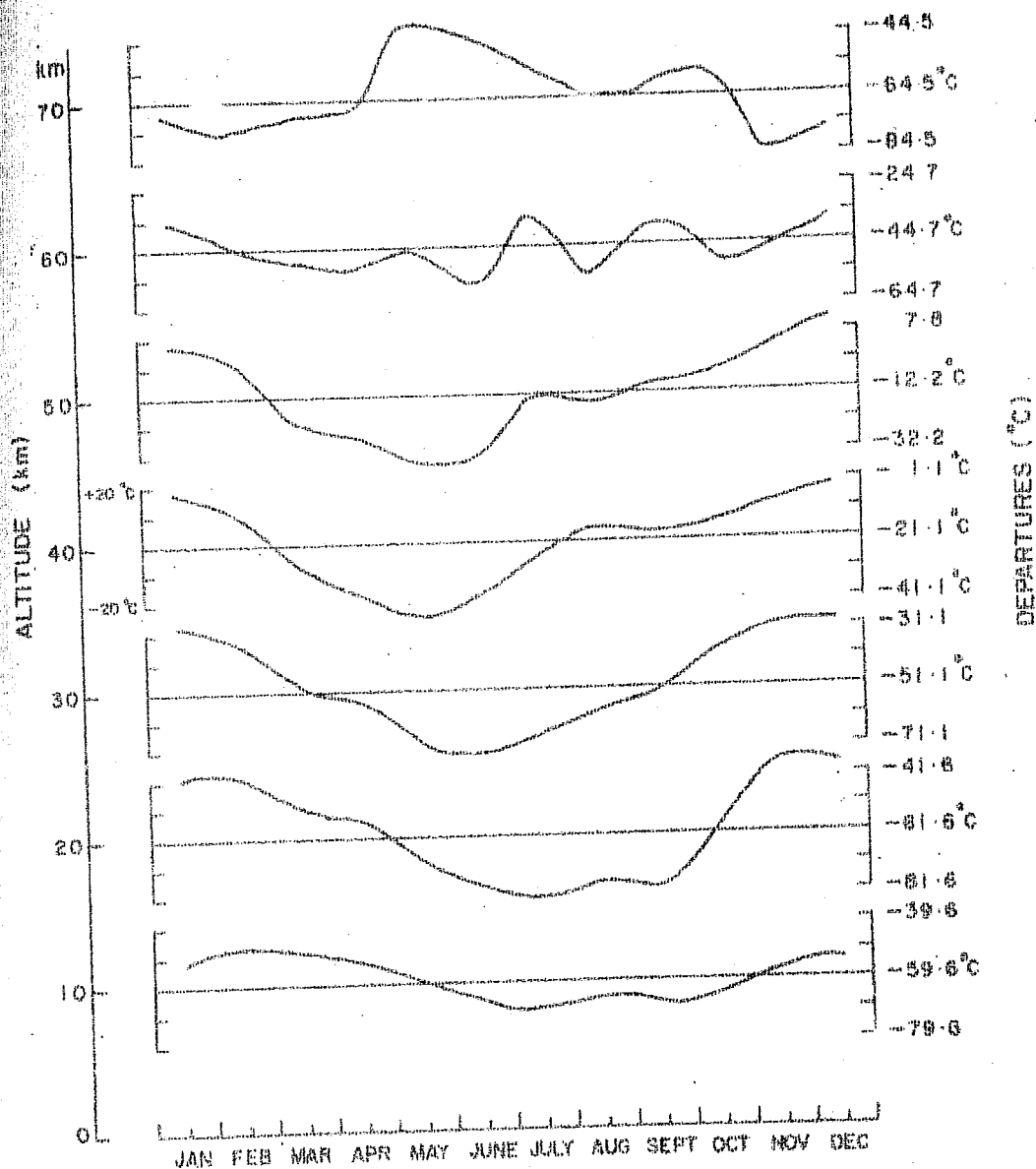
Departures (°C) of the monthly average temperatures from the annual
mean over Molodezhnaya, Antarctica in 1972

(Fig. 5·2)

Fig. 5.3 shows that in the southern summer months January-February the mesospheric temperatures in the region 50 to 80 km ranged from about 10 to -110°C with the summer maximum reached by about January 5 in the lower mesosphere and by about January 26 in the upper mesosphere. The disruption of the mesospheric winter regime by a period of stormy winds quite clear from Figs. 5.2 & 5.3. In the third week of May and the first week of July the upper mesosphere was subjected to a warming of more than 30°C in less than a week. The temperature distribution returned to normal by early September, but was again disrupted in about the third week.

5.2.2   Horizontal temperature gradients

Meridional and zonal temperature gradients are derived for altitudes of 65, 70 and 75 km from the corresponding upper wind and temperature results using the thermal wind equations

$$\frac{\delta T}{\delta y} = \frac{fT}{g} \left(\frac{\delta u}{\delta z} - \frac{u}{T} \frac{\delta T}{\delta z} \right)$$

$$\frac{\delta T}{\delta x} = \frac{-fT}{g} \left(\frac{\delta v}{\delta z} - \frac{v}{T} \frac{\delta T}{\delta z} \right)$$

where f is the coriolis parameter, g the acceleration due to gravity, T the absolute temperature at a particular level, x, y, z the eastward, northward and vertical axes, u, v the zonal and meridional components of winds with west and south positive, respectively. The horizontal temperature gradients are given in Table 5.2.
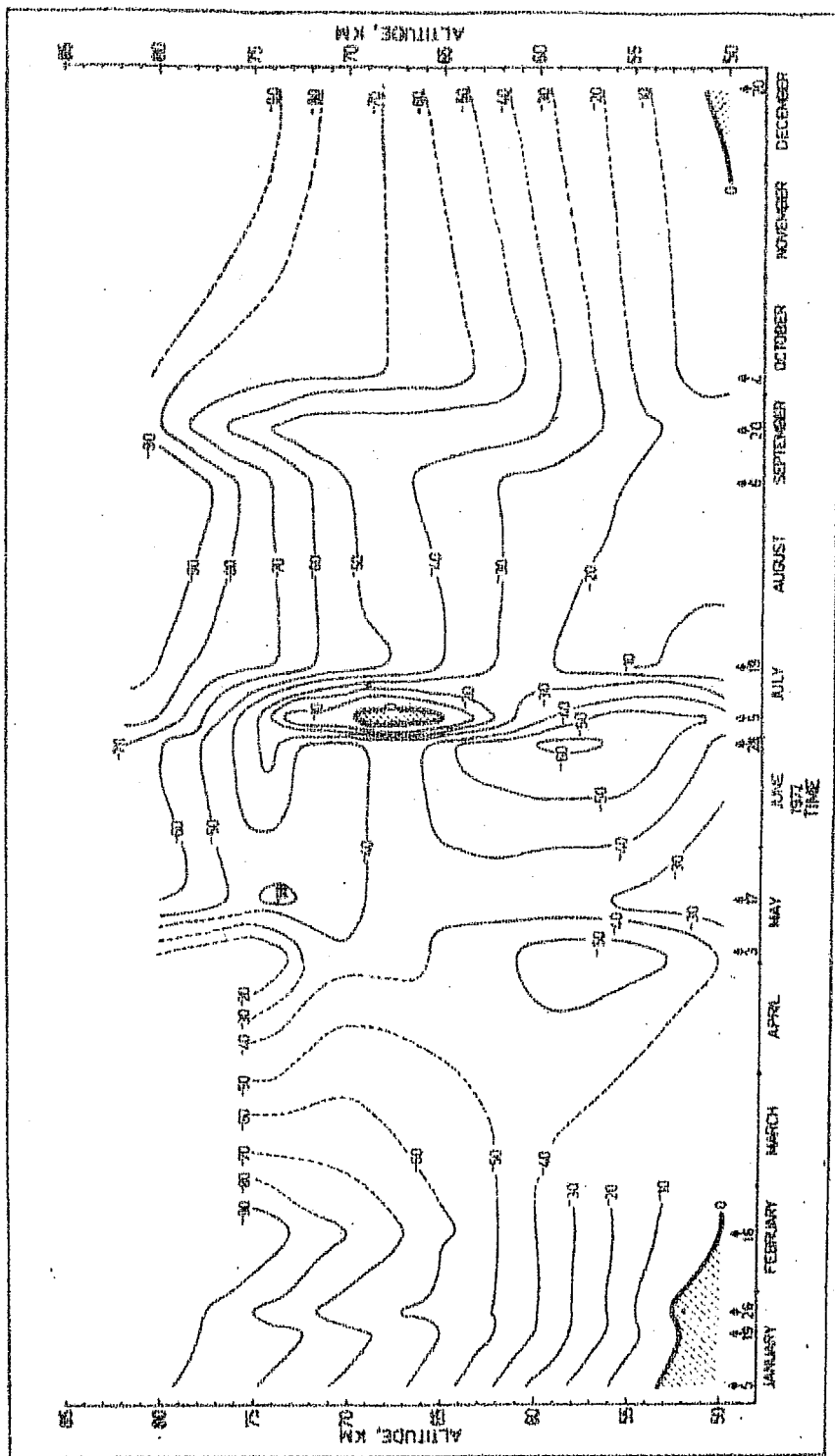
[Fig 5.3]

e-height cross section of the mesospheric temperatures (°C) at Molodezhnaya, Antarctica in 2. Dashed lines represent extrapolated data. Arrows above the abscissa show the dates on ch the data were obtained.

Table 5.2 shows that the horizontal temperature gradients at 65 km ranged from -37 to 10°C per 5° latitude with a maximum on September 6. At 70 km the range was -31 to 30°C with the maximum values on June 28 and May 17, whereas the gradients at 75 km ranged from -14 to 21°C per 5° latitude with the maxima on September 6 and May 17, respectively. Larger gradients were found from May to July indicating a disruption by stormy winds having large wind shears of about $10 \times 10^{-3} s^{-1}$ to $30 \times 10^{-3} s^{-1}$. A similar disruption occurred in September. The negative meridional temperature gradients represent a decrease of the zonal winds with altitude (the easterlies increase and the westerlies decrease with height) and the negative zonal temperature gradients represent an increase of the meridional winds with altitude(the easterlies increase and the westerlies decrease with height) and the negative zonal temperature gradients represent an increase of the meridional winds with altitude (the northerlies decrease and the southerlies increase with height). On May 17 at 70 km the meridional temperature gradient was 30.4, suggesting a disruption by strong easterlies which decreased with height.

Table - 5.2

Meridional and zonal temperature gradients at Molodezhnaya, Antarctica, in 1972 expressed in °C per 5° latitude

Date	65 km Temperature gradient		70 km Temperature gradient		75 km Temperature gradient	
	Meridional	Zonal	Meridional	Zonal	Meridional	Zonal
January 5	0.3	-2.1	- 6.3	-0.8	-1.7	3.1
January 19	- 2.0	-0.6	0.3	-6.5	2.5	1.4
January 26	0.8	3.0	- 1.7	2.6	10.6	- 1.7
February 16	- 9.4	-0.3	3.3	3.5	-5.0	- 5.9
May 3	- 9.3	-4.0	- 5.0	17.8	-1.0	- 2.1
May 17	-20.2	-8.1	30.4	-0.5	-4.8	20.9
June 28	5.2	2.3	-31.3	10.5	-7.1	5.5
July 5	-13.4	-7.8	-20.9	6.9	-7.5	- 1.0
July 19	-10.4	-3.7	8.2	5.6	9.1	1.9
September 6	-36.7	9.9	- 1.1	-1.7	9.1	-14.1
October 4	- 0.6	-3.8	- 5.4	5.4	2.7	- 2.2
December 20	0.1	0.7	4.2	-3.4	-0.2	3.7

5.2.3   Upper atmospheric warmings and coolings

Time sections of the upper atmospheric temperatures showing annual variations at 30, 50 and 70 km altitudes in 1972 are plotted in Fig. 5.4. Curve C in Fig. 5.4 shows that at 30 km the stratospheric temperatures in Antarctica fall as the sun sets, and that the minimum - 75°C is reached in June. A slow temperature rise begins as the Sun returns, but this becomes much more marked after early September when the sun's radiation reaches the lower strata. Curve B (50 km, around the boundary of the stratosphere and the mesosphere) shows a warming of 23°C during the second week of May followed by an equal cooling during the third week. During the second week of July there was a mid-winter stratospheric warming of 30°C. The temperatures at 50 km ranged from a maximum of 12°C in early December to a minimum of - 45°C at the end of May.

Curve A (70 km) in Fig. 5.4 reveals sudden 'explosive' changes in the upper mesospheric temperature distribution, particularly during the winter period May to July. During the third week of May, a warming of 26°C occurred, and in mid-winter there was a warming of 31°C during the first week of July followed by a 'sudden cooling' of 53°C during the second week. The temperatures at 70 km show a distinct maximum of - 12°C during the first week of July, after which the
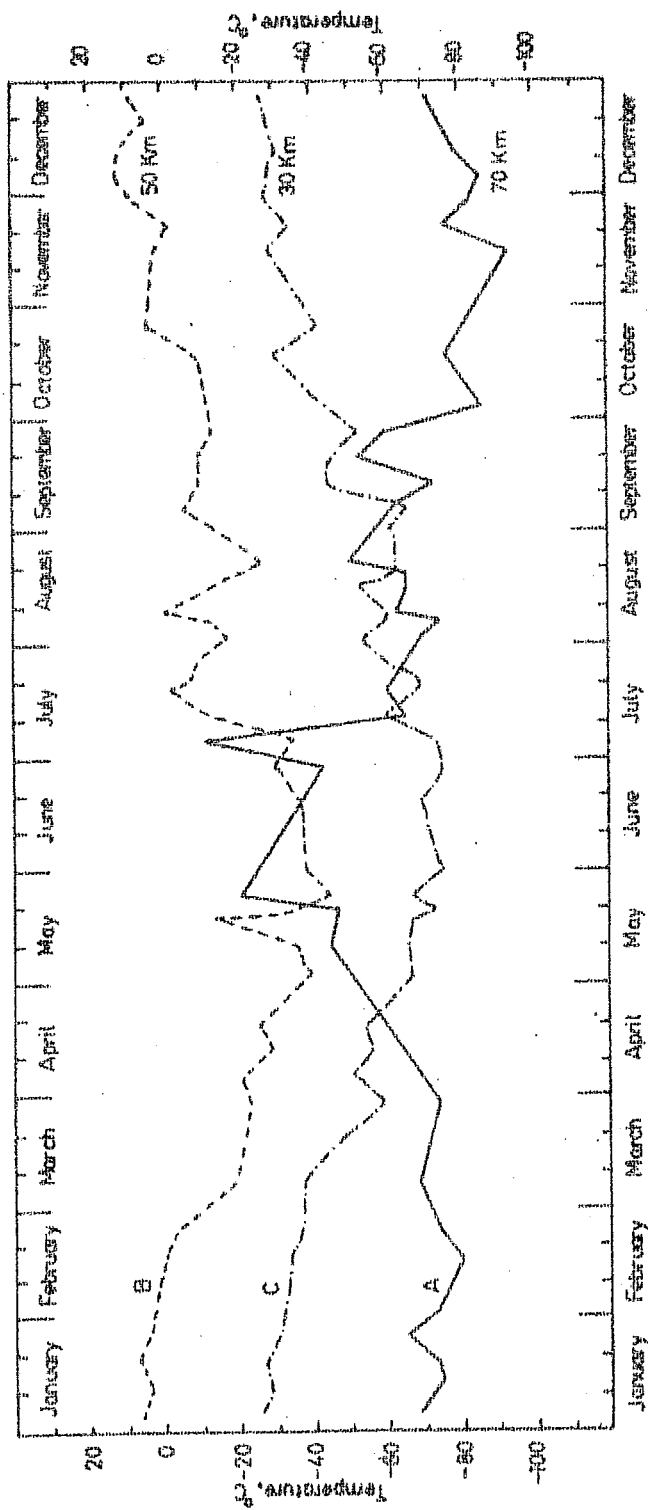
(Fig. 3.4)

Time section of annual variation of the upper atmospheric temperatures (°C) for the altitudes 30, 50 and 70 km at Molodezhnaya, Antarctica, in 1972.

temperature declines irregularly, attaining a minimum of $-93^{\circ}C$ in mid-November. Again in September there was a disruption with a warming of $20^{\circ}C$ followed by a cooling of $33^{\circ}C$ after which the temperature distribution returned to the normal summer regime.

Upper atmospheric warming and cooling of more than $15^{\circ}C$ over periods of less than 15 days during the winter period May to August and early spring are given in Table 5.3. It reveals that in May there was a significant warming both in the upper stratosphere and the mesosphere with a 'sudden warming' of $49^{\circ}C$ at 73 km from May 17 to 24. The warming was followed by a cooling of about $30^{\circ}C$ in the lower mesosphere. From June 28 to July 5, a warming of $37^{\circ}C$ was detected at 65 km. The upper stratosphere and the lower mesosphere were subjected to a warming from July 5 to 19, with a maximum of $38^{\circ}C$ at 55 km, whereas the upper mesosphere underwent a 'sudden cooling' which had a maximum value of $55^{\circ}C$ at 65 km from July 5 to 12. In August and September the warming in the mesosphere was less than $27^{\circ}C$ while the stratosphere at 40 km experienced a cooling of $26^{\circ}C$ from August 2 to 9, followed by a warming of $32^{\circ}C$ from August 9 to 16. At 40 km there was another warming of $39^{\circ}C$ from September 6 to 20, which was followed by a cooling of $20^{\circ}C$ from September 20 to 27.

Table - 5.3

Upper atmospheric warming (W) and cooling (C) of greater than 15°C over periods less than 15 days at Molodezhnaya, Antarctica, in 1972. Figures within brackets represent the corresponding dates of the warmings and coolings(°C)

May	May	June-July	July	July	July-Aug.	July-Aug.	August	August	Aug.-Sept.	September	September
Warming	Cooling	Warming	Warming	Cooling	Warming	Cooling	Warming	Cooling	Warming	Warming	Cooling
W 2	C 3	W 4	W 5	C 6	W 7	C 8	W 9	C 10	W 11	W 12	C 13
18 (10–17)	—	—	22 (5–12)	—	—	—	27 (9–16)	—	—	38 (6–20)	—
21 (10–17)	-18 (3–10)	—	29 (5–12)	—	21 (26– 2)	—	32 (9–16)	-26 (2– 9)	—	39 (6–20)	-20 (20–27)
26 (3–17)	-32 (17–24)	—	19 (5–12)	—	—	—	—	-22 (16–23)	—	17 (13–20)	—
24 (10–17)	-27 (17–24)	—	31 (5–19)	—	—	-23 (26– 2)	—	-26 (9–23)	21 (23– 6)	—	—
22 (10–17)	-28 (17–31)	19 (28– 5)	38 (5–19)	—	—	-26 (26– 2)	—	—	19 (23– 6)	—	26 (13–27)
36 (20–24)	—	37 (28– 5)	20 (12–19)	-55 (5–12)	—	-18 (26– 2)	18 (20–23)	—	15 (23– 6)	—	-27 (20–27)
26 (20–24)	—	31 (28– 5)	—	-53 (5–12)	—	—	22 (20–23)	—	—	19 (13–20)	-22 (20–27)
—	—	—	—	—	—	—	—	—	—	20 (13–20)	—

Table- 5.3 contd...2

2	3	4	5	6	7	8	9	10	11	12	13
49 (17-24)	-	-	-	-48 (5-12)	-	-	16 (6-20)	-	-	16 (13-20)	-
29 (17-24)	-	-	-	-25 (22-26)	-	-	16 (6-20)	-	-	-	-
36 (17-20)	-43 (20-24)	-	-	-39 (22-26)	22 (26- 2)	-	18 (16-20)	-	-	-	-

5.2.4   Discussion of results

The above investigation of the Antarctic upper atmosphere indicates that the most active period in south polar regions is the winter and the early spring. It is marked by large disruptions in the wind and thermal structure. The rapid shifts in both zonal and meridional components of the upper atmospheric winds, particularly during the winter period May to July were accompanied by sudden changes in the temperature distribution. Figure 5.4 shows that the stratospheric warming in May propagated upwards and was followed by the mesospheric warming. The stratospheric warming in July followed the mesospheric warming indicating downward in July followed the mesospheric warming indicating downward propagation of the disturbance which started above 70 km. Apparently, the polar winter warmings were caused both by an increase in the supply of energy by radiative and photochemical processes taking place in the upper atmosphere. During September, when the winter westerlies changed to the summer easterlies, the upper atmosphere was again disrupted with a warming of $39^{O}C$ at 40 km which is attributed to the increase in available heat brought about by the return of sun-light.

There is also an indication that pronounced stratospheric and mesospheric warmings over Antarctica occurred on geomagnetically disturbed days when aurora australis was also

observed. For example an intense aurora australis was visually observed from May 14 to 17 which was followed by a sudden warming of $49^{\circ}C$ at 73 km from May 17 to 24. Again, an intense auroral glow was observed on July 3 & 4 which was also followed by an explosive warming in the mesosphere and the stratosphere, e.g. a warming of $37^{\circ}C$ was detected at 65 km from June 28 to July 5. The aurora australis was also observed on August 7 & 8 followed by a warming of $32^{\circ}C$ from August 9 to 16 in the stratosphere. Apparently, there is a marked correlation of the strato-mesosphere warmings with auroral activity and consequently a dependence on the variability of the solar wind, i.e. solar corpuscular invasions causing and controlling auroral, magnetic, ozonal and thermal phenomena.

In the spring and early summer great changes take place in the stratosphere. The circulation that was strongly cyclonic with westerly winds averaging as much as 50 m/s changes abruptly. In the stratosphere and the mesosphere, warming of as much as $50^{\circ}C$ takes place during winter and early spring and westerly winds generally prevail. The polar warmings also appear to be due to the transport of warm air from lower latitudes and to adiabatic heating, i.e. an increase in air temperature as a consequence of internal processes of contraction caused by sinking motions over the continent. It is partly caused by absorption of solar

radiation in the atmosphere. During this period there is a sharp rise in surface pressure from the late wintertime minima that are noted almost everywhere over Antarctica to the summertime maxima. These pressure changes indicate that great masses of air are transported and as much as 15×10^7 tons of air are lost or gained over Antarctica from one month to another.

It was found that the annual variation of the atmospheric temperature over Antarctica was smaller at the surface and in the troposphere, while in the stratosphere and the mesosphere the variation was quite large. Also, the Antarctic upper atmosphere was subjected to large thermal perturbations during the winter regime causing significant warming and cooling in the stratosphere and mesosphere with larger amplitudes at higher altitudes. It was also found that a differential cooling was set in the atmosphere beginning early autumn which weakened the south polar tropopause and at times wiped it out thus forming a complex quasi-tropopause during the winter regime. The Antarctic winter stratosphere was colder than its summer counterpart, while the polar winter mesosphere in the southern hemisphere was found to be warmer which may be due to a large-scale meridional transport of heat resulting from a mean meridional atmospheric circulation or from large-scale eddy processes.

5.3   Atmospheric pressure and density variations

Time-height cross sections of the atmospheric pressure (mb) and density (gm^{-3}) over Antarctica from the M-100 meteorological rocket soundings carried out at Molodezhnaya in 1972 are drawn in Figs. 5.5 and 5.6 respectively. Annual mean and corresponding standard deviations of the pressure and density were computed as in Table 5.4. Departures of the monthly average pressure from the 1972 annual mean for the southern summer (December to February), autumn (April), winter (June to August) and spring (October) months in an altitude region from surface to 80 km at 5-km interval are worked out in Table 5.5. Monthly averages of the atmospheric density along with the 1972 annual mean are given in Table 5.6.

Fig. 5.5 shows that at high latitudes in winter there is a ridge of high pressure, and the pressure decreases rapidly polewards of this ridge. Compared to the lower latitudes or the summer hemisphere much greater variations of the atmsopheric pressure occur in the winter period over Antarctica. During the autumn the pressure in the stratosphere and the mesosphere decreases from the summer values till early winter. On May 17 a significant increase is detected in the mesospheric pressure which may be attributed to the sudden mesospheric warmings over Antarctica. Again, in July,
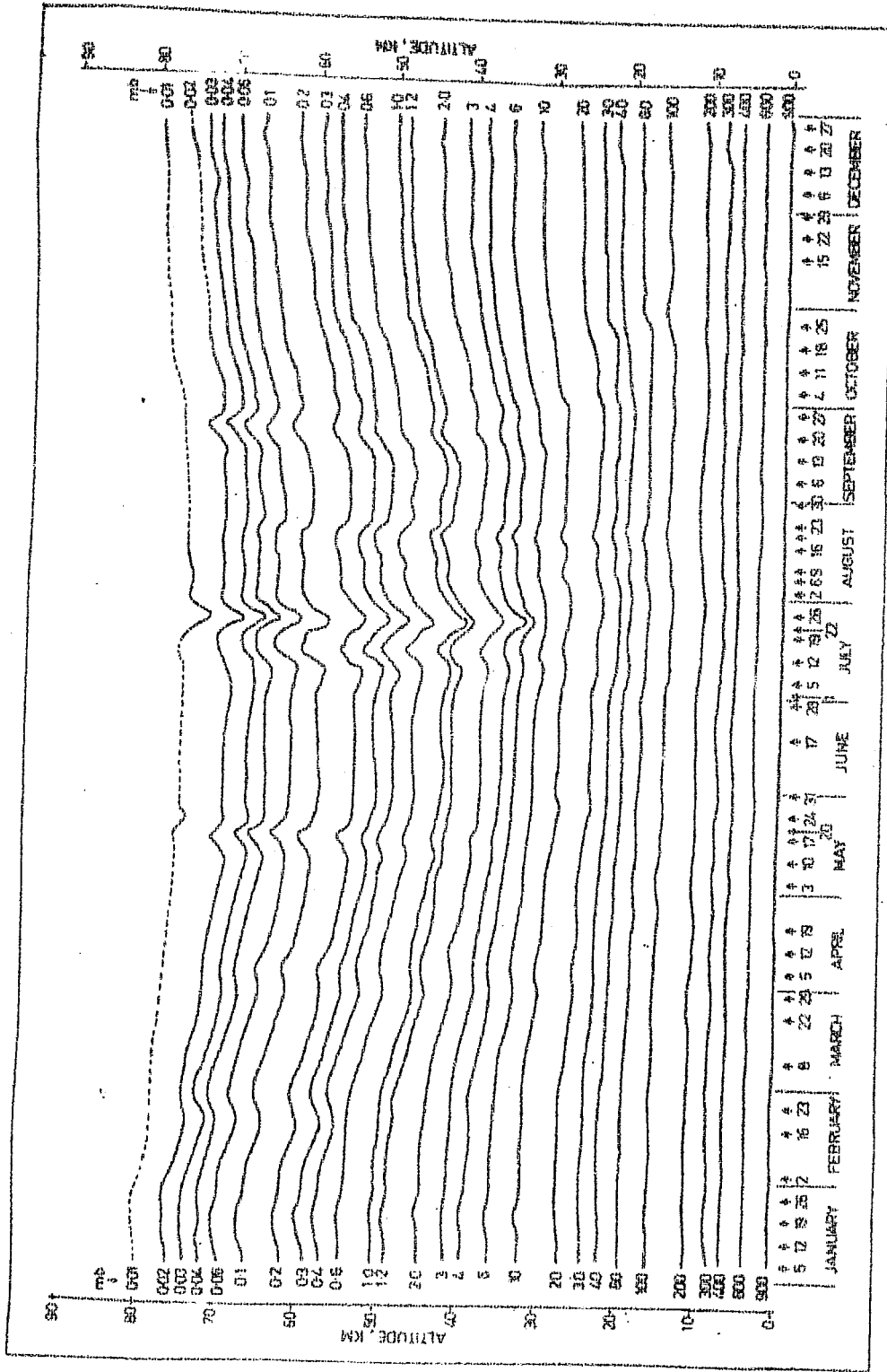
(Fig. 5)

Light cross section of the atmospheric pressure (mb) over Molodezhnaya, Antarctica. Dashed lines represent extrapolated data. Arrows above the abscissa show the dates when the data were obtained.

Table - 5.4

Annual mean and corresponding standard deviations of atmospheric pressure (mb) density (gm^{-3}) from M-100 rocket launchings at Molodezhnaya, Antarctica in 1972

Altitude (km)	Pressure (mb)		Density (gm^{-3})		No. of observations
	Annual Mean	Standard deviation	Annual Mean	Standard deviation	
1	2	3	4	5	6
0	987.2	9.2	-	-	49
2	763.5	7.7	-	-	49
4	579.6	9.2	-	-	49
6	434.2	9.0	-	-	49
8	320.0	9.7	-	-	49
10	233.4	7.9	387.8	9.9	49
12	171.4	7.7	275.5	8.6	49
14	123.1	7.8	201.1	7.0	49
16	89.4	7.1	146.6	4.6	49
18	65.1	6.7	106.7	4.1	49
20	49.1	6.4	77.6	5.1	49
22	34.1	5.3	56.2	5.1	49
24	24.8	4.5	40.7	4.2	49
26	18.0	3.8	29.4	3.7	49
28	13.2	3.0	21.1	3.4	46

more

Table - 5.4 contd...2..

1	2	3	4	5	6
30	9.76	2.51	15.14	2.89	46
32	7.23	1.50	11.09	2.31	46
34	5.40	1.50	8.01	1.85	46
36	4.05	1.34	5.89	1.50	46
38	3.09	1.00	4.36	1.19	46
40	2.351	0.827	3.243	0.953	46
42	1.813	0.634	2.439	0.768	46
44	1.402	0.512	1.855	0.590	46
46	1.087	0.408	1.432	0.473	46
47	0.958	0.365	1.260	0.421	46
48	0.878	0.323	1.112	0.372	46
50	0.658	0.264	0.870	0.297	45
52	0.512	0.210	0.682	0.249	45
54	0.395	0.167	0.543	0.203	44
56	0.298	0.130	0.428	0.170	43
58	0.229	0.094	0.337	0.137	42
60	0.1714	0.0757	0.2634	0.1090	42
62	0.1281	0.0565	0.2022	0.0888	40
64	0.0944	0.0436	0.1531	0.0741	40
66	0.0689	0.0308	0.1144	0.0526	40

Table - 5.4 contd..3..

1	2	3	4	5	6
68	0.0504	0.0215	0.0852	0.0393	39
70	0.0364	0.0151	0.0626	0.0294	39
72	0.0264	0.0103	0.0471	0.0209	35
74	0.0190	0.0083	0.0365	0.0200	25
76	0.0139	0.0052	0.0258	0.0118	20
78	0.0096	0.0037	0.0183	0.0085	14
80	0.0060	0.0020	0.0126	0.0057	11

Table – 5.5

Monthly average atmospheric pressure in mb (P) over Molodezhnaya, Antarctica in 1972 and the corresponding departures (D) from the annual mean

Alti-tude (km)	Pressure Departure	Southern summer			Autumn		Southern winter			Spring
		Dec	Jan	Feb	April	June	July	Aug		October
1	2	3	4	5	6	7	8	9		10
0	P	989.5	988.3	987.3	981.0	994.0	985.7	988.0		979.3
	D	2.3	1.1	0.1	-6.2	6.8	-1.5	0.8		-7.9
5	P	512.8	513.3	511.3	501.7	509.5	493.7	502.3		494.8
	D	10.0	10.5	8.5	-1.1	6.7	-9.1	-0.5		-8.0
10	P	242.0	245.5	242.7	233.0	236.0	223.3	232.1		227.3
	D	8.6	12.1	9.3	-0.4	2.6	-10.1	-1.3		-6.1
15	P	113.6	115.8	115.8	108.4	102.3	95.39	100.2		100.4
	D	8.7	10.9	10.9	3.5	-2.6	-9.51	-4.7		-4.5
20	P	54.58	55.60	55.70	50.00	43.27	39.46	42.14		44.90
	D	5.48	6.5	6.6	0.9	-5.83	-9.64	-6.96		-4.2
25	P	26.55	26.92	26.89	22.84	17.99	16.23	17.56		20.57
	D	5.42	5.79	5.76	1.71	-3.14	-4.90	-3.57		-0.56
30	P	13.09	13.23	13.15	10.41	7.565	6.768	7.615		10.04
	D	3.33	3.47	3.39	0.65	-2.19	-2.99	-2.14		0.28

More

Table – 5.5 contd..2..

| 1	2	3	4	5	6	7	8	9	10
35	P	6.614	6.756	6.596	4.849	3.333	3.084	3.554	4.968
	D	1.93	2.08	1.92	0.17	-1.35	-1.60	-1.13	0.29
40	P	3.465	3.572	3.410	2.324	1.574	1.491	1.777	2.537
	D	1.11	1.22	1.06	-0.03	-0.78	-0.86	-0.57	0.19
45	P	1.874	1.934	1.820	1.152	0.7834	0.7662	0.9350	1.385
	D	0.64	0.70	0.59	-0.08	-0.45	-0.47	-0.30	0.15
50	P	1.032	1.056	0.9864	0.5829	0.3939	0.4005	0.4977	0.7138
	D	0.374	0.398	0.328	-0.075	-0.264	-0.258	-0.161	0.056
55	P	0.5559	0.5708	0.5012	0.3074	0.1878	0.2071	0.2514	0.3761
	D	0.210	0.225	0.156	-0.038	-0.158	-0.139	-0.094	0.031
60	P	0.2827	0.2919	0.2402	0.1459	----	0.1036	0.1189	0.1868
	D	0.1113	0.1205	0.0688	-0.0255	----	-0.0678	-0.0525	0.0154
65	P	0.1335	0.1388	0.1119	0.0674	----	0.0503	0.0541	0.0754
	D	0.0528	0.0581	0.0321	-0.0133	----	-0.0304	-0.0266	-0.0053
70	P	0.0586	0.0622	0.0493	0.0312	----	0.0237	0.0243	0.0322
	D	0.0222	0.0258	0.0129	-0.0052	----	-0.0127	-0.0121	-0.0042
75	P	0.0239	0.0266	0.0201	----	----	0.0108	0.0105	0.0158
	D	0.0077	0.0104	0.0039	----	----	-0.0054	-0.0057	-0.0004
80	P	0.0096	0.0109	----	----	----	0.0044	0.0045	----
	D	0.0036	0.0049	----	----	----	-0.0016	-0.0015	----

Table - 5.6

Monthly average atmospheric density (gm^{-3}) over Molodezhnaya, Antarctica in 1972 from the M-100 rocket soundings

Alti-tude (km)	Southern summer			Autumn	Southern winter			Spring	Annual Mean
	December	January	February	April	June	July	August	October	
1	2	3	4	5	6	7	8	9	10
10	383.7	384.9	373.6	431.1	398.8	380.9	389.0	379.0	387.8
15	171.9	175.8	174.2	169.9	176.7	169.1	174.9	166.2	171.8
20	81.02	83.04	83.39	79.8	77.41	71.27	75.34	73.69	77.63
25	38.79	39.87	39.77	36.90	32.62	28.88	31.16	33.36	34.64
30	18.68	18.83	19.18	16.53	13.13	11.41	12.42	14.94	15.14
35	9.026	9.112	9.144	7.500	5.421	4.779	5.296	6.998	6.852
40	4.475	4.600	4.518	3.435	2.316	2.109	2.415	3.417	3.243
45	2.326	2.418	2.320	1.634	1.105	0.9914	1.224	1.739	1.637
50	1.2748	1.323	1.257	0.8190	0.5738	0.5360	0.6730	0.9264	0.8700
55	0.7405	0.7563	0.7226	0.4600	0.3005	0.2892	0.3725	0.5141	0.4876
60	0.4159	0.4278	0.3648	0.2302	0.1407	0.1519	0.1904	0.2472	0.2634
65	0.2184	0.2243	0.1848	0.1086	---	0.0769	0.0899	0.1290	0.1330
70	0.1043	0.1068	0.0867	0.0533	---	0.0380	0.0406	0.0583	0.0626
75	0.0471	0.0485	0.0389	---	---	0.0182	0.0178	0.0277	0.0297
80	0.0205	0.0219	---	---	---	0.0084	0.0082	---	0.0126

large pressure fluctuations were noticed in the stratosphere
and the mesosphere, e.g. from July 5 to 12 the upper atmos-
pheric pressure in an altitude range of about 30 to 80 km
increased significantly followed by an equal decrease up to
July 22 which again rapidly increased and attainred normal
winter values by July end. The pressure fluctuations were as
a result of the sudden stratospheric and mesospheric warming
during the winter period. The upper atmospheric pressure
gradually increased during the spring and subsequently
attained the normal summer values. Obviously, there was a
large seasohal variation with a pronounced semi-annual
variation in the upper atmospheric pressure particularly in
the stratosphere and the mesosphere, over Antarctica.

In the troposphere the pressure variations are
relatively less. The summer values of the atmospheric
pressure in the upper stratosphere and the mesosphere
exceed the winter values almost by a factor of two as is
obvious from the Table 5.5. The pressure data also indicates
a diurnal variation having the amplitudes smaller at lower
altitudes and larger at higher altitudes with significant
diurnal variation in the upper mesosphere.
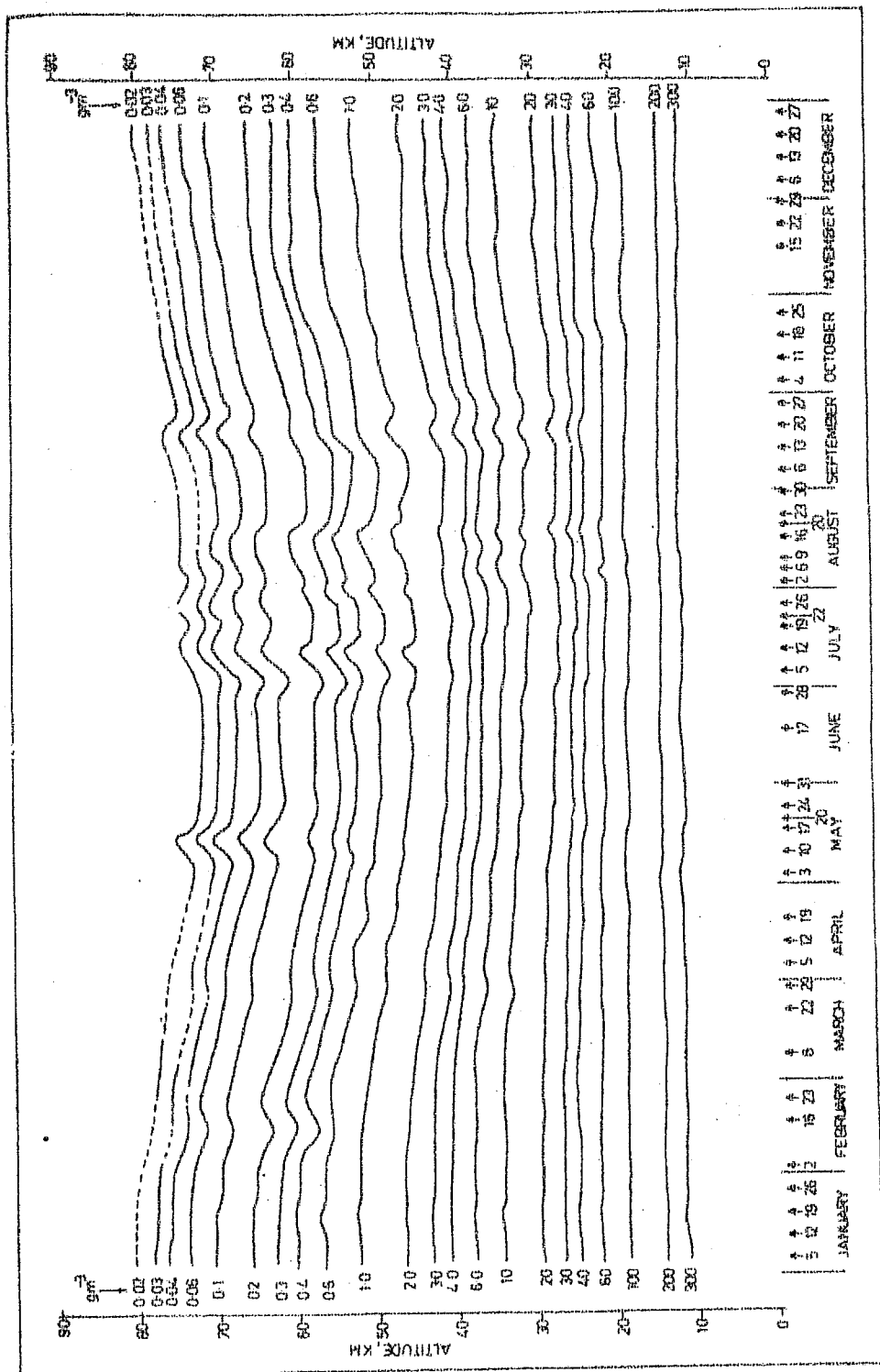
(Fig. 5.6)

Time-height cross section of atmospheric density (gm^{-3}) over Molodezinaya, Antarctica in 1972. Dashed lines represent extrapolated data. Arrows above the abscissa show the dates on which the data were obtained.

As shown by Fig.5.6 variations in the atmospheric density over Antarctica were similar to the pressure variations discussed above. The summer values of the density exceed the winter values almost by a factor of 2 as revealed by Table 5.6. In the upper stratosphere and mesosphere there were fluctuations with an increase and decrease in atmospheric density particularly during the early and mid-winter periods, e.g. on May 17 and July 12 a significant increase in density was observed in the mesosphere as shown by Fig. 5.6. This might have again resulted from the sudden warmings which occurred in the south polar stratosphere and mesosphere during the winter regime.

C H A P T E R - VI
═════════════════

STUDY OF EQUATORIAL ATMOSPHERIC STRUCTURE

A major portion, nearly 75 % of the total rocket launchings carried out from the Thumba Equatorial Rocket Launching Station ($8^{\circ}32'N$, $76^{\circ}52'E$), India have been of meteorological interest. The rocket sounding programme commenced from Thumba on July 14, 1964 with the launching of a Judi Dart rocket with copper chaff payload for measuring the upper atmospheric winds which was followed by 35 more flights up to August 1969. Rao (1967) has discussed the results derived from the chaff-borne Judi-Dart rocket flights carried out at Thumba and shown that in the middle stratosphere the flow is predominantly zonal while in the upper stratosphere and the lower mesosphere periodic meridional flow exists. The upper atmospheric wind and temperature measurements were also made in March 1970 with Skua rocket system.

The Indo-Soviet M-100 meteorological rocket sounding programme commenced from Thumba on December 9, 1970. Preliminary results of the M-100 meteorological rocket soundings from Thumba are reported by Narayanan and Fedynski (1973).

It is found that the quasi-bienniel oscillation of the equatorial stratospheric winds over Thumba was most evident in the zonal wind profiles. During 1971 and 1973 the westerly phase of the quasi-bienniel oscillation was predominant while in 1972 the easterly phase was present. The seasonal effects on the vertical distribution of the zonal wind component in the lower equatorial stratosphere in an altitude range of 17 to 38 km manifest themselves as an intensification of the easterly phase of the 26 month oscillation during the summer. The Berson westerlies make their appearance over Thumba every year for a period of about 5-7 months, October to May and are absent during the south-west monsoon period.

6.1   Equatorial circulation pattern

In 1972 about 52 meteorological M-100 rockets were launched from Thumba, mostly after sunset around 2000 IST (1430 GMT) and the average rocket apogee reached was about 89 km. Time-height cross sections of the zonal winds, meridional winds and of temperature are shown in Figs.6.1, 6.2 and 6.3 respectively. Seasonal averages of the zonal winds, meridional winds and of the temperatures for the northern summer (June to August), autumn (September to November), winter (December to February) and spring (March to May) are

ALTITUDE (km)

JANUARY FEBRUARY MARCH APRIL MAY JUNE JULY AUGUST SEPTEMBER OCTOBER NOVEMBER DECEMBER

—height cross section of the zonal winds (ms⁻¹) over Thumba, Equatorial India in 1972. Shaded areas with negative
es present easterly components while the blank areas with positive values depict the westerly wind components. Dashed
represent extrapolated data. Arrows on the abscissa show the dates on which the data were obtained.

(Fig. 6·1)

given in Tables 6.1, 6.2 and 6.3 respectively along with their annual mean showing the seasonal variation of the atmospheric wind and thermal structure over the equatorial station Thumba.

The equatorial upper troposphere from about 10 to 17 km is a region of easterly winds interrupted periodically by short spells of narrow westerlies during January to April, the duration of each spell varying from a few weeks to about two months as is obvious from Fig 6.1. Within the general easterly circulation, a week westerly stream prevailed during the period from June to September in the lower troposphere below 10 km. Fig. 6.2 shows that the meridional transport of air in the middle stratosphere is neglegible but there is a progressively increasing meridional flow as we go to higher altitudes. Meridional circulation index of the order of 30 to 40 m/s has been experienced in the lower mesosphere on certain occassions. For example, a northerly wind of 65 ms^{-1} was noticed at 48 km, the stratopause in the 3rd week of November 1972 with a southerly wind of 42 ms^{-1} at 40 km in November end. No regular pattern of meridional flow was observed over the equatorial region. The meridional winds were of variable nature with fluctuations of shorter durations and larger amplitudes.

In the middle stratosphere from about 25 to 35 km the westerlies and easterlies change biennially and in the layers within 10 to 17 , they change annually. The transition from the bienniel cycle above the stratonull or 25 km to the annual
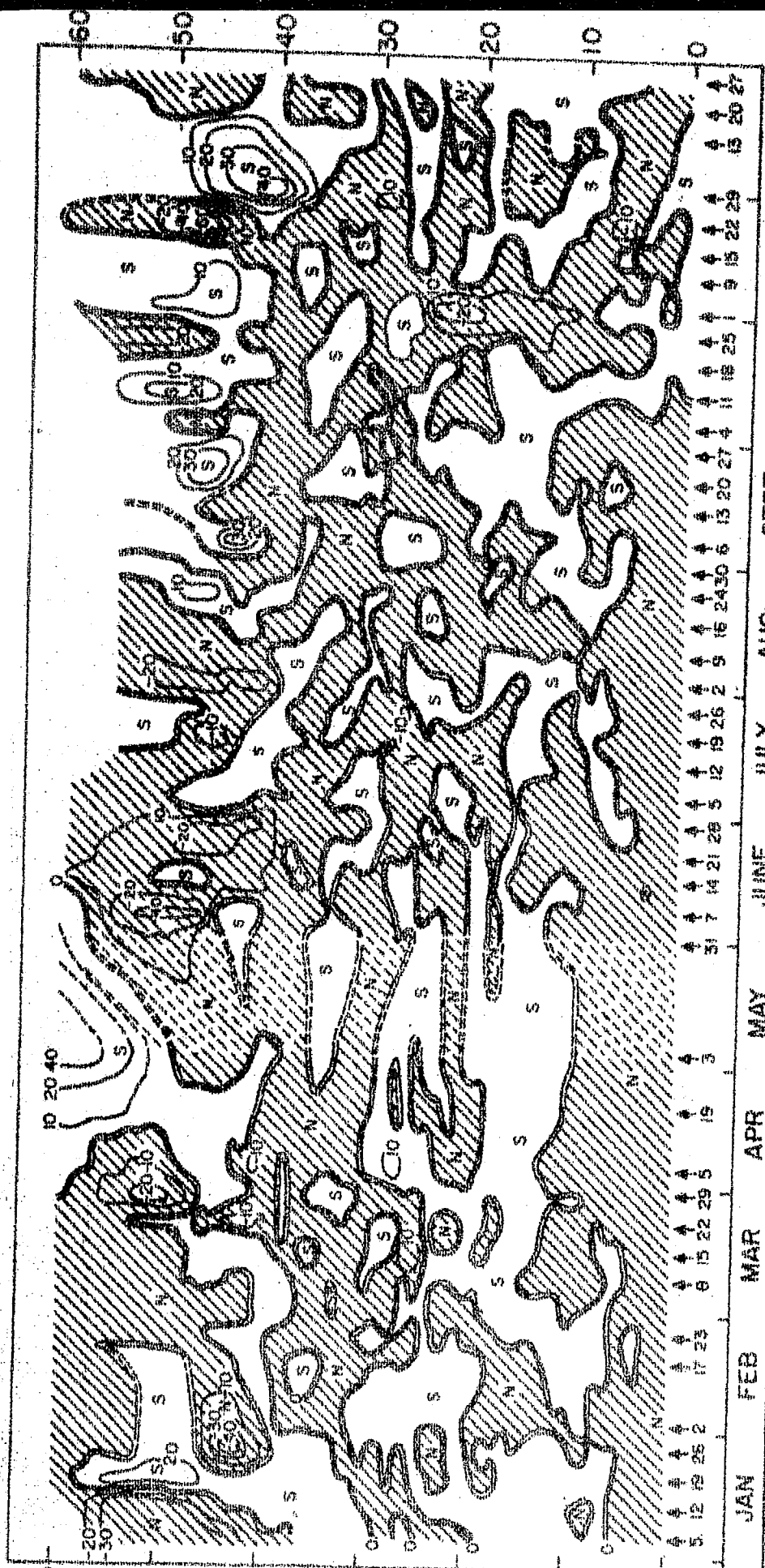
Time-height cross section of the meridional winds (ms⁻¹) over Thumba. Equatorial India in 1972. Shaded areas with negative values depict the southerly wind components while the blank areas with positive values present northerly components. Dashed lines represent extrapolated data. Arrows on the abscissa show the dates on which the data were obtained.

(Fig. 6.2)

cycle below the tropopause around 18 km takes place through a cyclic change of 15 months period in the intermediate layer between the tropopause and stratonull. The layers above 40 km have oscillations of semi-annual period and the transition layer between 36 and 40 km levels has an annual period. While the combined easterly-westerly oscillations in the middle stratosphere have a biennial period, it is seen that the period is slightly more than 24 months (George and Narayanan, 1975). Other workers have found a 26 months cycle for the stratospheric circulation over the Pacific Ocean area (Kats, 1970). While in no layer of the atmosphere the westerly regime lasts for more than 6 months, the easterly regimes have very long durations in the upper troposphere and in the lower and the middle stratosphere.

6.2   Berson westerly winds

The equatorial circulation in the lower stratosphere is strongly marked by the appearance of the westerly current every year at regular periodic intervals within the prevailing broad equatorial stratospheric easterlies. The westerly current occurring in the equatorial lower stratosphere is commonly known as 'Berson wind'. According to Palmer (1954), the narrow stream of Berson westerlies has its axis usually nearly $2^{\circ}N$ and extends through a latitudinal zone of not more than 7° on both sides of this axis. The Berson westerlies are noticeable in an altitude region from about 18 to 25 km as in

Fig.6.1 and extend up to the first week of June.

The easterly jet in the upper troposphere and the westerly Berson current in the lower stratosphere are apparently two complementary circulation systems, one appearing over Thumba when the other disappears. The Berson westerlies are known to exist over the equatorial region of the Indian Ocean throughout a year, while over Thumba they are found for about 8 months in a year and are generally absent during the SW monsoon period, June to September. The layers in which Berson current exists over Thumba vary from year to year with some similarities between the Berson currents of the alternate years. The Berson westerlies get displaced gradually to the southern hemisphere when the Indian summer starts. Average strength of the zonal components of the Berson current was about 10 to 20 ms^{-1}. A time-lag has been noticed between the appearance or disappearance of the westerlies and the easterlies on the periphery of either side of the equatorial zone. The manner in which the upper boundary of the Berson current over Thumba gradually increased and decreased in height would suggest that the vertical depth of the stream was maximum along the central axis decreasing gradually towards the northern and southern boundaries. There is an indication that the Berson westerly stream has its northern boundary extending beyond 10° N during the period of its maximum displacement to the

northern hemisphere. The above analysis suggests that the general pattern of zonal circulation in the lower stratosphere has certain amount of asymmetry about the equator as reported by Rao and Joseph (1971).

6.3   Strato-mesospheric circulation

The equatorial middle stratosphere from 25 to 35 km is a region of predominantly easterly circulation having biennial characteristics. A biennial westerly circulation prevails over certain layers of this region during September to April months of the alternate years. From October to December of these alternate years, westerlies predominate from lower stratosphere to lower mesosphere. The average zonal wind speed in the core of these westerlies above 30 km level was of the order of 30 ms^{-1}. In the 1970-71 season, October to April the westerlies were prominent with average zonal components of the order of 10 to 20 ms^{-1} reaching occassionally jet speed of 30-35 ms^{-1} in the core region. Owing to the quasi-bienniel periodicity the westerlies were absent in the 1971-72 season. They appeared again at the end of September 1972 and continued up to April 1973. The appearance of broad and very strong easterly jet stream during June to October period is an annual feature

of the middle stratospheric circulation. In 1972, the jet
stream covered the entire middle stratosphere and even
extended into the lower stratosphere and well into the
upper stratosphere as shown in Fig. 6.1. The average strength
in the core region was of the order of 40-50 ms^{-1}. In 1972
November end, the westerlies had a maximum speed of 84 ms^{-1}
at 35 km. In the years 1971 and 1973 the middle stratospheric
easterlies covered a relatively narrow region as compared with
the 1972 profiles.

   The upper stratosphere in an altitude region from 35
to 45 km is characterised by well marked semi-annual oscilla-
tion with easterlies during the northern winter (December to
February) and summer (June to August) and westerlies in
spring (March to May) and autumn (September to November)
as shown by Table 6.1, and Fig. 6.1. The pattern
and shape of the isotachs separating the westerlies and
easterlies in the upper stratosphere and mesosphere would
suggest that the westerlies in the upper stratosphere
are due to the mesospheric westerlies penetrating downwards
periodically. The region 35 to 40 km appears to be closely
linked with the semi-annual cycle above and the quasi-
biennial cycle below through a well defined annual cycle.
The easterlies had a larger period than the westerlies and
attained jet speeds with an average of about 30-50 ms^{-1}.

Table - 6.1

Seasonal variation of the zonal components of winds (EW) and corresponding standard deviations (SD) in m/s over equatorial Thumba (8°32'N, 76°52'E). Negative sign indicates easterly winds while the positive values give the westerlies. The number of observations for these northern seasons were 13 each.

Summer		Autumn		Winter		Spring	
June	August	September	November	December	February	March	May
EW	SD	EW	SD	EW	SD	EW	SD
2	3	4	5	6	7	8	9
2.7	2.1	1.7	2.1	0.2	2.9	3.3	1.9
10.0	3.5	0.7	4.3	-3.6	4.0	-4.6	4.1
6.7	5.3	-0.1	3.6	-3.2	5.7	-7.1	3.9
3.5	4.4	-3.1	5.2	-6.5	5.6	-6.0	5.0
-0.7	5.9	-4.3	4.2	-5.4	8.3	-0.9	4.5
-7.5	6.4	-5.4	4.0	-3.6	8.3	-0.1	7.6
-18.8	8.9	-9.2	5.4	-5.8	9.7	-2.3	8.4
-30.6	6.4	-12.6	6.8	-6.7	13.2	-3.7	8.1
-25.3	6.3	-11.5	6.7	-6.3	5.4	-6.5	8.6
-15.1	6.1	-8.8	4.8	0.2	5.4	0.9	4.9
-15.9	6.2	-16.6	3.1	9.4	2.3	8.6	5.4
-21.7	3.9	-25.3	3.9	9.8	3.6	4.9	8.3
-27.0	4.0	-27.7	6.4	2.2	5.4	-6.2	9.7

more

Table - 6.1 contd..2..

1	2	3	4	5	6	7	8	9
26	-32.5	3.3	-24.8	8.6	- 2.9	5.5	-16.9	5.4
28	-38.5	7.6	-15.5	16.4	-14.2	5.8	-23.2	6.0
30	-36.5	5.2	- 3.4	17.4	-20.8	6.2	-26.9	7.0
32	-35.2	5.4	4.8	13.5	-21.9	7.3	-27.1	9.0
34	-27.6	9.5	4.5	9.8	-21.4	8.1	-25.9	8.7
36	-24.8	11.3	9.5	9.9	-11.3	11.3	-22.8	7.0
38	-25.4	13.4	6.7	9.2	- 2.4	13.3	-19.5	13.1
40	-24.5	16.1	8.8	9.2	- 2.3	13.9	8.2	11.9
42	-21.7	17.8	10.5	11.4	- 6.5	22.2	- 0.3	10.4
44	-14.2	20.8	14.8	23.3	- 6.8	23.6	- 0.4	20.6
46	- 7.9	29.7	11.5	24.1	- 8.3	24.0	2.7	27.3
48	- 5.3	29.3	9.4	19.6	-11.2	28.2	2.9	25.6
50	- 5.9	26.6	10.9	21.7	-10.3	29.3	0.4	24.9
52	- 6.0	26.3	12.5	21.4	- 4.2	28.4	2.3	26.2
54	- 3.1	24.9	13.1	19.3	4.3	27.5	7.3	29.5
56	1.8	21.3	12.5	18.0	14.5	26.0	16.1	33.1
58	8.0	19.2	10.4	18.1	2C.0	29.4	27.8	38.1
60	14.7	27.2	7.9	21.4	26.8	34.1	33.8	33.0

The easterlies are stronger during the easterly phase of the quasi-biennial oscillation when the zonal wind speeds of more than 80 ms^{-1} were found in the core region on certain days.

Wind data for the equatorial mesosphere over Thumba were available up to an altitude of about 60 km. The semi-annual variation of the zonal circulation in the equatorial mesosphere is shown in Fig. 6.1. It is found that in the lower mesosphere region, the westerlies are of durations varying from 3 to 5 months followed by corresponding easterlies of shorter durations varying from 1 to 3 months. It is evident from Fig. 6.1 that the duration of the westerlies gradually increased and that of the easterlies decreased towards the higher levels of the mesosphere. The total combined duration of two consecutive periods of westerlies and easterlies in the lower mesosphere is about 6 months indicating a regular semi-annual cycle. Very strong winds having average zonal components of more than 50 ms^{-1} are quite common in the mesospheric region from about 45 to 60 km. The seasonal variation of the atmospheric winds, both zonal and meridional components over the equatorial station Thumba in 1972 are shown in Tables 6.1, and 6.2 respectively.

6.4   Relation with the tropospheric circulation

The steadiness factor (SF) computed from the ratio of the mean vector wind to the mean scalar wind expressed as a percentage is given in Table 6.2. It is found to vary significantly both during the northern summer and winter with larger values in the lower and the middle stratosphere and smaller values in the upper stratosphere and the lower mesosphere. Large variability was noticed in the spring and autumn reversal periods also with relatively higher values. Transient eddies as revealed by fluctuations in the zonal and meridional components of the winds are more frequent during the transitions from winter to summer and summer to winter with the meridional component exceeding 25-30 ms^{-1}. Their frequency is less during the equinoxes when the zonal winds are steady westerl, and the meridional winds rarely exceed 10 ms^{-1}. In the equatorial mesosphere the winds are generally westerly during the northern autumn and spring with an average speed of up to about 35 ms^{-1} and a standard deviation of the same order. During summer and winter the winds are predominantly easterly with speeds varying over a wider range, about + 10 to -40 ms^{-1} as is obvious from Table 6.1.

The analysis also shows that the equatorial tropospheric circulation is influenced to a great extent by

Table - 6.2

Seasonal variation of the meridional components of winds (NS) and corresponding standard deviations (SD) in m/s over equatorial Thumba (8°32'N, 76°52'E) in 1972. Negative sign indicates northerly winds while the positive values give the southerlies. Sf is the steadiness factor in %. The number of observations for these northern seasons were 13 each

Summer			Autumn			Winter			Spring		
(June	-	August)	(September	-	November)	(December	-	February)	(March	-	May)
NS	SD	SF	NS	SD	SF	NS	SD	SF	NS	SD	SF
2	3	4	5	6	7	8	9	10	11	12	13
-1.8	2.5	83.5	-0.5	1.6	68.9	1.2	2.7	44.7	-1.4	2.3	93.5
-5.1	3.5	100.0	-1.6	3.1	42.4	-1.9	3.2	77.1	-3.9	2.2	96.8
-2.8	1.9	89.5	-0.4	2.6	10.4	0.5	2.3	53.9	-2.8	3.1	99.3
-2.1	3.1	76.3	-1.7	3.2	59.3	0.7	3.8	88.7	-1.2	4.1	88.3
0.2	4.5	11.2	-1.3	2.9	73.6	1.2	2.6	62.7	-2.9	3.8	56.2
-1.5	3.9	89.3	-0.3	2.9	85.0	3.1	5.9	51.2	-1.5	4.5	21.6
-0.5	4.8	93.7	0.0	3.4	95.3	4.5	4.5	68.1	2.4	4.9	37.5
-0.8	5.3	99.1	-0.5	4.0	95.3	4.0	6.7	57.2	3.9	7.5	51.0
0.9	3.3	99.5	0.3	3.2	98.1	1.5	5.0	77.3	0.9	3.9	79.7
-0.7	1.8	99.5	0.7	2.2	97.6	0.7	3.3	12.9	1.3	2.8	34.8
-0.9	1.5	99.8	1.2	2.8	99.6	0.9	2.5	98.6	0.7	3.1	90.2
-1.5	3.4	99.6	0.5	1.8	99.8	-1.2	2.8	97.4	-2.5	3.9	60.6
-0.2	3.2	99.6	-0.8	2.2	99.8	-0.1	5.7	36.3	1.6	4.9	62.8

more

Table - 6.2 contd..2..

2	3	4	5	6	7	8	9	10	11	12	13
-1.1	3.8	99.7	0.0	7.3	97.9	2.2	3.8	54.2	0.4	6.5	96.3
-3.7	3.8	99.9	-1.2	8.7	80.5	-0.4	6.5	96.1	-0.6	6.3	97.3
-0.2	4.4	99.5	-1.3	3.8	24.4	-1.5	5.7	97.7	-1.9	5.6	98.8
-2.0	3.7	99.7	-0.9	6.0	39.9	0.2	4.2	98.7	-1.5	4.5	99.1
-1.9	7.3	98.1	-4.2	14.6	52.1	2.2	5.8	97.4	-0.6	4.9	99.0
-2.9	4.6	99.2	-2.5	9.9	70.4	1.1	3.8	87.0	-3.1	5.1	99.8
0.1	5.3	98.6	-5.4	8.7	79.7	-0.3	5.5	22.6	-1.0	6.5	96.8
-2.8	8.0	91.3	-3.8	3.4	78.7	1.2	5.3	25.0	-0.9	4.8	73.7
-5.3	15.4	83.1	0.9	11.7	70.7	-1.7	16.6	33.4	-5.0	15.2	38.7
-1.1	21.3	54.3	5.2	18.6	63.2	0.0	22.4	25.0	-4.6	20.3	21.9
-1.1	29.9	23.5	2.8	26.1	43.1	4.5	26.5	31.7	-3.9	15.0	18.6
-1.8	30.8	16.3	-0.1	29.5	32.0	5.1	27.4	36.1	-9.0	17.3	35.0
-5.6	25.5	27.9	-0.5	26.8	36.4	3.2	26.5	31.8	-13.4	21.2	44.8
-8.0	18.4	37.4	0.2	22.7	43.2	-2.4	23.7	14.8	-13.9	24.4	44.7
-7.5	14.6	33.4	1.1	18.7	50.8	-1.5	21.4	14.7	-9.5	26.8	35.8
-5.1	13.3	25.7	1.1	15.5	52.1	-2.2	18.3	52.8	-4.5	24.7	46.7
-1.9	13.7	38.3	0.2	12.1	47.5	-5.0	20.0	58.1	-2.4	22.6	68.5
2.0	16.8	57.6	-1.3	12.1	37.3	-5.7	26.2	63.8	7.6	21.9	78.0

the strato-mesospheric circulations, particularly, the Berson westerlies. The reversal in the zonal Stratospheric Circulation Index (SCI) from westerly to easterly flow and the meridional SCI showing strong southerly component in the 40-50 km layer gives a clue to the onset of the south-west (SW) monsoon. The zonal SCI reversal took place on May 3 in 1972 but westerlies reappeared on June 2 and remained as a strong current up to June 7 thus delaying the onset of the SW monsoon. SCI was reversed on June 14, 1973 thus favouring the advancement of the monsoon current. The burst of the SW monsoon took place on June 18 much later than usual 1st June showing that the reversal of the zonal SCI could predict the onset of the SW monsoon over the Indian Sub-continent.

6.5 Equatorial tropopause, stratopause and mesopause

The heights and temperatures of the equatorial tropopause, stratopause and mesopause were determined from the high altitude balloon and rocket soundings carried out at Thumba. The time-height cross section of the atmospheric temperature in 1972 is drawn in Fig. 6.3. Table 6.3 gives the corresponding seasonal variability the atmospheric thermal structure. It shows that the mean tropopause over Thumba in 1972 was at 17 km and had a temperature of $-79.2^{o}C$ with a standard deviation of $3.7^{o}C$. While there was no seasonal variability in the tropopause altitude, its temperatures

in the northern summer and winter were $-76.3^{\circ}C$ and $-78.4^{\circ}C$ with the values of $-79.2^{\circ}C$ in autumn and $-80.7^{\circ}C$ in the spring and standard deviations less than $4^{\circ}C$. The mean stratopause was located at 45 km and had a temperature of $-7.6^{\circ}C$ with a standard deviation of $4.1^{\circ}C$. The summer stratopause located at 45 km with a temperature of $-6.4^{\circ}C$ was warmer than the winter stratopause by $2.6^{\circ}C$ which was found at 47 km. The autumn and spring stratopause levels were also found at 45 km with temperatures of -8.3 and $-4.6^{\circ}C$ and standard deviations 2.8 and $3.4^{\circ}C$ respectively. The mean equatorial mesopause over Thumba was located at 76 km with the summer and winter mesopause at 75 km and the autumn and spring at 77 and 76 km, respectively. The mean mesopause temperature was $-82.1^{\circ}C$ with a standard deviation of $9.4^{\circ}C$, while the values in the summer, winter, autumn and spring were -82.1, -76.2, -89.9 and $-85.6^{\circ}C$ respectively. The winter mesopause over the equatorial station Thumba in the summer, winter, autumn and spring were -82.1, -76.2, -89.9 and $-85.6^{\circ}C$ respectively. The winter mesopause over the equatorial station Thumba was found to be about $6^{\circ}C$ warmer than the summer mesopause, while the mesopause in autumn and spring was cooler by about 10 to $14^{\circ}C$ than the winter mesopause as is obvious from the Table 6.3.

Table - 6.3

Seasonal variation of the atmospheric temperatures (T) and corresponding standard deviations (SD) in °C over equatorial Thumba (8°32'N, 76°52'E) in 1972. The number of observations for these northern seasons were 13 each

	Summer (June - August)		Autumn (September-November)		Winter (December-February)		Spring (March-May)		Annual	
	T	SD	T	SD	T	SD	T	SD	T	SD
	2	3	4	5	6	7	8	9	10	11
	28.2	1.8	28.8	2.8	30.6	1.5	31.6	1.9	30.0	2.6
	14.4	1.3	14.8	1.9	15.7	1.9	15.6	2.0	15.1	1.9
	4.9	0.9	4.8	1.9	4.6	1.7	5.3	1.4	4.9	1.6
	-6.2	1.3	-6.2	2.3	-7.2	1.8	-6.1	1.6	-6.4	1.8
	-17.8	1.9	-18.0	1.7	-19.4	2.2	-18.9	2.6	-18.5	2.2
	-33.4	2.3	-32.8	3.0	-34.5	2.2	-34.4	4.3	-33.5	3.3
	-49.4	2.3	-49.8	3.5	-51.3	1.8	-49.9	2.7	-49.8	2.8
	-66.1	1.8	-67.2	2.7	-67.4	1.9	-65.1	2.9	-66.3	2.7
	-75.8	1.8	-78.6	2.3	-77.9	2.1	-77.8	4.0	-77.3	3.0
	-76.3	2.6	-79.2	2.9	-78.4	2.6	-80.7	4.2	-79.2	3.7
	-72.0	2.3	-77.7	3.3	-73.8	2.9	-75.9	4.0	-75.6	4.5
	-65.3	1.9	-70.5	3.8	-65.2	3.1	-67.6	3.2	-67.8	3.9
	-59.5	1.9	-62.1	3.4	-60.0	2.2	-59.5	4.0	-60.5	3.4

Table – 6.3 contd./2.

2	3	4	5	6	7	8	9	10	11
-54.5	2.2	-55.8	3.0	-55.1	3.0	-54.4	4.3	-55.1	3.4
-50.1	2.2	-51.1	2.6	-50.5	2.5	-50.3	2.7	-50.9	2.6
-45.5	3.5	-45.6	4.1	-45.6	3.1	-45.0	2.8	-45.8	3.4
-41.8	2.7	-39.1	2.6	-42.3	3.2	-38.5	2.6	-40.5	3.3
-38.2	3.4	-33.7	3.3	-37.0	3.6	-34.0	2.6	-36.0	3.9
-32.5	3.4	-29.9	4.8	-31.2	3.4	-28.0	4.0	-30.9	4.5
-26.6	4.4	-24.3	3.7	-26.8	3.9	-23.7	4.4	-25.9	4.5
-21.5	4.3	-18.9	3.8	-22.1	3.9	-17.6	3.5	-20.3	4.3
-15.4	2.1	-15.3	3.2	-16.0	3.7	-12.6	3.4	-15.1	3.5
-10.0	1.9	-11.1	3.2	-12.4	3.8	-7.3	4.1	-10.5	4.1
-6.8	3.3	-8.5	2.8	-10.7	4.0	-4.9	3.9	-8.0	4.4
-6.4	3.0	-8.3	3.1	-9.8	4.4	-4.6	3.4	-7.6	4.1
-6.5	3.9	-8.7	3.5	-9.4	4.5	-4.9	3.6	-7.7	4.2
-6.8	4.1	-9.1	4.4	-9.0	4.3	-6.1	3.6	-8.1	4.2
-7.8	2.8	-9.3	4.9	-9.1	4.3	-7.4	3.7	-8.8	4.0
-8.8	3.0	-10.5	5.6	-8.9	3.9	-8.9	3.8	-9.8	4.3
-9.9	4.3	-11.8	6.6	-9.5	3.9	-10.4	3.5	-11.0	4.7
-15.8	2.8	-16.4	7.0	-12.8	5.2	-15.5	4.4	-15.8	5.2
-22.7	3.7	-22.8	7.5	-18.9	6.2	-20.7	5.6	-21.8	5.9
-30.8	5.7	-30.3	7.7	-27.2	6.6	-27.6	8.7	-29.3	7.4
-42.2	8.2	-38.8		-37.1	6.4	-36.0	12.0	-38.6	9.2

Table - 6.3 contd ..3..

2	3	4	5	6	7	8	9	10	11
-50.5	7.2	-47.5	7.5	-46.7	6.6	-44.6	14.8	-47.1	10.0
-58.2	8.2	-55.1	6.4	-55.1	5.8	-52.4	16.6	-54.7	10.8
-64.7	8.8	-61.9	5.6	-61.8	6.9	-60.0	17.6	-61.4	11.3
-69.8	8.3	-67.9	5.3	-67.8	6.9	-66.7	17.5	-67.2	11.1
-74.8	7.8	-74.2	5.7	-72.8	6.8	-73.4	17.0	-72.9	10.9
-78.8	7.5	-79.2	6.5	-75.8	6.6	-78.4	15.3	-77.1	10.5
-79.0	7.7	-81.2	7.3	-74.2	6.7	-80.6	13.4	-77.9	10.3
-81.5	8.3	-85.1	6.7	-76.1	7.2	-83.4	10.9	-80.9	9.5
-82.1	8.5	-86.8	5.9	-76.2	7.7	-85.1	9.7	-82.0	9.3
-81.8	8.6	-87.6	5.6	-76.0	8.7	-85.6	8.4	-82.1	9.4
-80.8	9.0	-89.9	5.6	-74.3	10.6	-85.5	7.6	-81.5	10.0
-79.2	9.3	-89.8	6.1	-74.8	11.5	-84.3	7.0	-80.8	9.7
-79.4	10.2	-88.1	6.4	-73.3	9.8	-84.5	7.5	-81.5	10.2
-81.1	10.1	-89.5	6.8	-73.1	9.0	-85.5	7.7	-81.0	10.3

6.6   Sudden mesospheric warming over equatorial region

A sudden mesospheric warming was noticed during February 17 to March 15 (late winter in the Northern Hemisphere) over the equatorial station Thumba with an explosive warming on March 1 as evidenced by the M-100 rocket soundings carried out in 1972. Table 6.4 gives quantitatively the warming and cooling which occurred in the equatorial mesosphere in an altitude region from 50 to 80 km during mid-February to mid-March 1972. The sudden mesospheric warming is also obvious from Fig. 6.3 as the isotherms experienced a sharp change in slope around March 1. From February 23 to March 1, the mesospheric temperature in an altitude region between 60 and 70 km increased by about 50 to 60°C with the maximum around 65 km showing an explosive warming over the equator. A core of positive temperatures of the order of 3°C was detected in a narrow altitude region from 58 to 63 km on March 1.

The upward slope of the isotherms in Fig.6.3 indicates atmospheric warming while the downward slope gives the subsequent cooling. As is obvious from the Table 6.4, the lower mesosphere in an altitude region from 50 to 65 km experienced a relatively weaker warming of about 5 to 17°C from February 17 to 23, while the upper mesosphere above 68 km was subjected to a cooling of about 4 to 14°C during that period.

Table -6.4

Mesospheric warming (W) and cooling (C) in °C during February 17 to March 15, 1972 over equatorial Thumba (8°32'N, 76°52'E) with an explosive warming on 1st March, 1972

	Atmospheric Temperature (°C)				Feb 17 - 23		Feb 23 - Mar 1		Mar 1 - 15	
	Feb 17	Feb 23	Mar 1	Mar 15	W	C	W	C	W	C
	2	3	4	5	6	7	8	9	10	11
	-15	- 6	-16	-13	9	–	–	-10	3	–
	-17	- 8	-17	-14	7	–	–	- 9	3	–
	-21	-10	-16	-15	11	–	–	- 6	1	–
	-25	-12	-14	-17	13	–	5	- 2	–	3
	-31	-16	-11	-19	15	–	12	–	–	8
	-36	-19	- 7	-23	17	–	20	–	–	-16
	-41	-24	- 4	-27	17	–	27	–	–	-23
	-45	-29	- 2	-32	16	–	35	–	–	-30
	-49	-34	1	-38	15	–	41	–	–	-39
	-53	-39	2	-44	14	–	47	–	–	-46
	-57	-44	3	-49	13	–	52	–	–	-52
	-61	-49	3	-56	12	–	56	–	–	-59
	-64	-54	2	-61	10	–	59	–	–	-63
	-67	-59	0	-56	8	–	59	–	–	-56
	-69	-63	- 3	-72	6	–	60	–	–	-69

Table - 6.4 contd..2..

1	2	3	4	5	6	7	8	9	10	11
65	-71	-67	-7	-77	4	--	60	--	--	-70
66	-73	-70	-11	-81	3	--	59	--	--	-70
67	-74	-74	-16	-85	0	--	58	--	--	-69
68	-76	-77	-21	-90	--	4	56	--	--	-69
69	-75	-79	-26	-92	--	4	53	--	--	-66
70	-74	-80	-32	-94	--	6	48	--	--	-62
71	-71	-81	-37	-96	--	-10	44	--	--	-59
72	-71	-79	-41	-96	--	8	38	--	--	-55
73	-72	-80	-46	-97	--	8	34	--	--	-51
74	-71	-82	-53	-98	--	9	29	--	--	-45
75	-71	-82	-59	-99	--	9	23	--	--	-40
76	-69	-81	-63	-97	--	-12	18	--	--	-34
77	-65	-79	-67	-95	--	-14	12	--	--	-28
78	--	--	-71	-92	--	--	--	--	--	-21
79	--	--	-73	-92	--	--	--	--	--	-19
80	--	--	-76	-94	--	--	--	--	--	-18

The equatorial mesospheric warming was the most pronounced from February 23 to March 1 with a temperature increase of about $10^{\circ}C$ per day between 62 and 68 km altitude region. The explosive warming was followed by an equal cooling as shown by the downward slope of the isotherms in Fig. 6.3. It is evident from the Table 6.4, that the mesospheric cooling ranged from 50 to $70^{\circ}C$ in an altitude region from 60 to 70 km during March 1 to 15 with the maximum cooling around 65 km, the altitude where the warming was also maximum. The rate of cooling was about 3 to $5^{\circ}C$ per day while the warming rate was greater than the cooling rate by about $5^{\circ}C$. The cooling in the lower mesosphere and the upper mesosphere was relatively smaller of the order of 1 to $3^{\circ}C$ per day. Besides this late winter sudden mesospheric warming event, some other weaker temperature fluctuations were also noticed in the equatorial atmosphere in 1972 as shown by the varying slope of the isotherms in Fig. 6.3, though none was as pronounced and significant as that of March 1.

Explosive warmings of the winter stratosphere and mesosphere to the extent of 50 to $60^{\circ}C$ outside the equatorial regions, particularly at high latitudes in the Northern Hemisphere are well known. Such sudden warmings have been attributed to horizontal and vertical transport of air mass from other regions. In the absence of closer network of observations in the equatorial region, it is difficult to attribute the

sudden warmings in the equatorial region to horizontal and vertical transport of air mass. For drawing definite conclusions about meridional transport of heat in the stratospheric and mesospheric region, it is necessary to have temperature observations at shorter intervals of time, preferably daily.

C H A P T E R - VII
=====================

SOUTH POLAR AND EQUATORIAL ATMOSPHERIC STRUCTURE COMPARISON

        Synoptic M-100 meteorological rocket launchings were
carried out weekly once from Molodezhnaya, Antarctica and
equatorial Thumba . The author worked at both these stations
and directly participated in data acquisition and processing.
Using these data, a comparative study of the South Polar and
the equatorial atmospheric structure is carried out and the
results of this investigation are presented in this Chapter.
Seasonal vertical profiles of zonal and meridional components
of winds, and of temperatures from Molodezhnaya, Antarctica
in January-February and July 1972 are compared with those of
the corresponding ascents from equatorial Thumba. The actual
results are also compared with the Groves atmospheric model
(Groves, 1971) and the corresponding departures of the actuals
from the Groves Model are worked out.

7.1   Antarctic and equatorial atmospheric structure in
         southern summer

        The vertical profiles of atmospheric winds and
temperatures over Molodezhnaya, Antarctica and Thumba
equatorial station in South India for the period January-
February (southern summer) are drawn in Fig. 7.1 and 7.3

and a brief summary of the flights carried out is given in Table 7.1. Radiosonde data are used for completing the profiles in the lower atmosphere as each rocket flight was preceded by a standard radiosonde release. Figs 7.1 and 7.3 show the monthly average profiles for January and February, while Fig 7.2 represents a typical summer profile of January 26. The actual results of the zonal winds and the temperatures in the altitude region from 25 to 85 km at an interval of 5 km are compared with the Groves atmospheric model (Groves, 1971) and the corresponding departures of the actuals from the Model are drawn in Figs 7.4 and 7.5 for January and February respectively.

As the values in the Groves Model apply to the first of each month, the Model average values are obtained from the data of two successive months for comparison. Thumba ($8^{\circ}32'N$) actuals for January are compared with the corresponding $10^{\circ}N$ profiles from the Groves (1971) Model. Since in the Groves Model, no data are available for $70^{\circ}S$, actual profiles over Molodezhnaya ($68^{\circ}S$) for January and February are compared with the $70^{\circ}N$ profiles from the Model shifted six months in time. Comparison of the actual monthly average profiles with the corresponding Groves profiles is shown in Figs 7.4 and 7.5. Tropospheric, Stratospheric and Mesospheric Circulation Indices (TCI, SCI & MsCI) are computed by using the method

devised by Webb (1964) and are given in Table 7.1. Structure of the Antarctic and equatorial atmosphere in southern summer, particularly for the months of January and February is discussed in this section.

7.1.1   Zonal winds

From the solid curve (A) of Fig 7.1 it is evident that average zonal wind components at Molodezhnaya, Antarctica in January 1972 were easterly throughout the atmosphere up to about 84 km. In the troposphere the easterlies were weaker with speeds less than 10 ms^{-1}. In the stratosphere the winds became stronger with speeds ranging from about 20 to 30 ms^{-1} around the stratospause. However, the wind maximum was found in the mesosphere at 70 km which had a speed of 47 ms^{-1}. Above 70 km the easterly winds decreased with height which had an average wind shear of about 0.004 s^{-1}.

The corresponding average zonal wind profile of January for Thumba equatorial station given by the dashed curve (a) in Fig 7.1 shows that up to about 7 km the winds were weak easterlies having speeds less than 7 ms^{-1}. Around 7 km the zonal winds changed to weak westerlies of speeds less than 11 ms^{-1} with the maximum at 21 km. From 25 km to 60 km the zonal winds were easterlies in toto, with speeds ranging from about 5 to 31 ms^{-1} having the maximum at 50 km,
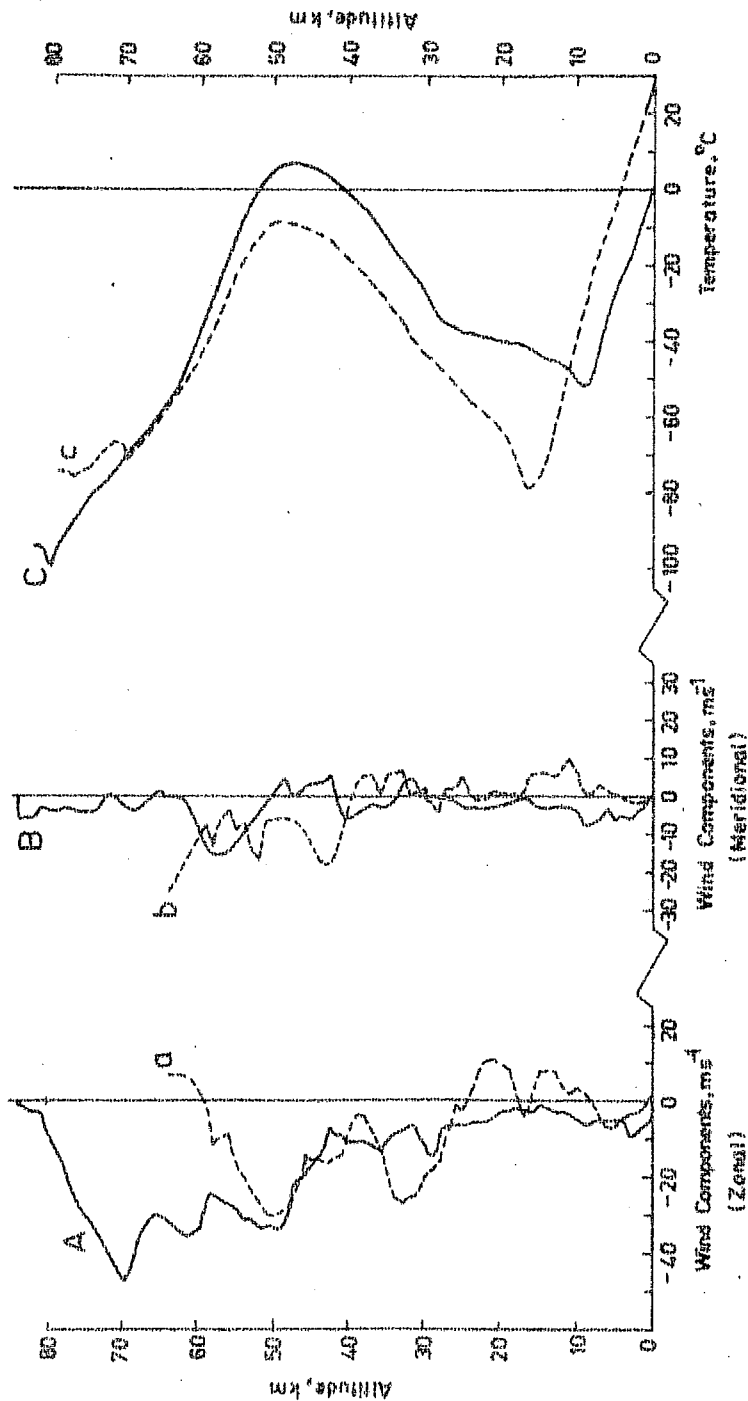
(Fig. 7.1)

Average vertical profiles of zonal winds (curves A,a), meridional winds (curves B,b) and temperatures (curve C,c) over Molodezhnaya, Antarctica (curves A,B,C) and Thumba equatorial station (curves a,b,c) in January 1972.

the stratospause. However, above 60 km the zonal winds showed a westerly trend.

It is obvious from the solid curve (A) of the typical summer profile shown in Fig 7.2 that on January 26, 1972 the zonal winds over Molodezhnaya, Antarctica were predominantly easterly in the atmosphere up to about 55 km altitude having tropospheric maximum wind speed of 22 ms^{-1} at 3 km and stratospheric maximum at 48 km with 43 ms^{-1} speed. In a narrow altitude region from 55 to 60 km westerly winds with speed ranging from 5 to 12 ms^{-1} were detected! In the mesosphere the winds were strong easterlies having maximum speed of 47 ms^{-1} at 70 km. However, in a narrow region from 78 to 85 km the easterly winds changed to westerlies with speeds ranging from about 5 to 13 ms^{-1} which again showed a reversal to easterlies aloft 85 km.

The corresponding dashed curve (a) in Fig 7.2 shows that on January 26 the zonal winds over Thumba equatorial station were weak and variable in the lower troposphere up to about 12 km altitude. From 12 to 23 km the winds were mainly westerly with a maximum speed of 15 ms^{-1} at 15 and 22 km showing a sudden reversal at 17 km (tropopause). The lower stratospheric weak westerlies changed to strong easterly winds at about 24 km and persisted in the stratosphere up to 45 km with a maximum speed of 61 ms^{-1} at 42 km which showed a
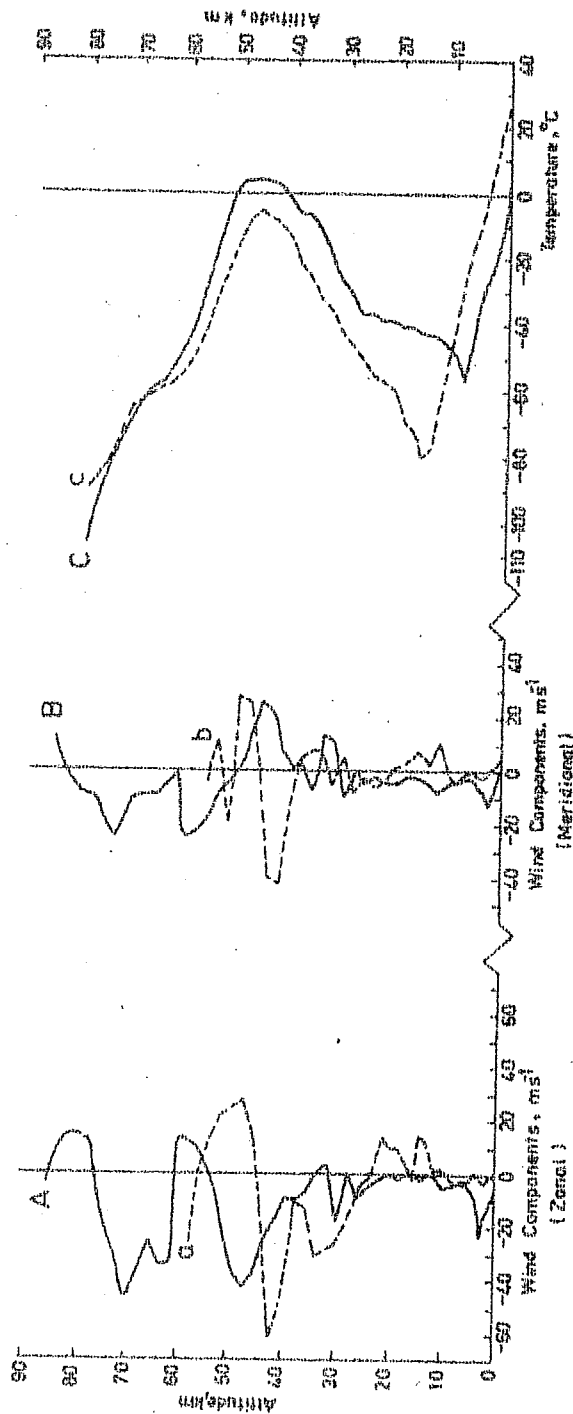
(Fig. 2)

Typical vertical profiles of zonal winds (curves A,a), meridional winds (curves B,b),
and temperature (curves C,c) over Molodezinaya, Antarctica (curves A,B,C) and Thumba
equatorial station (curves a,b,c) on January 26, 1972.

reversal to westerlies at about 46 km which attained a maximum speed of 28 ms^{-1} at 49 km, the approximate stratopause. The westerlies persisted in the lower mesosphere up to about 56 km and changed to easterly winds aloft.

Fig 7.3 gives an average profile for February, 1972. The solid curve (A) in the Figure shows that over Molodezhnaya, Antarctica the zonal winds were easterly with speeds less than 10 ms^{-1} up to about 10 km and were weak and variable in an altitude range of about 10 to 30 km. In the middle stratosphere, altitude region from 30 to 40 km, easterly winds of speed about 10 ms^{-1} were detected wihch showed a reversal to strong westerly winds in the upper stratosphere with a maximum speed of 36 ms^{-1} at 49 km, the approximate stratospause. The winds remained westerly in the lower mesosphere up to 60 km with speeds in a range of 20 to 30 ms^{-1}. A large wind shear of about 0.04 s^{-1} was detected around 60 km where the westerly winds showed a sudden reversal. The winds in the upper mesosphere were strong easterlies with speeds ranging from about 10 to 100 ms^{-1}. Around 80 km there was a wind shear of 0.02 s^{-1} with a wind speed of 96 ms^{-1} at 82 km.

The corresponding dashed curve (a) drawn in Fig 7.3 shows that in February 1972 the zonal winds over Thumba equatorial station were predominantly weak easterly with speeds less than 10 ms^{-1} up to 17 km (tropopause). The weak
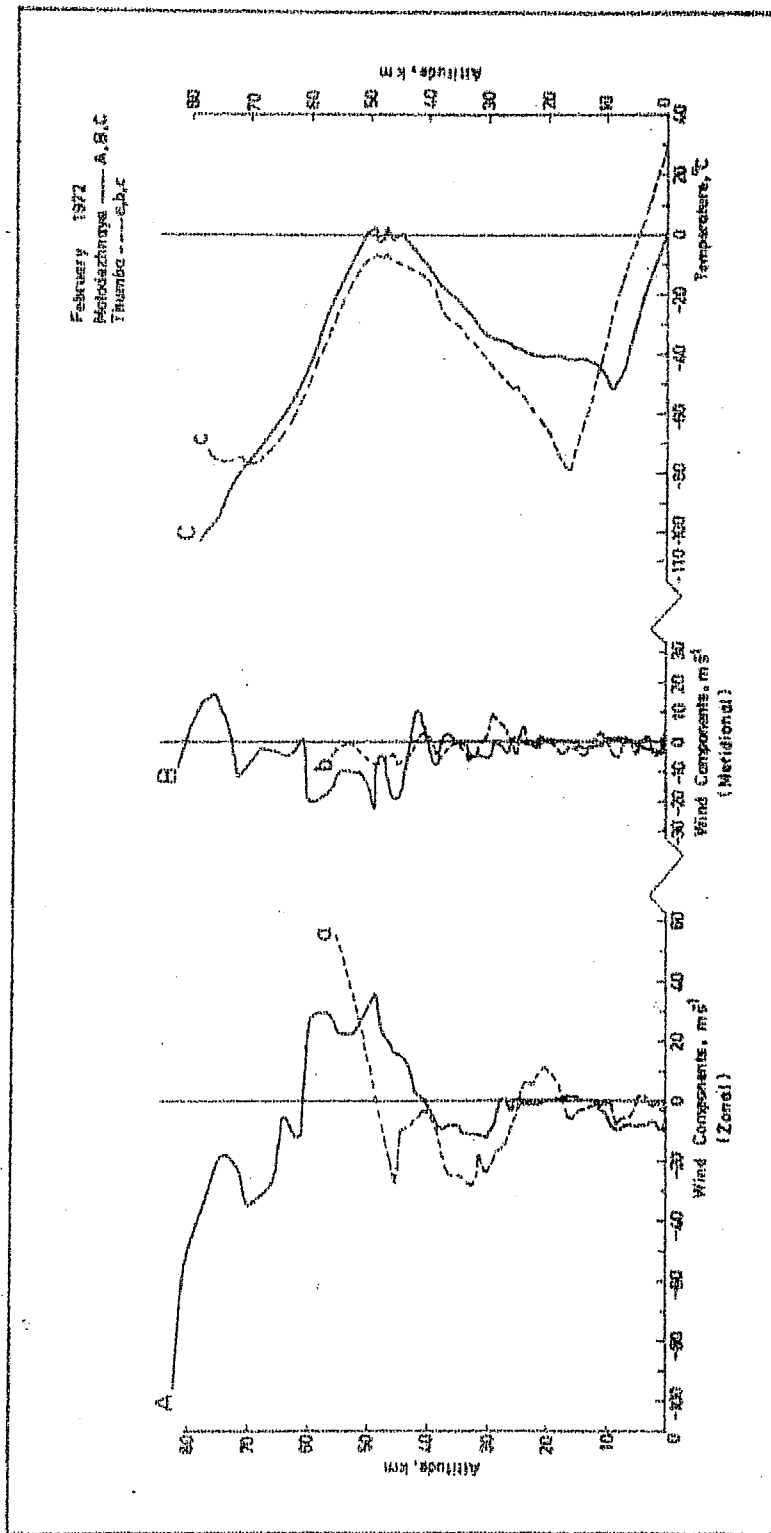
(Fig.7.3)

Average vertical profiles of zonal winds (curves A,a), meridional winds (curves B,b) and temperatures curves C,c) over Molodezhnaya, Antarctic (curves A,B,C) and Thumba equatorial station (curves a,b,c) in February 1972.

easterlies at the tropopause showed a reversal to weak
westerlies which again showed a reversal at 25 km. Strong
easterly winds persisted in the stratosphere from 26 to 49 km
which attained a maximum speed of 28 ms^{-1} at 33 km. The
stratospheric easterlies showed a reversal at 49 km around
the stratopause and changed into strong westerly winds with
speeds ranging from about 10 to 50 ms^{-1} in the lower
mesosphere.

7.1.2 Meridional winds

Average meridional wind profile, given by the solid
curve (B) in Fig 7.1 shows that in January the winds over
Molodezhnaya, Antarctica were predominantly northerly up to
the mesopause. Up to 30 km the northerlies were weak with
speeds less than 8 ms^{-1}. In the altitude region from 30 to
50 km the meridional components were weak and variable. In
the 50 to 60 km region the northerlies were relatively
stronger having a maximum speed of 16 ms^{-1} at 58 km which
again became weaker in the upper mesosphere.

The corresponding average profile for Thumba given by
the dashed curve (b) in Fig 7.1 shows that in January the
meridional winds over the equatorial station were weak and
variable up to about 40 km with speeds less than 10 ms^{-1}.
Above 40 km the winds were predominantly northerly with speeds
ranging from 5 to 25 ms^{-1}.

The solid curve (B) in Fig 7.2 shows that the meridional components of winds in the upper atmosphere over Molodezhnaya, Antarctica on 26th January 1962 were weak northerly up to an altitude of 27 km with wind speed less than 8 ms^{-1}. In an altitude region from 28 to 38 km the winds were variable with speed less than 20 ms^{-1}. In the upper stratosphere, altitude region 38 to 50 km, strong southerly winds were found which had a maximum speed of 26 ms^{-1} at 45 km. The stratospheric southerlies changed to mesospheric northerlies at about 50 km. In the mesosphere the northerly winds persisted up to 83 km having a maximum speed of 25 ms^{-1} at 74 km with a secondary maximum of 24 ms^{-1} at 60 km. Above 83 km the profile showed a southerly trend.

From the corresponding dashed curve (b) in Fig 7.2 it is obvious that the meridional winds over Thumba equatorial station on January 26 were variable with weaker winds of speeds less than 13 ms^{-1} up to 40 km and stronger winds aloft. In an altitude region from 40 to 45 km the meridional winds were strong northerlies which had a maximum speed of 47 ms^{-1} at 43 km. The upper stratospheric northerly winds showed a reversal to southerlies around 46 km which had a maximum speed of 28 ms^{-1} at 49 km. Above 50 km the meridional winds were again variable with speeds ranging from about 5 to 25 ms^{-1}. Thus the upper stratosphere and the lower mesosphere

were in a turbulent state having large wind shears with meridional winds rapidly shifting from northerlies to southerlies and vice versa.

The meridional wind components over Molodezhnaya, Antarctica in February 1972 are shown by the solid curve (B) in Fig 7.3. Up to an altitude of 43 km the winds were weak and variable with speed less than 11 ms^{-1}. Above 44 km the winds were predominantly northerly with a maximum speed of 23 ms^{-1} at 49 km, the stratopause. The northerlies persisted up to 73 km in the mesosphere with a maximum speed of 20 ms^{-1} around 60 km which showed a reversal to southerly winds at 74 km. The southerlies had wind speed ranging from 5 to 16 ms^{-1} in the upper mesosphere with the maximum at 76 km. Above 80 km the winds showed a northerly trend.

The corresponding average profile of the meridional winds over Thumba equatorial station in February given by the dashed curve (b) in Fig 7.3 shows that the winds were weak and variable up to 30 km with speeds less than 10 ms^{-1}. Above 30 km the winds were predominantly weak northerlies in the upper stratosphere and the lower mesosphere.

7.1.3   Atmospheric temperatures

Average temperature profile for January 1972 over Molodezhnaya, Antarctica given by the solid curve (C) in Fig 7.1 shows that the polar tropopause was at 9 km

altitude with air temperature of $-51.8^{\circ}C$. The lapse rate in the troposphere was $-5.6^{\circ}C$ km^{-1}. In an altitude region from 12 to 28 km a quasi-isothermal temperature structure prevailed with a lapse rate of $+ 0.5^{\circ}C$ km^{-1}.

In the upper stratosphere the lapse rate was about $2^{\circ}C$ km^{-1}. The profile shows that the stratopause was at 47 km with a temperature of $6.5^{\circ}C$. In the mesosphere the lapse rate was $- 3.8^{\circ}C$ km^{-1} with the mesopause at 80 km having a temperature of $-99^{\circ}C$.

The corresponding temperature profile for Thumba equatorial station is given by the dashed curve (c) in Fig 7.1. It shows that in January the equatorial tropopause was at 17 km with a temperature of $-78.8^{\circ}C$ and that the lapse rate in the troposphere was $-6.8^{\circ}C$ km^{-1}. In the stratosphere the lapse rate was $+ 2.4^{\circ}C$ km^{-1} with the stratospause at 50 km having a temperature of $-8.8^{\circ}C$ and the mesopause was at 77 km with a temperature of $-77.5^{\circ}C$.

The solid curve (C) in Fig 7.2 is the typical southern summer profile of January 26, 1972 over Molodezhnaya, Antarctica. It shows that the polar tropopause and stratopause were at 9 km and 49 km altitudes with temperatures of $-56^{\circ}C$ and $+ 4^{\circ}C$ respectively. The mesopause was however, not well defined.

The dashed curve (c) in Fig 7.2 is the corresponding profile of January 26 for Thumba equatorial station. It shows that the equatorial tropopause and stratopause were at 17 km and 48 km with temperatures of $-79^{\circ}C$ and $-7^{\circ}C$ respectively, while the mesopause was not well defined.

The solid curve (C) in Fig 7.3 gives an average temperature profile for February 1972 over Molodezhnaya, Antarctica. It shows that the polar tropopause and stratopause in late summer were at 9 km and 49 km with temperatures of $-52.3^{\circ}C$ and $2.0^{\circ}C$ respectively while the mesopause was not well defined. Temperature lapse rates in the troposphere, upper stratosphere, and mesosphere were -5.5, $+2.4$ and $-3.4^{\circ}C$ km^{-1} respectively, while in an altitude region from 12 to 28 km the lapse rate was very small, $+0.4^{\circ}C$ km^{-1} showing that the lower stratosphere was in a quasi-isothermal state.

The dashed curve (c) in Fig 7.3 gives the corresponding temperature profile of February for the equatorial station Thumba in South India. It shows that in late summer the equatorial tropopause and stratopause were at 16 km and 49 km with temperatures of $-79.3^{\circ}C$ and $-7.3^{\circ}C$ respectively. The mesopause was found in an altitude region from 70 to 75 km having a minimum temperature of -77.0° at 70 km with a secondary minimum of $-76.5^{\circ}C$ at 75 km. Temperature lapse rates in the troposphere, stratosphere and mesosphere were -7.2, $+2.4$ and $-4.3^{\circ}C$ km^{-1}, respectively.

7.2   Summer profiles comparison with Groves Model

The zonal winds and temperatures over Antarctica and equatorial Thumba in January and February 1972 (southern summer) are compared with the corresponding Groves model values and the results of this investigation are discussed in this section.

7.2.1   Zonal wind departures

The curve (A) in Fig 7.4 represents departures of the actual zonal winds at Molodezhnaya (about $68^{\circ}S$), Antarctica in January from the corresponding Groves profiles at $70^{\circ}N$ in July. The departures were less than 14 ms^{-1} in the stratosphere and there was a fairly good agreement between the two in the altitude region from 25 to 45 km. The winds were predominantly easterly in both the actual profile and the Groves profile. Maximum departure from the model was -23.5 ms^{-1} at 50 km with a wind speed of 34 ms^{-1} at Molodezhnaya and 20.5 ms^{-1} at $70^{\circ}N$ (from the Groves model). The negative departures in the Figure show that the actual easterly winds were stronger than the Model easterlies, while the positive departures show the reverse.

The curve (B) in Fig 7.4 gives the zonal wind departures of the actuals over equatorial Thumba (about $9^{\circ}N$) in South India from the Groves model profiles (at $10^{\circ}N$) in January. It shows that in January the zonal wind departures
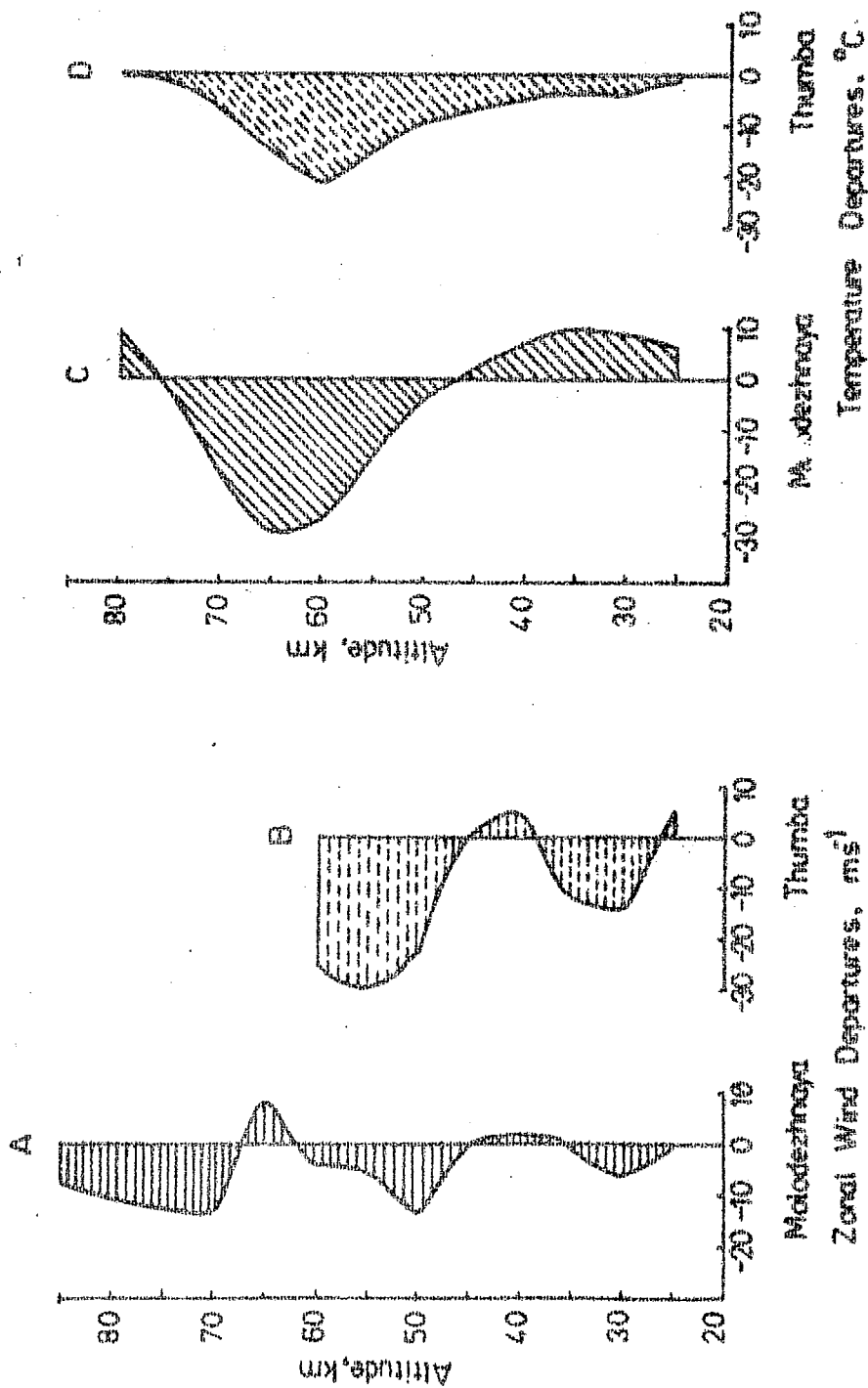
Fig. 7.4

Departures of the actual zonal winds and of temperatures from the Groves atmospheric model over Molodezhnaya, Antarctica (solid curves A,C) and Thumba equatorial station (dashed curves B,D) in January 1972.

in the stratosphere and the lower mesosphere were less than 30 ms^{-1}. The winds in the stratosphere were easterly with a westerly trend in the lower mesosphere in both the profiles, actual as well as Groves. Again, the negative departures mean that the Thumba zonal winds were stronger than the Model winds. However, at 60 km where the westerlies prevailed, the Thumba winds were weaker having a speed of 2.5 ms^{-1} and the departure from the Groves model was -25 ms^{-1}. A good agreement was found around 40 km where the departures were less than +4.7 ms^{-1} showing that the Groves easterlies were somewhat stronger than the actual Thumba easterlies. The curve (A) in Fig 7.5 gives the zonal wind departures of the Molodezhnaya actuals from the Groves model for February 1972. In the Groves profile the winds are predominantly easterly in the stratosphere and the mesosphere, while in the actual profile the winds were predominantly strong westerly in an altitude region from about 45 to 60 km which contributed to larger departures in this region with a maximum of + 35.5 ms^{-1} at 50 km and a secondary maximum of + 34.0 ms^{-1} at 60 km. The negative departures in the Figure show that the actual easterly winds over Molodezhnaya, Antarctica were stronger than the corresponding Groves winds.

February 1972
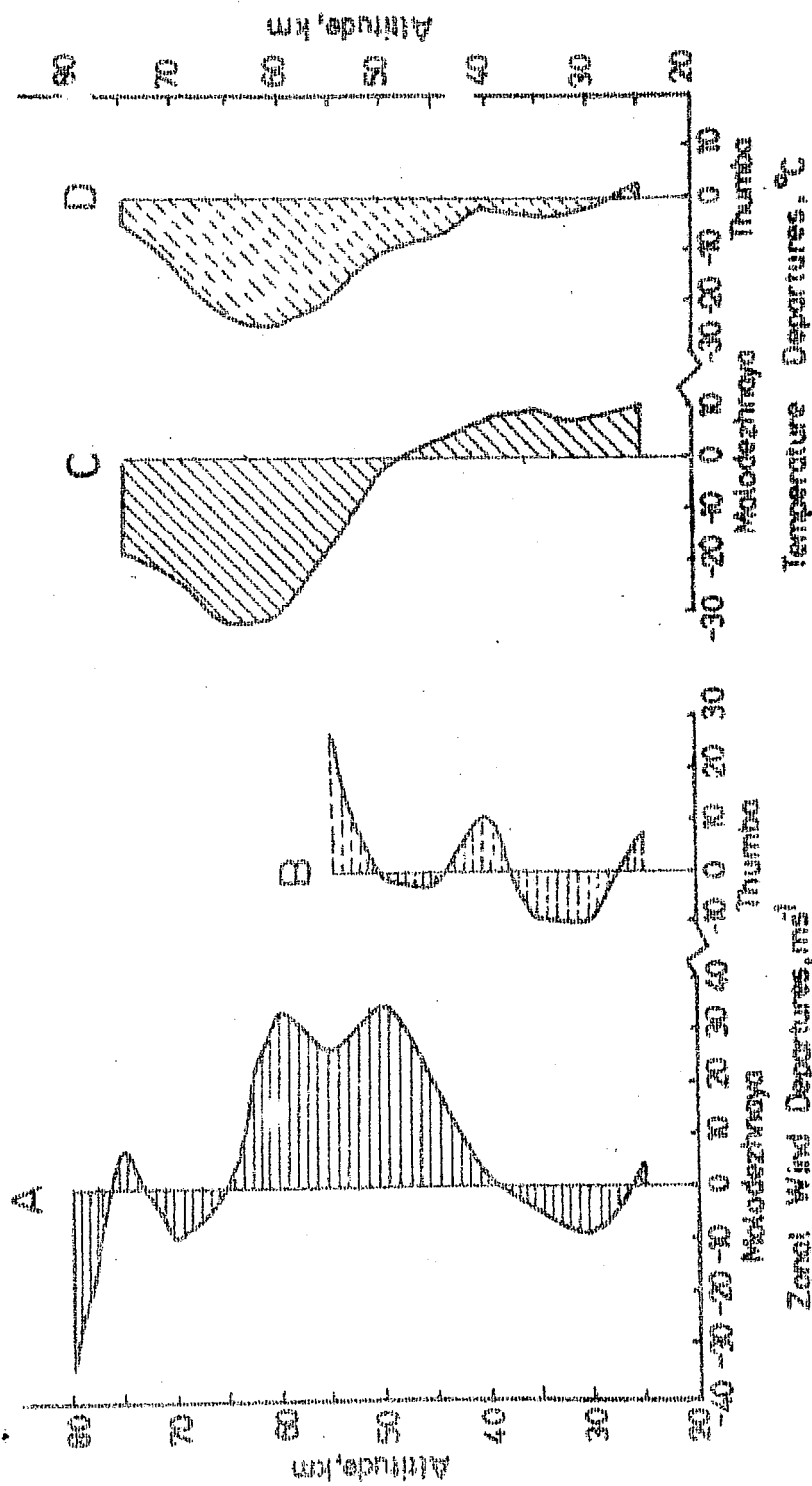
(Fig. 7.5)

Departures of the actual zonal winds and of temperatures from the Groves atmosphere model over Molodezhnaya Antarctica(solid curves A,C) and Thumba equatorial station (dashed curves B,D) in February 1972.

The corresponding zonal wind departures of the Thumba
actuals from the Model for February are shown by the curve (B)
in Fig 7.5. The winds were predominantly easterly in the
stratosphere with strong westerlies aloft, in both the actual
and the Model profiles. Maximum departure was + 26.5 ms^{-1} at
55 km with strong westerlies of 50.5 ms^{-1} at Thumba and
24.0 ms^{-1} from the Groves model. A good agreement between the
actuals and the Model was found around the stratopause in an
altitude region from 45 to 50 km with departures of about
-2 ms^{-1}. Again, the negative deviations from the model mean
that the actuals were stronger than the model winds, while
the positive departures mean the reverse.

7.2.2 Temperature departures

The curve (C) in Fig 7.4 gives temperature departures
of the Molodezhnaya actuals from the Groves atmospheric model
for January 1972. In the stratosphere the deviations from the
Model were less than + 10°C . Maximum departure was -30°C at
65 km and the minimum was + 1.8^{o}C at 45 km around the stratopause.
Positive departures in the Figure show that the actual
temperatures were greater than the Groves temperatures, while
the negative departures mean the reverse. It is thus obvious from
the Figure 7.4 that in January the stratosphere over
Molodezhnaya, Antarctica is warmer than the corresponding

Groves profile with a maximum of $10^{o}C$ at 35 km, while the Molodezhnaya mesosphere is colder than the Model with a maximum of $30^{o}C$ at 65 km. However, at 80 km around the mesopause the Molodezhnaya profile is about $8.5^{o}C$ warmer than the Groves profile.

The corresponding temperature departures of the Thumba actuals from the Groves Model for January are shown by the curve (D) in Fig 7.4. A sufficiently good agreement between the actuals and the Model was found in the stratosphere with departures ranging from -1 to $-9^{o}C$. Maximum departure was $-21.8^{o}C$ at 60 km. Negative departures in the Figure mean that the actual temperatures over Thumba, South India were colder than the corresponding Groves model temperatures.

The curve (C) in Fi 7.5 gives the temperature departures over Molodezhnaya, Antarctica from the Groves model for February 1972. Again, in the stratosphere the actual temperatures were warmer than the Groves temperatures with a maximum of $9.8^{o}C$ at 25 km, while in the mesosphere the actuals were colder with a maximum of $31.8^{o}C$ at 65 km.

The corresponding temperature departures of the Thumba actuals from the Model for February are shown by the curve (D) in Fig 7.5. It is obvious from the Figure that in February the Thumba actuals were colder than the corresponding Groves profile with a maximum of $24.8^{o}C$ at 60 km. There is a

sufficiently good agreement between the two in the stratosphere with departures ranging from about $-2^{\circ}C$ to $-10^{\circ}C$.

It is obvious from Figs 7.4 and 7.5 that the temperature departures of the actuals from the Groves Model in January had a good similarity with those in February both for Molodezhnaya, Antarctica and Thumba equatorial station. However, the zonal wind departures were different in the two cases.

7.3   Atmospheric circulation indices in southern summer

From the combined average values of the M-100 rocket soundings conducted in January-February 1972, a brief summary of which is given in Table 7.1, it is found that in the southern summer the polar tropopause and stratopause were at 9 km and 47 km with temperatures of $-52.1^{\circ}C$ and $4.8^{\circ}C$ respectively, while the mesopause was around 80 km with a temperature of about $-100^{\circ}C$. The corresponding equatorial tropopause, stratopause and mesopause were found to be at 17 km, 49 km and 75 km with temperatures of $-78.6^{\circ}C$, $-8.2^{\circ}C$ and $-75.0^{\circ}C$ respectively. Temperature lapse rates in the troposphere, stratosphere and mesosphere over Molodezhnaya, Antarctica were -5.5, $+2.2$ and $-3.6^{\circ}C$ km^{-1} while over Thumba equatorial station in South India the corresponding lapse rates were -7.0, $+2.4$ and $-4.0^{\circ}C$ km^{-1}. In an altitude region from 12 to 28 km, the temperature structure over Antarctica was found to be quasi-isothermal with a lapse rate of $+0.4^{\circ}C$ km^{-1}.

Table - 7.1

Summary of the M-100 meteorological rocket soundings from (i) Molodezhnaya, Antarctica (M), and (ii) Thumba equatorial station (T) in January-February and July 1972. TCI, SCI and MsCI denote Tropospheric, Stratospheric and Mesospheric Circulation Indices, respectively, while NS and EW are their meridional and zonal components. N/A means data not available

Station	Date	Time (GMT)	Wind Track (km)	Temperature track (km)	(i) 5-15 km (ii) 10-20 km TCI (m/s)		45-55 km SCI (m/s)		70-80 km MsCI (m/s)	
1	2	3	4	5	NS 6	EW 7	NS 8	EW 9	NS 10	EW 11
M	Jan 05	1450	80-10	82-10	-0.8	-1.7	-1.3	-35.6	2.4	-41.5
T	Jan 05	1433	55-10	70-10	0.7	-1.1	-32.5	-49.6	---	---
M	Jan 12	1425	48-10	78-10	-7.6	-4.0	N/A	N/A	---	---
T	Jan 12	1430	64-10	80-10	5.1	2.7	-42.5	-34.2	---	---
M	Jan 19	1440	84-62	73-10	-4.1	-9.0	N/A	N/A	5.5	-29.3
T	Jan 19	1431	65-10	70-10	5.7	8.5	29.6	-34.3	---	---
M	Jan 26	1435	86-10	80-10	-5.0	-2.7	2.1	-26.9	-16.4	-13.1
T	Jan 25	1655	58-25	80-25	3.9	6.6	10.1	20.7	---	---
M	Feb 02	1448	48-10	78-10	8.9	-5.8	N/A	N/A	---	---
T	Feb 02	1430	45-10	60-10	-2.4	2.0	N/A	N/A	---	---

more

Table - **7.**1 contd..2..

1	2	3	4	5	6	7	8	9	10	11
M	Feb 16	1535	82-10	76-10	-5.1	6.0	-19.1	27.8	5.1	-30.5
T	Feb 17	1430	56-10	77-10	-2.5	-2.5	**1.2**	6.4	--	--
M	Feb 23	1530	55-10	73-10	-4.5	-10.8	-21.6	33.8	--	--
T	Feb 23	1430	56-24	77-24	-0.1	-0.2	-0.5	18.1	--	--
M	July 1	1400	57-10	N/A	-2.5	18.5	-44.7	77.6	--	--
T	July 1				No launch					
M	July 5	1400	84-10	73-10	-3.2	5.2	1.9	57.0	14.7	32.5
T	July 5	1432	65-10	76-10	-4.7	-17.2	8.2	23.0	--	--
M	July 12	1400	40-10	75-10	-0.7	6.7	N/A	N/A	--	--
T	July 12	1430	65-10	**7**8-10	0.0	-22.3	-21.7	-10.8	--	--
M	July 19	1400	84-10	75-10	-6.5	7.8	5.5	52.5	-12.7	38.9
T	July 19	1505	55-10	39-10	0.0	-22.0	2.5	-10.9	--	--
M	July 22	1400	60-10	80-10	-2.7	3.0	25.3	40.3	--	--
T	July 22				No launch					
M	July 26	1400	60-10	80-10	-3.1	11.1	-14.4	52.7	--	--
T	July 26	1430	55-10	N/A	0.2	-21.8	2.9	-35.7	--	--

Using the method devised by Webb (1964), average
values of the wind speeds for the layers from 5 to 15 km, 10
to 20 km, 45 to 55 km and 70 to 80 km are computed for deriving
Tropospheric Circulation Index (TCI), Stratospheric Circulation
Index (SCI) and Mesospheric Circulation Index (MsCI) of the
appropriate layers. Average winds over the layer from 5 to
15 km give TCI for Molodezhnaya, Antarctica, while those from
10 to 20 km give TCI for Thumba equatorial station. This is
because the polar tropopause was found to be at 9 km, while
the equatorial tropopause was at 17 km. Average winds over
the layers from 45 to 55 km and from 70 to 80 km give the
corresponding SCI and MsCI. The Tropospheric, Stratospheric
and Mesospheric Circulation Indices computed for January-
February 1972 are given in Table 7.1. Positive values of the
circulation indices refer to south in the meridional flow and
to west in the zonal flow, while the negative values represent
north and east correspondingly.

7.3.1   Tropospheric Circulation Index (TCI)

Table 7.1 shows that the meridional components of the
Tropospheric Circulation Index (TCI) over Molodezhnaya,
Antarctica were predominantly northerly in January and
February (southern summer) with a maximum wind speed of
7.6 ms^{-1} on January 12. However, a wind reversal from weak

northerlies to weak southerlies of speed 8.9 ms^{-1}, occurred from January 26 to February 2 which again changed to weak northerlies by February 16. The corresponding meridional TCI over equatorial Thumba was weak southerly in January with a maximum wind speed of 5.7 ms^{-1} on January 19. The weak southerlies showed a reversal to weak northerlies from January 26 to February 2 which then persisted throughout the month. January 26 to February 2 thus seems to be a transition period for the meridional winds in the troposphere over Antarctica and equatorial station Thumba in South India.

The zonal components of the Tropospheric Circulation Index over Molodezhnaya, Antarctica in January-February were predominantly easterly having a maximum wind speed of 10.8 ms^{-1} on February 23 with a secondary maximum of 9 ms^{-1} on January 19. However, a wind reversal occurred around February 16 when the zonal flow became westerly with a speed of 6 ms^{-1}. The corresponding zonal TCI at equatorial Thumba in South India was predominantly westerly in January with a maximum wind speed of 8.5 ms^{-1} on January 19. The westerlies changed to weak easterlies during the 1st half of February which persisted later. Thus there seems to be a transition of the zonal winds both over Antarctica and equatorial India around mid-February.

7.3.2   Stratospheric Circulation Index (SCI)

Table 7.1 shows that the meridional component of the Stratospheric Circulation Index (SCI) over Molodezhnaya, Antarctica was predominantly northerly with a maximum wind speed of 21.6 ms^{-1} on February 23. However, a weak southerly trend with a wind speed of about 2 ms^{-1} occurred on January 26. The corresponding meridional SCI over equatorial Thumba in South India was found to be variable during January to February with a strong northerly flow of maximum speed 42.5 ms^{-1} on January 12 and a strong southerly flow of speed 29.6 ms^{-1} on January 19. The southerly flow persisted till about mid-February and again became northerly around February 23.

The zonal SCI over Antarctica was found to be predominantly easterly in January with a maximum wind speed of 35.6 ms^{-1} on January 5, and westerly during February with a maximum speed of 33.8 ms^{-1} on February 23. Wind reversal occurred sometime during January 26 to February 16. The corresponding zonal SCI over Thumba equatorial station also showed a strong easterly flow in January with a maximum wind speed of 49.6 ms^{-1} on January 5 and a westerly flow in February. The reversal of zonal winds from strong easterlies to relatively weaker westerlies occurred during January 19 to January 26. The westerly flow had a maximum speed of 20.7 ms^{-1} on January 26.

7.3.3   Mesospheric Circulation Index (MsCI)

Table 7.1 gives Mesospheric Circulation Index (MsCI) over Molodezhnaya, Antarctica for only those days when special chaff-borne M-100 meteorological rocket flights were carried out. It shows that the mesospheric meridional flow was predominantly weak southerly with a reversal to northerlies of speed 16.4 ms^{-1} on January 26, while the zonal flow was strong easterly which had a maximum speed of 41.5 ms^{-1} on January 5 with a secondary maximum of 30.5 ms^{-1} on February 16. Since no chaff flights were conducted from Thumba equatorial station in January-February, no MsCI is available for the equatorial station.

It is found that in the southern summer the polar tropopause and stratopause were about 27°C and 13°C warmer than the corresponding equatorial tropopause and stratopause, while the mesopause was about 25°C colder. At both the stations the zonal winds in the stratosphere were predominantly easterly in January with speed less than 50 ms^{-1}, and westerly in February with speed less than 35 ms^{-1}, while the meridional winds were variable. Zonal wind departures of the actuals from the Groves model were found to be in a range of about ± 35 ms^{-1} while the temperature departures were mostly negative by about 25°C.

7.4 Antarctic and equatorial atmospheric structure in southern winter

Vertical profiles of zonal and meridional components of winds, and of temperatures from the M-100 rocket soundings simultaneously carried out at Molodezhnaya, Antarctica and Thumba equatorial station in South India during July 1972 (southern winter) are discussed in this section. The vertical profiles of the Antarctic and equatorial winds and temperatures for the southern winter are drawn in Figs 7.6 (a to d) and a brief summary of the flights carried out at Molodezhnaya and Thumba in July 1972 is given in Table 7.1. Radiosonde data were used for completing the profiles in the lower atmosphere. Typical southern summer (January 5) and winter (July 5) Antarctic temperature profiles over Molodezhnaya (68°S) are compared with the corresponding Groves profiles (July 1 and January 1) at 70°N from the Groves atmospheric model (Groves,1971) as shown in Fig 7.7.

7.4.1 Zonal winds

In the southern winter month July, the zonal winds over Molodezhnaya, Antarctica as shown by the solid curves (1) in Fig 7.6 (a to d) were predominantly westerly throughout the upper atmosphere up to an altitude of about 80 km with weak easterlies near the surface. The westerlies built up in
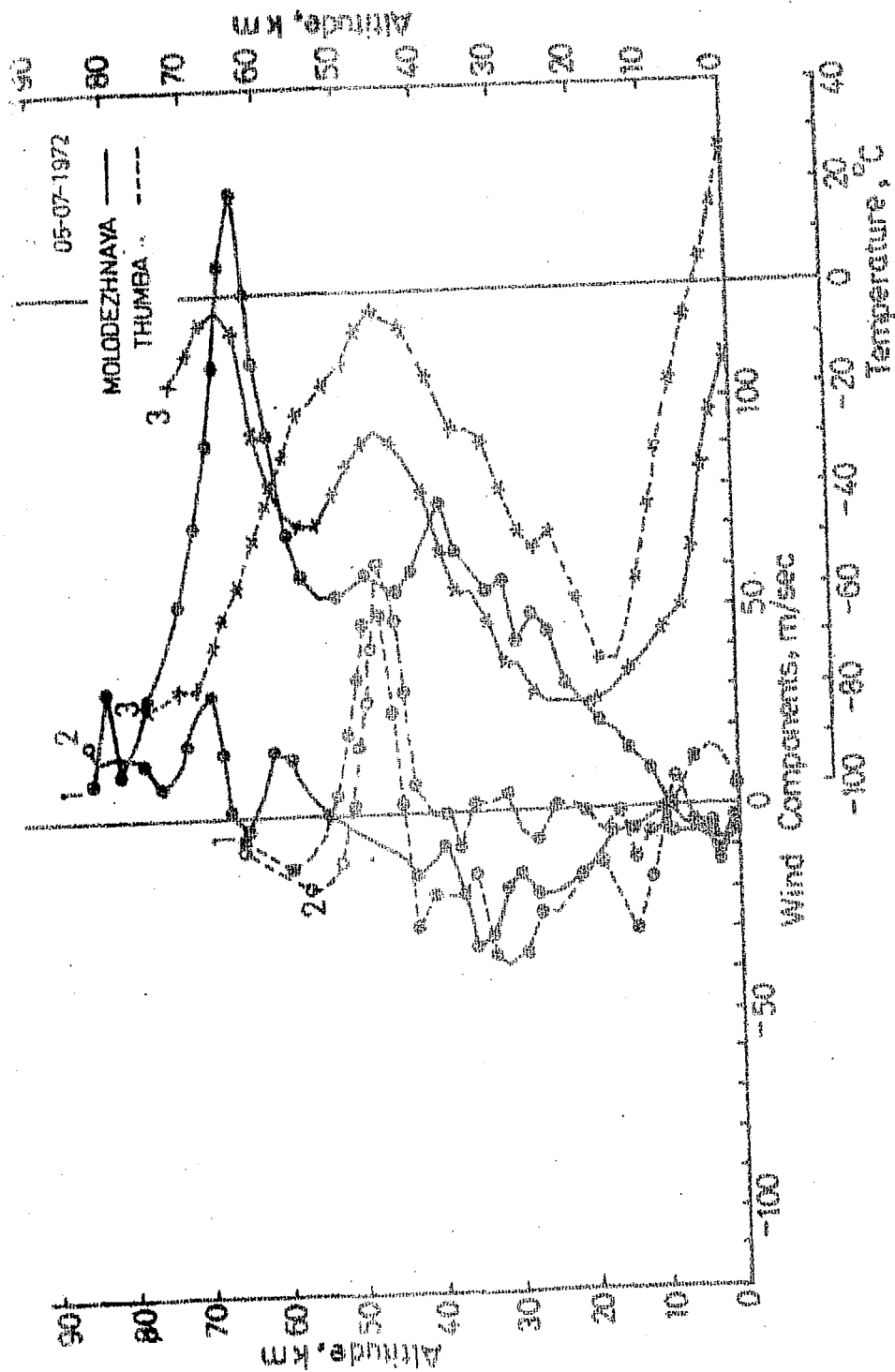
[Fig. 4(a)]

Vertical profiles of zonal winds (curves 1 through solid circles, meridional winds (curves 2 through open circles, and of temperatures (curves 3 through cross marks) over Molodezhnaya Antarctica (solid curves 1,2,3 and Thumba equatorial station (dashed curves 1,2,3) on July 5, 1972.
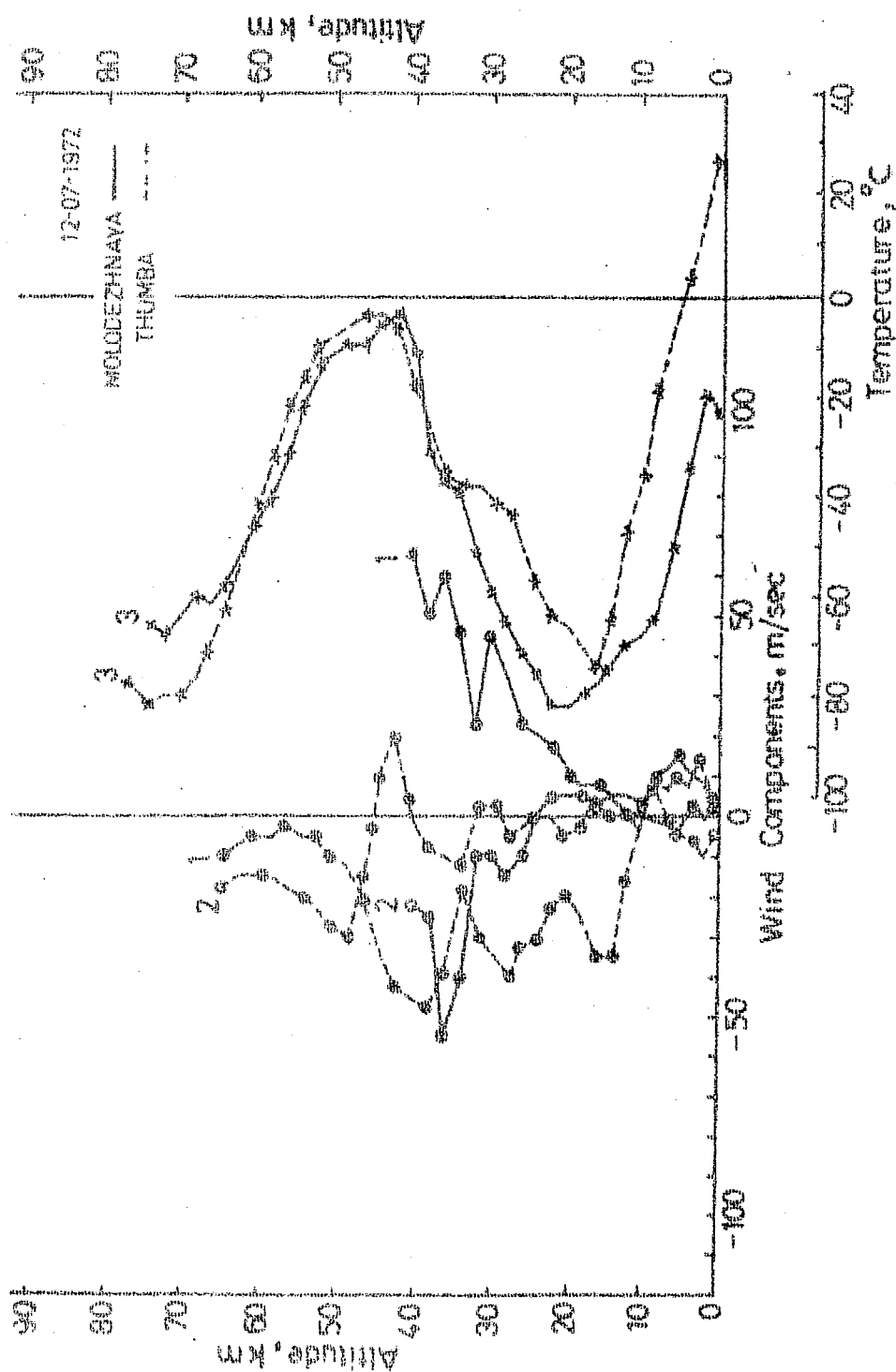
(Fig.7.6(b))

Vertical profiles of zonal winds (curves 1 through solid circles), meridional winds (curves 2 through open circles) and of temperatures (curves 3 through cross marks) over Molodezhnaya Antarctic solid curves 1,2,3) and Thumba equatorial station (dashed curves 1,2,3) on July 12, 1972.
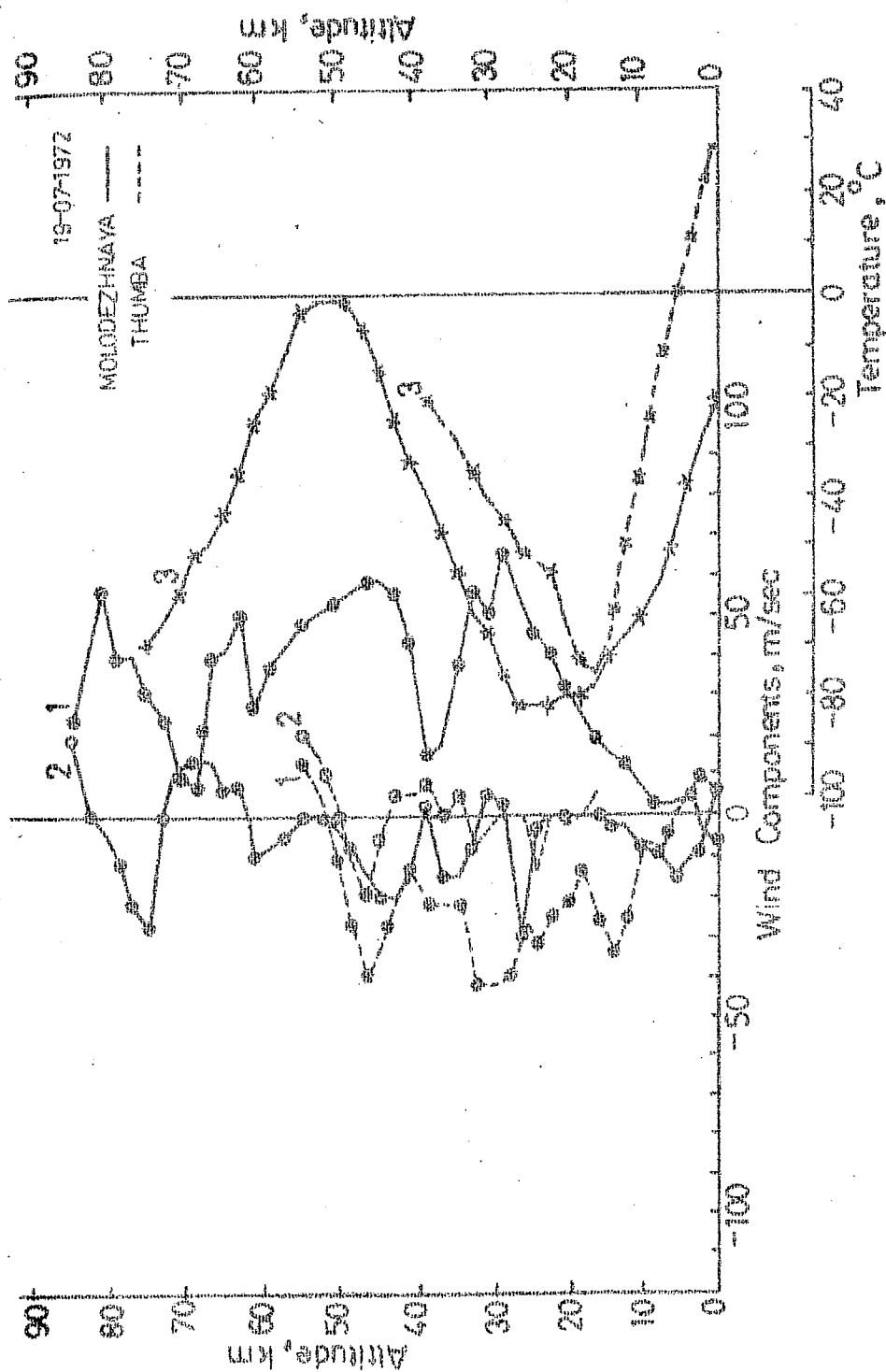
Vertical profiles of zonal winds (curves 1 through solid circles), meridional winds (curves 2 through open circles) and of temperatures (curves 3 through cross marks) over Molodezhnaya Antarctic solid curves 1,2,3 and Thumba equatorial station (dashed curves 1,2,3) on July 19, 1972.
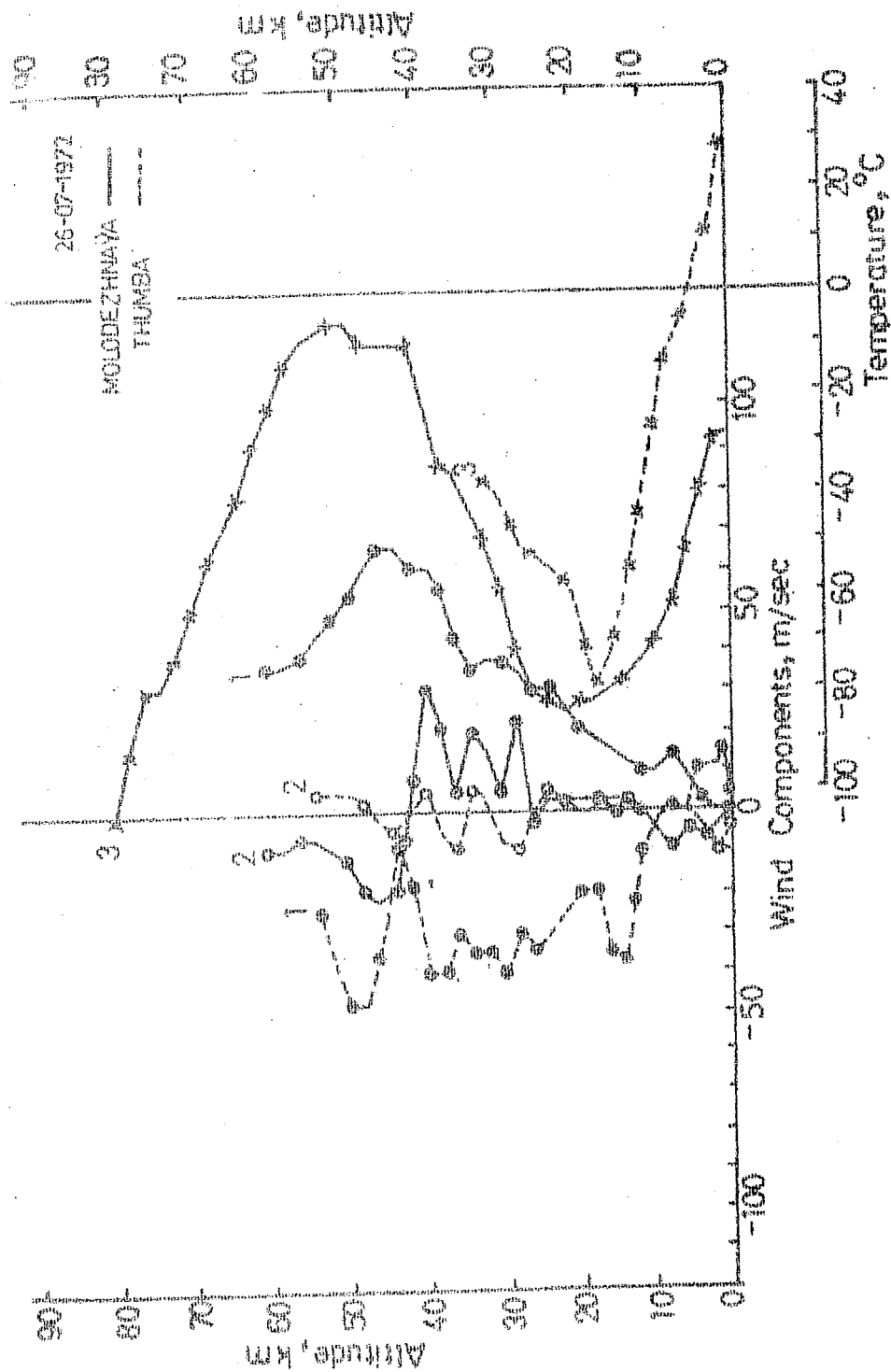
(Fig.7.6(a))

Vertical profiles of zonal winds (curves 1 through solid circles), meridional winds (curves 2 through open circles) and of temperatures (curves 3 through cross marks) over Molodezhnaya Antarctica (solid curves 1,2,3) and Thumba equatorial station. Dashed curves 1,2,3 on July 26, 1976.

the troposphere and the stratosphere and attained jet speed in the lower mesosphere. In the stratosphere the maximum wind speed was 82 ms^{-1} at 39 km on July 5 with secondary maxima of 66 ms^{-1} at 28 km and 58 ms^{-1} at 45 km on July 19 as is obvious from the solid curves (1) in Fig 7.6(a,c). In the mesosphere strong easterly winds having large wind shears were detected. Maximum wind speed was 157 ms^{-1} at 64 km on July 5 which indicated a sudden disruption in the atmosphere over Antarctica during the winter regime. The average values of the zonal winds in winter show that the zonal flow over Antarctica was totally westerly in winter with weaker winds in the lower atmosphere and stronger winds in the upper atmosphere. In the troposphere the westerly winds were of speeds less than 30 ms^{-1}, in the stratosphere the westerlies had a maximum wind speed of 59 ms^{-1} at 40 km and in the mesosphere the maximum speed was 99 ms^{-1} at 64 km. Strong westerly winds decreased with height in the mesosphere and attained a speed of 15 ms^{-1} at 84 km.

From the dashed curves (1) in Fig 7.6 (a to d) it is obvious that the zonal winds over Thumba equatorial station in July 1972 were predominantly easterly with speeds ranging from about 10 to 50 ms^{-1} up to about 45 km. Up to an altitude of about 10 km westerly winds of speeds less than 17 ms^{-1} prevailed. The stratospheric easterly winds had a maximum

speed of 49 ms^{-1} at 49 km around the stratopause on July 26 as shown in Fig 7.6 (d), It had a secondary maximum of 47 ms^{-1} at 39 km on July 12 as shown by the dashed curves (1) in Fig 7.6 (b). A core of strong westerly winds with a maximum speed of 53 ms^{-1} at 47 km was detected in an altitude region from about 44 to 52 km on July 5. The average values of zonal winds at Thumba in July show that the winds were weak westerly of speeds less than 13 ms^{-1} up to an altitude of about 10 km. Above 10 km the zonal winds were totally easterly up to an altitude of 65 km in the lower mesosphere. The easterlies were stronger in the stratosphere with a maximum speed of 39 ms^{-1} at 31 km and weaker in the mesosphere with speeds less than 10 ms^{-1}.

7.4.2   Meridional winds

The solid curve (2) in Fig 7.6 (a) shows that the meridional winds over Antarctica on July 5 were predominantly northerly in the troposphere and the stratosphere with a maximum speed of 33 ms^{-1} at 33 km, and were predominantly southerly in the mesosphere with a maximum wind speed of 31 ms^{-1} at 68 km. On July 12 the meridional winds were weak and variable with speed less than 6 ms^{-1} up to an altitude of about 25 km and strong northerly aloft with a maximum speed of 54 ms^{-1} at 36 km as shown in Fig 7.6 (b). On July 19, the meridional components were predominantly northerly having a maximum wind speed of 30 ms^{-1} at 26 km with a secondary

maximum of 28 ms^{-1} at 74 km. However, in an altitude region from about 62 to 72 km, a core of weak southerly winds with speed less than 14 ms^{-1} was detected as shown in Fig 7.6 (c). On July 26 the winds were variable with southerly components of speed less than 30 ms^{-1} in the middle stratosphere and northerly components of speed less than 23 ms^{-1} above 42 km in the upper stratosphere, Fig 7.6 (d). From the July average values it is found that the meridional winds over Antarctica in winter were predominantly northerly with speed less than 20 ms^{-1} up to 57 km and southerly aloft with a maximum speed of 23 ms^{-1} at 68 km.

The dashed curves (2) in Fig 7.6 (a to d) show that the meridional winds over the equatorial station Thumba were variable in July. On July 5 the winds were predominantly southerly in the stratosphere with a maximum speed of 65 ms^{-1} at 45 km and northerly in the lower mesosphere with speed less than 17 ms^{-1}, Fig 7.6 (a). On July 12 the winds were variable up to 45 km with speed less than 20 ms^{-1} and northerly aloft with a maximum speed of 30 ms^{-1} at 48 km around the stratopause, Fig 7.6 (b). On July 19 the meridional winds were variable of speed less than 20 ms^{-1} up to 55 km with weaker winds in the troposphere and the lower stratosphere and stronger winds in the upper stratosphere, Fig 7.6 (c), while on July 26 the winds were again weak and variable of speed less than 10 ms^{-1}

as is obvious from the dashed curve (2) in Fig 7.6 (d). The
average values of the meridional wind components show that the
winds over the Equator in July were weak and variable of speed
less than 12 ms^{-1} in the troposphere and the stratosphere, and
northerly in the lower mesosphere having a maximum speed of
17 ms^{-1} at 56 km.

7.4.3 Atmospheric temperature

The solid curves (3) in Fig 7.6 (a to d) give the
vertical temperature profiles over Molodezhnaya, Antarctica in
July 1972. In the southern winter the polar tropopause was
located in an altitude region from 20 to 25 km with a
temperature varying from about -80 to -87°C while the
stratopause was located between 43 and 52 km with a temperature
ranging from -1 to -8°C. The mesopause was agin ill-defined.
However, on July 12 the polar mesopause was located at 73 km
with a temperature of -70°C. In an altitude region from
about 15 to 25 km where the winter polar tropopause was located,
the temperature variation was found to be quite small. The
July average temperature values over Molodezhnaya, Antarctica
show that in the southern winter the polar tropopause was
not well defind due to its multiple occurrence, while the
stratopause was at 48 km with a temperature of -12.4°C. The
mesopause was also ill-defined. The temperature lapse rates
in the troposphere, stratosphere and mesosphere were found

to be about -2.7, $+3.1$ and $-1.9^{\circ}C$ km^{-1}, respectively. In an altitude region from 15 to 26 km where the tropopause was located the temperature lapse rate was very small, $-0.35^{\circ}C$ km^{-1} which showed a quasi-isothermal temperature structure in that layer.

The dahsed curves (3) in Fig 7.6 (a to d) give the corresponding vertical temperature profiles over Thumba, equatorial India in July 1972. It is found that in the southern winter the equatorial tropopause was located at 17 km with a temperature varying from -74 to $-80^{\circ}C$, while the stratopause was lying around 45 km with a temperature of about $-5^{\circ}C$. The mesopause was again found to be ill-defined. However, on July 12, the equatorial mesopause was found at 74 km with a temperature of $-82^{\circ}C$. The corresponding average temperature profile over Thumba, Equatorial India shows that in July , the southern winter the equatorial tropopause and stratopause were located at 17 km and 46 km with temperatures of $-77.3^{\circ}C$ and $-4.5^{\circ}C$, respectively, while the mesopause was not very well defined due to the meagre data available in that particular region. The temperature lapse rates in the troposphere, stratosphere and mesosphere were found to be -6.2, $+2.3$ and $-2.7^{\circ}C$ km^{-1}, respectively.

7.5   Typical temperature profiles comparison

Typical southern summer (January 5) and southern winter (July 5) vertical temperature profiles obtained from the M-100 meteorological rocket soundings conducted at Molodezhnaya, Antarctica in 1972 are compared with the corresponding Groves atmospheric model profiles at 70°N on July 1 and January 1, respectively in Fig 7.7.

The thick dashed curve (C) in Fig 7.7 is the typical southern summer actual temperature profile, while the curve (D) is the corresponding Groves model profile. These two curves show that the deviations of the Actuals from the Model ranged from -26°C to $+17^\circ$C with a maximum of -26°C (absolute value) at 65 and a minimum of -1°C (absolute value) at 45 km. The curves also show that the deviations in the stratosphere were smaller with absolute values less than 10°C while the deviations in the mesosphere were larger with absolute values less than 26°C. This indicates that the temperatures in summer in the Model are given somewhat in excess in the mesosphere, while there is a reasonably good agreement in the stratosphere.

The thick solid curve (A) in Fig 7.7 gives the typical southern winter temperature profile, while the curve (B) gives the corresponding Groves atmospheric model profile. The curve (A) shows a sudden disruption in the Antarctic
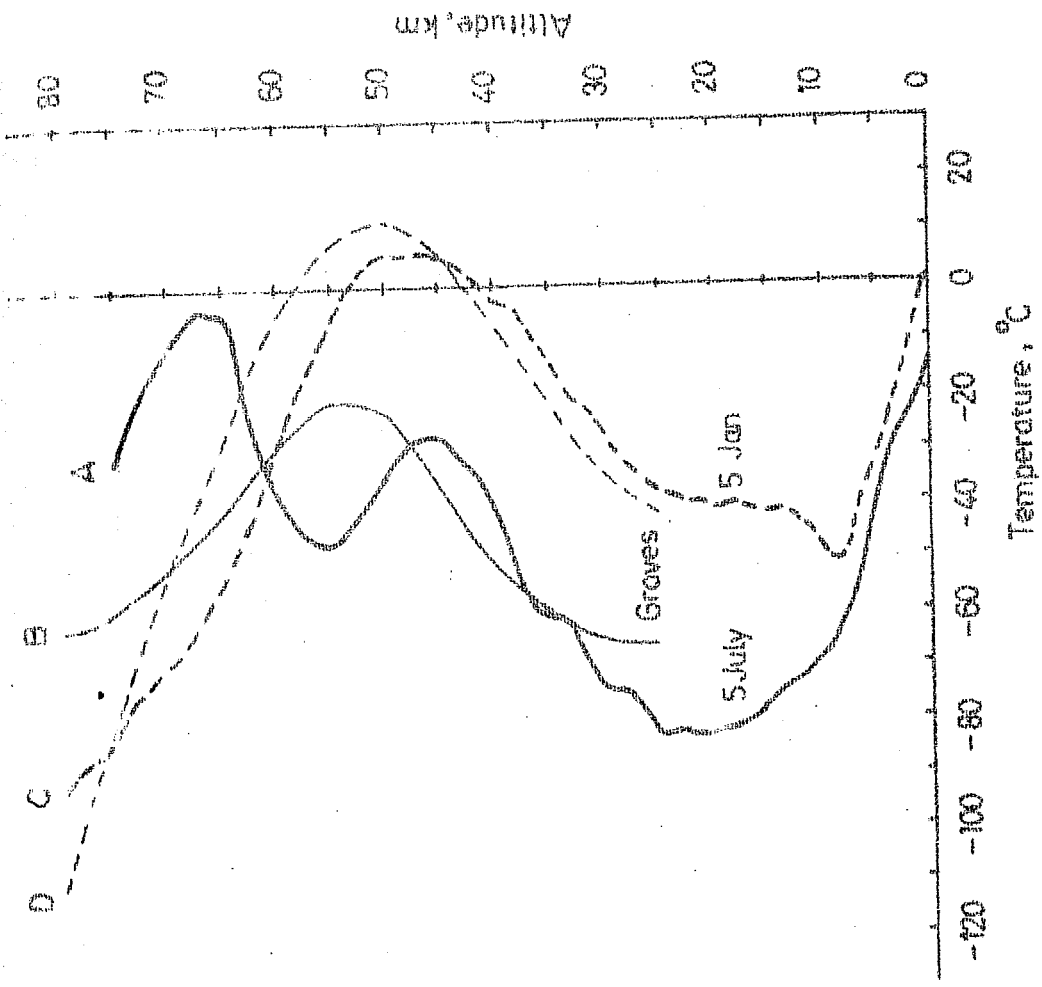
(Fig. 7.7)

Comparison of the typical southern summer (January 5) and southern winter (July 5)
vertical temperature profiles (curves C and A) at Molodezhnaya (67°40'S, Antarctica
in 1972 with the corresponding Groves atmospheric model profiles curves b and B)
at 70°N.

upper atmosphere in the winter regime. The polar stratosphere and the mesosphere were subjected to a significant cooling and warming in the southern winter(Sehra, 1975 , 1976a).

Due to this disruption, in winter the departures of the Actuals from the Model were quite large ranging from -26 to + 39°C as is obvious from the curves (A) and (B) in Fig 7.7. The absolute value of the deviation was minimum 1^{O}C at 35 and maximum 39°C at 70 km. In the stratosphere the departures were smaller with absolute values less than 12 ^{O}C, while in the mesosphere the departures were larger with values lying in a range of about -10 to + 40°C. The larger departures may be due to the upper atmospheric disruption in the winter regime.

7.6   Discussion and interpretation of results

The atmospheric zonal winds in the southern hemisphere over Antarctica were predominantly easterly in the southern summer. However, there was a marked wind reversal from easterlies to westerlies at 40 to 60 km altitude between January and February, while the winds at the northern high latitudes in summer are known to be notably steady. The zonal winds over the equatorial station Thumba were mostly easterly in the upper atmosphere above 25 km in January-February with

a pronounced westerly trend between 45 and 55 km on January 26.
The meridional winds both over the South Polar and the
Equatorial regions were variable.

A remarkable wave-like structure was detected in the
vertical profiles of wind components both over the south
polar and the equatorial regions. These observations indicate
that the recurrent wave structure might have been caused by
the wind fluctuations due to atmospheric gravity waves. It is
also obvious from the Figures 7.1 to 7.4 that these irregular
waves were predominantly horizontal, had amplitudes that
increased with height and also the dominant scale size of the
vertical wave length increased with height which may be due
to gravity waves. The amplitude of the irregular waves
increased rapidly with height owing to the rapid decrease in
atmospheric density. It appears that both the processes i.e.
internal manifestations in the wind field due to atmospheric
gravity waves and irregular fluctuations set up due to
turbulent motions might cause the wave-like structures in the
vertical wind profiles.

From the combined average values of the M-100 rocket
soundings carried out at Molodezhnaya in January-February
1972, it is found that in the southern summer the Antarctic
tropopause and stratopause were located at 9 km and 47 km
having temperatures $-52.1^{\circ}C$ and $4.3^{\circ}C$, while the equatorial

tropopause and stratopause were at altitudes 17 km and 49 km with temperatures - 78.6°C and -8.2°C , respectively. From the meagre upper mesospheric data, the south polar and the equatorial mesopause were apparently found around 80 km and 75 km with temperatures of about -100°C and -75°C . During January-February average temperature lapse rates in the troposphere, stratosphere and mesosphere over Antarctica were about -5.5, + 2.2 and -3.6°C km^{-1}, while over the equator the corresponding lapse rates were about -7.0, + 2.4 and -4.0°C km^{-1} . In an altitude region from 12 to 28 km the temperature structure over Antarctica was found to be quasi-isothermal with a lapse rate of + 0.4°C km^{-1}.

The summer polar tropopause and stratopause in the Southern Hemisphere over Antarctica were found to be about 27°C and 13°C warmer than the corresponding equatorial tropopause and stratopause while the Antarctic mesopause was apparently about 25°C colder. Also, the south polar tropopause and stratopause were located at altitudes about 8 km and 2 km lower than their corresponding equatorial counterparts while the Antarctic mesopause seemed to be located at an altitude about 5 km higher than the corresponding equatorial mesopause in the southern summer. The primary reason of the warmer polar tropopause and stratopause is the availability of more solar radiation in Antarctica due to

almost continuous sunlight there in summer. Furthermore,
in Antarctica there is less convection which forms the
tropopause at a lower altitude around 9 km. Since the
tropospheric temperature lapse rate extends over a smaller
altitude range the polar tropopause becomes warmer as compared
with the equatorial tropopause which is located at a higher
altitude around 17 km as a consequence of greater degree of
convection at the equator.

Again, in the southern summer the Antarctic stratosphere
receives more solar radiation almost continuously which
penetrates into it perhaps to a greater depth (lower
altitude) where the ultraviolet radiation gets absorbed by
ozone . Apparently, in the southern summer the ozone maximum
may be at lower level where there is maximum absorption thus
heating the stratosphere and forming the stratopause at a
lower altitude and with a warmer temperature as compared with
its equatorial counterpart. The summer polar mesopause in
the Southern Hemisphere may be colder than its equatorial
counterpart due to strong adiabatic cooling in the Antarctic
mesosphere. It is because upward motions exist to some degree
in summer polar areas due to the expansion of stratospheric
regions. Initial phases of upward motions of this meridional
current at the stratopause could well be supported by ozone
heating in that region. As the air lifts towards the

mesopause, adiabatic cooling would become a very strong effect and consequently the polar mesopause becomes colder and also shifted somewhat upwards.

It is found that the south polar tropopause and stratopause in summer were about $30^{o}C$ and $20^{o}C$ warmer than the corresponding winter tropopause and stratopause, while the equatorial tropopause and stratopause did not show any significant seasonal differences. In July during the southern winter the south polar tropopause and stratopause were found to be about $5^{o}C$ and $8^{o}C$ colder and at higher altitudes, about 3 km and 2 km respectively, than the corresponding equatorial tropopause and stratopause contrary to the summer time atmospheric structure.

The situation is reversed because of the absence of sunlight over Antarctica during the southern winter. Compared to the equatorial tropopause the Antarctic tropopause is colder because the surface temperature in winter is too low due to a quasi cut-off of solar radiation there. It is located at a higher altitude possibly because the radiation balance is somehow effected only at a higher level and the altitude of tropopause is determined by the radiation balance, the convection being practically absent. The steep lapse rate of the Antarctic troposphere stops around 10 km which is lower than the equatorial tropopause.

The winter Antarctic stratopause is colder than the corresponding equatorial one due to lesser solar radiation received by the south polar stratosphere. It is located at a higher altitude because the ozone maximum might be occurring at a higher altitude in winter which is related to the penetration of weak solar radiation to lesser extent, and therefore, to a greater height from the earth's surface.

The zonal winds over Antarctica were predominantly easterly in the southern summer and westerly in the southern winter, while over the Thumba equatorial station, the winds were predominantly easterly in both the seasons with weak westerlies in the troposphere in January (southern summer). The meridional winds were variable both over the Antarctic and the Equator. During the southern winter a sudden disruption followed by sizeable perturbations in the atmospheric winds and thermal structure is detected over Antarctica, while over the Equator the structure was found to be relatively steady.

Departures of the actual zonal winds from the corresponding Groves atmospheric model over Antarctica varied from -14 to + 8 ms^{-1} in January and -34 to + 36 ms^{-1} in February while the corresponding equatorial departures ranged

from -30 to + 5 ms^{-1} and -9 to + 27 ms^{-1} between the two

months. The atmospheric temperature departures of the actuals

from the Groves profiles varied from -32 to + 10°C over the

south polar region and from -25 to + 2°C over the equatorial

region in the southern summer. Deviations of the actual

temperatures over Antarctica and equatorial region in the

southern winter from the corresponding Groves model profiles

were found to be quite significant lying in a range of -30

to + 40°C with smaller departures in the mesosphere.

The departures over Antarctica are apparently because

the Groves atmospheric model is based on the data from the

Northern Hemisphere which differs from the Southern Hemisphere

in many respects. Antarctica is as continental as the Arctic

at the surface, but the dominant water surface outside the

polar regions in the Southern Hemisphere and the extensive

areas of land surrounding the Arctic are the important

factors controlling various changes in the atmospheric

winds and temperatures in the Southern and the Northern

Hemispheres. The higher albedo over Antarctica than over

the Arctic explains the much lower summer temperatures of

the Antarctic. The **coldness** of the air at middle southern

latitudes in summer, compared with the same northern

latitudes, owes more to the physical properties of the

immense southern oceans than to the presence of an ice-covered

polar continent. The departures may also be due to the

reasons that the Southern Hemisphere is more symmetric and has a vigorous general circulation and that the Antarctic continent is located at a higher elevation than the Arctic.

Likewise for the Thumba latitude in the Eastern Hemisphere , the Groves Model is based on data from all longitudes mostly from the Western Hemisphere. Departures of the equatorial actuals from the Groves profiles may, therefore, be the evidence of longitudinal asymmetries between the Eastern and the Western Hemispheres. Thus the discrepancy between the actuals and the Groves Model may be largely attributed to the specificity of geographical locations of the station Molodezhnaya, Antarctica and the equatorial station Thumba in India.

C H A P T E R - VIII
=====================

INTERHEMISPHERIC COMPARISON OF ATMOSPHERIC STRUCTURE

The Meteorological Rocket Network (MRN) has forced a renewed analysis of the spatial and time distribution of each atmospheric parameter. However, longitudinal inhomegenieties in the atmospheric structure still exist due to the lack of observations particularly from the Eastern Hemisphere. Since 1971, meteorological rocket soundings have been regularly carried out along two selected meridional zones : 40-90°E in the Eastern Hemisphere and 35-95°W in the Western Hemisphere. The stratospheric and mesospheric upper-air data for the Southern Hemisphere, particularly over the ocean areas are obtained with the help of research vessels.

One of the primary functions of the networks is to provide data which allow comparisons of the stratospheric behaviour of the Northern and the Southern Hemispheres and also find out differences in the Eastern and the Western Hemispheric atmospheric structures. Information that we require from both hemispheres would allow answers to questions regarding the differences in the intensities of the thermal and circulation fields, the differences in the preferred areas of winter-time warm and cold air centres
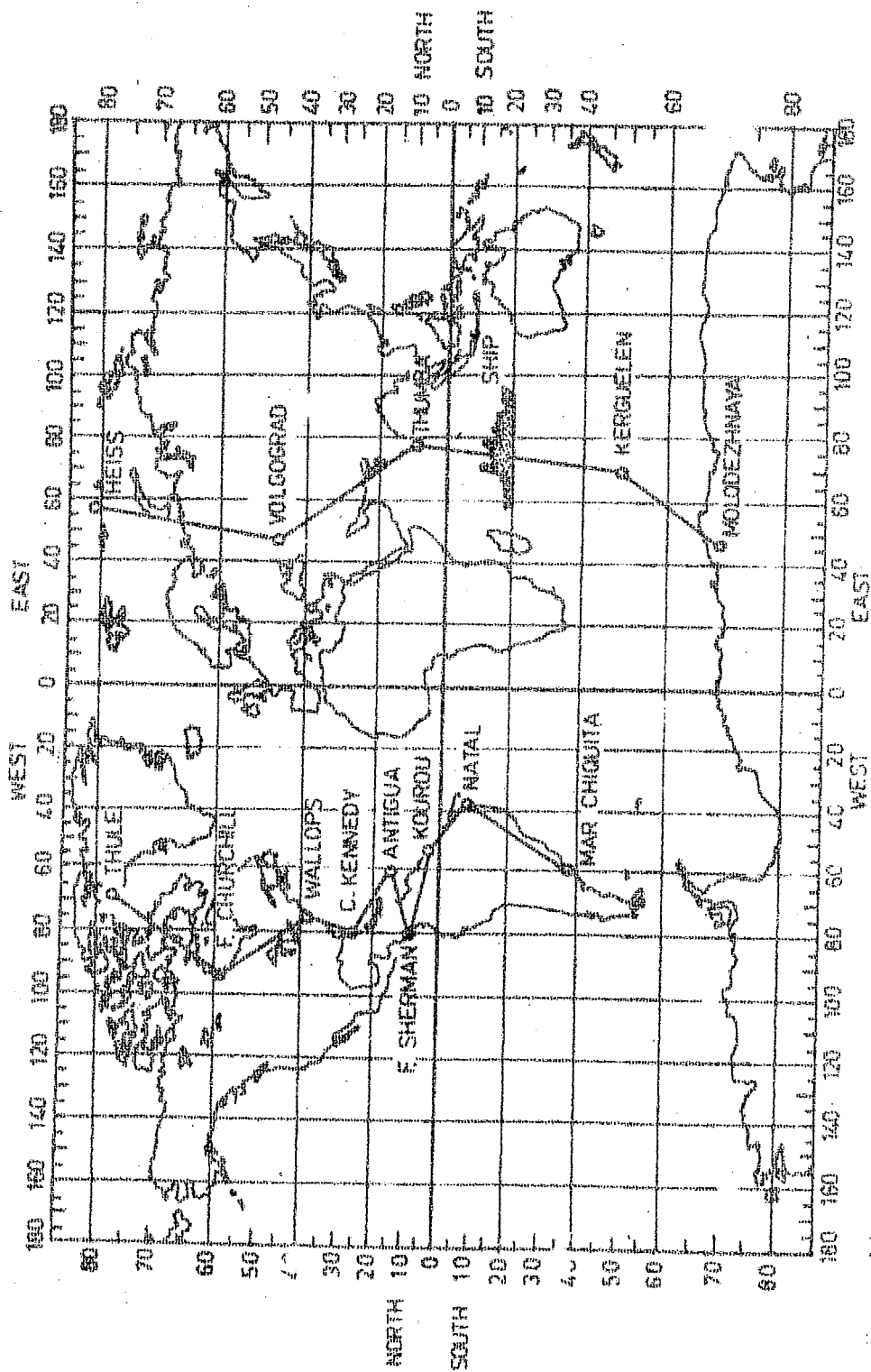
Location of the various stations in the Eastern and the Western hemispheres used in meridional cross section analysis.

(Fig 3.1)

and also the differences in the models of stratospheric warmings. The results of the new observations derived from the meridional cross section analysis are discussed here with illustrations.

The location of the various stations in the Eastern and the Western Meridional Network is shown in Fig 8.1. A summary of the rocket soundings carried out and that of the data used for the meridional cross section analysis in the Eastern and the Western Hemispheres is given in Tables 8.1 and 8.2 respectively.

8.1   Atmospheric structure over Heiss Island

Using the standard linear interpolation method, time-height cross sections of the zonal and meridional components of winds and those of the atmospheric temperatures up to an altitude of about 60-80 km over Heiss Island ($80^{\circ}37'N$, $58^{\circ}03'E$, Franz-Josef Land in the Arctic) and over Volgograd ($48^{\circ}41'N$, $44^{\circ}21'E$) located in the northern part of Eastern Hemisphere are drawn in Figs 8.2, 8.3, 8.4 and Figs 8.5, 8.6, 8.7 respectively. The data used in these cross sections are for the year 1972. The broken curves T and S in Figs.8.4 and 8.7 represent the corresponding tropopause and stratopause variations.
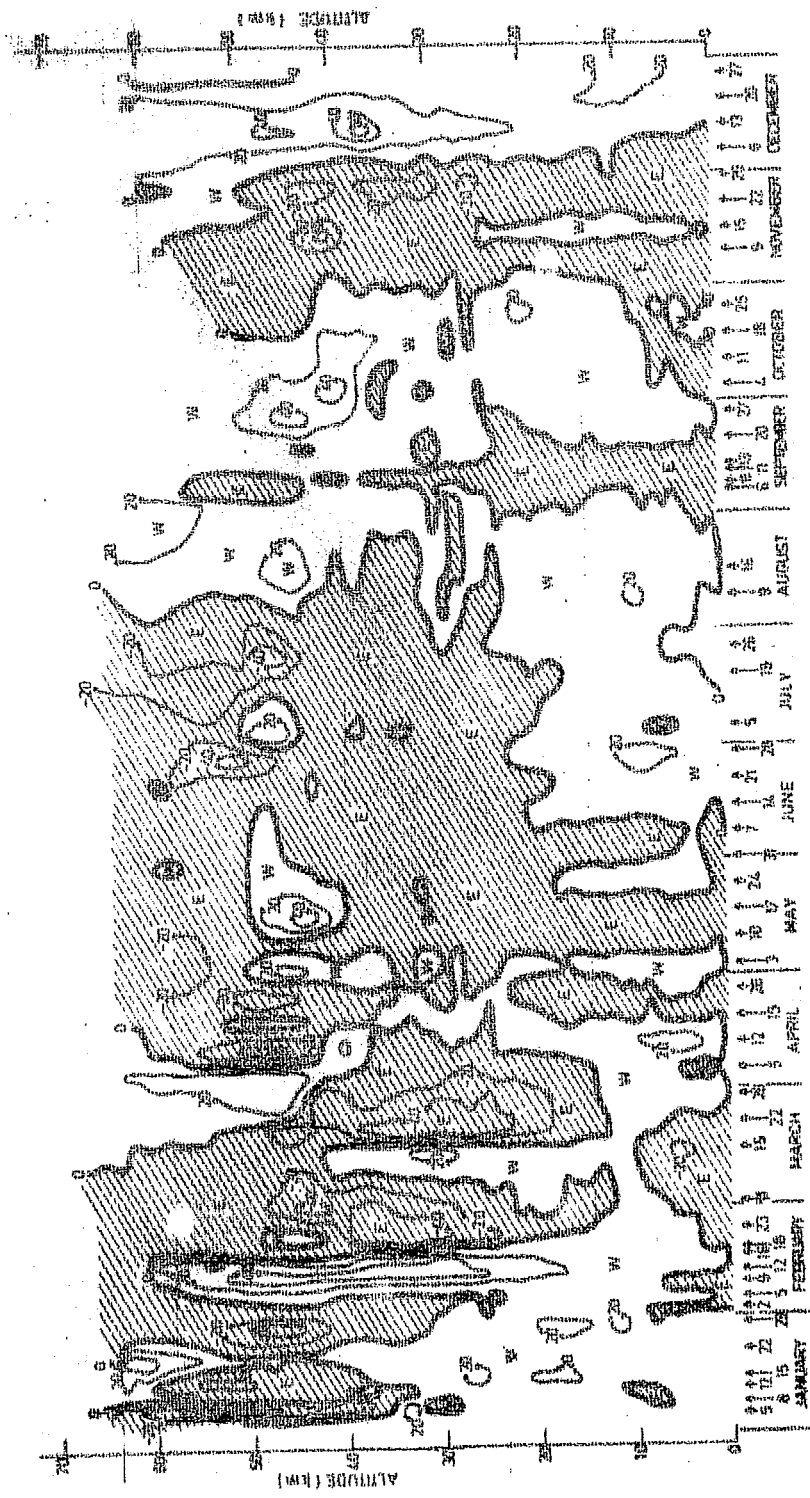
Time-height cross section of the zonal winds (ms⁻¹) over Heiss Island, Arctic in 1972. Shaded areas with negative values present easterly components while the blank areas with positive values depict the westerly wind components. Dashed lines represent extrapolated data. Arrows on the abscissa show the dates on which the data were obtained.

(Fig. 8-2)
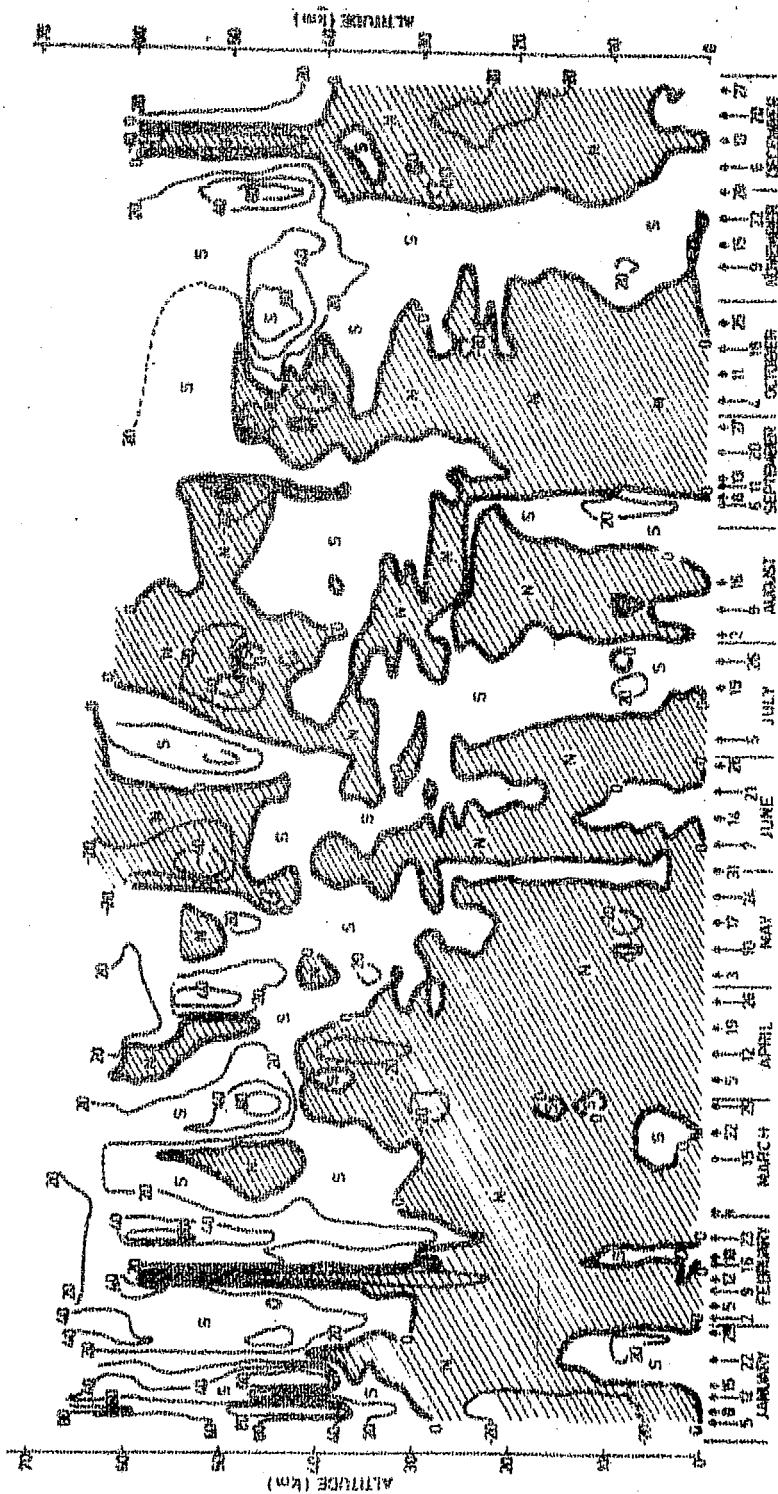
Time-height cross section of the meridional winds (m s⁻¹) over Heiss Island, Arctic in 1977. Shaded areas with negative values present northerly components while the blank areas with positive values depict the southerly wind components. Dashed lines represent extrapolated data. Arrows on the abscissa show the dates on which the data were obtained

(Fig. 8.3)
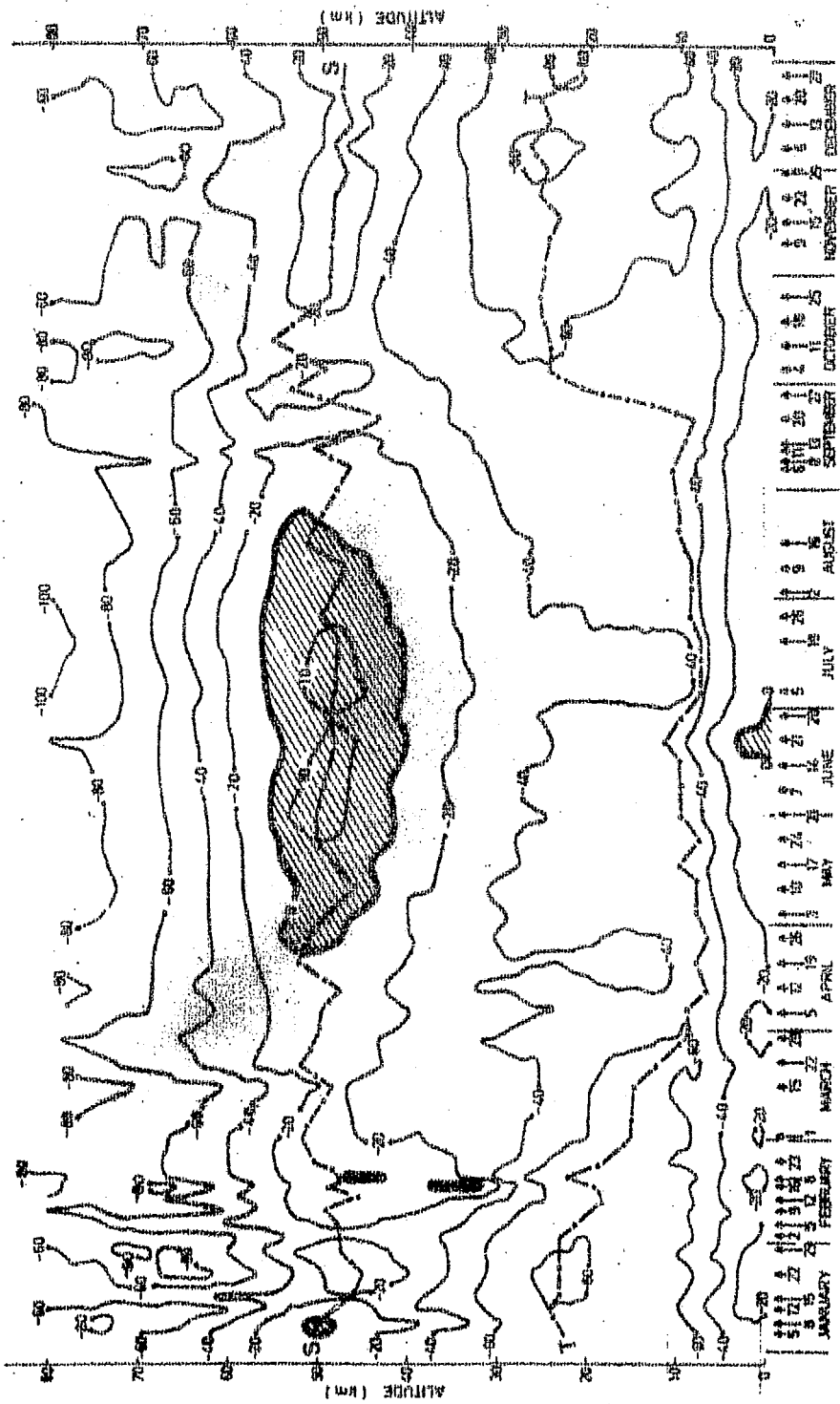
Time-height cross section of the atmospheric temperature (°C) over Heiss Island, Arctic in 1972. Shaded areas present positive temperatures and the dashed lines extrapolated data. Arrows on the abscissa show the dates on which the data were obtained.

(Fig. 8.4)

The time-height cross sections for Heiss Island indicate seasonal trends in the zonal and meridional wind components in the upper atmosphere as shown in Figs 8.2 and 8.3. A marked characteristic of the zonal wind distribution over Heiss Island is the predominance of a significant easterly component in the polar night period as is obvious from Fig 8.2. It may be due to the displacement of the polar vortex from the polar region to the European and Asian sectors of the Arctic and to stratospheric warmings. Maximum speeds of westerly winds in the upper stratosphere are recorded in autumn and in late winter. On the other hand, southerly wind components have been observed in the upper stratosphere during the winter season as illustrated in Fig 8.3.

Rocket soundings over Heiss Island give an indication of the disturbed character of winter thermal and wind regimes most strikingly corroborated by stratospheric warmings. Local temperature variations for the warming period in early February can be visualised in Fig 8.4. The monthly mean temperature maximum at the stratopause level in mid-summer approaches + 15°C, while the minimum temperature of the stratopause was observed in early winter as shown in the Figure 8.4. In the central Arctic the warming was most intensive in the middle and upper stratosphere.

## 8.2   Atmospheric structure over Volgograd

The disturbed character of the winter regime of the upper atmosphere is displayed in both high and middle latitudes. It is illustrated by the time-height cross sections of the wind and temperature fields in the upper atmosphere over Volgograd ($48^{\circ}41'$N, $44^{\circ}21'$E) as shown in Figs 8.5, 8.6 and 8.7.

The wind regime of the upper stratosphere over Volgograd was marked by seasonal change of westerly and easterly components as shown in Fig 8.5. High speeds of westerly winds in the winter months reaching about 100-150 ms^{-1} at the height of about 40-50 km were noted. The meridional winds over Volgograd were predominantly northerly with erratic southerlies having a maximum speed of about 100 ms^{-1} around 58 km in mid-December as shown in Fig 8.6. As is generally known, the summer regime of the upper atmosphere is characterised by low variability. This is corroborated by the Volgograd time-height cross sections. With the approach of autumn there was some increase of variability in the atmospheric structure in the stratosphere and mesosphere.

There was a large variability of the stratopause height over Volgograd ranging from 41 to 55 km as is obvious from Fig 8.7. Non-periodic temperature fluctuations with the range reaching 15-20°C at the stratopause level were also
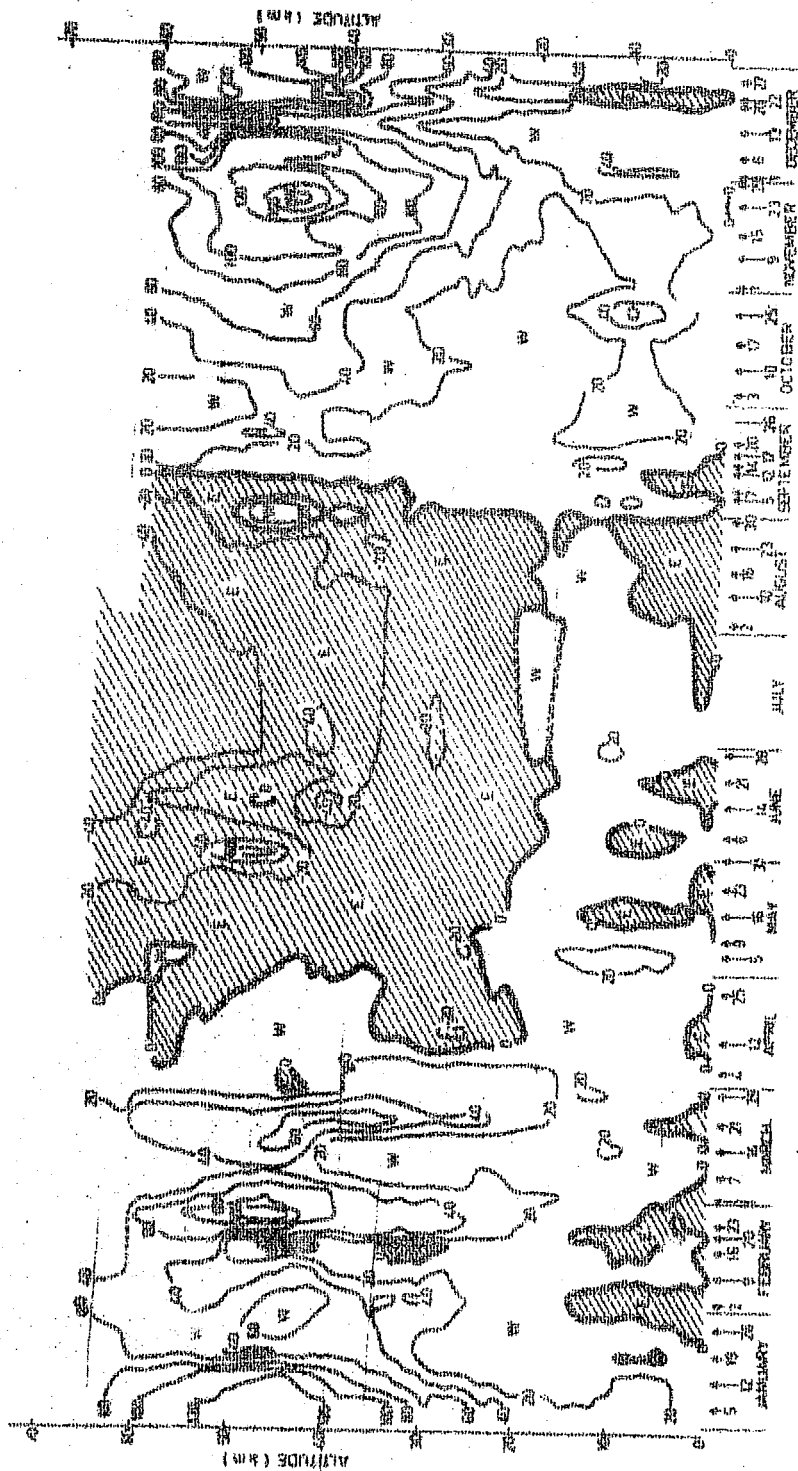
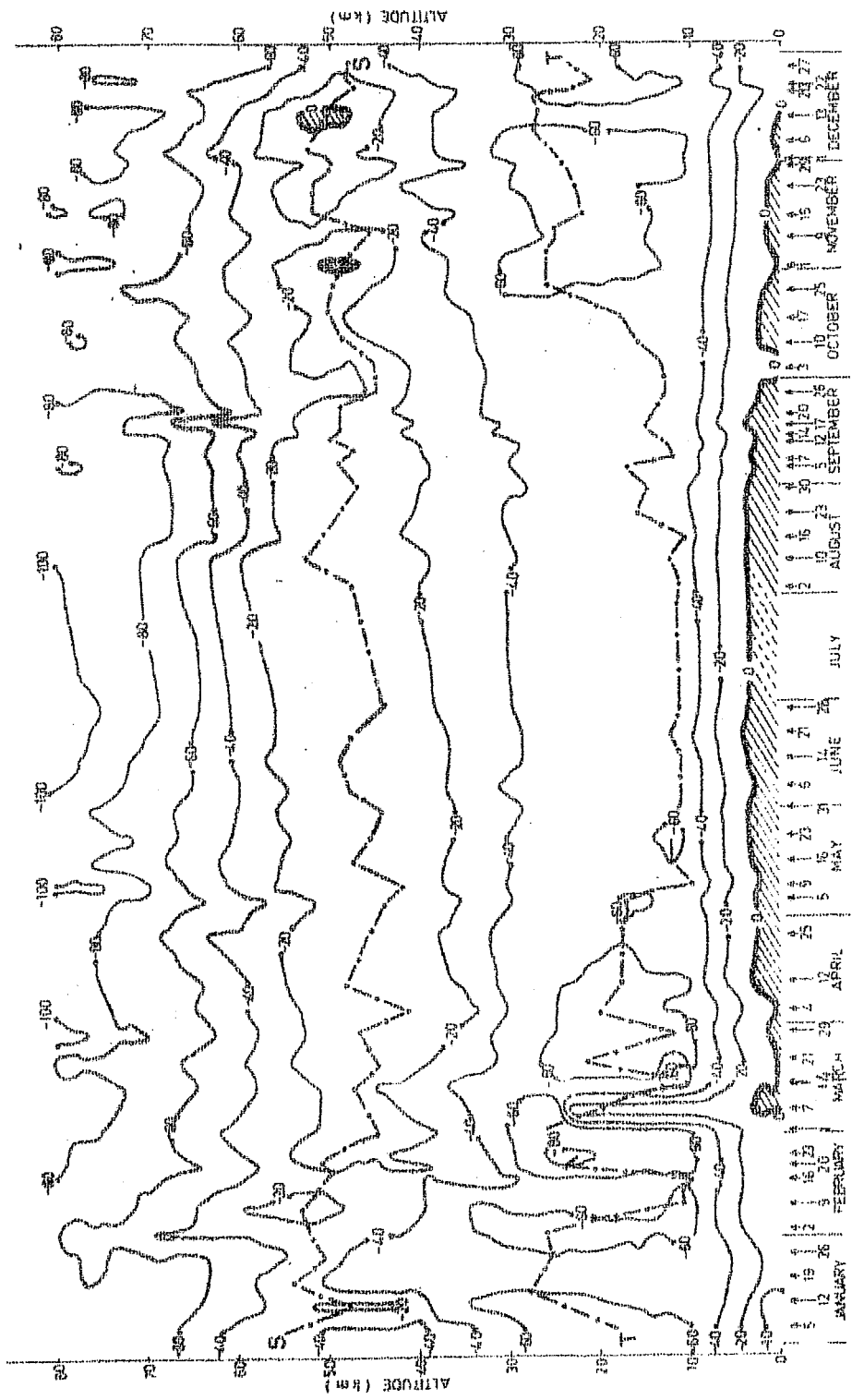Time-height cross section of the zonal winds (m s⁻¹) over Volgograd, USSR in 1972. Shaded areas with negative values present easterly components; the blank areas with positive values depict the westerly wind components. Dashed lines represent u, updated data. Arrows on the abscissa show the dates on which the data were obtained

(Fig. 8.5)
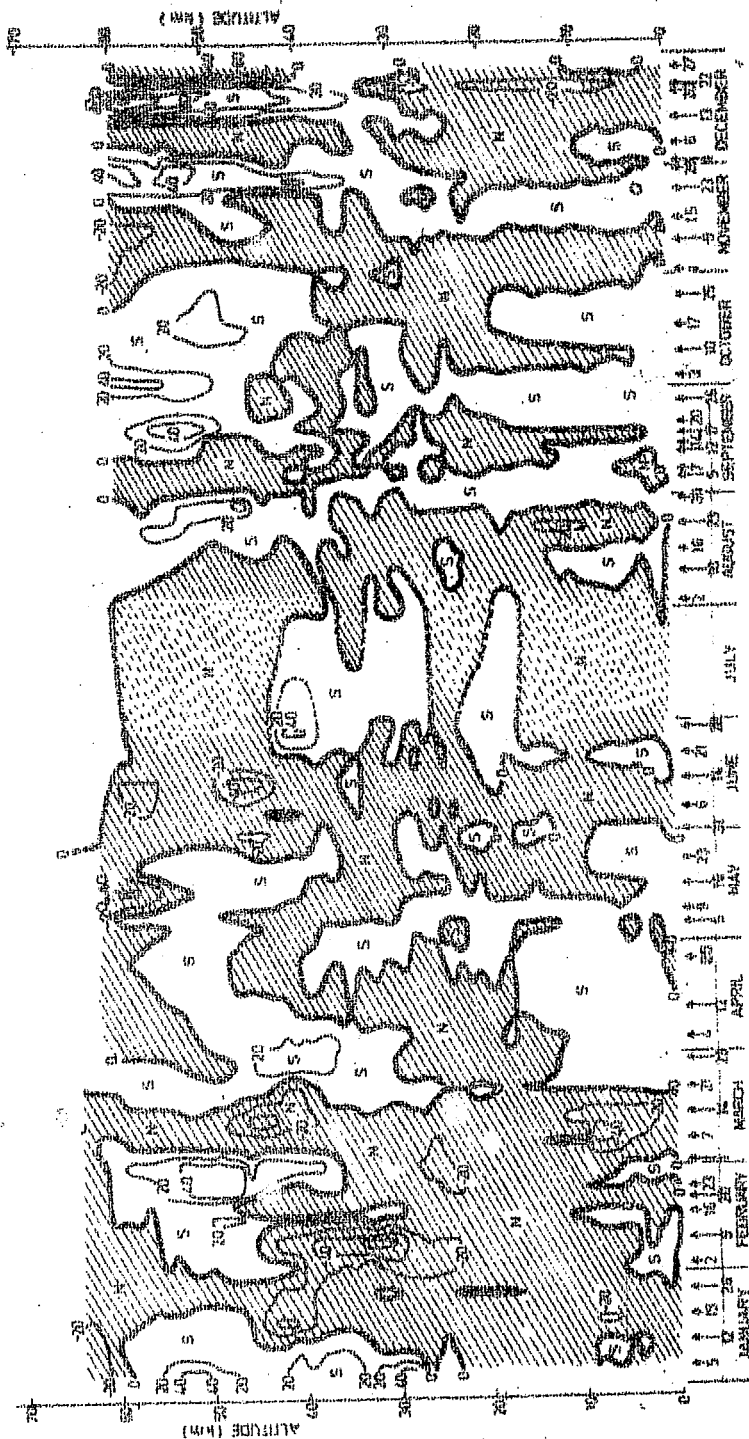
Time-height cross section of the meridional winds (m s⁻¹) over Volgograd, USSR, in 1972. Shaded areas with negative values denote northerly components while the blank areas denote southerly components. Dashed lines represent extrapolated data. Arrows on the abscissa show the dates on which the data were obtained.

(Fig. 8.6)

Time-height cross section of the atmospheric temperature (°C) over Volgograd, USSR in 1972. Shaded areas present positive temperatures and the dashed lines extrapolated data. Arrows on the abscissa show the dates on which the data were obtained.

(Fig. 8.7)

noticed in the upper stratosphere. The observed seasonal temperature trends over Volgograd were in accordance with the concepts generally accepted. Temperature changes in the stratosphere and lower mesosphere on one hand and in the upper mesosphere on the other hand were found to be out of phase in middle latitudes as well as in polar regions.

## 8.3   Antarctic-Arctic atmospheric structure

From the available data monthly average of January and July 1972 were computed for the stations Molodezhnaya ($67^{o}40'$S, $45^{o}51'$E), Thumba ($8^{o}32'$N, $76^{o}52'$E) and Heiss Island ($80^{o}37'$N, $58^{o}03'$E) and the corresponding results of summer and winter were compared. January and July were taken as the representative southern summer and winter, and northern winter and summer respectively. Some of the results of this intercomparison (southern summer versus northern summer and vice versa) are discussed here. Typical temperature and wind profiles over the Antarctic station Molodezhnaya and the Arctic station Heiss Island are shown in Figs 8.8(a) and 8.8(b).

In summer the Antarctic tropopause, stratopause and mesopause were found to be at altitudes of 9 km, 47 km and 80 km with temperatures of about -52°C, 7°C and -99°C respectively. The corresponding values at the equator(Thumba)
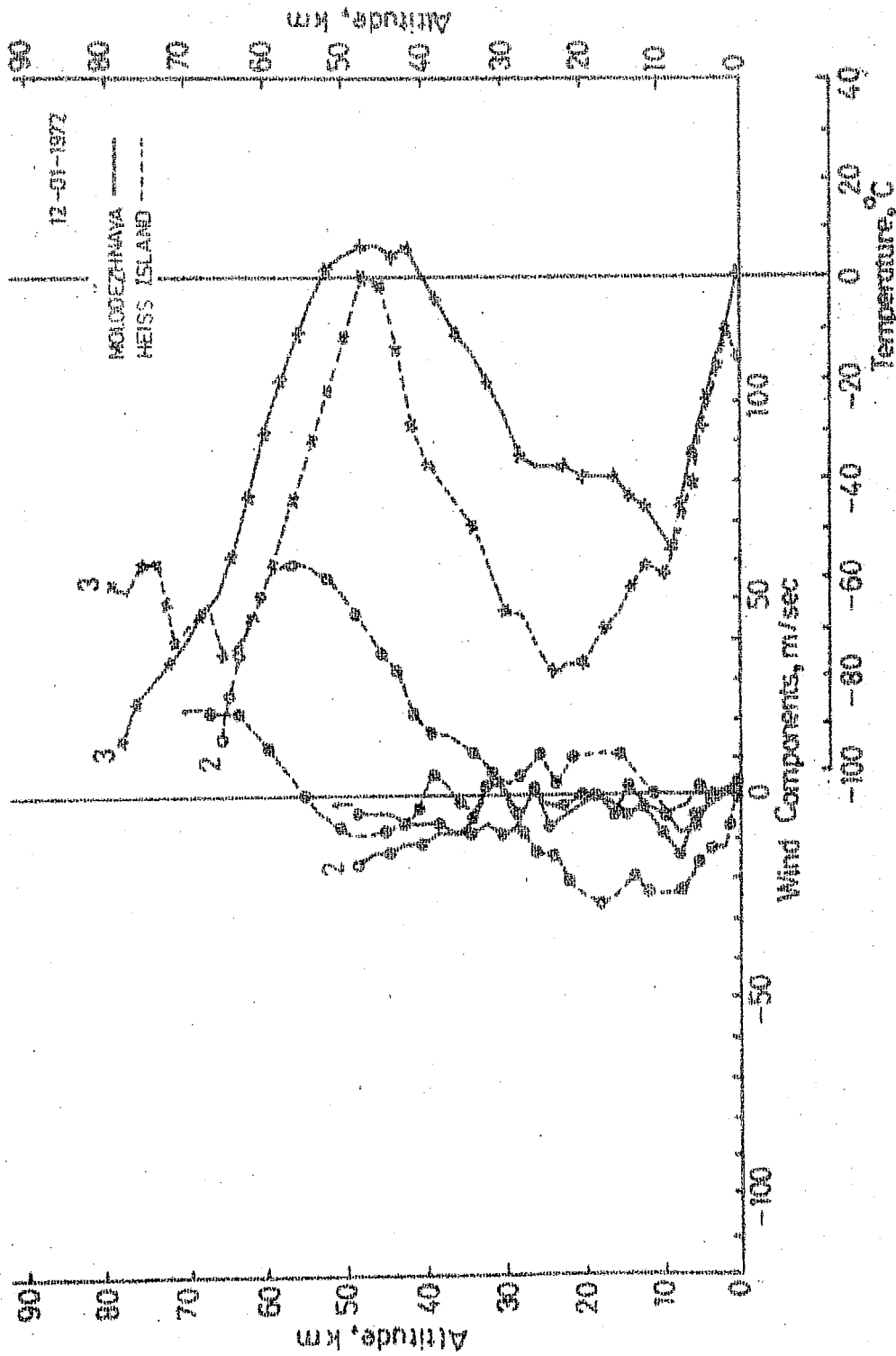
(Page 66 a)

Typical profiles of zonal winds (curves 1) meridional winds (curves 2) and temperatures (curves 3) over Molodezhnaya, Antarctica (solid lines) and Heiss Island, Arctic (dashed lines) on January 12, 1972.
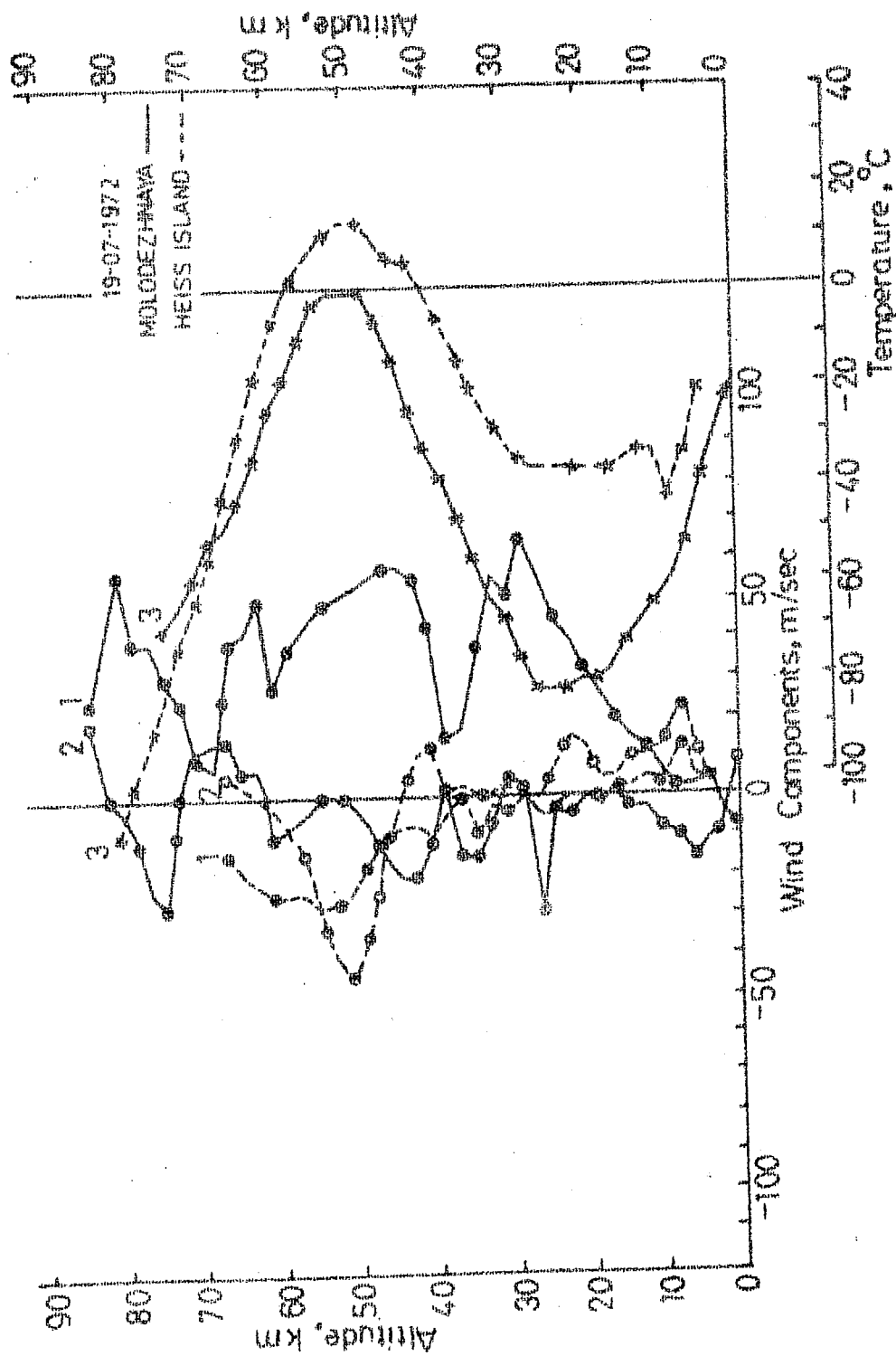
(Fig.8.8(b))

Typical profiles of zonal winds (curves 1, meridional winds (curves 2) and temperatures curves 3) over Molodezhnaya Antarctica (solid lines) and Heiss Island, Arctic (dashed lines) on July 19, 1972.

were 17 km, 46 km and 75 km with temperatures $-77^{O}C$, $-5^{O}C$ and $-82^{O}C$. Over the Antarctic, the tropopause and the stratopause were located at 9 km and 48 km with temperatures $-44^{O}C$ and $11^{O}C$ respectively, while the mesopause was ill-defined. Thus the South Polar tropopause was about $25^{O}C$ warmer and the stratopause about $12^{O}C$ warmer than the corresponding equatorial tropopause and stratopause. However, the South Polar mesopause was found to be about $17^{O}C$ colder. The Antarctic tropopause was about $8^{O}C$ colder and the stratopause about $4^{O}C$ colder than the corresponding Arctic tropopause and stratopause.

It is found that in summer the winds in the lower atmosphere up to about 25 km altitude over Antarctica were weak and easterly with speeds less than 10 ms^{-1}. Over the equatorial region also the winds were with speed less than 13 ms^{-1} but westerly up to 10 km. The south polar stratosphere and equatorial stratosphere were marked by strong easterly winds having speeds less than 40 ms^{-1}. Over the equatorial station Thumba the maximum speed was about 40 ms^{-1} at 30 km. The Antarctic mesospheric zonal winds were characterised by strong easterlies with a maximum speed of 47 ms^{-1} at 70 km, while the meridional winds were weaker northerlies having a maximum speed of 16 ms^{-1} at 58 km. Over the Arctic the winds were weak with speeds less than 10 ms^{-1} up to the

stratopause. In the lower mesosphere the zonal winds were easterlies ranging from about 10 to 25 ms^{-1} and the meridional winds were southerlies with speeds less than 20 ms^{-1}.

In winter the Antarctic stratopause was located at 48 km with a temperatures of about $-12^{\circ}C$, while the tropopause and mesopause were ill-defined. The corresponding values at the equator (Thumba) were about 17 km, 50 km and 77 km with temperatures around $-80^{\circ}C$, $-9^{\circ}C$ and $-76^{\circ}C$ respectively. Over the Arctic the tropopause, the stratopause and the mesopause were apparently located at altitudes of about 22 km, 48 km and 72 km with temperatures of $-79^{\circ}C$, $-6^{\circ}C$ and $-71^{\circ}C$. However, the tropopause was not well defined due to its multiple occurrences between 10 and 25 km. The South Polar stratopause was thus about $3^{\circ}C$ colder than the corresponding equatorial stratopause. The Antarctic tropopause was found to be about $3^{\circ}C$ colder and the stratopause about $6^{\circ}C$ colder than the corresponding Arctic tropopause and stratopause in the winter period.

It is found that in winter the zonal winds over Antarctica were westerly in toto, up to 84 km having a maximum speed of about 100 ms^{-1} at 64 km. The meridional winds were northerlies up to about 60 km with a maximum speed of 19 ms^{-1} at 35 km and southerlies aloft with a

maximum of 23 ms^{-1} at 68 km. Over the equatorial region (Thumba) the zonal winds were easterlies in the stratosphere having a maximum speed of 31 ms^{-1} at 50 km. The meridional winds were weak and variable up to 40 km, and northerlies ranging from 5 to 25 ms^{-1} from 40 to 64 km. Over the Arctic the zonal winds were westerlies having speeds less than 15 ms^{-1} up to 35 km and easterlies aloft with a maximum speed 22 ms^{-1} at 49 km. Up to about 30 km the meridional winds were predominantly northerly with speed less than 20 ms^{-1} and above 30 km they were strong southerlies having a maximum speed of 58 ms^{-1} at 64 km. The departures of the actual zonal winds and temperatures over the polar and the equatorial regions from the corresponding profiles of the Groves (1971) atmospheric model were of the order of 30 ms^{-1} and 30°C respectively.

From this analysis, the annual temperature range in the Antarctic stratosphere appears to be much greater than that over Heiss Island in the Arctic. The differences in thermal regimes of the two polar regions are related generally to the specific features of the orography of their underlying surface and circulation. In the Antarctic minimum temperature in the stratosphere is observed in the middle of the polar night while in the Arctic it is displaced to the first half of the night period.

The effect of winter stratospheric warmings is quite noticeable in the southern polar region which is marked by a sudden disruption in the wind and thermal regimes. There is also an indication that the spring transformation of the circulation in the Antarctic starts one or two months later than in the Arctic.

8.4   Eastern-Western hemispheric atmospheric structure

The Eastern and Western Meridional Networks with stations in both the Northern and the Southern Hemispheres are located near the 70°E and 70°W meridians as shown in Fig 8.1. The Eastern Meridional Network covers Heiss Island ($80^{\circ}37'$N, $58^{\circ}03'$E), Volgograd ($48^{\circ}41'$N, $44^{\circ}21'$E), Thumba ($8^{\circ}32'$N, $76^{\circ}52'$E), Ships in the Indian Ocean (within 20°N- 50°S) and Molodezhnaya ($67^{\circ}40'$S, $45^{\circ}51'$E). The Western Meridional Network comprises of the stations Thule ($76^{\circ}33'$N, $68^{\circ}49'$W), Fort Churchill ($58^{\circ}44'$N, $93^{\circ}49'$W), Wallops Island ($37^{\circ}50'$N, $75^{\circ}29'$W), Cape Kennedy ($28^{\circ}27'$N, $80^{\circ}32'$W), Antigua ($17^{\circ}09'$N, $61^{\circ}47'$W), Fort Sherman ($9^{\circ}20'$N, $79^{\circ}59'$W), Natal ($5^{\circ}55'$S, $35^{\circ}10'$W) and Mar Chiquita ($37^{\circ}45'$S, $57^{\circ}25'$W). A summary of the meteorological rocket soundings carried out in the Eastern and the Western Hemispheres during the period December to February and June to August 1972 and that of the data used for cross section analysis is given in Tables 8.1

and 8.2 respectively. Some of the data were also taken from 1969-71 as the rocket soundings at a few stations in the Western Hemisphere e.g. Thule, Antigua, Natal and Mar Chiquita were practically nil or very few in 1972. The number of rocket launchings carried out in the Western Hemisphere exceeded those in the Eastern Hemisphere as is obvious from the Tables 8.2 and 8.1.

The meridional analysis was carried out by drawing latitude-height cross sections of the atmospheric winds and temperatures from the seasonal averages for the periods December to February and June to August using the standard linear interpolation method. The latitude-height cross sections of the zonal and the meridional components of winds for the periods December to February and June to August are given in Figs 8.9, 8.10, and Figs 8.11, 8.12 respectively, while Figs 8.13 , 8.14 present the corresponding cross sections of the temperatures. An intercomparison of the actual atmospheric temperatures at the altitudes 25, 50 and 75 km averaged over December to February and June to August in the Eastern and the Western Meridional Networks with the corresponding average profiles from the Groves Atmospheric Model (Groves, 1971) is illustrated in Fig 8.15.

Table – 8.1

Summary of the meteorological rocket soundings in the Eastern Hemisphere in 1972

Eastern Meridional Network (40°E – 90°E)

Rocket launching dates/(No.of launches)

Station (latitude.)	December	January	February	June	July	August
1	2	3	4	5	6	7
Heiss Island (80°37'N)	6,13,20, 27 (4)	5,8,12, 12,22,29 (6)	2,5,9,12 16,18,23 (7)	7,14,21, 28 (4)	5,19,26 (3)	2,9,16 (3)
Volgograd (48°41'N)	1,6,13, 20,22,27 (6)	5,12,19, 26 (4)	2,9,16, 20,23 (5)	6,14,21, 28 (4)	---	2,10,16, 23,30 (5)
Thumba (8°32'N)	13,20, 27 (3)	5,12,19, 26 (4)	2,17,23 (3)	7,14,21, 28 (4)	5,12,19, 26 (4)	2,9,16, 24,30 (5)
Ships (23°N to 50°S)	---	---	---	1(23°N) 3(14°N) 30(24°S) (3)	26(15°S) 15(30°S) 7(35°S) 8(40°S) 9(45°S) 10(50°S) (6)	1(6°N) 9(5°S) 8(9°S) (3)
Molodez–naya (67°40'S)	6,13,20, 27 (4)	5,12,19, 26 (4)	2,16,23 (3)	17,28 (2)	1,5,12,19, 22,26 (6)	2,6,9,16, 20,23,30 (7)

Table - 8.2

Summary of the meteorological rocket soundings in the Western Hemisphere

Western Meridional Network (35°W - 95°W)

Rocket launching dates/(No. of launches)

Region (latitude)	December 1971	January 1972	February 1972	June 1972	July 1972	August 1972
1	2	3	4	5	6	7
...le 33'N	1969-71 (11)		1969-72 (16)		1969-72 (14)	1969-72 (10)
...rchill °44'N	1,2,3,6,7, 8,9,10,10, 10,13,15,16, 17,20,21,22, 23,24,28,28, 29,29,30,30, 31 (26)	4,5,6,7,15, 17,18,19, 20,21,24, 26,28,31 (14)	1,2,3,4,7,8, 10,11,12,15, 15,16,17,18, 22,23,24 (17)		5,14,21,26 (4)	2,6,11,14,16, 18,21,23,25, 28,30 (11)
...lops and °50'N	1,3,8,10,13, 16,17 (7)	3,5,6,6,7, 12,14,17,21, 21,24,26, 27,28,31,31 (17)	1,4,7,9,11, 16,23,28 (8)	2,5,7,9,12, 15,16,19,22, 28,30 (11)	6,7,12,14, 17,19,21,24, 26,28,31 (11)	2,4,9,11,14, 16,18,18,21, 23,25,25,30 (13)

more

Table - 8.2 contd..2..

	2	3	4	5	6	7
edy 27'N)	1,1,6,10, 13,15,15,15, 15,16,17,20, 22,27,29,29 (17)	3,5,7,11,12, 14,17,19,21, 21,24,26,26, 26,28,12 (16)	2,7,9,9,11, 14,15,15,15, 16,16,17,18, 18,23 (15)	2,5,7,12,14, 17,19,20,20, 20,21,21,22, 22,22,23,23, 28,29,30 (20)	3,7,10,12, 14,17,19, 21,24,25,25, 26,26,26,27, 28,28,31 (18)	2,2,4,7,9,11, 16,18,23,28, 30 (11)
gua 09'N)	1969-71 (11)	1969-72 (23)	1969-72 (19)	1969-72 (14)	1969-72 (20)	1969-72 (16)
nan 0'N)	3,8,10,13, 16,20,22, 28,29,30 (10)	3,5,7,10,12, 14,17,19,21, 24,26,28,31 (13)	4,7,11,14, 18,22,23,25, 28 (9)	2,5,7,9,12, 14,16,19, 21,23,26,28 (12)	3,5,7,10, 14, 12,17,19, 21,24,26, 28 (12)	16,18,21,25, 28,30 (6)
l 5'S)	1969-71 (4)	1969-72 (3)	1969-72 (3)	1969-72 (3)	1969-72 (5)	------------
ita 45'S)			------------			

8.4.1   Hemispheric zonal flow

The cross section for December to February in Fig 8.9
shows conditions characteristic of this time of the year with
fairly strong westerlies of the winter circulation prevailing
in the Northern Hemisphere and with relatively weaker
easterlies typical of summer in the Southern Hemisphere. The
quasi-bienniel oscillation is known to have been in its
easterly phase at this time accounting for the easterly winds
over Thumba in the Eastern Hemisphere and Fort Sherman in the
Western Hemisphere. The wind regime of the southern part of
the Indian Ocean during the winter displays wind speeds which
exceed mean values generally recorded in the Northern
Hemisphere and amount to 90 ms^{-1} at the altitude of about
50 km. The height of the maximum **wind** layer in the mesosphere
lowers considerably from tropical regions towards middle
latitudes. A core of moderately strong westerly winds with
speeds less than 40 ms^{-1} was detected in the summer easterly
regime in the Southern Hemisphere, which was located in an
altitude region from surface to 25 km between the latitude
belt 20°S to 65°S in the Eastern Hemisphere as illustrated
in Fig 8.9. Spring and autumn advanced in the Northern and
Southern Hemisphere respectively by about the beginning of
April. There were then winds with weak easterly components
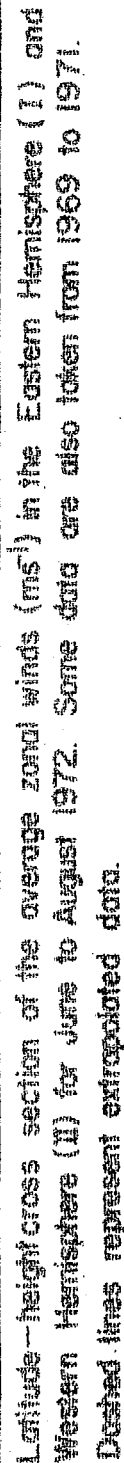at high and middle latitudes of the Northern Hemisphere
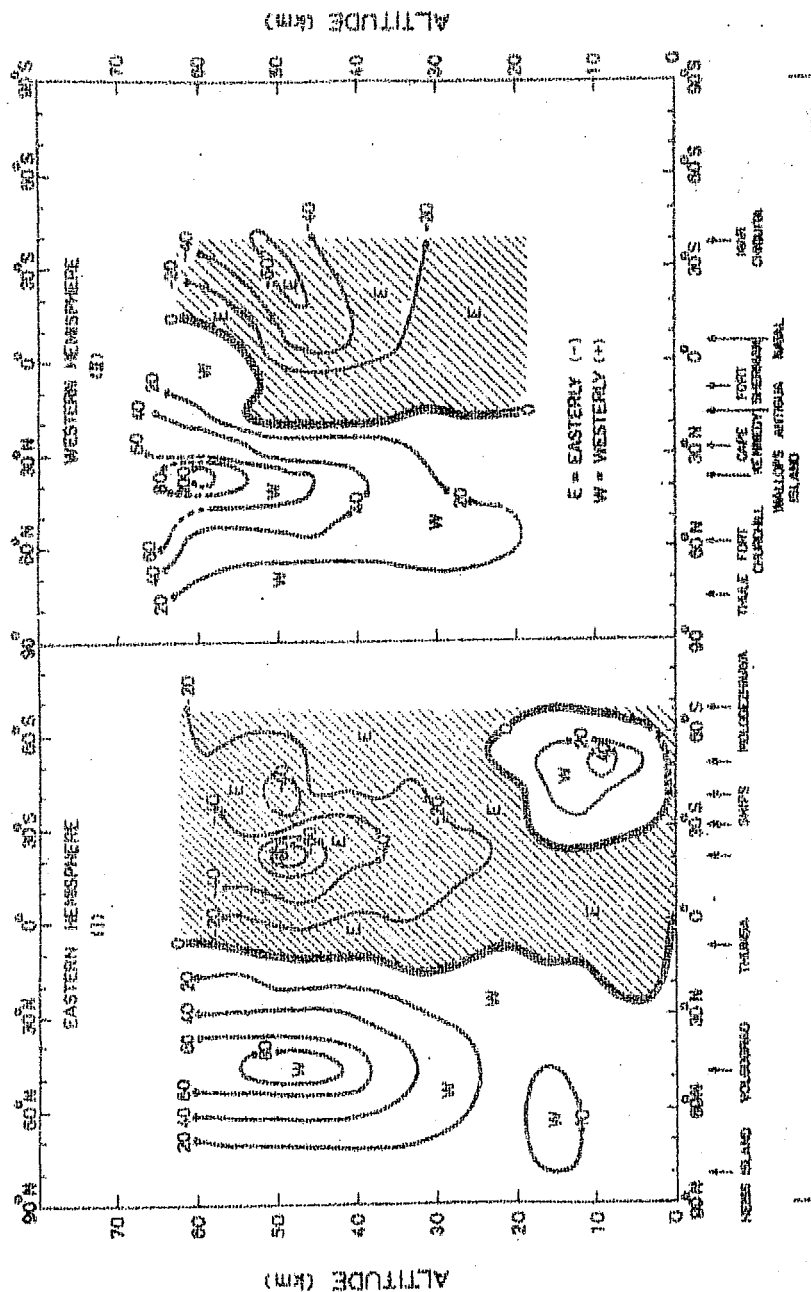
(Fig. 6.9)

Latitude-height cross section of the average zonal winds (m/s) in the eastern
hemisphere (I) and the western hemisphere (II) for December to February 1972.
Some data are also taken from 1969 to 1971. Dashed lines represent extrapolated

extending to altitudes greater than 50 km, while the Antarctic station Molodezhnaya indicated moderately strong westerlies in the polar area. By the end of May the transition from winter to summer in the Northern Hemisphere and from summer to winter in the Southern Hemisphere was completed.

The latitude-height cross section of the average zonal winds during June to August drawn in Fig 8.10 shows that the easterly winds prevailed throughout the stratosphere and lower mesosphere in the Northern Hemisphere, while in the Southern Hemisphere the winds were predominantly strong westerly with speeds less than 80 ms^{-1}. Mar Chiquita station showed stronger westerlies. The steady character of the summer circulation is displayed in slight wind fluctuations around the predominant easterly direction. It was found that in summer the growth of the easterly winds in the stratosphere was faster with altitude south of the equator than north of it. On the other hand, in winter the growth of the easterlies with altitude was faster in the Northern Hemisphere than in the Southern Hemisphere. The summer maximum of easterlies in the upper stratosphere in low latitudes of the Southern Hemisphere was higher than that in the Northern Hemisphere. In summer the wind speed in the upper stratosphere was found to be considerably higher south of the equator than north of it. It appears that this discrepancy was not a local

Latitude-height cross section of the average zonal winds (ms) in the Eastern Hemisphere (I) and Western Hemisphere (II) for June to August 1972. Some data are also taken from 1969 to 1971. Dashed lines represent extrapolated data.

(Fig. 8.10)

phenomenon but it reflected differences in circulation between the two hemispheres.

In middle latitudes of the Southern Hemisphere the information gained so far is rather scant. It may, however, noted that there was a gradual reduction with latitude of differences between hemispheres in the summertime easterly circulation. Thus in summer the speed the easterly stratospheric flow of the Southern Hemisphere did not differ much from that of the Northern Hemisphere in middle latitudes but exceeded the latter in tropical regions. Strong winds observed in low latitudes of the Southern Hemisphere determined the shift of the axis of the easterly flow towards lower latitudes in the Southern Hemisphere as compared with the Northern Hemisphere. Apparently, it is not justifiable to use rocket data obtained in one hemisphere for describing the wind pattern in the opposite hemisphere. The magnitude of the wind differences between hemispheres in summer amounting to about 20 or 30 ms^{-1} around 10° and 20° latitude makes it reasonable to take them into consideration when compiling atmospheric wind models. In winter easterly wind speeds at $10^{o}S$ were lower in the Southern Hemisphere at altitudes of 40 and 50 km than in the Northern Hemisphere. The comparison for 20° latitude was hampered by lack of data in the Southern Hemisphere. In higher latitudes the westerlies were more
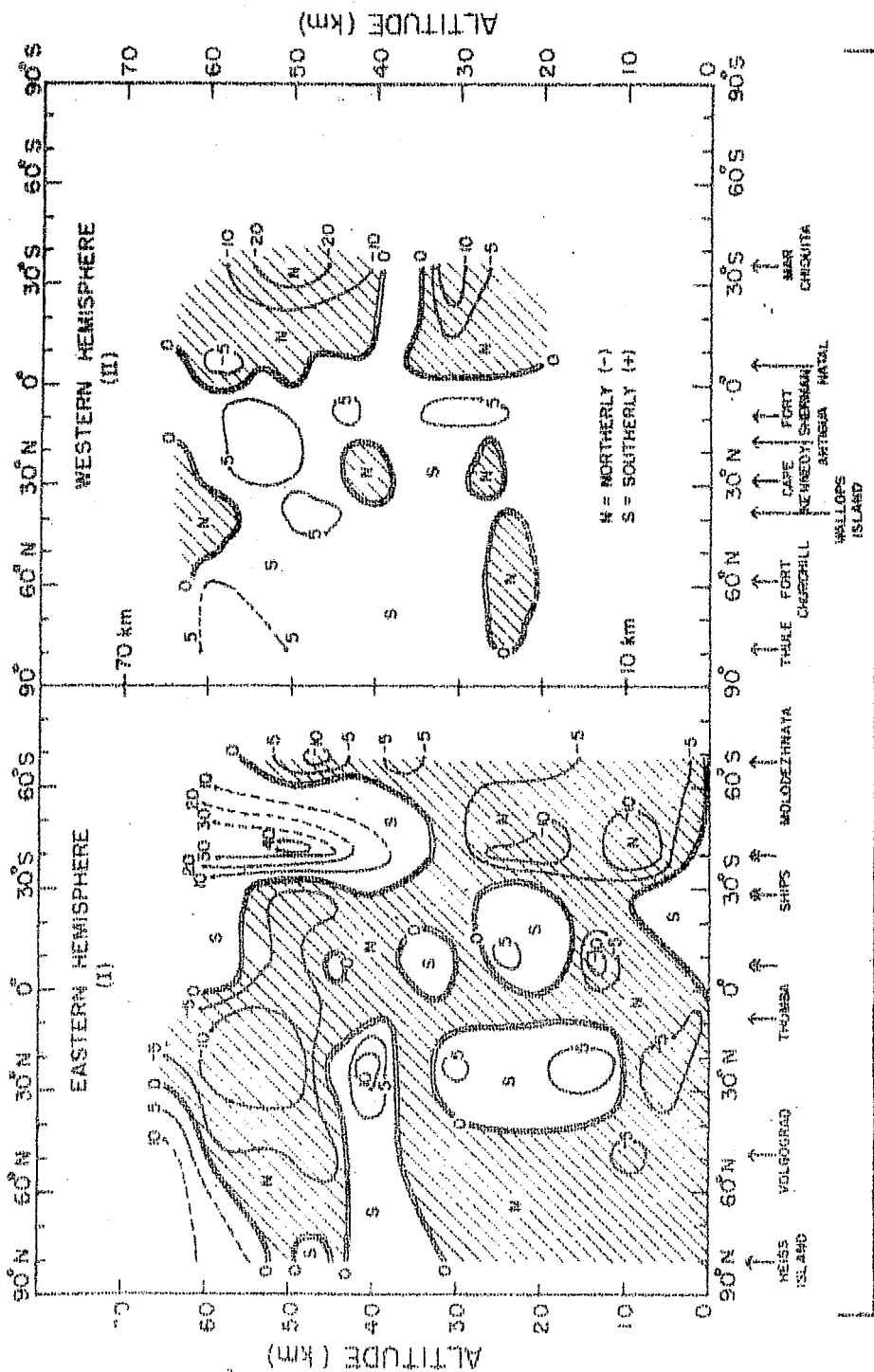
MERIDIONAL WINDS

DECEMBER – FEBRUARY
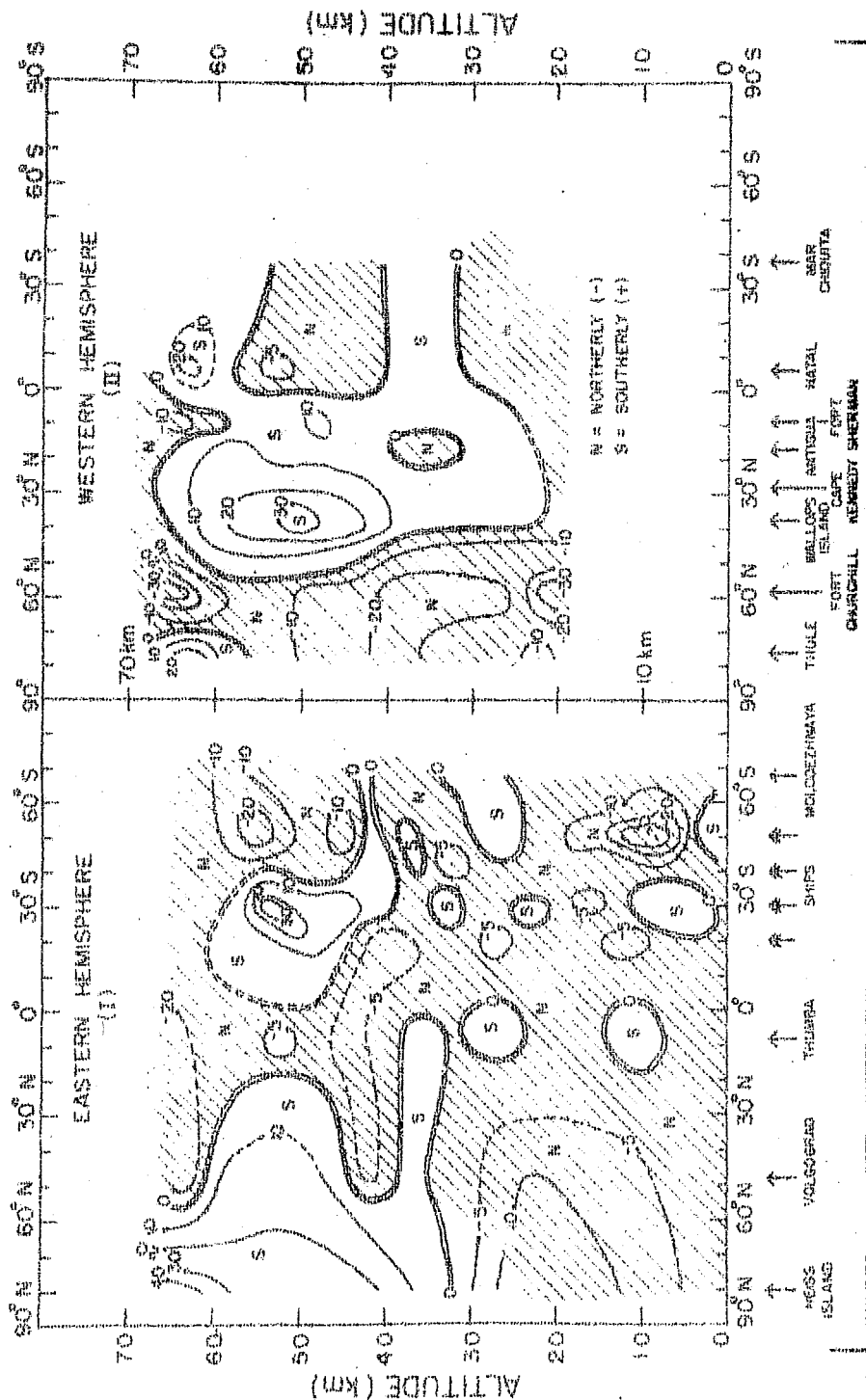
Latitude-height cross section of the average meridional winds (ms⁻¹) in the Eastern Hemisphere (I) and the Western Hemisphere (II) for December to February 1972. Some data are also taken from 1969 to 1971. Dashed lines represent extrapolated data.

(Fig. 8.11)

MERIDIONAL WINDS
JUNE – AUGUST

Latitude-height cross section of the average meridional winds (ms^{-1}) in the Eastern Hemisphere (I) and the Western Hemisphere (II) for June to August 1972. Some data are also taken from 1969 to 1971. Dashed lines represent extrapolated data.
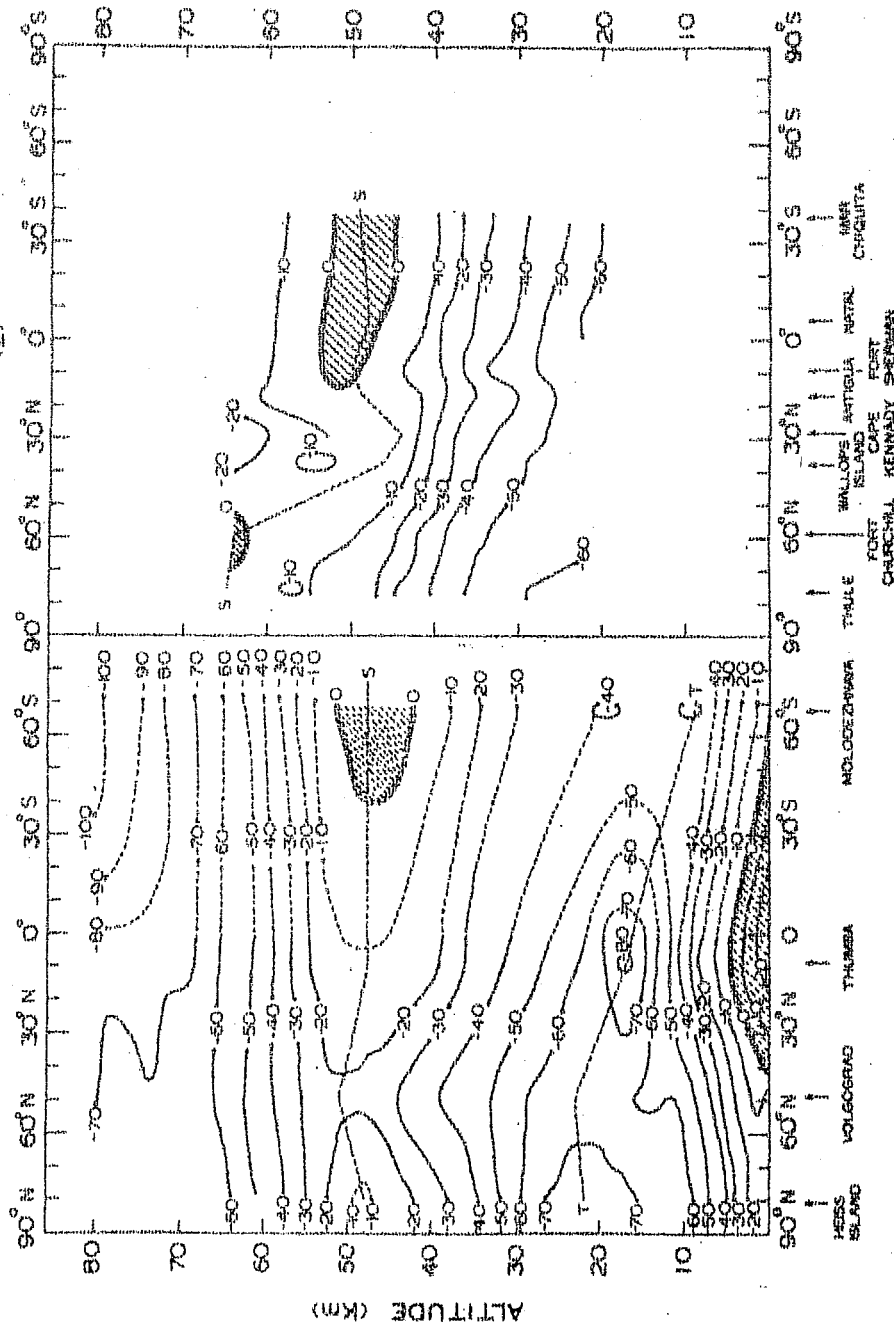
(Fig. 8.12)

intense in the Southern Hemisphere. In low latitudes maximum
differences in wind speed between hemispheres were observed
at an altitude of about 40-50 km.

The latitude-height cross sections of the meridional
components of winds in the Eastern and the Western Meridional
Networks showing the corresponding hemispheric differences
during the periods December to February and June to August
are illustrated in Figs 8.11 and 8.12 respectively. Northerly
and southerly wind components were found to be erratically
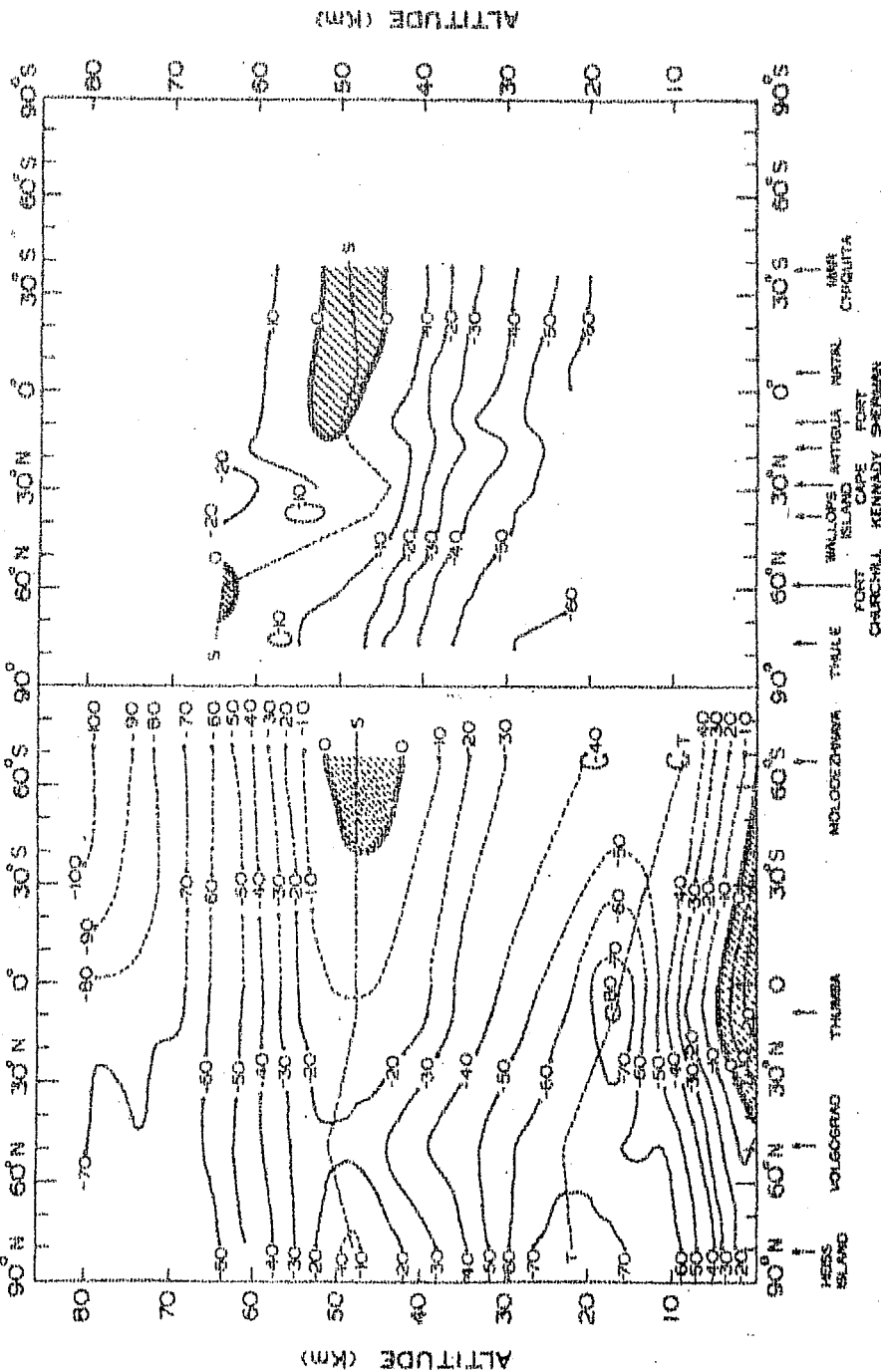distributed.

8.4.2   Hemispheric temperature variations

As is seen from Figs 8.13 and 8.14 the temperature
regime of the stratosphere in low latitudes is marked by
considerable stability and minor latitudinal variations.
The cross sections presented provide a spectacular illustration
of the sharp temperature variations which might occur in
the stratosphere and mesosphere over the Arctic and the
Antarctic regions. The dashed curves T and S in the Figs 8.13
and 8.14 present the latitudinal variations of the tropopause
and the stratopause during the periods December to February
and June to August, respectively. Rocketsonde data obtained
in the polar regions showed large variability of temperature
and wind in the winter mesosphere. The maximum range of

(Fig.8.13)

Latitude-height cross section of the average atmospheric temperature (°C) in the Eastern Hemisphere (I) and the Western Hemisphere (II) for December to February 1972. Some data are also taken from 1969 to 1971. Dashed lines represent extrapolated data.

Fig. 14)

Latitude-height cross section of the average atmospheric temperatures (°C) in the eastern hemisphere (i) and the western hemisphere (ii) for June to August 1972. Some data are also taken from 1969 to 1971. Dashed lines represent extrapolated data.

temperature fluctuations was about 40 to 80°C in 7 to 10 days in the mesosphere. Temperature fluctuations gradually diminished in the stratosphere towards a minimum in the lower stratosphere. Warmings and coolings in the upper atmosphere preceeded those in the lower layers. Warm and cold regions were observed overlying each other.

During winter period notable temperature variations were observed in the Southern Hemisphere particularly south of 30°S and the meridional gradient reached maximum values in the 40°S latitude region as shown in Fig 8.14. Marked temperature changes occurred between 20°S and 45°S with the upper stratosphere undergoing a significant cooling and the upper mesosphere a considerable warming around 40°S. Fig 8.14 shows that the upper mesosphere over the equator was also subjected to a significant warming indicating that the mesospheric warming was global in character. It was difficult to determine the precise position of the mesopause on account of the data limitations.

It was found that in the period analysed in high latitudes of the Southern Hemisphere, the mesopause level was located considerably higher and had lower temperature values than those ascertained in the Groves Atmospheric Model (Groves, 1971) as shown in Fig 8.15. The Fig 8.15 illustrates the inter-hemispheric comparison of the
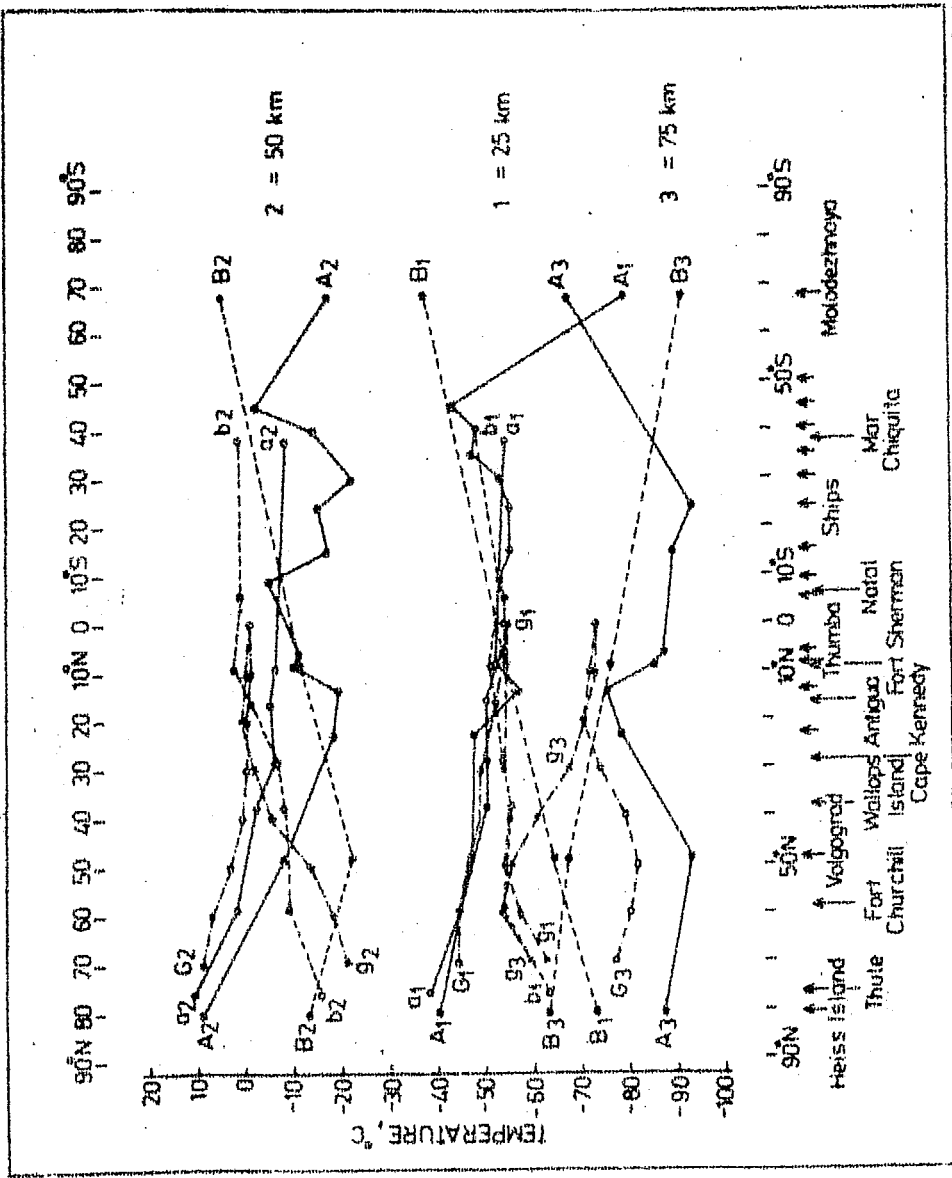
(Fig. 8.15)

Constant-height latitude cross section of atmospheric temperature (°C) in 1972.
Curve A = Eastern Hemisphere cross section for June to August
Curve B = Eastern Hemisphere cross section for December to February
Curve a = Western Hemisphere cross section for June to August
Curve b = Western Hemisphere cross section for December to February
Curve G = Cross section according to Groves (1971) Model for June to August.
Curve g = Cross section according to Groves (1971) Model for December to February
Suffixes 1, 2 and 3 represent the heights 25, 50 and 75 km, respectively.

atmospheric temperatures at 25,50 and 75 km altitudes averaged over the periods December to February and June to August.

8.4.3   Upper atmospheric warmings and coolings

The meridional cross section analysis illustrated in Figs 8.9 to 8.15 shows that significant disturbances of temperature and wind velocity distribution were observed in the Antarctic mesosphere during the southern winter regime, which exceeded similar variations at lower levels. The period of oscillations at the altitudes of 60-70 km ranged from one to three weeks, and changes of temperature were from 20 to 70°C. The strengthening of westerly flows in the middle and upper mesosphere as well as in the stratopause layer were accompanied by warming, while the weakening of a westerly flow, the increase of meridional components and the appearance of easterly components coincided with cooling in this part of the atmosphere. Strong cooling in the upper mesosphere was accompanied by warming in the stratopause layer. These features of temperature and wind variations suggest that along with the relative stability of the Southern Hemisphere winter polar cyclone in the stratosphere and the lower mesosphere, its intensity and centre position apparently varied in the middle and upper mesosphere.

Again, from rather south-easterly flows that occurred during winter in the upper mesosphere, it may be assumed that a disturbance of the cyclonic vortex possibly changed to anticyclonic circulation.

The latitude-height cross sections illustrated in Figs 8.9 to 8.15 show that large temperature and wind variations occurring in the winter Antarctic mesosphere are also typical of northern high latitudes. This is evidenced by results of rocket soundings at Fort Churchill and at Heiss Island during their winter period. A rather interesting feature of the Antarctic circulation is that in the upper mesosphere easterly wind components were predominant for about 8-9 months. Also, these periods of easterly winds corresponded to a period of low temperatures, while the periods of westerly flow corresponded to short duration mid-winter warmings in the upper mesosphere.

The main differences between hemispheres in the intensity of various physical processes in the stratosphere occurred in the winter period. Frequent break-up of mid-winter zonal circulation accompanied by warmings have been observed in the stratosphere of the Northern Hemisphere, while in the Southern Hemisphere these processes were relatively less. Direct cause of stratospheric warmings is commonly

assumed as descending motions. According to Perry (1967), these may be accompanied by ascending motions in the tropical stratosphere of the Northern Hemisphere. Cooling of the stratosphere has usually been observed in the tropical regions and in the summer Southern Hemisphere at least to 30°S simultaneously warming in the Northern Hemisphere (Fritz and Soules, 1970).

There is an indication of the development of ascending motions in the tropical stratosphere of both hemispheres during the period of warming in middle and high latitudes of the Northern Hemisphere. As warmings are more frequent and intense during the winter period of the Northern Hemisphere than during that of the Southern Hemisphere, it may be supposed that ascending motions in low latitudes should attain greater intensity in January or February than in July or August. The resulting effect would be decrease of temperature over the equator at the beginning (and end) of a year and increase in the middle of it. Hence the annual cycle caused by radiation will be strengthened north of the equator and radially changed south of it, which leads to the anomalous annual variation observed in this region.

8.5   Epilogue

The latitude-height cross sections of the atmospheric winds and temperatures in the Eastern and the Western Meridional Networks during the periods December to February and June to August illustrated in Figs 8.9 to 8.15 provide a valuable information on the relative symmetry between phenomena of the Northern and the Southern Hemispheres. For example, the springtime transition from westerlies to easterlies outside the tropics appeared to take place in a more regular fashion in the Southern Hemisphere. This is in no doubt related to differences in dynamic and radiational warming patterns between the two hemispheres. It may be due to differences in topographical characteristics.

In both hemispheres there is a marked tendency for the westerlies to replace the easterlies before the autumnal equinox and to persist after the vernal equinox. Both wintertime westerlies and summertime easterlies appear to be stronger on the average between 20 and 60 km over the Southern Hemisphere than over the Northern Hemisphere. The above analysis shows that the winter polar vortex and the summer anticyclone spread up to the mesosphere while tropical anti-cyclone are confined to the stratosphere. It is noted that large-scale disturbances of the thermal field and circulation caused by winter warmings of planetary scale appear most significant in the mesosphere.

SUMMARY AND PRINCIPAL CONCLUSIONS

The investigation of the Atmospheric Structure : Exploration over Antarctica and Interhemispheric Comparison carried out in the thesis leads to a number of new results which are discussed in the previous Chapters. A resume of the work done and the principal conclusions drawn from this study are summarised in this Chapter.

The author participated in the Soviet Antarctic Expedition during 1971-73 and carried out the M-100 rocket soundings at Molodezhnaya as reported by Caffin (1975). The upper atmospheric wind and temperature results from these soundings have been discussed earlier (Sehra, 1974,1975,1976a, 1976b,1976f) and also compared with the corresponding equatorial results (Sehra, 1976c,1976d, 1976e).

In 1972, 52 flights were successful out of which 16 carried an additional wind sensor 'chaff' for measuring upper mesospheric winds. The chaff and parachute wind data were obtained simultaneously. Based on all these data, seasonal variations of the winds in the Antarctic troposphere, stratosphere and mesosphere are studied. The results are also compared with the Groves atmospheric model (Groves,1971)

and the corresponding departures in the two hemispheres are worked out.

The zonal winds over Molodezhnaya, Antarctica in 1972 were predominantly easterly in the southern summer and westerly in the winter with reversal of winds from easterly to westerly during the autumn and from westerly to easterly during the spring. The Antarctic winter westerly winds increased in strength as the season advanced and attained jet speed of about 90 m/s. Complete reversal of winds from easterlies to westerlies occurred in the first week of February in the stratosphere and in February end in the troposphere. The reversal from westerlies to easterlies occurred in the third week of November in the stratosphere. It was found that the reversal first occurred in the upper layers and subsequently in the lower layers indicating a downward propagation of the disturbance similar to Miers(1963).

It is found that the summer to winter shift was a relatively rapid change while the winter to summer shift was slow and gradual. Also, the most unsettled period in the south polar region was the winter and early spring which was marked by large perturbation in wind and thermal structures accompanied by stratospheric and mesospheric warmings and coolings (Sehra,1975).These results are in close agreement with those obtained by Briggs (1965) and Koshelkov (1972).

It is found that in the southern summer (December to February), average zonal flow over Antarctica was easterly throughout the atmosphere from surface up to 80 km. The flow had a speed less than 13 m/s in the tropsophere and the stratosphere. It became stronger in the mesosphere and attained a speed of 41 m/s at 70 km with a standard deviation of about 7 m/s.In an altitude region from about 10 to 20 km the zonal winds were very weak and calm with speeds less than 3 m/s indicating that there was no turbulence' at the boundary of the troposphere and the stratosphere in the summer.

Average wind profile for the southern winter (June to August) over Antarctica show that in the winter the zonal winds were strong westerly throughout the atmosphere from about 5 to 80 km with weak easterly winds of speed less than 8 m/s in the lower troposphere below 5 km. The winter westerly flow attained jet speed in the stratosphere and the mesosphere which had a maximum of 90 m/s at 64 km with a secondary maximum of 71 m/s at 44 km. The winter westerly flow persisted in the spring with the stratospheric maximum of 39 m/s at 28 km and mesospheric maximum of 56 m/s at 61 km. It is found that the meridional wind components were variable throughout the atmosphere with weaker winds from surface up to the lower mesosphere and relatively stronger aloft.

The atmospheric temperatures over Antarctica were obtained up to an altitude of 80 km. The results showed that the variation of the Antarctic temperatures was smaller in the troposphere and larger in the stratosphere and the mesosphere. The summer polar tropopause was located between 8 and 11 km with the temperature varying from -50 to $-60^\circ C$, while the winter tropopause was not found to be well defined due to its multiple occurrences between 10 and 25 km. A differential cooling was set in the atmosphere beginning early autumn which weakened the South Polar tropopause and at times wiped it out thus forming a complex quasi-tropopause during the winter regime. The differential cooling might be due to the ventilation of the Antarctic atmosphere by warm marine air with intense horizontal advection in the troposphere and a weak advection through the strong stratospheric jet stream encircling Antarctica.

The average polar stratopause over Antarctica was located at 47 km and the winter stratopause was colder than its summer counterpart by about $19^\circ C$. The Antarctic stratosphere was colder in the southern winter because there was very little warm air advection through the strong stratospheric jet-stream encircling Antarctica thus permitting the average stratospheric temperature to fall

steadily at the rate of about 0.25°C per day. The Antarctic upper stratosphere and the lower mesosphere appears to gain energy through radiative processes in the southern summer and to lose it during the winter regime.

The mesosphere over Antarctica in an altitude region from about 64 to 80 km in the summer was found colder than its winter counterpart. The average summer and winter temperature departures from the annual mean were found to be in a range of about -22 to +7°C. The polar winter mesosphere in the Southern Hemisphere may be warmer due to a large-scale meridional transport of heat in one form or another by the atmosphere resulting from a mean meridional circulation or from large-scale eddy diffusion processes.

The Antarctic upper atmosphere was subjected to large thermal perturbations during the winter regime causing significant warmings and coolings in the stratosphere and the mesosphere with larger amplitudes at higher altitudes. Apart from this, there were a few instances when sudden warmings also occurred, e.g. on May 17 and July 5, 1972. The polar warmings might be due to an increase in the supply of energy caused by radiative processes.

As noted by the author (Sehra, 1974, 1975), in the southern winter there were significant disturbances of temperature and wind velocity distribution in the Antarctic

mesosphere exceeding similar variations at lower levels. The period of oscillations at heights of 60-70 km ranged from one to three weeks and changes of temperature were from about 20 to 70°C (Sehra, 1976a). The strengthening of westerly flows in the middle and upper mesosphere as well as in the upper stratosphere were accompanied by warming, while the weakening of a westerly flow, the increase of meridional components and the appearance of easterly components coincided with cooling.

A rather interesting fact is that in the upper mesosphere easterly wind components are predominant for about 8-9 months and these periods of easterly winds correspond to a period of low temperatures. Periods of westerly flow correspond to short duration mid-winter warmings in the upper mesosphere.

A remarkable wave like structure was detected in the vertical profiles of wind components both over the South Polar and the equatorial regions. These observations indicate that the recurrent wave structure might have been caused by the wind fluctuations due to atmospheric gravity waves. It is also found that these irregular waves were predominantly horizontal, had amplitudes that increased with height and also the dominant scale size of the vertical wave length increased with height which may be due to gravity waves. The amplitude of the irregular waves increased

rapidly with height owing to the rapid decrease in atmospheric density. Turbulent motions causing the irregular waves over rough terrain and about local circulations such as clouds, as a result of local instabilities can be expected to make their influence felt at remote points in the atmosphere. Thus it appears that both the processes i.e. inetrnal manifestations in the wind field due to atmospheric gravity waves and irregular fluctuations set up due to turbulent motions might cause the wave like structures in the vertical wind profiles.

The summer polar tropopause and stratopause in the Southern Hemisphere over Antarctica were found to be about $27^{\circ}C$ and $13^{\circ}C$ warmer than the corresponding equatorial tropopause and stratopause while the Antarctic mesopause was apparently about $25^{\circ}C$ colder. Also, the south polar tropopause and stratopause were located at altitudes about 8 km and 2 km lower than their corresponding equatorial counterparts while the Antarctic mesopause seemed to be located at an altitude about 5 km higher than the corresponding equatorial mesopause in the southern summer. The primary reason of the warmer polar tropopause and stratopause is the availability of more solar radiation in Antarctica due to almost continuous sunlight.

The summer polar mesopause in the Southern Hemisphere may be colder than its equatorial counterpart due to strong adiabatic cooling in the Antarctic mesosphere. It is because upward motions exist to some degree in summer polar areas due to the expansion of stratospheric regions. Initial phases of upward motions of this meridional current at the stratopause could well be supported by ozone heating in that region. As the air lifts toward the mesopause, adiabatic cooling would become a very strong effect and consequently the polar mesopause becomes colder and also shifted somewhat upwards.

During the southern winter the South Polar tropopause and stratopause were found to be $5^{\circ}C$ and $8^{\circ}C$ colder and at higher altitudes, about 3 km and 2 km respectively than the corresponding equatorial tropopause and stratopause. The situation is reversed because of the absence of sunlight over Antarctica during the southern winter. Some of the key experimental results in the northern polar region are presented by Palmer (1959) and Webb (1961). Departures of the actual zonal winds from the corresponding Groves atmospheric model over Antarctica varied from -14 to $+8$ ms^{-1} in January and -34 to $+36$ ms^{-1} in February while the corresponding equatorial departures ranged from -30 to $+5$ ms^{-1} and -9 to $+27$ ms^{-1} between the two months.

The temperature departures   of the actuals from the Groves profiles were   -30 to +10°C over the South Polar region and   -25 to + 2°C over the equatorial region in the southern summer.

The departures over Antarctica are apparently because the Groves atmospheric model is based on the data from the Northern Hemisphere which differs from the Southern Hemisphere in many respects. Antarctica is as continental as the Arctic at the surface, but the dominant water surface outside the polar regions in the southern Hemisphere and the extensive areas of land surrounding the Arctic emerge as the important factors controlling various changes in the atmospheric winds and temperatures in the Southern and the Northern Hemispheres similar to Holcombe (1958). The higher albedo over Antarctica than over the Arctic explains the much lower summer temperatures of the Antarctic. The coldness of the air at middle southern latitudes in summer, compared with the same northern latitudes, owes more to the physical properties of the immense southern oceans than to the presence of an ice-covered polar continent.

The departures may also be due to the reasons that the Southern Hemisphere is more symmetric and has a vigorous general circulation and that the Antarctic continent is located at a higher elevation than the Arctic. Likewise for

the Thumba latitude in the Eastern hemisphere, the Groves Model is based on data from all longitudes mostly from the Western Hemisphere. Departures of the equatorial actuals from the Groves profiles may, therefore, be the evidence of longitudinal asymmetries between the Eastern and the Western Hemispheres. Thus the discrepancy between the actuals and the Groves Model may be largely attributed to the specificity of geographical locations of the sounding stations.

The meridional cross section analysis carried out using the data from the Eastern and the Western Hemispheres shows that the main differences between hemispheres in the intensity of various physical processes in the upper atmosphere occurred in the winter period. Frequent break-up of mid-winter zonal circulation accompanied by warmings have been observed in the stratosphere of the Northern Hemisphere. In the Southern Hemisphere these processes were relatively less. In 1972 the wind and thermal field over Antarctica were subjected to sizeable perturbations accompanied by significant warmings and coolings including a few cases of sudden explosive warming.

According to Perry (1967), these temperature changes may be accompanied by ascending motions in the tropical stratosphere of the Northern Hemisphere. The present

investigation gives an indication of the development of ascending motions in the tropical stratosphere of both the hemispheres during the period of warming, in middle and high latitudes. As warmings are generally more frequent and intense during the winter period of the Northern Hemisphere, ascending motions in low latitudes may be supposed to attain greater intensity in January or February (northern winter) than in July or August (southern winter) .The resulting effect would be decrease of temperature over the equator at the beginning and end of a year and increase in the middle of it.

Ad finem, it may be added that it is very essential to collect more meteorological data particularly in the relatively less explored South Polar region and fill up the data gaps over oceanic areas in the Southern Hemisphere in order to fully understand the physical processes influencing the weather and climate all over the globe and solve the intricate problems connected with weather forecasting. The First GARP Global Experiment (FGGE) of the Global Atmospheric Research Programme (GARP) to be carried out during 1978-79 is one of the most complex and ambitious international projects ever conceived to solve these problems.

R E F E R E N C E S

Angell, J.K. and Korshover, J.	1962	Mon. Weath. Rev., Vol. 90 p. 127
Angell, J.K. and Korshover, J.	1965	J. Geophsys. Res., Vol.70 , p. 3851
Ballard, H.N. and Rofe, B.	1969	In Stratospheric Circulation, Webb, W.L.(ed), Academic Press, New York, p. 142
Barnett, J.J. et al	1971	Nature, Vol. 230, p. 47
Batten, E.S.	1961	J. Met., Vol. 18, p. 283
Belmont, A.D. and Dartt, D.G.	1970	J. Geophys. Res., Vol. 75, p. 3133
Beyers, N.J.	1969	In Stratospheric Circulation, Webb, W.L.(ed), Academic Press, New York, p. 94
Bhavsar, P.D. and Ramanuja Rao, K.	1968	Space Research VIII,p.655
Bollermann, B.	1970	NASA CR-1529, Parts 1 & 2
Briggs, R.S.	1965	J. Appl. Met., Vol.4, p.238
Caffin, J.M.(ed).	1975	Antarctic, published quarterly by the New Zealand Antarctic Society, Vol. 7, No.7, pp. 224-225.
Dartt, D.G. and Belmont, A.D.	1970	Quart. J. Roy. Met. Soc., Vol. 96, p. 186

Deb, S.   1953   J. Atmos. Terr. Phys.,
                                                       Vol. 4, p. 28

Ebdon, R.A.   1960   Quart. J. Roy. Met. Soc.,
                                                       Vol. 86, p. 540

Finger, F.G., Teweles, S.   J. Geophys. Res., Vol. 68,
and Mason, R.B.   1963   p. 1377

Finger, F.G. and   NASA TM-X-1346, and,
Woolf, H.M.   1967a   J. Atmos. Sci. Vol.24, p.387

Finger, F.G. and   J. Atmos. Sci., Vol. 24,
Woolf, H.M.   1967b   p. 230

Gaigerov, S.S. et al   1969   In Stratospheric Circulation,
                                                       Webb, W.L.(ed), Academic
                                                       Press, New York, p. 323

Gaigerov, S.S. et al   1974   Space Research XIV, p. 55

George, P.A. and   Indian J. Met. Hyd. Geophys.,
Narayanan, V.   1975   Vol. 26, p. 443

Groves, G.V.   1967   Space Research VII, p. 986

Groves ,G.V.   1968   Space Research VIII,p. 741

Groves, G.V. and
Makarious, S.H.   1968   Space Research VIII,p. 857

Groves, G.V.   1969   J. Brit. Interplan. Soc.,
                                                       Vol. 22, p.285

Groves, G.V,   1971   Report No.AFCRL-71-0410,
                                                       Air Force Cambridge Research
                                                       Laboratories, Bedford,
                                                       Massachusetts

Hines, C.O.   1963   Quart. J. Roy. Met.Soc.,
                                                       Vol. 89, p. 1

Hines, C.O.   1966   J. Geophys. Res., Vol. 71,
                                            p. 1453

Holcombe, R.M.   1958   Polar Atmosphere Symposium,
                                            Part I, R.C.Sutcliffe,(ed),
                                            Pergamon Press, pp. 9-17

Johnson, K.W.   1969   Mon. Weath. Rev., Vol. 97,
                                            p. 553

Johnson, K.W. and   Mon. Weath. Rev., Vol. 98,
McInturff, R.M.   1970   p. 635

Julian, P.R.   1967   J. Appl. Met., Vol. 6, p.557

Kantor, A.J. and   J. Geophys. Res., Vol. 69,
Cole, A.E.   1964   p. 5131

Kats, A.L.   1970   Stratospheric and Mesospheric
                                            Circulation,Israel Program
                                            for Scientific Translations,
                                            Keter Press,Jerusalem

Kellog, W.W.   1961   J. Met., Vol. 18, p. 373

Kellog, W.W. and
Schilling, G.F.   1951   J. Met., Vol. 8, p. 222

Kennedy, J.S. and
Nordberg, W.   1967   J.Atmos. Sci.,Vol. 24, p.711

Kokin, G.A. and   Processing of Rocket Data,
Koshelkov, Y.P.   1968   Central Aerological Obser-
                                            vatory, Moscow.

Koshelkov, Yu.P.   1972   Meteorol. i Gidrol., No.5,1972

Koshelkov, Yu.P.   1974   Space Research XIV, p. 49

Kriester, B.	1968	In Winds and Turbulence in the Stratosphere,Mesosphere and Ionosphere, Rawer,K(ed), North-Holland Publ.Co., Amsterdam, p. 81
Labitzke, K.	1969	Quart. J. Roy. Met. Soc., Vol. 94, p. 279
Lally, V.E. and Leviton, R.	1958	Air Force Surveys in Geophysics, No.93, AFCRC-TN-58-213, Bedford,Massachusetts
Lindblad, B.A.	1967	Space Research VII, p. 1029
Lindblad, B.A.	1968	Space Research VIII, p. 835
Lindzen, R.S.	1967	Quart. J. Roy. Met.Soc., Vol. 93, p. 18
MacDowell, J.	1960	Proc. Roy. Soc., Series A, Vol. 256, p. 149
Maeda, K.	1963	J. Geophys. Res., Vol. 68, p. 185
Miers, B.T.	1963	J. Atmos. Sci., Vol.20, pp. 87-93
Miller, A.J., Finger, F.G. and Gelman, M.E.	1970	NASA TM X - 2109
Müller, H.M.	1966	Planet. Space. Sci., Vol.14, p. 1253
Murgatroyd, R.J.	1957	Quart. J. Roy. Met. Soc., Vol. 83, p. 417
Murgatroyd, R.J.	1965	Proc. Roy. Soc., Series A, Vol. 288, p. 575

Murphy, C.H.   1969   J. Geophys. Res. , Vol.74,
                                            p. 339

Narayanan, V. and   J. Indian Rocket Soc.,
Fedynski, A.V.   1973   Vol. 3, p. 127

Newell, R.E., Wallace,J.M.
and Mahoney, J.R.   1966   Tellus, Vol. 18, p. 363

Palmer, C.E.   1954   Weather, Vol. 9, p.341

Palmer, C.E.   1959   J.Geophys. Res.,Vol. 64,
                                            pp.749-764

Pant, P.S.   1956   J. Geophys. Res., Vol.61,
                                            p. 459

Perry, J.S.   1967   J. Atmos. Sci., Vol. 24,
                                            No.5, p. 539

Quiroz, R.S.   1966   J. Appl. Met., Vol.5,p.126

Quiroz, R.S. and   Mon. Weath. Rev., Vol. 95,
Miller, A.J.   1967   p. 635

Quiroz, R.S.   1969   Mon. Weath. Rev., Vol. 97,
                                            p. 541

Rahmatullah, M.   1968   Space Research VIII, p.761

Ramanathan, K.R.   1963   XIII General Assembly IUGG,
                                            Paper No.C-11-24

Rao, K.S.R. and   Indian J. Met. Geophys.,
Joseph, K.T.   1969   Vol. 20, p. 213

Rao, K.S.R. and   J. Appl. Met., Vol. 10,
Joseph, K.T.   1971   p. 133

Rao, M.S.V.	1967	J. Appl. Met., Vol.6, p.401
Reed, R.J.	1964	Quart. J. Roy. Met.Soc., Vol. 90, p. 441
Reed, R.J.	1965	J. Atmos. Sci, Vol.22, p. 331
Reed,R. J.	1966	J. Geophys.Res.,Vol.71,p.4223
Reed, R.J., McKenzie, D.J. and Vyverberg, J.C.	1966	J. Atmos. Sci., Vol. 23, p. 416
Reed, R.J., Oard, M.J. and Sieminski, M.	1969	Mon. Weath. Rev., Vol. 97, p. 456
Rotolante, R.A. and Parra, A.M.	1965	J. Geophys. Res., Vol. 70, p. 749
Scherhag, R.	1960	J.Met., Vol.17, p. 575
Sehra, P.S.	1974	Nature, Vol. 252, pp.683-686
Sehra, P.S.	1975	Nature, Vol. 254, pp.401-404
Sehra, P.S.	1976a	J.Geophys.Res.,Vol.81, No.21, pp.3715-3718
Sehra, P.S.	1976b	Geophys. Res. Lett.,(in press)
Sehra, P.S.	1976c	Indian J. Met. Hyd.Geophys., Vol.27,No.3,(in press)
Sehra, P.S.	1976d	Indian J.Radio Space Phys., Vol.5, No.1, pp. 66-74
Sehra, P.S.	1976e	J.Met.Soc.Japan, Vol.54, No.2, pp. 105-117
Sehra, P.S.	1976f	Exploration of atmospheric wind structure in Antarctica, To appear in Tellus,(1976/1977)

Shen, W.C., Nicholas,G.W. and Belmont, A.D.	1968	J. Appl. Met., Vol. 7, p. 268
Sheppard, P.A.	1963	Reports on Progress in Physics and Physical Soc., London, Vol. 26, p.213
Smith, O.E., McMurray,W.M. and Crutcher, H.L.	1961	NASA TN D-1641
Sparrow, J.G. and Unthank, E.L.	1964	J. Atmos. Sci., Vol. 21, p. 592
Sprenger, K., Greisiger,K.M. and Schminder, R.	1969	Ann.Geophys., Vol.25, p.505
Sprenger, K. and Schminder, R.	1969	J. Atmos. Terr. Phys., Vol. 31, p.217
Staley, D.O.	1963	J. Atmos. Sci,Vol.20,p.506
Teweles, S.	1965	In WMO Tech. Note No.70,p.107
Theon, J.S. and Horvarth, J.J.	1968	NASA TN D-4264
Thiele, O.W.	1966	J.Atmos.Sci,Vol.23, p.424
Tucker, G.B.	1965	Quart. J. Roy. Met. Soc., Vol. 91, p.356
Tucker, G.B. and Hopwood, J.M.	1968	J.Atmos.Sci,,Vol.25, p. 293
Webb, W.L.et al	1961	Bull. Amer. Met. Soc., Vol. 42, pp. 482-494
Webb, W.L.	1964	Astronaut. Aeronaut., Vol. 2, No. 3, p. 62

Webb, W.L.	1966	Structure of the Stratosphere and Mesosphere, Academic, Press, New York
Webb, W.L.	1969	Stratospheric Circulation, Academic Press, New York,
Wexler, H.	1959	Quart. J. Roy. Met. Soc., Vol. 85, p.196
Willet, H.C.	1968	J. Atmos. Sci., Vol. 25, p. 341
Woodrum, A., Justus, C.G. and Roper, R.G.	1969	J. Geophys. Res., Vol. 74, p. 4099

IN MEMORY OF

All Polar Explorers

who sacrificed themselves in the harshest and the

most hostile polar regions with a self denial

of comfort in search of new scientific

knowledge for the common good

of all mankind